Optical Mapping of Human Embryonic Stem Cell-Derived Cardiomyocyte
Graft Electrical Activity in Injured Hearts

Dominic Filice

A dissertation

submitted in partial fulfillment of the

requirements for the degree of

Doctor of Philosophy

University of Washington

2015

Reading Committee:

Michael A. Laflamme, Chair

Charles E. Murry

Deok-Ho Kim

Program Authorized to Offer Degree:

Bioengineering

University of Washington

Abstract

Optical Mapping of Human Embryonic Stem Cell-Derived Cardiomyocyte Graft
Electrical Activity in Injured Hearts

Dominic Filice

Chair of the Supervisory Committee:
Associate Professor Michael A. Laflamme
Department of Pathology

Human embryonic stem cell-derived cardiomyocytes (hESC-CMs) show

tremendous promise for cardiac repair. hESC-CMs can be efficiently generated in high

numbers for cardiac transplantation, have been shown to form stable grafts within

animal models of cardiac injury and mediate beneficial mechanical effects on recipient

hearts. However, the successful development of hESC-CM-based therapies requires

improved tools to investigate their behavior after transplantation. Here, we utilized

hESC-CMs that stably express the calcium-sensitive fluorescent protein GCaMP3 to

visualize their activity in hearts ex vivo. By this method, we found the first direct

evidence that GCaMP3+ hESC-CMs can integrate with host myocardium, although with

variable success. Specifically, GCaMP3+ hESC-CMs coupled in 100% of uninjured,

~60% of recently injured, and ~38% of chronically injured guinea pig hearts. Further,

activation kinetics measured by GCaMP3 fluorescence revealed grafts residing in injury

scar of recipient hearts were considerably slower than grafts within healthy tissue.

When we attempted to measure host-graft electrical interactions by optical mapping with

conventional voltage-sensitive fluorescent dyes, we found hESC-CM grafts failed to label. Thus, to overcome this limitation we developed and validated an alternative strategy based on the simultaneous imaging of GCaMP3+ hESC-CM grafts (providing a graft autonomous reporter of activation) and optical action potentials (APs) from a water-soluble, voltage-sensitive fluorescent dye (di-2-ANEPEQ) that labels both graft and host tissue. By this approach, we found GCaMP3+ hESC-CM grafts from two hESC lines (RUES2 and H7) exhibited multiple potentially pro-arrhythmic properties, including conduction velocities <10% of that in adjacent host myocardium, incomplete host-graft and graft-graft coupling, and spatially heterogeneous patterns of activation that vary from beat-to-beat. GCaMP3+ RUES2 hESC-CM grafts displayed significantly longer AP durations than equivalently prepared H7-derived grafts as well as a significantly lower, near zero rate of host-graft coupling. We provide evidence that these ultra-long APs in RUES2 hESC-CMs may be an idiosyncratic response to GCaMP3 expression in this cell line. Despite this unanticipated off-target effect of GCaMP3 on AP duration, the simultaneous imaging of this graft-autonomous reporter and di-2-ANEPEQ nonetheless allowed us to acquire the first unambiguously hESC-CM graft-derived optical APs and yielded critical insights into the electrical behavior of engrafted hearts.

Table of Contents

List of Figures

List of Tables

Acknowledgements

I would like to thank my advisor Dr. Michael A. Laflamme, as well as committee members Dr. Charles E. Murry, Dr. Bertil Hille and Dr. Deok-Ho Kim for their guidance and support during my studies.

Dedication

This document is dedicated to my wife, who has been with me since the beginning of my PhD program and has been a constant source of support, love, and joy. I also dedicate this document to my parents, whose sacrifices when I was young allowed me to get the best education possible growing up. Without you I would not be here today.

Chapter 1: Introduction

1.1 Motivation

A myocardial infarction (MI) occurs when the flow of oxygen-rich blood to the heart muscle itself becomes blocked. If blood flow is not quickly restored, the infarction results in the death of heart muscle and thus a decrease in the heart's ability to pump blood throughout the body. Although there is some suggestion of ongoing cardiomyocyte cell cycle activity and proliferation[1, 2], for all practical purposes the heart is considered a non-regenerative organ and simply cannot replace the ~1 billion cardiomyocytes typically lost due to MI[3]. As a result of this shortcoming, over time this once active muscle is replaced with non-contracting and non-conducting scar, leading to the initiation of heart failure. This disease of the heart is of global significance and is the number one cause of death worldwide[4]. In the United States alone, heart disease is responsible for 1 in every 4 deaths and comes with a burden of $32 billion dollars each year[5].

While there have been advances in treatment options[6], the 5 year survival rate after diagnosis of ischaemic heart failure is only 50%[7]. At the root of this is the fact that most current treatment options are only palliative (e.g. medication, diet, and exercise), and although they can improve quality of life they cannot compensate for the loss of heart pumping function. To date, the only treatment option available to restore heart function is whole organ transplantation, however with demand greatly exceeding supply and co-morbidity from non-cardiac diseases precluding many from this option, few receive this treatment. The development of mechanical left ventricular assistive devices that take over for the left ventricle altogether is another option, however these devices

are typically implemented as a destination therapy and come with their own significant complications such as a need for a power supply and an increased risk of infection and stroke[8]. For all of these reasons, healing the heart by regenerating the tissue lost from the ischemic event is a very attractive goal, and has motivated preclinical work with a number of replacement cell therapies. The focus of this body of work is on the use of human embryonic stem cell derived cardiomyocytes for this purpose, which explained below have emerged as one of the most promising cell populations in preclinical work today.

1.2 Background

1.2.1 Cell-based therapies

A multitude of cell-based therapies have been studied in preclinical models of cardiac injury. To meet the criteria for true cardiac regeneration, a cell type must be capable of surviving in the injured heart and forming a stable cardiac graft, exhibit contractile properties to restore lost pumping function, and electrically sync with host myocardium. Described next is a brief summary of the positive findings and limitations of several exogenous cell types studied to date.

The use of exogenous cells to treat failing hearts began in the 1990s with the transplantation of fetal and neonatal cardiomyocytes (CMs) into uninjured and injured mice, rat, and canine hearts[9-15]. These cell types proved capable of forming stable intracardiac grafts, exhibited shared intercalated discs containing gap junctions with host myocardium, and mediated beneficial improvements in injured heart end diastolic dimensions and function[9-15]. As definitive cardiomyocytes, these cell populations meet

all criteria for cardiac regeneration. However, using fetal and neonatal CMs as a cell source have proven practically unworkable, facing both strong moral and political opposition, so although they served as early proof-of-concept, research of different cell types for clinical transplantation has ensued.

The cardiac transplantation of skeletal myoblasts for repair also began in the 1990s, due to their functional and histological similarities to cardiac myocytes. A variety of syngeneic, allogeneic, and xenogeneic transplantation studies in injured rat, rabbit, and sheep hearts showed skeletal myoblasts were capable of forming stable intra-cardiac grafts and improving mechanical function[14, 16-21]. These positive attributes aside, skeletal myoblasts were found to lack the capacity to form functional intercellular communication pathways with host myocardium by shared gap junctions[14, 19, 22]. Thus, the formation of intra-cardiac skeletal myoblast grafts was hypothesized to result in local conduction block, pre-disposing hearts to re-entrant phenomena and ventricular arrhythmias[23]. Indeed, a higher incidence of ventricular arrhythmias was found in human patients receiving this therapy[24]. Further, no evidence was found that they could transdifferentiate into CMs[25].

Another non-cardiomyocyte cell source that has received considerable attention are bone marrow-derived cell sources, namely bone marrow-derived mononuclear cell derivatives and mesenchymal stem cells. Early work in injured mice showed vast engraftment of these cells, transdifferentiation into myocyctes, and improvement in heart mechanical function[26, 27], leading to rather rapid translation of this cell-therapy based on the relative ease at which large numbers of these cells could be obtained and their already proven clinical safety. The results from clinical trials, however, have not

shown the same robust improvements in injured heart function[28-31]. Furthermore, cells from these sources have not been found to persist in the infarct environment or differentiate into cardiomyocytes after transplantation[32, 33] (disputing earlier work[26, 27]), thus they lack the inherent potential to remuscularize injured hearts directly or contribute force generating units that beat in sync with host myocardium. As such, the modest benefits observed from studies with these cell populations have been attributed to paracrine effects on host hearts[34-39].

Cardiac-derived cells (CDCs), so named because they are derived from myocardial biopsies and expanded in vitro for later transplantation, are another cell source that has transitioned to the clinic. Initially, CDCs were considered to be cardiac progenitor cells capable of a cardiomyocyte cell fate, and were shown to engraft and improve function in injured mouse hearts[40, 41]. However, like bone marrow-derived cell sources, recent data from several trials questions their capacity to form stable grafts in injured hearts, and while they have been shown to reduce infarct scar size and improve functional outcomes this action is likely only through paracrine mechanisms as well[42-45].

In contrast to all the aforementioned cell sources, CMs derived from pluripotent stem cells offer a renewable supply of bona fide CMs with the potential to meet all criteria for cardiac regeneration. First isolated in 1998, human embryonic stem cells (hESCs) opened the door for preclinical studies involving the very translationally relevant human CM[46]. The electrophysiological properties of hESC-derived CMs and preclinical experience with this promising cell type are covered in more detail next in sections 1.2.2 and 1.2.3.

1.2.2 Electrophysiology of hESC-derived versus adult ventricular myocytes

The ability to generate large quantities of relatively pure CMs from hESC sources (upwards of 70% cardiac purity) as a result of recent advances in differentiation protocols has enabled the widespread study of this promising cell source for cardiac repair[47, 48]. Beyond the differences in metabolism, morphology, contractility, and proliferation between the immature hESC-CMs from these protocols and adult ventricular myocytes[49-59], hESC-CMs also show differences in their electrical properties as covered below.

At the single cell level, hESC-CMs show immature action potential (AP) properties, including a more depolarized maximum diastolic membrane potential, more rapid spontaneous rate, and slower AP upstroke[60, 61]. Further, hESC-CMs exhibit significant automaticity and AP phenotypes that have been classified as either nodal- or ventricular-like[62, 63]. In patch clamp studies, hESC-CMs have been found to exhibit most of the key cardiac ion currents, however with reduced flux as compared to adult myocytes (see Figure 1.1 for a representation)[64]. Currents reported include L- and T-type Ca^{2+}, pacemaker, fast sodium, and transient outward and inward rectifier K^+ currents[61, 62, 65]. Similar to adult myocytes, fast depolarization in hESC-CMs is mediated primarily by Na^+ influx[65]. Further, depolarization activates L-type Ca^{2+} channels in hESC-CMs, which results in a calcium-induced calcium release from sarcoplasmic reticulum stores similar to adult myocytes[66-68]. Encouragingly, the electrical properties of hESC-CMs have been shown to mature with time in culture[61].
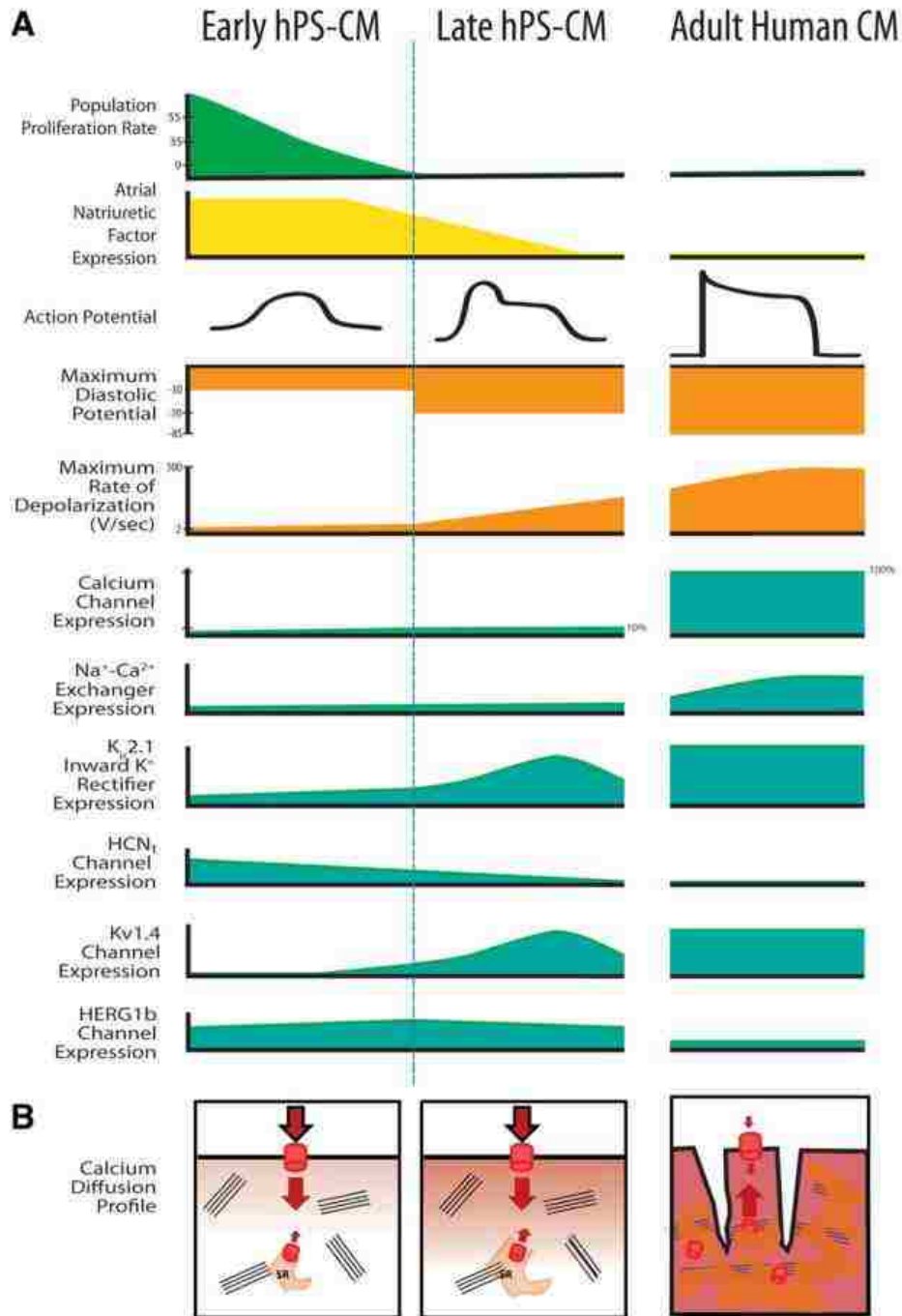
Figure 1.1. Visual comparison of early human pluripotent stem cell-derived cardiomycotyes (hPS-CMs), late hPS-CM and adult CM phenotype. A: An overview of major changes seen with increasing time in culture. Large changes in action potential characteristics (orange) are seen with time in culture, as well as expression of key ion channels (teal). **B:** Calcium influx profiles for early and late hPS-CM compared with adult CM. Note that in early hPS-CM, almost no calcium is released from the sarcoplasmic reticulum, leading to slow, diffusion-limited calcium influx. Late hPS-CM perform better, but still show slow influx compared to adult. Abbreviation: hPS-CM, human pluripotent stem cell-derived cardiomyocytes. Figure from review by Robertson et al[64] with permission.

Differences are also observed in the electrical properties of multicellular preparations of hESC-CMs versus adult cardiomyocytes. Reports of hESC-CM conduction velocity in 2D monolayers and 3D patches have varied between ~4 and ~21 cm/s[69-71], considerably lower than adult human myocardium on the order of ~35 to ~50 cm/s[72, 73]. Correspondingly, this difference have been found to be associated with the relatively smaller size and fewer and more isotropically distributed Cx43-forming gap junctions between interconnected hESC-CMs than adult myocytes[69-73].

1.2.3 Preclinical experience with hESC-CM transplantation

Transplantation studies with hESC-CMs began in uninjured rodent hearts[74, 75], followed by studies in rodent models of acute or subacute infarction[47, 76-79]. These early studies showed transplanted hESC-CMs could form stable intra-cardiac grafts and preserve mechanical function, importantly versus control populations of non-cardiac hESC derivatives. In a long-term evaluation of hESC-CM engraftment, however, van Laake et al. found the initial improvements in mechanical function were lost 3 months post-transplantation, highlighting the need for longer term endpoints[77]. More recently, our group evaluated the electrical and mechanical consequences of hESC-CM engraftment in a guinea pig model of subacute injury[80]. Similar to previous observations, hESC-CMs remuscularized injured hearts and preserved their ejection fraction versus non-cardiac hESC derivatives. More importantly, hESC-CM transplantation resulted in a reduction in spontaneous and induced arrhythmias relative to controls[80]

Transplantation studies with hESC-CMs have also been performed in chronically injured hearts, however with not as promising results as in recently injured hearts. Fernandes et al. found that after transplantation into chronically injured rat hearts, stable intra-cardiac engraftment of hESC-CM was not accompanied by beneficial effects on contractile function[81]. Further, our group found hESC-CM transplantation in a chronic guinea pig cardiac injury model similarly failed to preserve ventricular dimensions and fractional shortening, and had no effect on the incidence of spontaneous arrhythmias[82]. This data is concerning, since this therapy will likely be first applied clinically in end-stage heart failure patients.

Work with hESC-CMs in large animal models has also been studied. Over a decade ago, Kehat et al. assessed for the ability of hESC-CMs derived from beating embryoid bodies to integrate in uninjured porcine hearts after complete atrioventricular block[83]. In this model, they reported the ability of the transplanted hESC-CMs to ectopically pace host hearts, as concluded by correlating the source of ectopy by electroanatomical mapping with histology. Although their source of hESC-CMs was rather crude by currently available differentiation techniques, involved a very short duration, and was based on mapping technology that lacks fine spatial resolution, this was a key study for the field.

1.3 Summary

Myocardial infarction (MI) remains a leading cause of death worldwide[4]. For those that survive the initial ischaemic event, the tissue lost is eventually replaced with an akinetic and non-electrically conductive scar. This loss of viable tissue comes with a

reduction in cardiac output, initiating compensatory mechanisms that eventually spiral downward into full heart failure. Ultimately, the root of the problem is the loss of contractile myocardium, which the heart cannot replace. To date, whole organ transplantation is the only treatment available to restore this lost function, however when considering supply greatly under-meets demand[84], treatments that can potentially replace lost myocardium have considerable appeal. For this reason, strategies based on cell transplantation have garnered much interest and research attention.

Among the potential sources for a cell-based therapy, hESCs have emerged as a particularly attractive cell source due to their highly proliferative nature, virtually unlimited capacity to self-renew, and ability to differentiate into nascent cardiomyocytes. Further, reliable methods exist for the large scale cardiac differentaion of these cells[47, 48], enabling their use in cardiac transplantation studies. Furthermore, hESC-CM transplantation can remuscularize scar tissue and improve cardiac function in animal models of cardiac injury.

While promising, many challenges must be overcome before cell-based cardiac therapy with hESC-CM technology can become widespread in clinical use. Electrical integration is of particular importance when considering these relatively immature cells could provide an arrhythmic substrate in recipients where electrical instability is already a concern and leading cause of post-MI morbidity[85]. To this end, novel technologies to assess the integration and electrical activity of hESC-CM grafts are required to refine this potential treatment and continue to solve preclinical barriers. This scientific body of work contributes new methods to investigate graft electrical integration as well as a novel means to improve this important factor.

Chapter 2: Electrical Integration of Human Embryonic Stem Cell-Derived Cardiomyocyte Grafts in a Guinea Pig Subacute Infarct Model

2.1 Introduction

Preclinical studies with human embryonic stem cell-derived cardiomyocytes (hESC-CMs) have provided exciting proof-of-concept for the use of these cells in cardiac repair[47, 76, 86-88], but concerns remain about their electrophysiological behavior in injured hearts[89-93]. Our group has reported that their transplantation into recently injured guinea pig hearts resulted in improved contractile function and a reduction in spontaneous and induced arrhythmias relative to controls[80]. While the mechanistic basis for this anti-arrhythmic effect remains undetermined and its relevance to human or large animal models uncertain, it is consistent with prior observations in other systems, including transplantation studies with primary murine fetal cardiomyocytes injected into cryoinjured mouse hearts[94] and an in vitro arrythmogenic model involving the co-culture of hESC-CMs and rat neonatal cardiomyocytes[95].

Here, we use the same guinea pig model to investigate whether hESC-CMs are capable of undergoing electrical integration with host myocardium following their transplantation in uninjured and injured hearts. Although there is indirect evidence for their ability to couple with host myocardium following transplantation in uninjured hearts[83, 96], direct graft activity could not be measured. Further, the healthy heart is a very different context from that of the injured heart, where both inflammation and fibrosis are expected to function as barriers to host-graft integration. While we have shown

hESC-CMs are capable of forming stable cardiac tissue grafts with the potential to electrically sync with host tissue via shared intercalated discs in injured guinea pig hearts[80], we also did not have the tools to show direct evidence for host-graft electrical communication. To resolve this uncertainty, we transplanted hESC-CMs that stably express the genetically-encoded fluorescent calcium sensor GCaMP3. GCaMP3+ hESC-CMs exhibit robust fluorescent transients with each contractile cycle, which after transplantation can be used to visualize directly the kinetics of graft activation as well as the extent of graft coupling with recipient hearts. The following Chapter describes our findings using this innovative approach.

2.2 Materials and Methods

2.2.1 Production of GCaMP3+ hESC-CMs

Transgenic H7 hESCs (WiCell Research Institute, NIH Stem Cell Registry #hESC-10-0061) that stably express GCaMP3[97] were generated by zinc finger nuclease-mediated gene insertion as previously reported in detail by our group.[48, 80, 98] GCaMP3+ H7 hESCs were then expanded and differentiated into cardiomyocytes using methods previously detailed[47, 80, 99, 100]. In brief, prior to cardiac induction, hESC cultures were switched to high-density, monolayer conditions and fed with mouse embryonic fibroblast conditioned medium (MEF-CM) supplemented with basic fibroblast growth factor (bFGF). To induce cardiogenesis, cultures were serially treated with activin-A (day 0) and bone morphogenic protein-4 (day 1) in insulin-free RPMI-B27 medium. The latter was exchanged with insulin-free RPMI-B27 medium without exogenous growth factors on day 5, followed by re-feedings with insulin-free medium on

days 7 and 9 and insulin-supplemented medium on days 11, 13, 15 and 17. By this protocol, spontaneous beating and expression of cardiomyocyte markers are typically observed on or before day 10[99]. On day 19, hESC-CMs were transiently heat-shocked with 42º C medium to improve their survival post-transplantation.[101] On day 20, they were then harvested enzymatically and cryopreserved as previously described.[99] GCaMP3+ hESC-CM purity measured 74±10% by troponin I flow cytometry based on this protocol.

For in vitro imaging experiments involving GCaMP3+ hESC-CMs, cultures were enzymatically dispersed to single-cells and replated onto gelatin- and polyethylenimine-coated glass coverslips at 1.5×10^5 hESC-CMs per coverslip as previously described[66] or formed into three-dimensional aggregates by suspension culture.

2.2.2 Cardiac cryoinjury and GCaMP3+ hESC-CM transplantation

All animal procedures adhered to protocols approved by the University of Washington Institutional Animal Care and Use Committee (IACUC) and were conducted in accordance with federal guidelines. We have previously described in detail our methods for the cardiac cryoinjury procedure, intra-cardiac cell injection, and subsequent harvesting of the heart for ex vivo imaging[48, 80, 82]. Figure 2.1 depicts the timeline for experiments intended to assess the electrical integration of hESC-CM grafts in uninjured (n=9) and subacutely injured (n=22) hearts using the guinea pig model reported by our group[80].
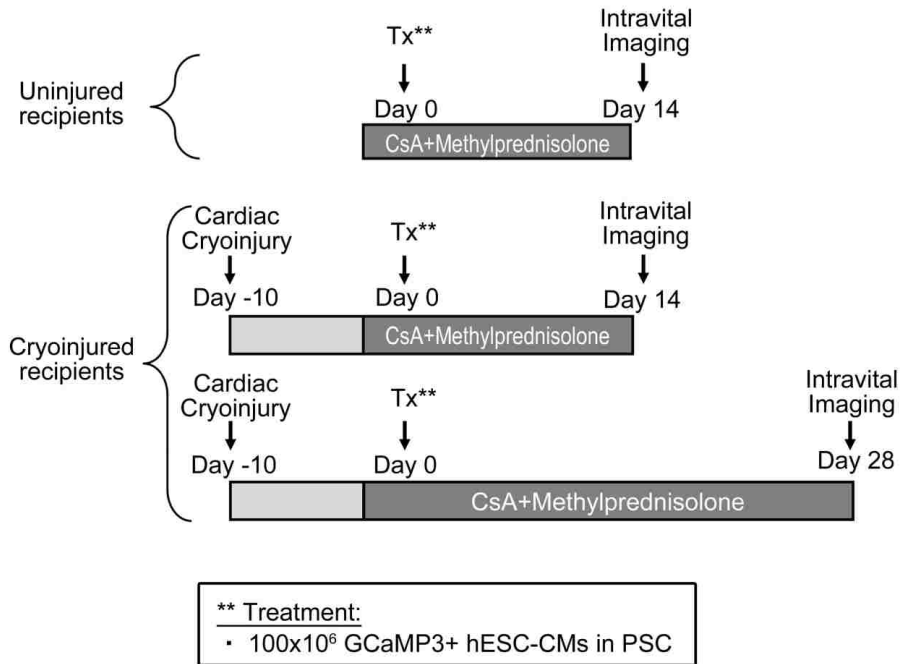
Figure 2.1. Experimental design. To determine the electrical integration of hESC-CM grafts in uninjured and cryoinjured recipients, guinea pigs underwent intra-cardiac injection of GCaMP3+ hESC-CMs at the indicated time-points. To ensure xenograft survival, all animals were treated from day -2 relative to cell transplantation until intravital imaging with cyclosporine A (CsA) and methylprednisolone. Intravital imaging of grafts in cryoinjured recipients was performed at 14 or 28 days post-transplantation. All grafts in uninjured recipients were already fully coupled at 14 days, so later timepoints were not examined in this model. Figure previously published[80].

In brief, 650-700 g male Hartley guinea pigs were anesthetized with ketamine-xylazine induction, intubated with a pediatric laryngoscope and maintained with 1.5% isoflurane anesthesia. To produce cardiac injury, a small thoracotomy was performed to expose the left ventricle, and the anterior epicardial surface contacted with an 8-mm diameter, liquid-nitrogen-cooled aluminum probe for 30 seconds duration times four. 10 days later to model transplantation in a subacute cardiac injury, or without previous injury to study transplantation in uninjured hearts, a repeat thoracotomy was performed, and the heart directly injected with 1×10^8 GCaMP3+ H7 hESC-CMs suspended in a pro-survival cocktail of factors that we have previously shown enhances graft survival[47]. To prevent

immune rejection of the graft cells, we treated the recipient animals with a regimen of cyclosporine (SQ, 15 mg/kg/day x 7 days, followed by 7.5 mg/kg/day maintenance thereafter) and methylprednisolone (IP, 2 mg/kg/day), starting two days prior to cell injection and continuing until the heart was harvested at euthanasia two-weeks (n=16) or four-weeks post-transplantation (n=15).

2.2.3 Imaging of GCaMP3+ hESC-CM engrafted hearts

As directly reported by our group[80], intravital imaging of hearts with GCaMP3+ hESC-CM grafts was performed on days 14 and 28 after transplantation using either an open-chest or ex vivo preparation. For the open-chest preparation, guinea-pigs were anaesthetized, mechanically ventilated and outfitted for standard surface ECG recordings. The anterior epicardium was then exposed by a wide thoracotomy and visualized using an epifluorescence stereomicroscope (Nikon, SMZ 1000) equipped with an EXFO X-Cite illumination source. GCaMP3 was excited at 450 to 490 nm and bandpass filtered (500 to 550 nm) before detection by an electron-multiplying, charge-coupled device camera (Andor iXon 860 EM-CCD) controlled by Andor Solis software. GCaMP3 image acquisition was typically at 80 to 140 frames per second (fps). Signals from the charge-coupled device (CCD) camera and the surface ECG were fed through a computer for digital storage and off-line analysis using Andor software and custom Matlab scripts (MathWorks). Some engrafted hearts were also imaged ex vivo after mechanical arrest to eliminate motion artifacts. For these experiments, the heart was collected, rapidly mounted on a gravity-fed Langendorff apparatus and then perfused with modified Tyrode's solution at 37°C. The epicardial GCaMP3 signal was then

recorded before and after supplementation of the perfusate with an excitation-contraction uncoupler, either 2,3-butanedione monoxime (BDM, 20 mM)[102, 103] or blebbistatin (10 µM)[104]. The utility of blebbistatin was limited by its substantial blue-green fluorescence[105], which interfered with the acquisition of the GCaMP3 signal, so BDM was used in experiments except where otherwise indicated. All quantitative comparisons were carried out using hearts treated with the same uncoupler. The electrical activity of the isolated heart was continuously monitored by placing positive and negative ECG leads at the apex of the left ventricle and right ventricular base, respectively. Although most imaging experiments were carried out under spontaneous conditions, a subset of hearts was also imaged during external pacing at rates from 3 to 6 Hz (ML866 PowerLab 430 Data Acquisition System). Experiments involving pacing at rates of greater than 5 Hz were sometimes limited by the occurrence of irreversible tachyarrhythmias.

In a subset of hearts, GCaMP3 activation maps were generated by determining the interval between a pacing stimulus (or the host QRS complex) and the initial rise in GCaMP3 fluorescence, as recently detailed by our group[48]. For this analysis, raw data from the green fluorescence and ECG channels were read into a custom Matlab script for analysis. The GCaMP3 fluorescent signal was median filtered in time to reduce noise, smoothed with a spatial conical filter, and background subtracted. Regions of graft were user defined and then analysed to determine the relative GCaMP3 activation time on a per-pixel basis. Relative GCaMP3 activation times for each pixel were then averaged over several stimuli to generate GCaMP3 activation maps.

2.2.4 Ex vivo voltage-mapping studies

As directly reported by our group[80], the preceding imaging system and experimental preparation was also used in optical mapping studies with the potentiometric dye RH237. RH237 was selected as our dye of choice, given our past experience with this indicator and its reasonable spectral separation from GCaMP3. When examined in the same heart, GCaMP3 (green-channel) and RH237 (red-channel) fluorescent signals were acquired consecutively by an exchange of filter cubes, not simultaneously. In brief, cryoinjured hearts with or without 28-day-old GCaMP3-positive hESC-CM grafts were mounted on a Langendorff apparatus and loaded with RH237 (40 mM) by a bolus injection (in 10 ml buffer) into the aorta. After an initial stabilization period, RH237-stained hearts were then imaged during both spontaneous and paced rhythms. RH237 was excited at 520 to 550 nm, and emitted light was long-pass filtered (670 nm) before detection at 500 fps using the high-speed EM-CCD system mentioned above. The resultant fluorescent signals were analyzed as described previously[106-108]. In brief, background fluorescence was subtracted and the signal at each pixel was smoothed using a median temporal filter and a spatial cone filter. The signal at each pixel was then scaled as a percentage of the maximum optical action potential amplitude for all the pixels. Although not simultaneously acquired, RH237 and GCaMP3 signals could be partially correlated in a subset of paced hearts by aligning repetitive signals relative to the stimulating electrode.

2.2.5 Histology

Histological endpoints were obtained using methods previously detailed by our group[47, 74, 80, 81]. In brief, hearts were evaluated by histochemical stains (hematoxylin-eosin, picrosirius red) and immunofluorescence. For immunostaining, we used primary antibodies against GFP (rabbit polyclonal) and β-myosin heavy chain (clone A4.951) with species-specific fluorescent (Life Sciences) secondary antibodies.

2.2.6 Statistical analysis

GraphPad Prism (GraphPad Software, La Jolla, California, USA) was used to perform all statistical analyses. To test for synchrony between GCaMP3+ hESC-CM graft-derived fluorescence and ECG signals, intervals were compared using 1-way ANOVA and then a post-hoc Dunnett's test. A p value less than 0.05 was considered significant. All values herein are expressed as mean±standard error.

2.3 Results

2.3.1 GCaMP3+ hESC-CM graft coupling in uninjured hearts

As previously reported by our group[80], to test the hypothesis that intra-cardiac hESC-CM grafts could electrically integrate with host myocardium we transplanted GCaMP3+ H7 hESC-CMs into uninjured guinea pig hearts and imaged them 14 days post-transplantation in vivo via an open chest preparation and ex vivo using a modified Langendorff apparatus. For this, we used a custom-built EM-CCD-based system to acquire the hESC-CM graft-derived GCaMP3 signals, which increase in fluorescence

upon contraction and provide a direct readout of graft activity. This GCaMP3 signal, when correlated with the host ECG, provided a convenient way to assess the extent of hESC-CM graft coupling after transplantation.

We found large GCaMP3+ H7 hESC-CM grafts in all uninjured hearts (n=9) transplanted. In these hearts, we observed extensive host-graft contact with little intervening scar tissue (see Figure 2.2A). Further, all visible GCaMP3+ hESC-CM grafts displayed 100% host-graft coupling, as evidenced by complete 1:1 synchronization of the graft-derived GCaMP3 calcium signals and the host ECG (see Figure 2.2B) as measured in vivo. This uniform 1:1 host-graft coupling persisted in all hearts then harvested and imaged ex vivo after mechanical arrest with either BDM or blebbistatin, ruling out confounding motion artifacts or stretch-mediated activation of graft cells. In addition, GCaMP3+ hESC-CM grafts in uninjured hearts remained fully coupled to the host during ventricular pacing at rates $\geq$5 Hz (see Figure 2.2C).
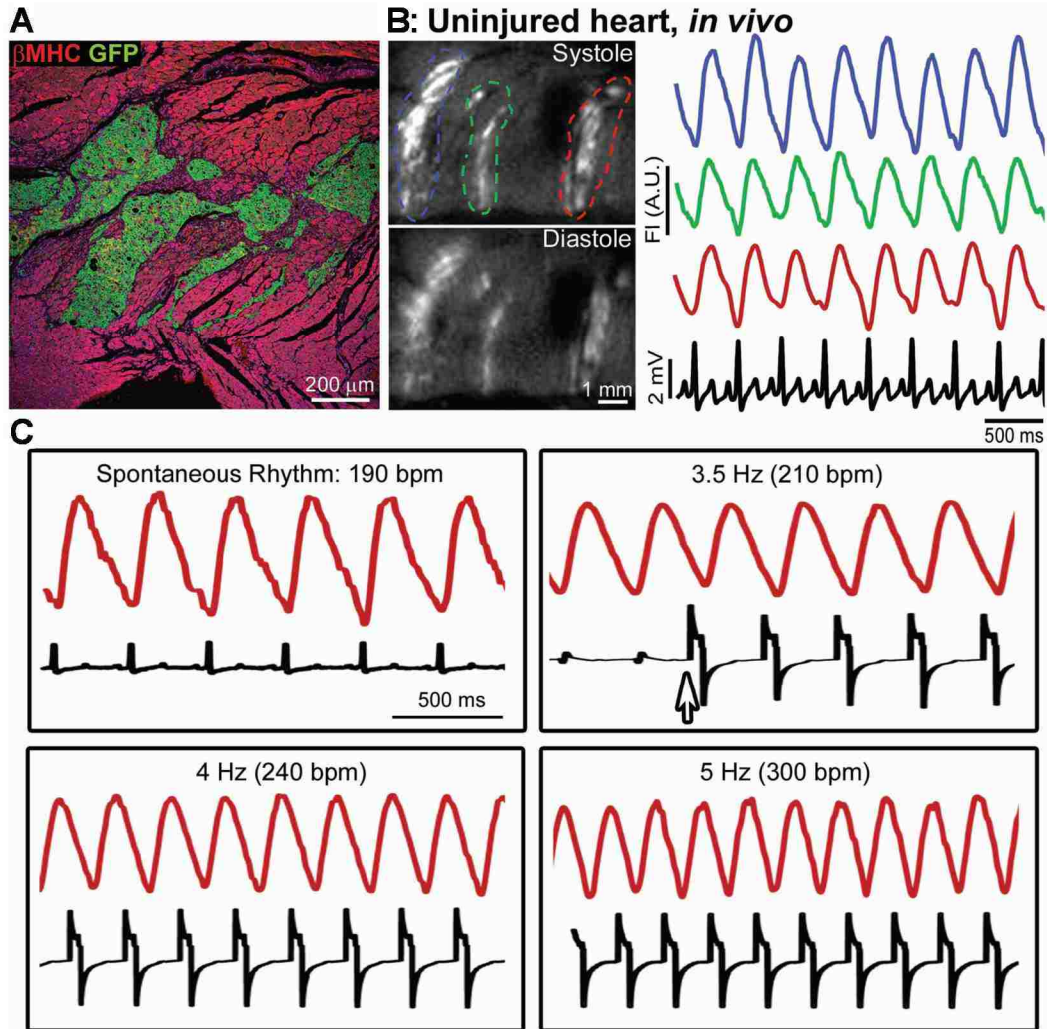
Figure 2.2. hESC-CM grafts in uninjured hearts show 1:1 coupling with host myocardium. A: GCaMP3-positive hESC-CM graft in an uninjured heart immunostained for GFP (green) and bMHC (red), showing extensive host–graft contact with minimal intervening scar. **B:** Left, GCaMP3-positive hESCCM graft in an uninjured heart during systole and diastole, acquired using an open-chest preparation at 14 days after transplantation. Right, GCaMP3 fluorescence intensity (FI) versus time for the red, green and blue regions of interest indicated in the left panel, as well as the host ECG (black). GCaMP3 fluorescent transients in all three regions occurred with 1:1 coupling with QRS complexes of the host ECG. a.u. arbitrary units. **C:** GCaMP3 fluorescent signal (red) and ECG (black) from a representative hESC-CM graft in an uninjured heart, imaged ex vivo under mechanical arrest. 1:1 host–graft coupling occurred during spontaneous beating and pacing at rates ≥5 Hz. Arrow, onset of pacing. Figure previously published[80].

2.3.2 GCaMP3+ hESC-CM graft coupling in subacutely injured hearts

As also reported previously[80], to then test the ability of hESC-CM grafts to couple in recently injured hearts we transplanted GCaMP3+ H7 hESC-CMs into hearts 10 days after cryoinjury and imaged them ex vivo at either 14 or 28 days after transplantation (n=7 and n=15, respectively). In these hearts, we observed surviving grafts at both time points that were found to predominantly reside completely within the central injury scar, however did find occasional points of host-graft contact at the injury border zone (see Figure 2.3A). As in uninjured hearts, GCaMP3+ hESC-CM grafts exhibited robust fluorescence transients when imaged in vivo, however with much greater variability in relation to the host ECG. Thus, assessments of GCaMP3+ hESC-CM graft coupling in the injured heart context were all carried out ex vivo after mechanical arrest. By this approach, we found ~60% of hearts at both the 14 and 28 day time points after transplantation to contain graft regions that were 1:1 synchronized to the host ECG (4 out of 7 and 9 out of 15, respectively; see Figure 2.3B and Tables 2.1 and 2.2 for details). Additionally, there was a trend towards greater host-graft coupling over time in the subset of hearts that had some areas of visibly coupled graft, although this did not reach significance (66%±10% vs 87±6% of visible graft coupled at 14 and 28 days, respectively). Uncoupled graft regions showed cyclic GCaMP3 fluorescence transients with periods unrelated to neighboring graft regions and the host ECG, typically at a rate slower than the host (graft rate of 96±11 vs host rate of 176±9 beats per minute at 28 days). Further, no graft regions were found to display intermittent or partial coupling to the host. When paced ventricularly, coupled grafts in injured hearts remained coupled

at rates up to 4 Hz, but did exhibit a loss of coupling with increased rates (see Figure 2.4).

Coupled graft regions in injured hearts were not limited to locations at the injury border zone, as we found examples of coupled grafts that by epicardial imaging appeared to be completely isolated within the injury region but later by histology found to be in contact with surviving host endocardium. The activation kinetics of hESC-CM graft regions, assessed by mapping a color to the interval between the host ECG or pacing stimulus and the initial rise in graft-derived GCaMP3 fluorescence, however, was dependent on location. We found that graft regions completely within healthy host tissue activated uniformly and within approximately 10 ms, likely a result from many points of host-graft contact leading to synchronous activation. Coupled grafts within the injury area, however, activated much slower (some requiring >50 ms for complete activation), likely reflecting their limited contact with host tissue, the relatively harsh environment of the injury region[109, 110], and slower propagation within the immature graft (see Figure 2.3C-D).
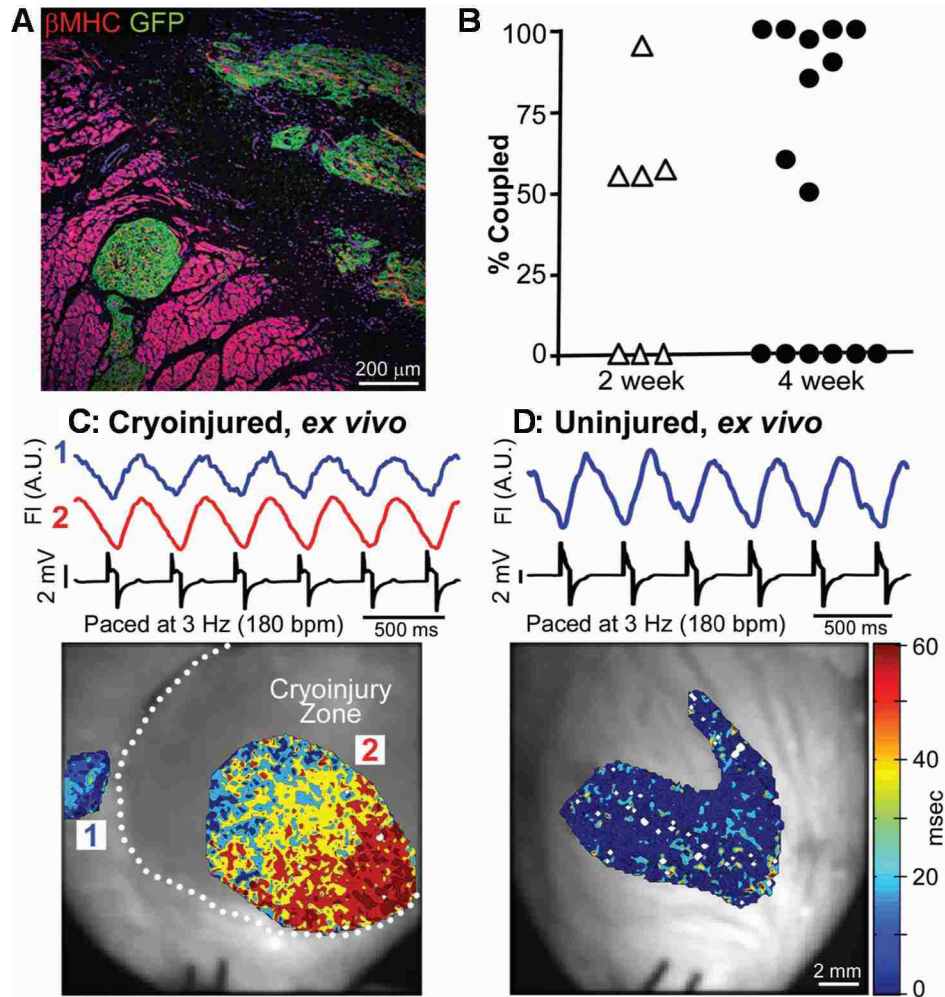
Figure 2.3. hESC-CM grafts show 1:1 host–graft coupling in the majority of injured recipient hearts, but the extent of coupling and pattern of activation is variable. **A:** GCaMP3-positive hESC-CM graft in a cryoinjured heart immunostained for GFP (green) and bMHC (red). Small graft nests were located in host muscle within the border zone, but most of the graft was in scar. **B:** Percentage of visible GCaMP3-positive hESC-CM graft in each cryoinjured heart that showed 1:1 host–graft coupling at 14 and 28 days after transplantation (n=7 and n=15 animals, respectively). **C:** Representative 28-day-old GCaMP3-positive hESC-CM graft in a cryoinjured heart imaged ex vivo during mechanical arrest with blebbistatin and pacing at 3 Hz. Top, traces of mean fluorescent intensity versus time for graft regions located within host muscle (1, blue font) and the cryoinjury zone (2, red font). Both were activated in a 1:1 correlation with the host ECG (black). Bottom, corresponding activation map showing the interval (in ms) between the stimulus pulse and the local rise in GCaMP3 fluorescence. Graft in host muscle (1) showed uniformly rapid activation, whereas the graft in the scar (2) activated first in center of the scar and then gradually progressed towards the border zone. On other occasions, graft activation started at the border zone and radiated into the scar. **D:** Top, traces of GCaMP3 fluorescence and EGG. Bottom, the activation map for a representative GCaMP3-positive hESC-CM graft in a blebbistatin-arrested uninjured heart. This graft showed 1:1 host–graft coupling and a brief interval between stimulus and GCaMP3 transient upstroke. Figure previously published[80].

.

1:1 Host-Graft Coupling?	Fraction of Graft Regions Showing Coupling (% of Graft Area Coupled)	Host RR Interval (in ms)	Cycle Length of GCaMP Transients (in ms, by graft region)
Yes	1/3 graft regions (55%)	540±1.3	540±3 681±3** 642±5**
Yes	1/2 regions (95%)	431±4.0	424±2 726±7**
Yes	1/3 regions (55%)	567±6	560±6 735±2** 1103±61 **
Yes	1/3 regions (57%)	538±8.5	541±11 671±8** 702±20**
No	0/1 regions (0%)	409±5.6	ND
No	0/1 regions (0%)	347±1.2	470±1†
No	0/2 regions (0%)	553±1.6 481±5.2	510±2† 666±6†

- All hearts examined at this timepoint were mechanically arrested with BDM.
- *p<0.05, ** p<0.01, †p<0.001 for comparison between GCaMP cyclic length (i.e. interval between successive GCaMP3 fluorescence troughs) and host RR interval.
- ND= not determined, as GCaMP fluorescent transients in this animal showed no consistent rate or rhythm.

Table 2.1. Outcomes during intravital imaging of GCaMP3+ hESC-CM grafts in injured guinea pig hearts at 14 days post-transplantation (n=7, examined ex vivo during mechanical arrest).   Table previously published[80].

1:1 Host-Graft Coupling?	Fraction of Graft Regions Showing Coupling (% of Graft Area Coupled)	Host RR Interval (in ms)	Cycle Length of GCaMP Transients (in ms, by graft region)
Yes[+]	1/1 region (100%)	302±3.2	303±2
Yes[+]	1/2 regions (97%)	380±1.5	379±9 2018±77†
Yes[+]	1/3 regions (85%)	400±4.7	403±8 1574±39† 1779±48†
Yes[+]	1/4 regions (60%)	276±5.1	276±2 508±8 † 501±20† 1309±22†
Yes[#]	1/1 regions (100%)	394±2.0	393±13
Yes[#]	2/2 regions (100%)	280±19.1	272±4 272±4
Yes[#]	1/1 regions (100%)	368±1.9	366±7
Yes[#]	1/2 regions (90%)	289±6.0	289±11 268±4*
Yes[#]	1/3 regions (50%)	341±0.3	341±2 764±72† 502±4†
No[+]	0/6 regions (0%)	322±8.1	662±138** 1010±13† 1070±222† 1102±24† 273±11† 270±5†
No[#]	0/2 regions (0%)	421±0.5	385±3† 453±11*
No[#]	0/3 regions (0%)	295±1.0	492±5† 1083±49† 648±57†
No[#]	0/4 regions (0%)	599±3.4	732±3† 638±3† 814±20† 880±18†
No[+]	0/1 regions (0%)	361±0.1	1131±8†
No[+]	0/2 regions (0%)	288±2.0	643±7† 887±28†

- Hearts were mechanically arrested with either blebbistatin (+) or BDM (#).
- *p<0.05, ** p<0.01, †p<0.001 for comparison between GCaMP cyclic length (i.e. interval between successive GCaMP3 fluorescence troughs) and host RR interval.

Table 2.2. Outcomes during intravital imaging of GCaMP3+ hESC-CM grafts in injured guinea pig hearts at 28 days post-transplantation (n=15, examined ex vivo during mechanical arrest). Table previously published[80].
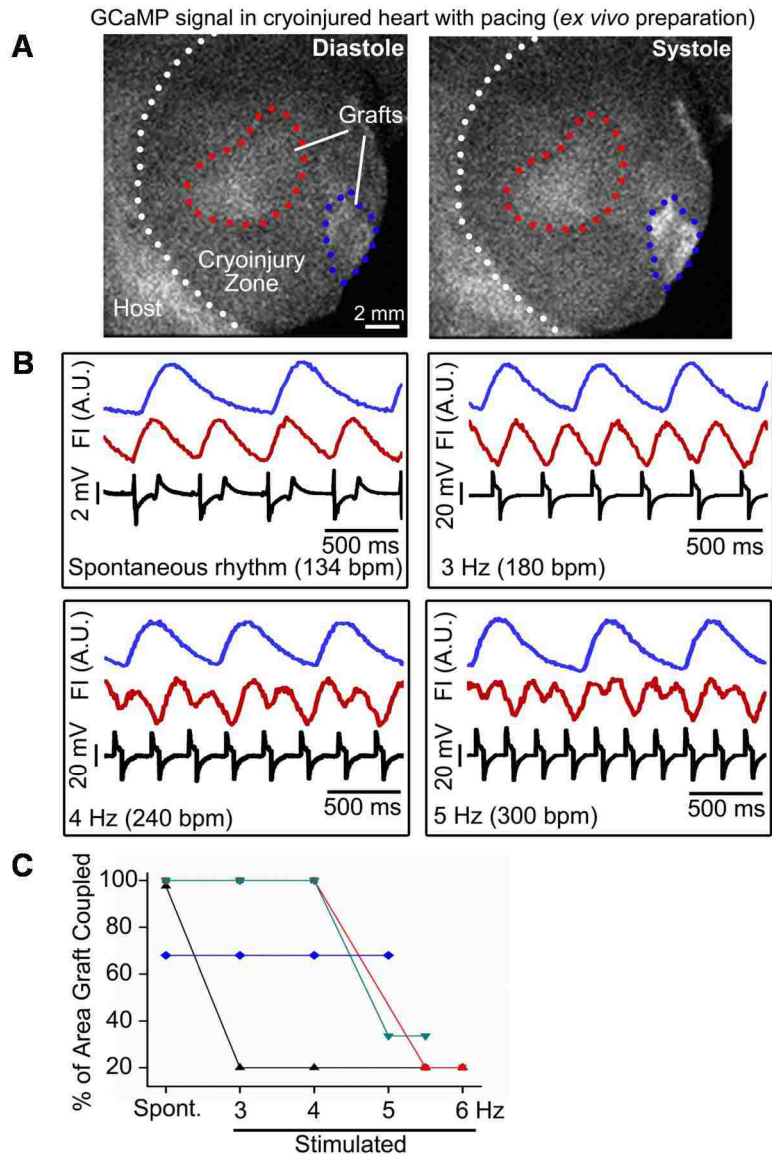
Figure 2.4. Intravital imaging of GCaMP3+ hESC-CM graft in injured hearts under stimulated conditions. For this experiment, injured hearts with GCaMP3+ hESC-CM grafts were harvested at 28-days post-transplantation and maintained ex vivo under mechanical arrest with blebbistatin. Hearts were then imaged under spontaneous conditions or with stimulation at rates up to 6.0 Hz (increased from the sinus rate in 0.5 Hz increments). **A:** Representative cryoinjured heart with graft ROIs circled in red and blue. The dotted white line indicates the border between cryoinjury scar and viable host muscle. Both graft regions were subsequently confirmed to reside within the cryoinjury scar by correlative histology (i.e. graft regions were marked by India Ink, which was later located in histological sections). **B:** Corresponding GCaMP3 fluorescent signals for each graft ROI and the host ECG under each condition. **C:** Plot showing the percentage of visible graft in each animal that showed consistent 1:1 coupling at each examined rate of stimulation. Note that, in 3 of 4 animals, graft regions that were coupled under spontaneous conditions (mean sinus rate of 186 ± 36 bpm) tended to remain coupled with stimulation at rates <5 Hz. A fifth animal showed no host-graft coupling under spontaneous or stimulated conditions. Figure previously published[80].

2.3.3 Voltage mapping of hESC-CM engrafted hearts

As reported[80], we attempted to map the voltage activity of both host and hESC-CM graft tissue to assess the electrical interactions between these tissues. Unexpectedly, we found transplanted hESC-CM grafts to be entirely refractory to labeling with the commonly used voltage dyes RH237 and di-4-ANEPPS (see Figure 2.5), although they did label in vitro (see Figure 2.6).
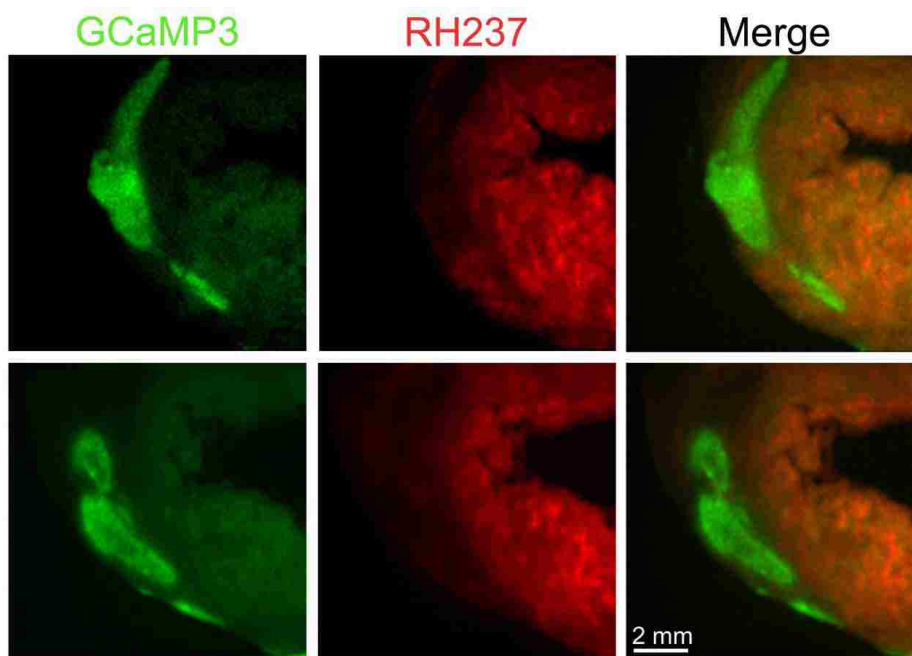
Figure 2.5. RH237 labels host muscle but not hESC-CM graft myocardium. Injured hearts with GCaMP3+ hESC-CM grafts were harvested at 28-days post-transplantation and were loaded with RH237 by retrograde perfusion. The upper and lower panel series show transverse slices from a representative heart, visualized in the green (GCaMP3) and red (RH237) channels. Note that, while host myocardium was strongly stained by RH237, corresponding GCaMP3+ graft regions lacked detectable RH237 signal. Note that this was true for graft regions located both within the cryoinjury scar and surviving host muscle. In the depicted examples, no significant RH237 labeling of graft myocardium was obtained despite perfusion for >30 minutes with 40 µM RH237, while being immersed in dye-containing buffer. Similarly poor graft labeling was obtained when using the structurally unrelated styryl dye di-4-ANEPPS (data not shown). Taken collectively, these data indicate that hESC-CM grafts are refractory to loading with commonly employed potentiometric indicators. Figure previously published[80].
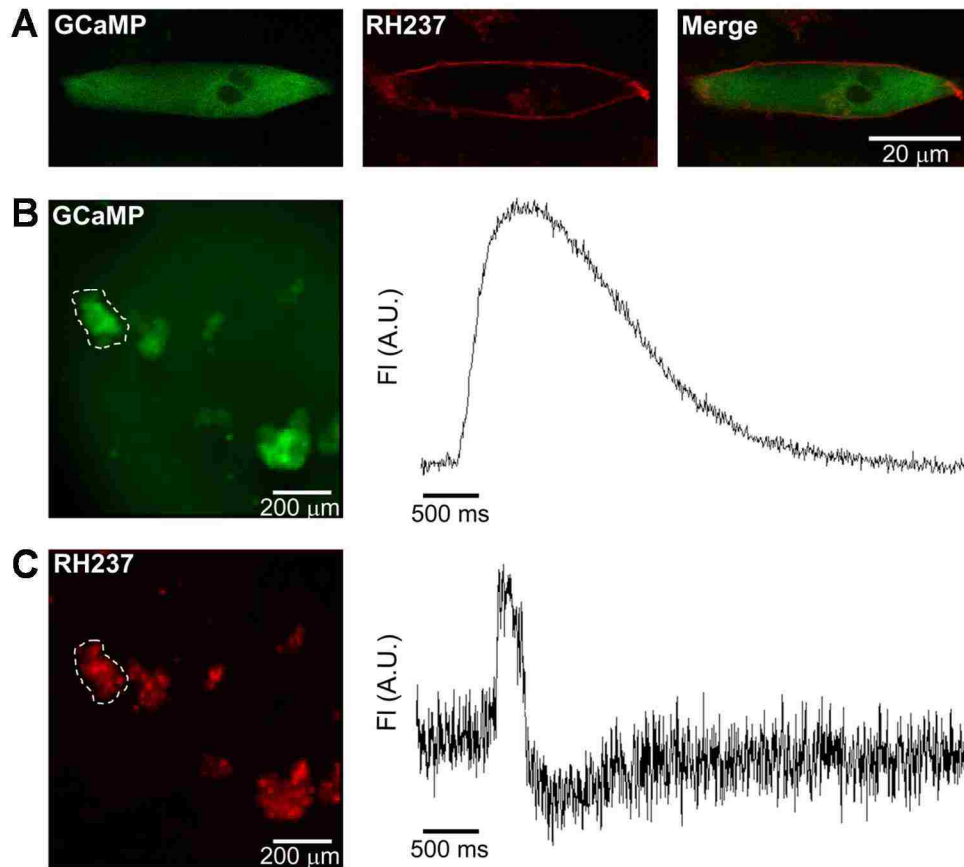
Figure 2.6. GCaMP3+ hESC-CMs can be labeled in vitro with the potentiometric dye RH237. To assess the ability of RH237 to label our cells in vitro, we prepared both GCaMP3+ hESC-CMs plated out at low density and three-dimensional aggregates of GCaMP3+ hESC-CMs formed via suspension culture. Both preparations were then loaded by exposure to 10 µM RH237 for 5 minutes. **A:** Confocal microscopy of a representative GCaMP3+ hESC-CM showing the expected GCaMP3 (green cytoplasmic) and RH237 (membranous) fluorescence. **B-C:** Small, spontaneously contracting aggregates of GCaMP3+ hESC-CMs were labeled with RH237, mechanically arrested with BDM and then visualized using our high-speed EM-CCD imaging system. Individual clusters showed robust GCaMP3 (**B**) and RH237 (**C**) fluorescent transients. Because these recordings were obtained at room temperature, both spontaneous activity and the kinetics of individual transients were relatively slow. Figure previously published[80].

While this lack of hESC-CM labeling in injured hearts may be a result of sluggish perfusion of graft tissue relative to host via relatively nascent graft-supplying host vasculature[111], host tissue labeling was successful. Thus, we compared the electrical properties of cryoinjured hearts with and without hESC-CM grafts (n=6 and n=4,

respectively) after labeling with RH237. We found no significant differences in host

tissue optical action potential amplitudes (see Figure 2.7) or activation kinetics (see

Figure 2.8). Further, in all hearts we observed fast activation in uninjured tissue with a

reduction of kinetics and optical action potential amplitudes in injured tissue.

A: Cryoinjured heart imaged ex vivo with two graft regions in synchrony with host ECG
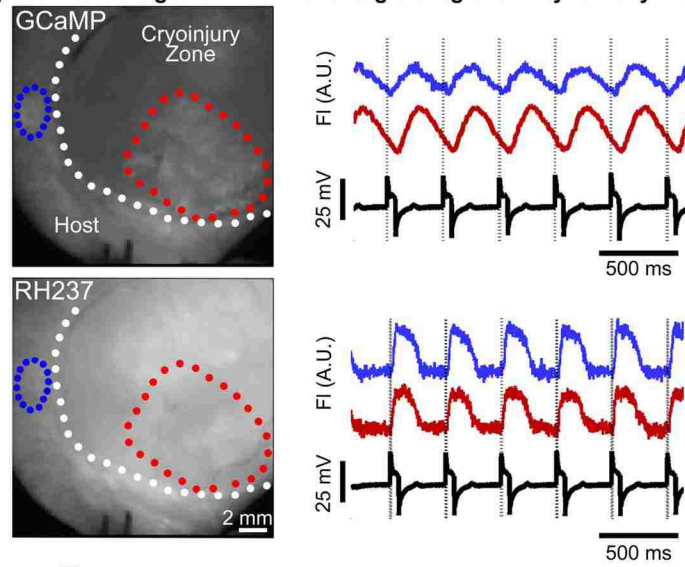
B: Cryoinjured heart imaged ex vivo with two graft regions not in synchrony with host ECG or RH237 signals
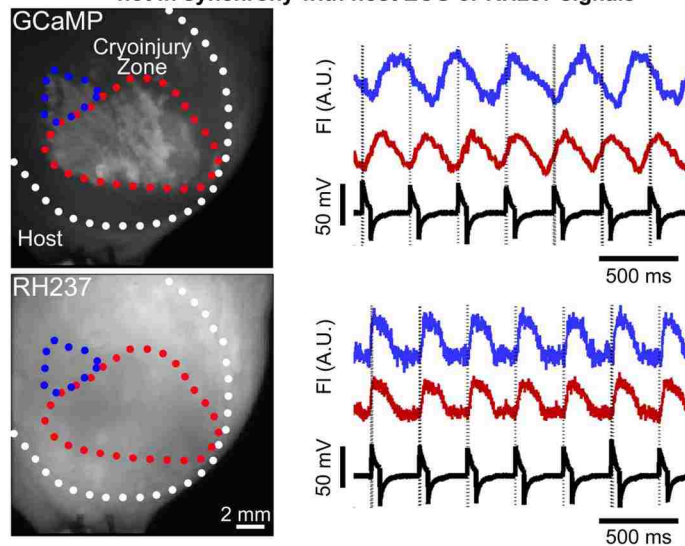
Figure 2.7. Representative imaging of cryoinjured hearts with GCaMP3+ hESC-CM grafts after loading with the voltage dye RH237. **A:** Representative GCaMP3 and RH237 fluorescent images from a cryoinjured heart in which all of the visible GCaMP3+ hESC-CM graft showed 1:1 host-graft coupling. In the still images to the left, the border between cryoinjury scar and viable host muscle is indicated by the dotted white line, while two representative graft ROIs are circled in red (in scar but abutting the border zone) and blue (in adjacent host muscle). As indicated in the traces to the right, both graft ROIs showed GCaMP3 and RH237 fluorescent transients that occurred in a 1:1 correspondence with the QRS complex of the host ECG. **B:** Representative GCaMP3 and RH237 fluorescent images from a cryoinjured heart in which all visible GCaMP3 hESC-CM graft regions were uncoupled from the host. Note that, while GCaMP3 cyclic fluorescent transients in both the red and blue ROIs were uncoupled from the host ECG, RH237 transients from these same areas did coincide with the host QRS. This lack of concordance between the two fluorescent signals implies that the voltage RH237 signal reflects activation of residual host muscle and not graft. Figure previously published[80].
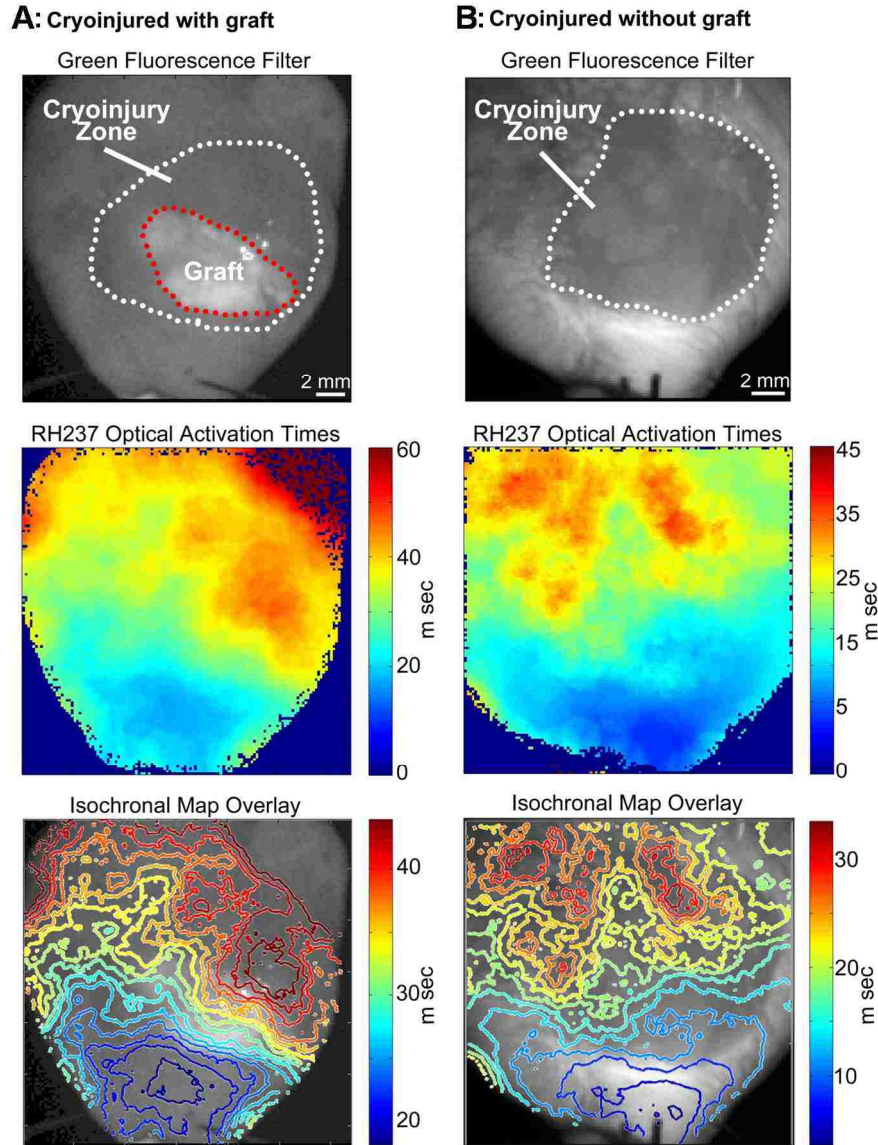
Figure 2.8. Voltage activation maps from cryoinjured hearts with and without GCaMP3+ hESC-CM grafts.
Voltage mapping from representative cryoinjured guinea pig hearts with (**A**) and without (**B**) 28-day old GCaMP3+ hESC-CM grafts. The upper panels show still images acquired on the green channel from each heart, with dynamic GCaMP3 graft and cryoinjury zones indicated by red and white dotted lines, respectively. Note that blebbistatin contributes significant background fluorescence in this channel, which is why the host myocardium also shows significant staining. The middle panels show voltage activation maps for each heart, determined using potentiometric RH237 fluorescent signals detected on the red channel. The lower panels show computer-generated isochronal maps of activation times overlaid on the corresponding green channel images. Note that, as in the two examples, control and engrafted hearts showed similar patterns and kinetics of activation, including more tightly spaced and irregularly contoured isochrones within the injured zone. Our inability to detect any difference between the two groups in these experiments likely reflects the fact that the RH237 signal reported only host electrical activity. Figure previously published[80].

2.4 Summary

As reported[80], here we investigated the electrical integration of hESC-CM grafts in uninjured and recently injured hearts using the same guinea pig subacute cardiac injury model in which we found hESC-CM transplantation protects against arrhythmias and mediates improvements in mechanical function. Importantly, for these studies we utilized hESC-CMs that stably express the fluorescent calcium reporter GCaMP3[97], which provided the first and direct visualization of hESC-CM graft activity after transplantation. Using this novel method, we found that hESC-CM grafts couple with host myocardium 100% of the time in uninjured hearts, however coupling in the injured heart was more variable at ~60%. Coupled hESC-CMs were found to keep pace with host hearts at rates $\geq$ 4 Hz, but showed slower speeds of activation if residing in scar tissue versus uninjured host myocardium. In addition, for the first time we report the inability of conventional voltage dyes to label hESC-CM graft tissue, a discovery enabled by the use of hESC-CMs expressing the graft-autonomous calcium reporter GCaMP3. This limitation aside, this study supports the continued development of hESC-CM-based therapies for the regeneration of injured hearts.

Chapter 3: Electrical Integration of Human Embryonic Stem Cell-Derived Cardiomyocyte Grafts in a Guinea Pig Chronic Infarct Model

3.1 Introduction

As reported in Chapter 2, hESC-CMs successfully engrafted following their direct injection into uninjured and recently injured guinea pig hearts. When we imaged GCaMP3+ hESC-CM grafts in uninjured guinea pig hearts, we found that the graft-derived fluorescent transients always occurred in a 1:1 relationship to the QRS complex of the host electrocardiogram (ECG), indicating seamless host-graft electromechanical integration[80]. On the other hand, when we imaged GCaMP3+ hESC-CM grafts transplanted into hearts 10 days after injury, we observed 1:1 host-graft coupling in only ~60% of hearts, and many of the latter hearts contained both coupled and uncoupled graft regions[80]. While this outcome indicates that we still have more work to do to optimize the integration of stem cell-derived grafts in recently injured hearts, intravital imaging of GCaMP3-expressing grafts provides a tool to assess host-graft integration and to test novel strategies to enhance this parameter.

Importantly, the aforementioned imaging studies were performed using a guinea pig model of subacute cardiac injury, i.e. in animals that underwent cell transplantation at 10 days post-injury. As such, these observations do not necessarily apply to outcomes following hESC-CM transplantation in chronically injured hearts with already established dysfunction and infarct scar tissue. Indeed, our group has already reported important differences in outcomes between these two contexts in the rat and guinea pig

models: hESC-CM transplantation at 4 days and 10 days post-injury, respectively, mediated robust improvements in left ventricular dimensions and fractional shortening, but these beneficial effects were not observed following cell transplantation at 28 days post-injury[81, 82]. In addition, the arrhythmia protection observed with hESC-CM transplantation in the subacute guinea pig injury model did not translate to chronically injured hearts. Hence, we decided that it would be important to specifically revisit electromechanical integration at this same late time-point to gain insights into the differences in outcomes between these injury models, especially since this late timing better reflects the end-stage heart failure patient population in which any novel hESC-derived therapy would likely be tested first.

3.2 Materials and Methods

3.2.1 Production of GCaMP3+ hESC-CMs

Transgenic H7 hESCs (WiCell Research Institute, NIH Stem Cell Registry #hESC-10-0061) and RUES2s (The Rockefeller University, NIH Stem Cell Registry #hESC-09-0013) that stably express GCaMP3[97] were generated by zinc finger nuclease-mediated gene insertion as previously reported in detail by our group.[48, 80, 98] GCaMP3+ H7 and RUES2 hESCs were then expanded and differentiated into cardiomyocytes as described in section 2.2.1.

3.2.2 Cardiac cryoinjury and GCaMP3+ hESC-CM transplantation

All animal procedures adhered to protocols approved by the University of Washington Institutional Animal Care and Use Committee (IACUC) and were conducted

in accordance with federal guidelines. Figure 3.1 depicts the timeline for experiments intended to assess the electrical integration of hESC-CM grafts in the guinea pig model of chronic cardiac injury recently reported by our group[82].
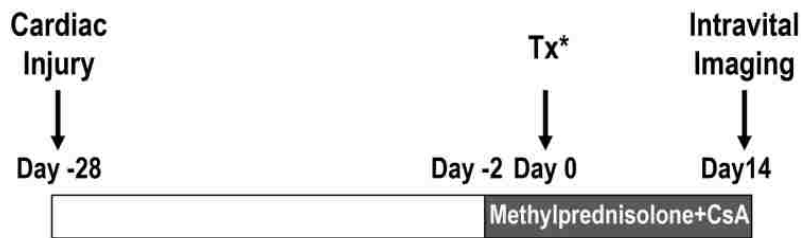
Figure 3.1. Experimental design. To assess the electrical integration of hESC-CM grafts in a chronic injury model, guinea pigs underwent intra-cardiac injection of GCaMP3+ hESC-CMs at 28 days post cryoinjury. To prevent host rejection of xenografts, animals were treated from day -2 relative to cell transplantation until intravital imaging with cyclosporine A (CsA) and methylprednisolone. Intravital imaging was performed at 14 days post-transplantation. Figure previously published[82].

Please see section 2.2.2 for methods pertaining to cardiac cryoinjury and hESC-CM transplantation; however note the difference in timeline per Figure 3.1.

3.2.3 Imaging of GCaMP3+ hESC-CM engrafted hearts

To assess the electromechanical integration of hESC-CMs in chronically injured hearts, intravital imaging of GCaMP3+ hESC-CM grafts was performed on day 14 post-transplantation as previously described[82] and detailed in section 2.2.3. In this study, as in our previous work[80], hearts were mechanically arrested by perfusion with either 2,3-butanedione monoxime (BDM) (n=9) or blebbistatin (n=4) to remove potentially confounding motion artifacts and indirect graft activation through passive stretch. Both mechanical uncouplers functioned to arrest all motion for imaging.

3.3 Results

3.3.1 A subset of hESC-CM grafts in chronically injured hearts are coupled with host myocardium

As directly reported recently[82], to investigate the ability of hESC-CM grafts to couple with host myocardium in hearts with fully established injuries we conducted experiments in which animals were transplanted with GCaMP3+ hESC-CMs at 28 days post-injury (n=13).   We harvested their engrafted hearts at 14 days post-transplantation (corresponding to six weeks post-injury) and then performed intravital imaging during mechanical arrest ex vivo. We then correlated the timing of cyclic GCaMP3 fluorescent transients with QRS complexes of the host ECG and found that only 38% (5 of 13) of recipient hearts contained some regions of visible graft with 1:1 host-graft coupling (see Figure 3.2A-B and 3.2C-D for representative examples of hearts with either coupled or uncoupled GCaMP3+ hESC-CM graft tissue, respectively).
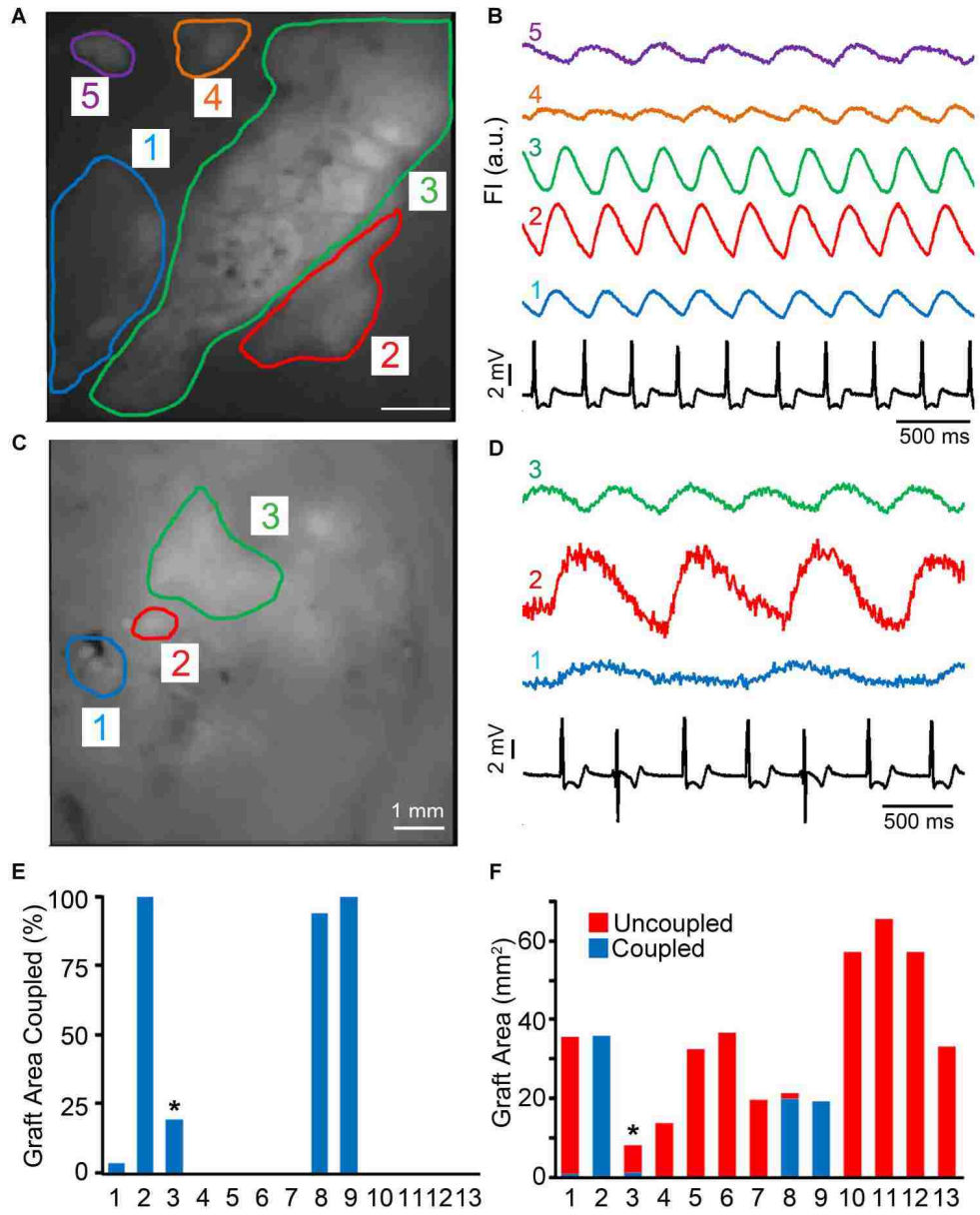
Figure 3.2. hESC-CM graft coupling in chronically cryoinjured guinea pig hearts. Intravital imaging of chronically injured hearts with GCaMP3+ hESC-CM grafts was performed at 14 days posttransplantation. **A:** Still image of the epicardial surface of a representative heart with 5 separate regions of GCaMP3+ graft. **B:** Corresponding GCaMP3 fluorescence traces over time for each region of interest (ROI), as well as the simultaneously recorded host ECG (black trace). Note that transients in ROIs 1 to 4 occurred in a 1:1 relationship with QRS complexes of the host ECG, while uncoupled RO1 5 (purple) activated independently. **C:** Still image from a different heart with 3 graft ROIs, all of which activated independently from the host ECG (**D**). **E:** Percentage of the visible GCaMP3+ hESC-CM graft footprint in each of the 13 hearts analyzed that showed 1:1 coupling with the host ECG. The asterisk indicates the 1 heart in which all of the 1:1 coupled graft resided in healthy host myocardium adjacent to cryoinjury zone. The images depicted in panels A and B were from heart #8. **F:** Area of coupled (blue) and uncoupled (red) GCaMP3+ hESC-CM graft in each of the 13 hearts analyzed. Figure previously published[82].

36

Among these five hearts that had at least some regions of 1:1 coupled graft, four had

coupled graft located within the injury scar, and the extent of coupled graft in these

varied considerably (Figure 3.2E-F). In two hearts, 100% of the visible graft area was

coupled with the host ECG, while others had 94% and only 3% coupled graft. A fifth

heart had hESC-CM graft located both within the injury scar and the viable host

myocardium adjacent to the border zone; and, in this case, 1:1 coupled graft was limited

to the latter area (accounting for 19% of the total graft footprint). Interestingly, the

hearts described above with host-graft coupling were all recipients of H7-derived

GCaMP3+ hESC-CM grafts (hearts 1-9). Hearts transplanted with RUES2 derived

grafts (hearts 10-13) showed no areas of host-graft coupling.

During these imaging studies, the mean R-R interval of the host ECG measured

368 +/- 19 ms. Uncoupled graft regions fired rhythmically but varied widely in terms of

their periodicity, and their activation did not occur in any obvious relationship to the host

ECG (i.e. no 1:2, 1:3 or higher order coupling was detected). Finally, although these

quantitative analyses were performed on mechanically arrested hearts, GCaMP3 hESC-

CM grafts displayed qualitatively similar behavior prior to motion arrest except as noted

in section 3.3.2 below.

3.3.2 BDM can negatively affect the electrical activity of uncoupled hESC-CM grafts in chronically injured hearts

We observed apparently sporadic and rapid bouts of GCaMP3+ hESC-CM graft

activation in 2 of the 14 engrafted hearts imaged. Upon further examination, however,

we found this abnormal graft activity to be associated with the administration of the

mechanical uncoupling agent BDM. Figure 3.3 details this finding, which presented as

a general reduction in graft activity within minutes of perfusing BDM-containing buffer ex

vivo. Concerned with this apparent reduction in graft activity, which in both cases was

only present in hearts with completely uncoupled hESC-CM grafts to begin with, we

closely examined all other 7 of the 9 hearts mechanically arrested with BDM but found

no such adverse effects. Thus, while this is the first instance of directly recorded off-

target effects from BDM on the electrical behavior of transplanted hESC-CM grafts, and

no loss of host-graft electrical coupling was observed with BDM use, we standardized

on the alternative mechanical uncoupling agent blebbistatin for the remaining hearts of

this study. Reassuringly, no such effects were found with the use of the blebbistatin

(n=4).
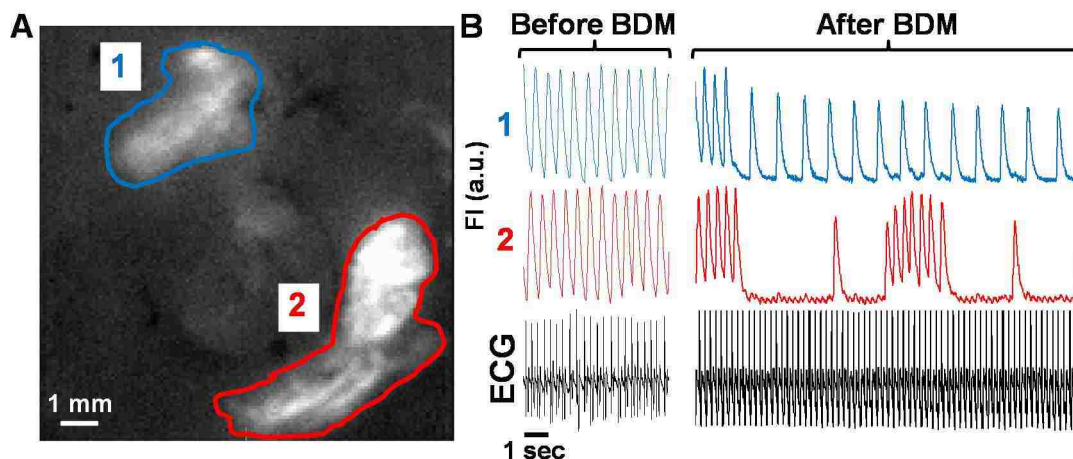
Figure 3.3. BDM can negatively affect the electrical activity of uncoupled hESC-CM grafts. A: Epicardial stilll image of one of the two hearts in this study that displayed reduced graft electrical activity after BDM. **B:** Corresponding graft ROI GCaMP3 fluorescence traces over time immediately before and three minutes after the addition of BDM to the Langendorff perfusate ex vivo. Before BDM both uncoupled graft regions exhibited typical cyclic behavior; after BDM both graft ROIs showed reduced electrical activity. Host electrical activity was not affected in this instance (see simultaneously recorded ECG in black trace).

3.4 Summary

As recently reported[82], here we describe the first study to investigate the electrical integration of hESC-CM grafts in injured hearts using a chronic cardiac injury model. In this work, we found that hESC-CMs reliably formed implants of human myocardium within the scarred injury zone, but the electrical integration of hESC-CM grafts in chronically injured guinea pig hearts was more limited than we had previously found to be the case for equivalent grafts in more recently injured hearts[80]. While this reality underscores the critical need for new strategies to improve the electrical integration of hESC-CM grafts in the end-stage failing heart, our report does describe imaging tools and an animal model that should be useful in the testing of such interventions. Further, our finding that the mechanical uncoupling agent BDM can adversely affect the electrical behavior of transplanted hESC-CM grafts gives a word of caution to the field as to the potential off-target effects of commonly used tools employed in ex vivo cardiac imaging.

Chapter 4: Optical Mapping of Human Embryonic Stem Cell-Derived Cardiomyocyte Graft Electrical Activity in Injured Hearts

4.1 Introduction

Human embryonic stem cells (hESCs) have a number of potentially useful properties for the repair of infarcted hearts, including tremendous capacity for expansion in vitro and the ability to differentiate into phenotypically unambiguous cardiomyocytes[51, 53, 56, 60-62, 112, 113]. The transplantation of hESC-derived cardiomyocytes (hESC-CMs) has been shown to partially remuscularize injured hearts and to mediate beneficial effects on contractile function in mouse, rat and guinea pig models of myocardial infarction[47, 76, 77, 80-82, 114]. Our group has also shown that these cells form implants of human myocardium that are capable of at least partial electrical coupling and synchronous contraction with host myocardium during systole, a sine qua non of cardiac regeneration[80, 82]. However, perhaps reflecting the immature phenotype of hESC-CMs and the significant electrophysiological mismatch between graft and host myocardium, we found that hESC-CM transplantation in a non-human primate infarct model results in transient bouts of non-lethal ventricular tachycardia[115]. Given that other concerns about teratoma formation, scalability and immune rejection did not prove to be a problem in the latter study, this phenomenon of graft-related arrhythmias has arguably emerged as the greatest barrier to the successful development of hESC-CM-based cardiac therapies. To address this issue, the field must develop new, more powerful tools to

investigate the electrophysiological properties of hESC-CM engrafted hearts and to test strategies to improve their electrical stability.

Our group has previously reported one approach by which we obtained useful insights into the electrical integration of hESC-CM grafts in normal and injured hearts[80]. For this work, we generated transgenic hESC-CMs that stably expressed the calcium-sensitive fluorescent protein GCaMP3 and exhibited robust fluorescent transients with each contractile cycle[97, 116, 117]. We transplanted these GCaMP3+ hESC-CMs into guinea pig[80, 82] and non-human primate hearts[115], which were then harvested at various time-points post-transplantation and imaged ex vivo. By correlating the graft-autonomous GCaMP3 fluorescent signal with the host ECG, we were able to determine what fraction of the GCaMP3+ hESC-CM graft was electrically active and/or coupled with the ventricular myocardium of the recipient. In the guinea pig model, we found that 100% of hESC-CM grafts in uninjured hearts were reliably 1:1 coupled with host myocardium, but outcomes were more complicated following transplantation into injured hearts. When we transplanted GCaMP3+ hESC-CMs in a subacute cardiac injury model (injecting cells at 10-days post-injury), we found that ~60% of engrafted hearts later showed some degree of 1:1 host-graft coupling[80]. Electromechanical integration was even worse when cells were injected into a chronic injury model (at 28-days post-injury) with better established fibrosis and contractile dysfunction, in which case only ~38% of recipient hearts showed 1:1 host-graft coupling[82].

While this approach based on GCaMP3 imaging alone provided crucial insights into the integration of hESC-CM grafts, it does have a number of important limitations.

First, the rise in intracellular calcium is delayed relative to membrane depolarization and GCaMP3 is a particularly slow calcium sensor[116], so GCaMP3 fluorescence transients significantly lag actual electrical activation in hESC-CMs. Second, GCaMP3 imaging provides no information as to electrical activation in host myocardium, precluding study of the complex spatiotemporal electrical interactions between graft and host tissue. One attractive route for overcoming these limitations would be to apply optical voltage mapping, a powerful tool that has provided critical insights into normal cardiac propagation and mechanisms of arrhythmogenesis[118-124]. This technique involves labeling hearts with a fluorescent voltage-sensitive dye, imaging the resultant dye-derived optical action potentials (oAPs) with a high-speed camera or photodiode array, and post-processing of this imaging data to extract electrophysiological parameters of interest. Critical parameters including the pattern of electrical activation, action potential duration (APD), and tissue conduction velocity (CV) can all be acquired using this technique, making optical mapping an attractive tool for evaluating cell-engrafted hearts. Indeed, there have been previous attempts to apply this technology to study the electrical activity of hESC-CM grafts after transplantation into uninjured hearts[83, 96]. However, as is further detailed below, our group has recently shown that hESC-CM grafts are not efficiently labeled by conventional voltage-sensitive dyes and that all observed oAPs actually result from host rather than graft tissue[80].

We report here our efforts to overcome these limitations using a novel approach that involves the simultaneous imaging of GCaMP3, the aforementioned genetically-encoded calcium-sensitive fluorescent protein that functions as a graft-autonomous reporter of graft activation, and di-2-ANEPEQ, a water-soluble voltage dye that we show

labels both host and graft tissue. While this approach presents its own challenges, it nonetheless allows one to reliably distinguish between host- and graft-derived oAPs, and we use it here to obtain previously-unavailable electrophysiological measurements of hESC-CM graft tissue in injured hearts.

4.2 Materials and Methods

4.2.1 Production of GCaMP3+ hESC-CMs

Transgenic H7 hESCs (WiCell Research Institute, NIH Stem Cell Registry #hESC-10-0061) and RUES2s (The Rockefeller University, NIH Stem Cell Registry #hESC-09-0013) that stably express GCaMP3[97] were generated by zinc finger nuclease-mediated gene insertion as previously reported in detail by our group.[48, 80, 98] GCaMP3+ H7 and RUES2 hESCs were then expanded and differentiated into cardiomyocytes as described in section 2.2.1.   GCaMP3+ hESC-CM purity measured 84±2% by troponin I flow cytometry based on this protocol.

For patch-clamp and in vitro imaging experiments involving isolated hESC-CMs, cultures were enzymatically dispersed on day 20 to single-cells and replated onto gelatin- and polyethylenimine-coated 23 mm fluorodishes at $2x10^5$ hESC-CMs per fluorodish as previously described[66]. For other in vitro imaging experiments, we prepared ~300 µm diameter aggregates of hESC-CMs. For this, we enzymatically dispersed and replated day 20 hESC-CM cultures into the commercially available AggreWell 800 system (StemCell Technologies, Vancouver, BC, Canada) at $3.6x10^6$ hESC-CMs per well per manufacturer recommendations.

4.2.2 Spectral analysis of GCaMP3 and di-2-ANEPEQ in hESC-CMs

We used spectrofluorimetry and spectral confocal microscopy to define the excitation and emission spectra of GCaMP3 and di-2-ANEPEQ in intact cardiomyocytes. WT and GCaMP3+ hESC-CMs were prepared as described above, and, where appropriate, cells were stained by incubation with di-2-ANEPEQ (5 µM) at 37°C for 10 minutes, after which they were spun down, switched to dye-free buffer and used immediately. For spectrofluorimetry experiments, we employed a Spectra Max M2 microplate reader (Molecular Devices, Sunnyvale, CA, USA) and 96-well plates loaded with $2x10^6$ hESC-CMs per well in a 200 µL volume. Absorbance was measured from 350 to 700 nm in 5 nm steps, while emission was determined from 500 to 800 nm in 5 nm steps following excitation at 480 nm (with a 495 nm cutoff filter). Confocal experiments were performed using a Zeiss LSM510-Meta confocal microscope (Carl Zeiss GmbH, Gottingen, Germany) operated in lambda-scanning mode, with excitation set to 488 nm and emission detected from 502 to 748 nm in 11 nm steps (the smallest interval available). Where indicated below, we also simultaneously recorded GCaMP3 and di-2-ANEPEQ fluorescence transients by confocal microscopy in time-series mode using 505-530 nm and 650-754 nm bandpass filters, respectively.

4.2.3 Cardiac cryoinjury and hESC-CM transplantation

All animal procedures adhered to protocols approved by the University of Washington Institutional Animal Care and Use Committee (IACUC) and were conducted in accordance with federal guidelines. Please see sections 2.2.2 for methods pertaining to cardiac cryoinjury and hESC-CM transplantation; note $1x10^8$ GCaMP3+ RUES2 or

H7 hESC-CMs were transplanted at either 10 days (subacute injury model per Figure 2.1) or 28 days (chronic injury model per Figure 3.1) post-injury.

4.2.4 Simultaneous GCaMP3 and di-2-ANEPEQ imaging of hearts ex vivo

To optically map GCaMP3+ hESC-CM engrafted hearts, we harvested hearts at two weeks post-transplantation, which were then mounted on a modified Langendorff apparatus and perfused with the following buffer (in mM): 25.0 NaHC0$_3$, 1.2 MgSO$_4$, 4.7 KCl, 118.0 NaCl, 1.2 KH$_2$PO$_4$, 11.0 glucose, 1.0 Na-pyruvate and 1.8 CaCl$_2$, bubbled with 95% O$_2$/5% CO$_2$, pH adjusted to 7.35, and warmed to 37°C. To arrest motion during ex vivo imaging, this perfusate was supplemented with blebbistatin (10µM, Cayman Chemical, Ann Arbor, Michigan, USA). For a small subset of initial experiments, we instead used 2,3-butanedione monoxime (20mM, Sigma-Aldrich, St. Louis, Missouri, USA) to avoid the spectral interference of blebbistatin (which emits strongly in the 500-530 nm range) when assessing the colocalization of voltage dyes and GCaMP3+ hESC-CM grafts. To label hearts with the conventional lipophilic voltage dye RH237, hearts were either perfused with RH237-containing buffer (40µM) for 30 minutes or bolus-loaded with RH237 (80µM in 5 ml volume) over 5 minutes. Identical results were obtained with either method. To label hearts with the water-soluble di-2-ANEPEQ (Assay Biotechnology, Sunnyvale, California, USA), hearts were continuously perfused with dye-containing buffer (20µM) via a recirculation loop.

Please see Figure 4.1 for a detailed schematic of the imaging system used to acquire GCaMP3 and voltage dye (RH237 or di-2-ANEPEQ) signals. In brief, epicardial fluorescent transients were acquired using a modified epifluorescence dissecting

microscope (Nikon SMZ1000, Kawasaki, Kanagawa, Japan) outfitted with a 0.5x objective (N.A. 0.05, W.D. 123 mm). Excitation light was provided by an external mercury lamp (EXFO X-Cite 120W, Mississauga, Ontario, Canada) and filtered to 450-490 nm. Emitted light was passed to a dichroic system (Photometrics DC2 dual-channel splitter, Tucson, Arizona, USA) outfitted with a 565nm dichroic mirror to separate GCaMP3 and voltage dye signals. The GCaMP3 signal ("green" channel) was bandpass-filtered to 500-530 nm, while the voltage dye signal ("red" channel) was longpass-filtered at >716 nm for RH237 or >650 nm for di-2-ANEPEQ. These signals were simultaneously detected by two high-speed, high-sensitivity EM-CCD cameras (Andor iXon 860 EM-CCDs, Andor, Belfast, United Kingdom) operated via Andor Solis software. The field of view with this optics was approximately 2.3 cm x 2.3 cm.
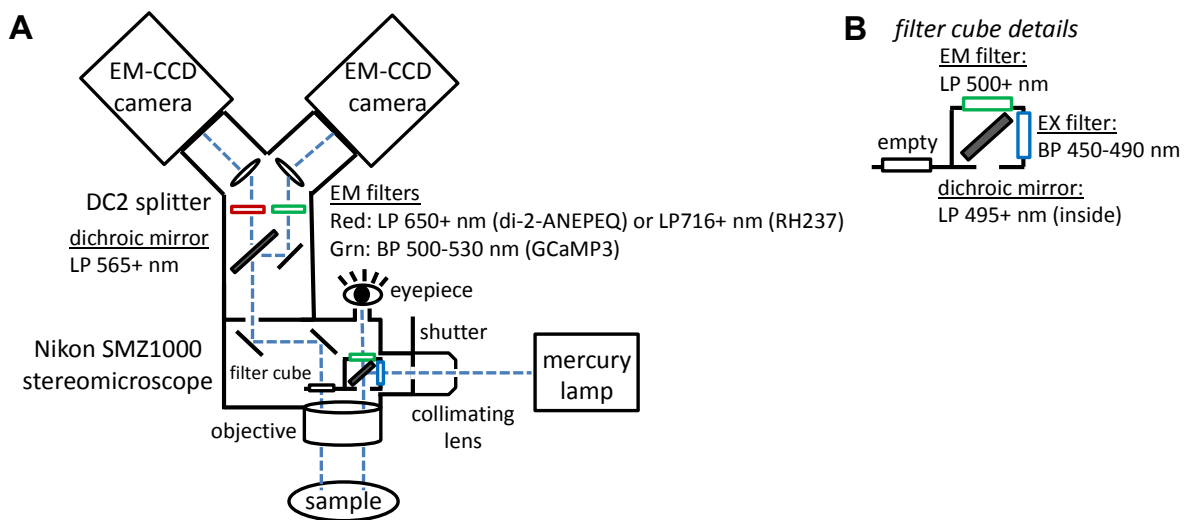
Figure 4.1. High speed dual channel imaging system. Schematic of our dual EM-CCD-based imaging system (**A**) with details of the filter set inside the stereomicroscope base (**B**). In brief, excitation light was collimated and bandpass filtered to 450-490 nm before being reflected onto Langendorff-mounted hearts. Emitted light was collected and split into the "green" and "red" channels first by a 565 nm longpass dichroic mirror inside the DC2 dual-channel splitter. The "green" channel (i.e. GCaMP3) signal was then further bandpass filtered to 500-530 nm before being detected by an EM-CCD camera, while the "red" channel (i.e. voltage dye) signal was longpass filtered at 650+ nm for di-2-ANEPEQ imaging or 716+ nm for RH237 imaging before being detected on a separate EM-CCD camera operated simultaneously.

46

During these ex vivo imaging experiments, a pseudo-ECG was acquired using a PowerLab 430 Data Acquisition System (Model ML866) outfitted with a bioamplifier (Model ML136, ADInstruments, Colorado Springs, Colorado, USA), with the resultant signals analyzed and aligned with camera outputs via Labchart software. For recordings obtained under paced conditions, we used the PowerLab 430 system connected to a pencil point concentric electrode (325 µm outer diameter stainless steel, 125 µm diameter inner iridium, FHC, Bowdoin, Maine, USA) placed into the LV apex. For a subset of experiments, we obtained simultaneously intracellular voltage recordings via sharp electrodes, using methods adapted after Omichi et al[125]. For this, we impaled host or graft myocardium with pure iridium-tipped (1-2 µm diameter, 5×10^6 ohm) electrodes coated with parylene-C insulation (World Precision Instruments, Shanghai, China). The resultant signals were amplified using a high-impedance intracellular electrometer with variable-capacity neutralization (Warner Instruments IE-251A intracellular electrometer, Hamden, Connecticut, USA) and then fed into the PowerLab system.

Please see Figure 4.2 for a timeline depicting the sequence of procedures during a typical imaging experiment involving the simultaneous acquisition of GCaMP3 and di-2-ANEPEQ signals. For this, we typically harvested and cannulated the heart and then perfused the organ for ~10 minutes with dye- and blebbistatin-free buffer to obtain stable electrical activity. We then switched the heart to blebbistatin-containing buffer to obtain mechanical arrest (typically requiring ~10 minutes) before turning on a recirculating loop for continuous perfusion with both dye- and blebbistatin-containing buffer (for at least 30 minutes). In most cases, the heart was then switched-back to

dye-free buffer to determine the kinetics of dye washout, followed by serial wash-in and washout experiments as indicated.
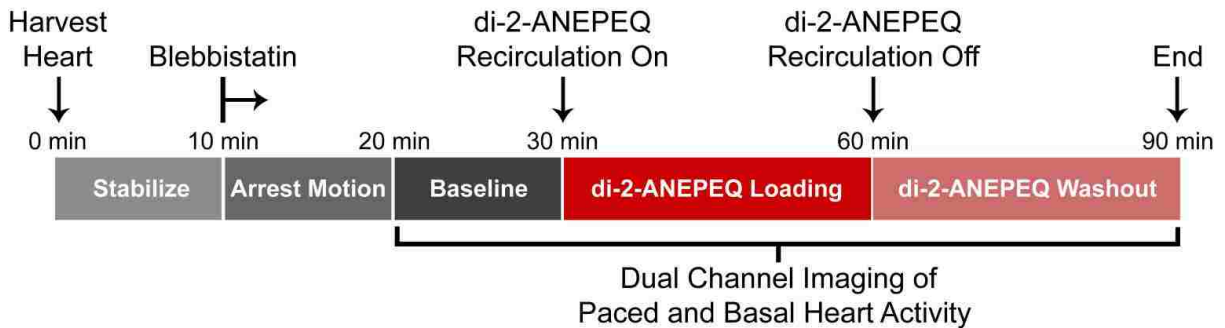
Figure 4.2. Protocol for imaging di-2-ANEPEQ in hearts ex vivo. Overview of the experimental protocol used to image hearts ex vivo with di-2-ANEPEQ. First, hearts were rapidly excised, mounted ex vivo on a modified Langendorff apparatus and allowed to stabilize electrically (~10 minutes). Next, hearts were treated with blebbistatin in the perfusate to arrest motion (~10 minutes) before recordings were taken prior to the administration of di-2-ANEPEQ ("baseline", ~10 minutes). Then, recordings were taken while di-2-ANEPEQ- and blebbistatin-containing buffer was recirculated through the heart ("di-2-ANEPEQ loading", ~30 minutes), as well as after the switch back to dye-free but blebbistatin-containing buffer ("di-2-ANEPEQ washout", ~30 minutes). During all periods, recording were taken under either sinus rhythm or paced conditions.

4.2.5 GCaMP3 and di-2-ANEPEQ imaging analysis

We generated custom Matlab (MathWorks) scripts to analyze imaging data (see Chapter 5). In brief, time-synchronized fluorescent signals and ECG recordings (from Andor Solis and LabChart software packages, respectively) were imported into the Matlab environment, and the former were subjected to the following sequence of initial processing steps. First, the imaging data was masked to exclude signals outside the heart, then spatial, low pass frequency, and temporal filters applied to improve signal quality. The results of filtering were then assessed at the single pixel level before removing signal drift. Next, the data was inverted for voltage dye-signals (which exhibit

48

a decrease in fluorescence intensity upon tissue depolarization), and a pseuodocolored movie of activation based on the z-score of each pixel through time played to screen for the easy identification of active graft regions. Next, we manually selected regions of interest (ROIs) and plotted their mean fluorescence intensity over time (with signals normalized to that of the region with the largest range in hearts with multiple ROIs). Activation maps of tissue were created by determining the timepoint at which the maximum slope in fluorescence occurs between the start and peak of a single activation. To aid in this determination, further drift removal, normalization, and careful utilization of a Savitzky-Golay filter were performed. CVs were then determined from activation maps, given the known field of view (FOV). Optical action potential durations (oAPDs) and cycle lengths were measured using AndorSolis software after selecting a 10x10 pixel ROI and manually determining the start and end of each action potential from the region's mean fluorescence intensity through time. The oAPD for a single graft ROI was then assigned as the mean of 30 measured oAPDs. To rate-correct graft-derived oAPDs, we utilize Fridericia's formula[126], where the corrected oAPD equals the cycle length divided by the cube root of the measured oAPD.

4.2.6 In vitro hESC-CM aggregate and single cell imaging and analysis

In addition to imaging oAPs of GCaMP3+ hESC-CM grafts in injured hearts ex vivo, we measured the oAPs of WT and GCaMP3+ hESC-CMs derived from both the RUES2 and H7 lines in vitro. For this we generated hESC-CM aggregates to replicate the bulk electrical behavior of hESC-CM grafts, then separately measured the electrical activity of individual hESC-CMs plated at low density (prepared as described above).

To assess the oAPDs of hESC-CM aggregates, 8 days after plating into Aggrewells formed aggregates were loaded with di-2-ANEPEQ (20μM) for 5 minutes at 37°C, then dispersed and transferred into the center of a 23mm well Fluorodish for imaging in dye-free buffer maintained at 37°C. For imaging, the 0.5x objective of our ex vivo imaging system was replaced with a 1x objective (N.A. 0.1, W.D. 70 mm) for an overall FOV of 4 mm x 4 mm. This magnification allowed for the high-throughput acquisition of optical voltage transients from many aggregates at once without the need for a mechanical uncoupling agent, as any small motion due to aggregate beating was not discernible at this zoom. Aggregates were field stimulated via a custom-made parallel 0.25 mm diameter silver wire electrode using the same PowerLab system used in ex vivo imaging, incrementally from 0.1 to 0.5 Hz by 0.1 Hz steps, then at 1 Hz with pulse duration set at 5 ms and voltage from 6 to 10 V. Aggregate oAPDs were measured using AndorSolis software after selecting a ROI per single aggregate and manually determining the start and end of each action potential from the aggregate's mean fluorescence intensity through time. The oAPD for a single aggregate was then assigned as the mean of >5 measured oAPDs. Group oAPDs were then determined from >12 aggregates spanning 3 biological replicates at each 0.5 and 1Hz.

To assess the oAPDs of individual hESC-CMs, cells were loaded with RH237 (2μM) for 5 minutes at 37°C, then imaging in dye-free buffer maintained at 37°C via an Andor iXon 860 camera mounted to an Olympus IX71 inverted microscope (Olympus, Shinjuku-ku, Tokyo, Japan). Fluorescent excitation was bandpass-filtered to 532-588 nm, while RH237-derived fluorescence emission was bandpass-filtered to 608-683 nm. 5 FOVs were imaged per dish, and the oAPD for a single hESC-CM determined as the

mean of >4 measured oAPDs using AndorSolis. Group oAPDs were then determined

from >5 hESC-CMs. Last, Fridericia's rate correction was applied to all measured

action potentials, the same as was done for hESC-CM graft oAPDs measured ex vivo.

4.2.7 Histology of GCaMP3+ hESC-CM engrafted hearts to assess structure and gap junction expression

Histological endpoints were obtained using methods previously detailed by our

group[47, 74, 81]. In brief, hearts were evaluated by histochemical stains (hematoxylin-

eosin, picrosirius red, masson's trichrome), DAB immunocytochemistry and/or

immunofluorescence. For immunostaining, we used primary antibodies against GFP

(rabbit polyclonal), N-cadherin (mouse monoclonal), Cx43 (obtained from A. Boynton[127],

and Cx43IF1 raised against amino acids 360-382[128]), and β-myosin heavy chain (clone

A4.951), as well as species-specific biotinylated (Vector Labs) or fluorescent (Life

Sciences) secondary antibodies.

Structural comparisons were measured from slides immunocytochemically

stained for GFP and counterstained with Picrosirius Red. These slides were digitally

scanned and a blinded observer manually quantified graft area, scar area, LV area, and

any perimeter contact between host and graft tissues. hESC-CM graft cadherin and

Cx43 expression were assessed from scanned images of immunocytochemically

stained slides by a blind observer. Immunofluorescence was imaged using a Zeiss

LSM 780 NLO confocal microscope (Jena, Germany) and processed with Image J (NIH

Image).

4.2.8 hESC-CM L-type calcium channel current recording and analysis

We compared L-type calcium current ($I_{Ca,L}$) in WT and GCaMP3+ hESC-CMs using perforated patch-clamp techniques previously reported by our group[63]. In brief, $I_{Ca,L}$ was elicited and recorded from individual hESC-CMs at 0.33 Hz using a HEKA EPC-10 patch-clamp amplifier (HEKA, Lambrecht, Germany) operated in voltage-clamp mode. All experiments were performed at 37°C, and hESC-CMs were perfused by the following solution (in mM): 140.0 NaCl, 5.0 CsCl, 2.0 $CaCl_2$, 1.0 $MgCl_2$, 10.0 HEPES, 10.0 Glucose, and pH = 7.4 with NaOH. The pipette solution was as follows (in mM): 130.0 CsCl, 10.0 TEA-Cl, 5.0 Mg-ATP, 10.0 HEPES, 10.0 Glucose, and pH = 7.2 with CsOH. To inactivate the fast sodium current, cells were depolarized from a holding potential of -60 mV and subjected to a 50 ms "pre-pulse" to -40 mV. Next, to activate $I_{Ca,L}$, they were depolarized from -40 mV to a range of voltages from -30 mV to +60 mV at 10 mV increments. To compare $I_{Ca,L}$ inactivation kinetics in WT and GCaMP3+ hESC-CMs, we fitted the decay of currents elicited at 0 mV using one- and two-phase exponential decay equations. The equation models were compared using an *F*-test, resulting in the two-phase decay being the best fitting equation[129, 130].

4.2.9 Statistical analysis

GraphPad Prism (GraphPad Software, La Jolla, California, USA) was used to perform all statistical analyses. All data groups were first checked for normality by submission to the D'Agostino-Pearson omnibus test, and parametric data herein presented as mean±standard error of the mean. Two-sample comparisons were made using a 2-tailed Student's t-test, paired or unpaired as appropriate with Welch's

correction for unequal variances as necessary. Multiple comparisons were made using 1-way Anova with Tukey's multiple comparison test correction. A p value less than 0.05 was considered significant, and asterisks (*) used in figures to indicate a significant difference between groups as specified.

4.3 Results

4.3.1 Conventional, lipophilic voltage-sensitive dyes do not label hESC-CM graft tissue, but the water-soluble dye di-2-ANEPEQ does label graft

Our group has previously reported that when hESC-CM-engrafted hearts are stained with commonly employed voltage-sensitive fluorescent dyes (e.g. RH237, di-4-ANEPPS), these dyes label host but not graft tissue[80]. To confirm this earlier finding, we transplanted GCaMP3+ hESC-CMs into guinea pig hearts at 10 days post-injury, harvested the engrafted hearts at two weeks post-transplantation, and then imaged them ex vivo after perfusion with the dye RH237 (n=3). For these imaging experiments, we used a custom-built, dual-channel, EM-CCD-based system (Figure 4.1) to simultaneously acquire the RH237 (red channel) and GCaMP3 (green channel) signals. As in our previous work[80], we consistently encountered hearts in which GCaMP3 fluorescence transients activated independently from host myocardium, and yet RH237-derived oAPs from these same graft regions occurred synchronously with the QRS complex of the host ECG (Figure 4.3A-B). Hence, while the genetically-encoded, graft autonomous indicator of graft activation (GCaMP3) proves that these grafts were in fact uncoupled from the host, the simultaneously acquired voltage dye signal could be interpreted as indicating 1:1 host-graft coupling. We were able to account for these

apparently discordant results by transversely sectioning these hearts after dye labeling

and examining them on a dissecting fluorescence stereomicroscope. While all of the

examined hearts showed strong, uniform staining of host myocardium by RH237,

GCaMP3+ graft regions were entirely devoid of RH237 fluorescence (Figure 4.3C).

Taken collectively, these observations support our earlier conclusion that ostensibly

graft-derived RH237-derived oAPs from such hearts are factitious, and that these

signals instead arise from subendocardial host tissue located deep to the graft that

shine through to the epicardial surface[80].

hESC-CM grafts known to have an immature, sinusoidal-like vascular supply[111]

so we hypothesized that lipophilic dyes such as RH237 may fail to stain hESC-CM graft

tissue simply because the dye partitions fully into host tissue before ever reaching the

relatively poorly-perfused graft. If this is correct, we predicted that better labeling of

hESC-CM graft tissue might be obtained by switching to the use of a water-soluble

voltage-sensitive dye. Water-soluble dyes have been used less commonly in optical

mapping experiments because they have to be constantly included in the perfusate, but

we predicted that this situation might be advantageous for our own application because

it would allow the dye to penetrate through to the graft. To test this, we prepared

equivalently injured hearts with GCaMP3+ hESC-CM grafts and then perfused them

with the water-soluble voltage di-2-ANEPEQ (n=3). In contrast to our prior experience

with RH237, when these hearts were transversely sectioned and examined, we

observed strong, uniform staining of both host and GCaMP3+ graft tissue by di-2-

ANEPEQ (Figure 4.3D).
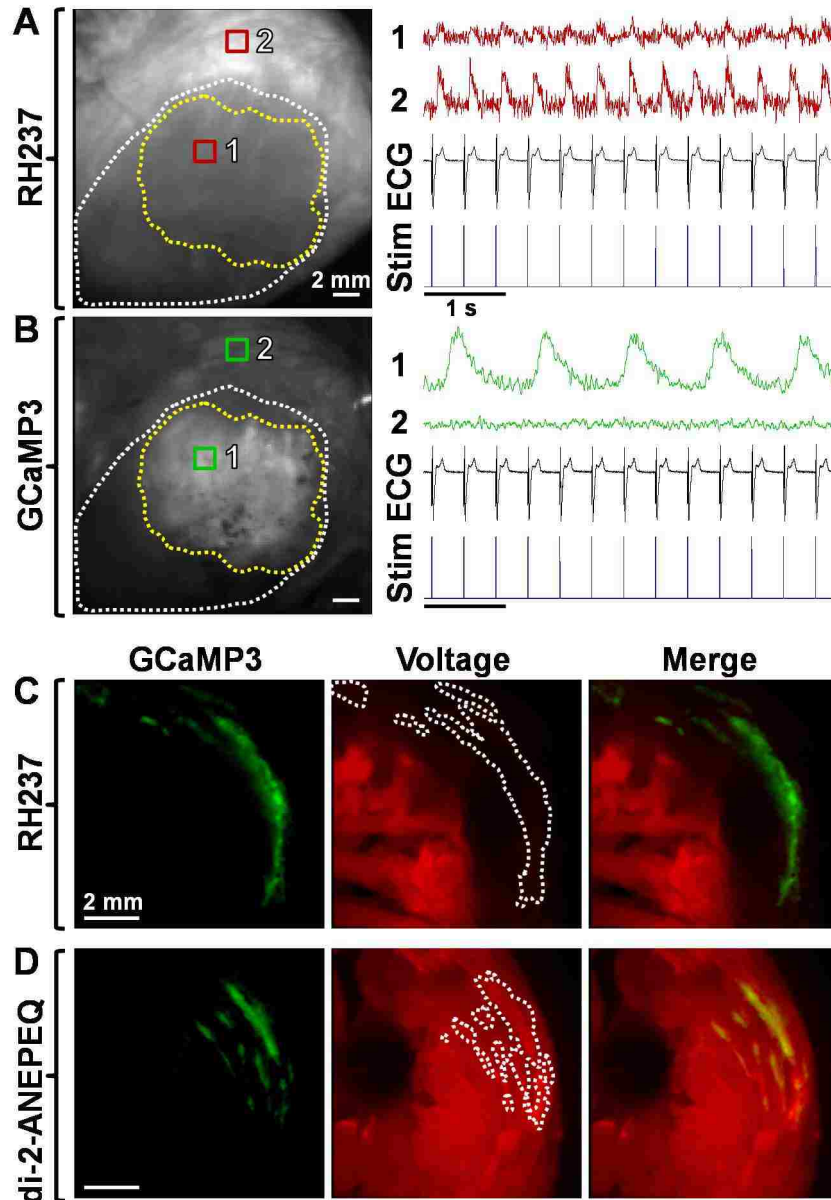
Figure 4.3. Conventional voltage dyes do _not_ label hESC-CM graft tissue. Still images and corresponding fluorescence traces from two regions of interest (ROIs) on the epicardial surface of a representative injured heart with GCaMP3+ hESC-CM graft, as acquired on the "red" RH237 (**A**) and "green" GCaMP3 (**B**) channels. Please note that ROI1 is located in hESC-CM graft tissue (yellow dotted line), while ROI2 is located in viable host myocardium outside of the cryoinjury zone (white dotted line). While RH237-derived optical action potentials (oAPs, red traces) from both ROIs occurred in 1:1 synchrony with QRS complexes of the simultaneously-acquired host ECG (black) and applied stimulus (blue), GCaMP3 fluorescence transients (green traces) from graft RO1 clearly activated independently from host myocardium. **C:** When this heart was transversely sectioned, slices showed uniform staining of host myocardium with RH237 (red fluorescence), but GCaMP3+ graft tissue (green) was completely devoid of RH237 staining. **D:** By contrast, when an equivalently injured and transplanted heart was sectioned after perfusion with the water-soluble voltage dye di-2-ANEPEQ, comparable dye staining of host and graft tissue was observed.

55

4.3.2 Water-soluble di-2-ANEPEQ can be spectrally separated from the graft-autonomous calcium reporter GCaMP3 and reliably reports myocardial electrical activity

While the preceding observations suggest that di-2-ANEPEQ might be useful as a voltage reporter in hESC-CM graft tissue, additional characterization of the dye was required before testing our strategy of using dual-imaging of di-2-ANEPEQ and GCaMP3 fluorescent signals to map electrical activity in engrafted hearts. We began with studies to ensure good spectral separation between the two fluorophores, including determination of the excitation and emission spectra of di-2-ANEPEQ by spectrofluorimetry (Figure 4.4A). Next, we used confocal emission fingerprinting to precisely define the emission spectra of GCaMP3+ and di-2-ANEPEQ-loaded hESC-CMs, both at rest and during depolarization (Figure 4.4B-D). In brief, these studies revealed that both fluorophores are efficiently excited at 488 nm and that their emission are readily separated using 500-530 nm band-pass (GCaMP3) and 650 nm long-pass (di-2-ANEPEQ) filters. Moreover, discrimination between the two signals is further simplified by the fact that depolarization causes changes in the opposite direction with the preceding filter sets, i.e. cardiomyocyte activation produces an *increase* in GCaMP3 fluorescence intensity but a *decrease* in di-2-ANEPEQ fluorescence (Figure 4.4E). That said, please note that all di-2-ANEPEQ-derived oAPs hereafter have been inverted (i.e. depicted as $-\Delta F/F$) to match convention.
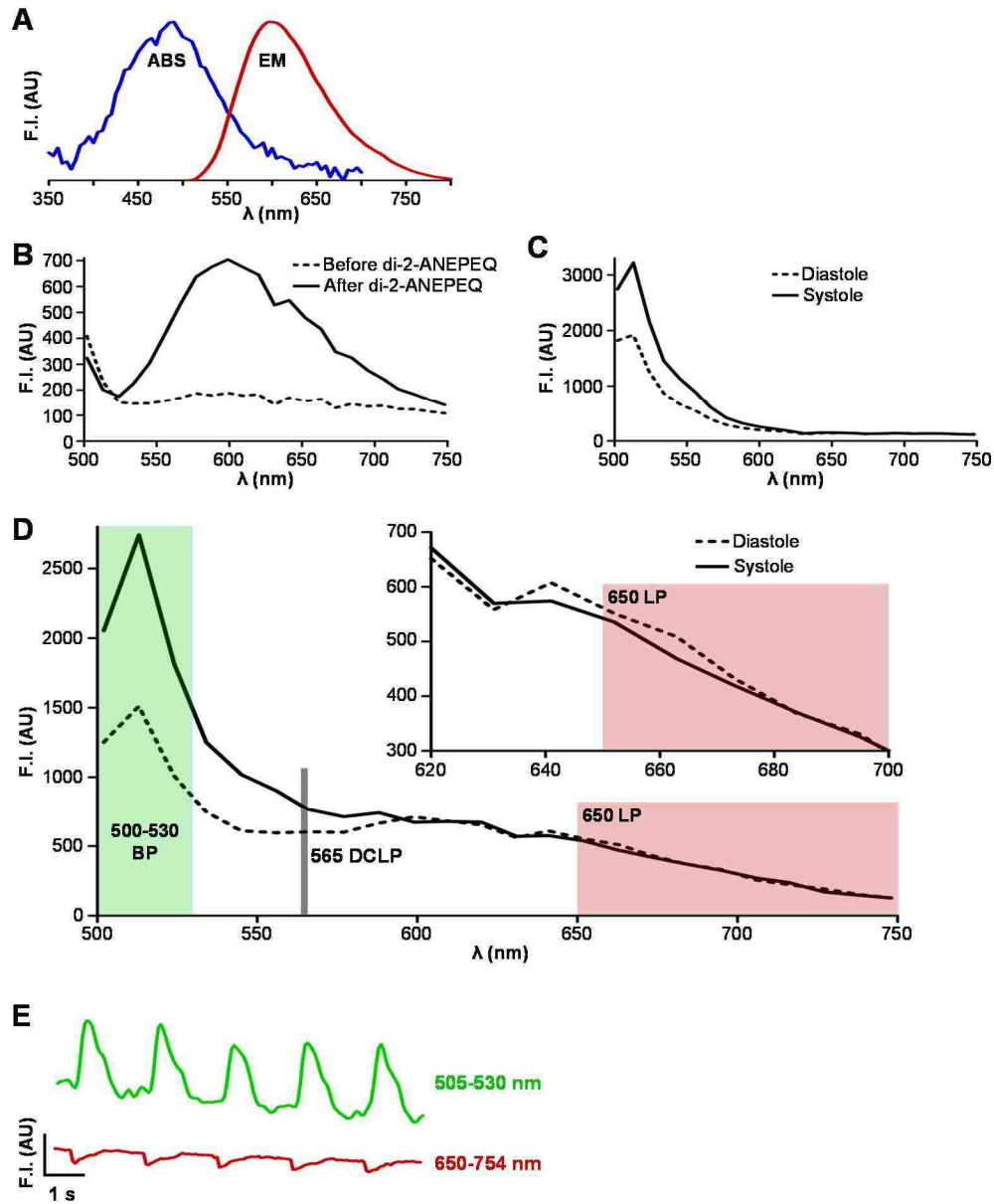
Figure 4.4. GCaMP3 and di-2-ANEPEQ spectrally separate in hESC-CMs. A: Absorbance and emission spectra of di-2-ANEPEQ in hESC-CMs by spectrofluorimetry. Note di-2-ANEPEQ-loaded hESC-CMs absorb with a peak ~488 nm, and emit with a peak ~600 nm. **B:** Emission spectra of WT hESC-CMs before and after loading with di-2-ANEPEQ, as determined by confocal lambda scanning. **C:** Emission spectra of GCaMP3+ hESC-CMs during systole and diastole (solid and dotted traces, respectively). **D:** Emission of GCaMP3+ hESC-CMs after loading with di-2-ANEPEQ recorded in both systole and diastole. As can be seen at the far left side of the plot, GCaMP3 mediates a large increase in fluorescence intensity during systole, however di-2-ANEPEQ emission undergoes a very small shift as seen at the right side of the plot and within the inset. **Overlaid** are the filter sets selected to spectrally separate these fluorophores. **E:** Mean fluorescence activity through time from a GCaMP3+ hESC-CM loaded with di-2-ANEPEQ acquired through the filter sets overlaid in panel **D**. Again, while GCaMP3 fluorescence intensity increases upon depolarization, di-2-ANEPEQ fluorescence intensity actually decreases when longpass filtered as shown.

57

Because di-2-ANEPEQ has not been previously used for cardiac optical mapping to our knowledge, we also performed experiments to verify its suitability as a myocardial voltage reporter. For this, we first imaged uninjured (n=2) and injured (n=3) guinea pigs hearts without grafts after dye labeling and consistently detected robust di-2-ANEPEQ-derived oAPs (Figure 4.5A-B). We next compared host di-2-ANEPEQ-derived oAPs to simultaneously acquired direct electrode recordings[131] and to RH237-derived oAPs, the latter obtained within the same heart after washout of di-2-ANEPEQ and staining with R237, and found excellent correlations in terms of activation times, action potential morphology and APDs (Figure 4.5C-E, n=2). For example, APD_{90} measurements based on di-2-ANEPEQ-and direct electrode recordings were 154.2±2.4 vs 155.5±1.7 ms (p=0.6), while APD_{90} measurements based on di-2-ANEPEQ and RH237 were 146.2±1.5 vs 144.7±1.3 ms (p=0.3). Of note, the change in fluorescence with di-2-ANEPEQ oAPs were greater than those obtained with RH237 in the same heart (4.7% vs 2.4% ΔF/F), an encouraging finding given our goal of detecting oAPs in graft tissue, which might be expected to be smaller amplitude[63, 66].
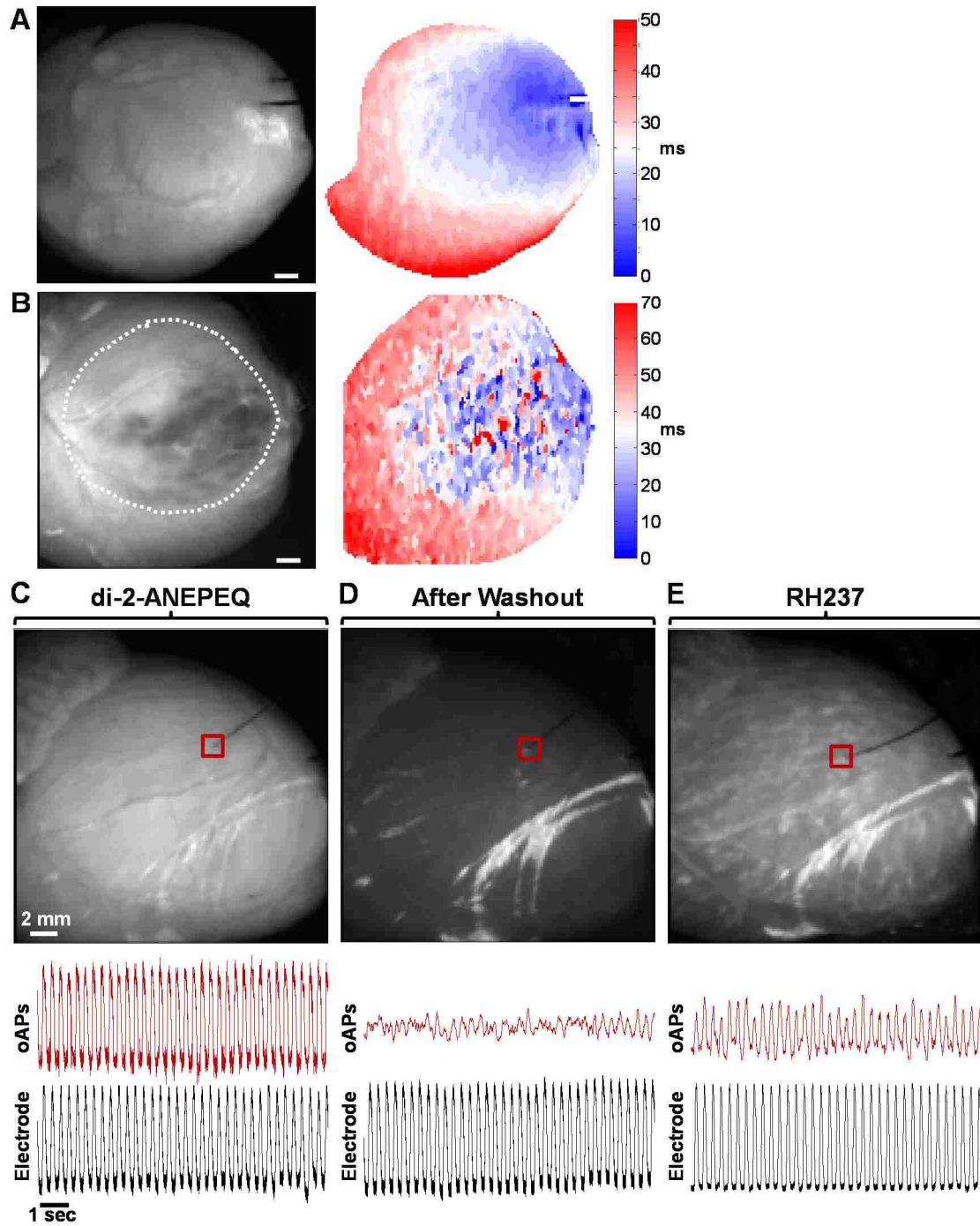
Figure 4.5. di-2-ANEPEQ is a reliable myocardial voltage reporter. A-B: Representative voltage activation maps of uninjured (**A**) and injured (**B**) hearts after loading with di-2-ANEPEQ ex vivo. To the left are still images of the di-2-ANEPEQ loaded hearts, and to the right are corresponding pseudocolored activation maps for a single beat indicating early (blue) to late (white to red) activation. Note the white dotted line of **B** indicates the cryoinjury region. **C-D:** Representative simultaneous electrode and optical action potential (oAP) recordings in an uninjured heart. We imaged the electrical activity of this uninjured heart (red traces) after di-2-ANEPEQ loading (**C**), after

di-2-ANEPEQ washout (**D**), and then after loading with RH237 (**E**) while simultaneously recording host activation directly by sharp electrode (black traces). Note that the ROIs selected in each panel to assess host-derived oAPs are centered over the termination of the recording electrode in the LV free wall. As shown in panel **C**, oAPs from host tissue loaded with di-2-ANEPEQ were robust (4.7% ΔF/F) and in excellent agreement with the simultaneously captured direct electrode recordings. As expected and as shown in panel **D**, after di-2-ANEPEQ washout oAPs from host tissue dropped significantly in amplitude whereas the electrode still registered robust action potentials. After then loading this same heart with RH237 and as shown in panel **E**, oAPs from host tissue returned and were again in excellent agreement with the direct electrode recordings, however RH237 oAPs were of smaller amplitude (2.4% ΔF/F) than di-2-ANEPEQ-derived signals.

4.3.3 Host and graft-derived electrical activity can be reliably detected via the simultaneous imaging of di-2-ANEPEQ (host and graft voltage) and GCaMP3 (graft-only calcium) fluorescent signals

Having validated the spectral compatibility of di-2-ANEPEQ with GCaMP3 as well its utility as a myocardial voltage reporter, we next moved to test these two fluorophores in combination for the optical mapping of hESC-CM-engrafted hearts. We hypothesized that di-2-ANEPEQ fluorescence (red channel) would report electrical activity in both graft and host tissue, while GCaMP3 fluorescence (green channel) would function as a critical graft-autonomous reporter of graft activation. If successful, this approach would provide us with a reliable means of distinguishing between host- and graft-derived electrical signals with high spatial and temporal resolution.

To test this approach, we transplanted 1×10^8 GCaMP3+ hESC-CMs into cryoinjured guinea pig hearts at either 10 or 28 days post-injury (with n=5 animals receiving GCaMP3+ cardiomyocytes derived from the RUES hESC line and n=7 animals receiving equivalently prepared myocytes derived from the H7 hESC line). We then harvested engrafted hearts at 2-weeks post-transplantation and imaged them ex vivo using the previously described dual-channel CCD-based system (Figure 4.1) and

following the experimental protocol depicted in Figure 4.2. In brief, each heart was perfused ex vivo, mechanically arrested with blebbistatin and then imaged on both channels before perfusion with di-2-ANEPEQ, during perfusion with di-2-ANEPEQ, and after dye washout. Recordings were acquired from hearts under both spontaneous and paced conditions.

Figure 4.6 depicts the findings from a representative imaging experiment, which in this case were obtained from a cryoinjured heart in which the hESC-CM graft was not electrically coupled with host myocardium (i.e. in which graft-derived GCaMP3 fluorescent transients occurred in no relationship to the host ECG or the applied rate of stimulation). As expected given our earlier spectral analyses, prior to perfusion with di-2-ANEPEQ, we detected strong GCaMP3 fluorescence transients in graft ROIs in the GCaMP3 (green) channel, but there was no "bleed-through" of this signal into the di-2-ANEPEQ (red) channel (see left-most panels of Figure 4.6B&D). Upon perfusion with di-2-ANEPEQ, we observed a differential time-course of dye labeling in host and graft tissue during perfusion with di-2-ANEPEQ, an outcome consistent with our hypothesis that hESC-CMs grafts have relatively sluggish perfusion. Maximal labeling of host tissue occurred 4.5±0.2 minutes after the addition of dye to the perfusate, but it took 13.4±1.3 minutes of perfusion to obtain comparable staining in graft tissue (n= 12 hearts examined). As expected, ROIs in host myocardium showed di-2-ANEPEQ-derived oAPs that occurred in 1:1 synchrony with the host ECG (and the applied stimuli in paced hearts), and oAPs from host tissue within the injury zone showed a smaller amplitude than oAPs from intact host myocardium (2.4±0.1% vs 4.7±0.3% ΔF/F). At early time-points following the onset of dye perfusion, graft ROIs also showed similar

small-amplitude oAPs that we attributed to host tissue located deep to the graft.

However, over time, these same graft ROIs showed the gradual emergence of *graft-derived* oAPs that were superimposed on the continuing host-derived oAPs (see the middle panels of Figure 4.6B&D). Proving their graft origin, these graft-derived oAPs occurred synchronously with the simultaneously acquired, graft-autonomous GCaMP3 fluorescence transients and not necessarily with the host ECG, behavior consistent with expectations for intra-cardiac grafts that are not always coupled with host myocardium[80, 82]. The duration of graft-derived oAPs were also distinct from their counterparts in host tissue, as detailed further below.

Interestingly, we observed the reverse sequence with regard to dye washout from host and graft tissues. Host tissues lost all detectable oAPs within 15.3±1.9 minutes after the switch to di-2-ANEPEQ-free perfusate, while graft tissue showed graft-derived oAPs— now no longer with the superimposed host-derived oAPs— that persisted for at least 30 minutes. At this late time point, graft-derived oAPs were of reduced dynamic range relative to before washout started, but still exhibited a ΔF/F of 2.3±0.2% that allowed for reliable quantitation. (See right-most panels of Figure 4.6B&D for representative traces during dye washout.) Note that this differential labeling phenomenon provided us with two independent means to reliably discriminate between graft- and host-derived signals. First, we correlated all apparent graft-derived oAPs based on di-2-ANEPEQ with the simultaneously acquired graft-autonomous GCaMP3 signal, and we always found excellent agreement between the two reporters. (For example, graft cycle lengths measured independently by these reporters had a correlation coefficient of R^2=0.997, and as shown in Figure 4.7A-B graft activation maps

recorded on the red and green channels showed similar patterns of spatial activation)
Second, by performing serial dye wash-in and washout experiments, we were able to
reliably isolate graft- and host-derived di-2-ANEPEQ signals.

To further validate the reliability of this system to distinguish between host- and
graft-derived electrical signals, we attempted direct microelectrode recording of
engrafted hearts during dual-imaging of GCaMP3 and di-2-ANEPEQ. Because this
procedure is technically challenging, we were successful in impaling and recording from
graft tissue in only 1 of 4 hearts attempted, but we did find excellent agreement in this
instance (Figure 4.8A-B). For example, measurements of graft APD were very similar
based on di-2-ANEPEQ and direct electrode recordings (APD_{90} 232.6±4.8 vs 234.0±3.0
ms, p=0.8). Taking collectively with our earlier experience, this outcome supports the
combined use of a water-soluble voltage dye and a graft autonomous reporter of graft
activation to study electrical activation in hESC-CM-engrafted hearts.
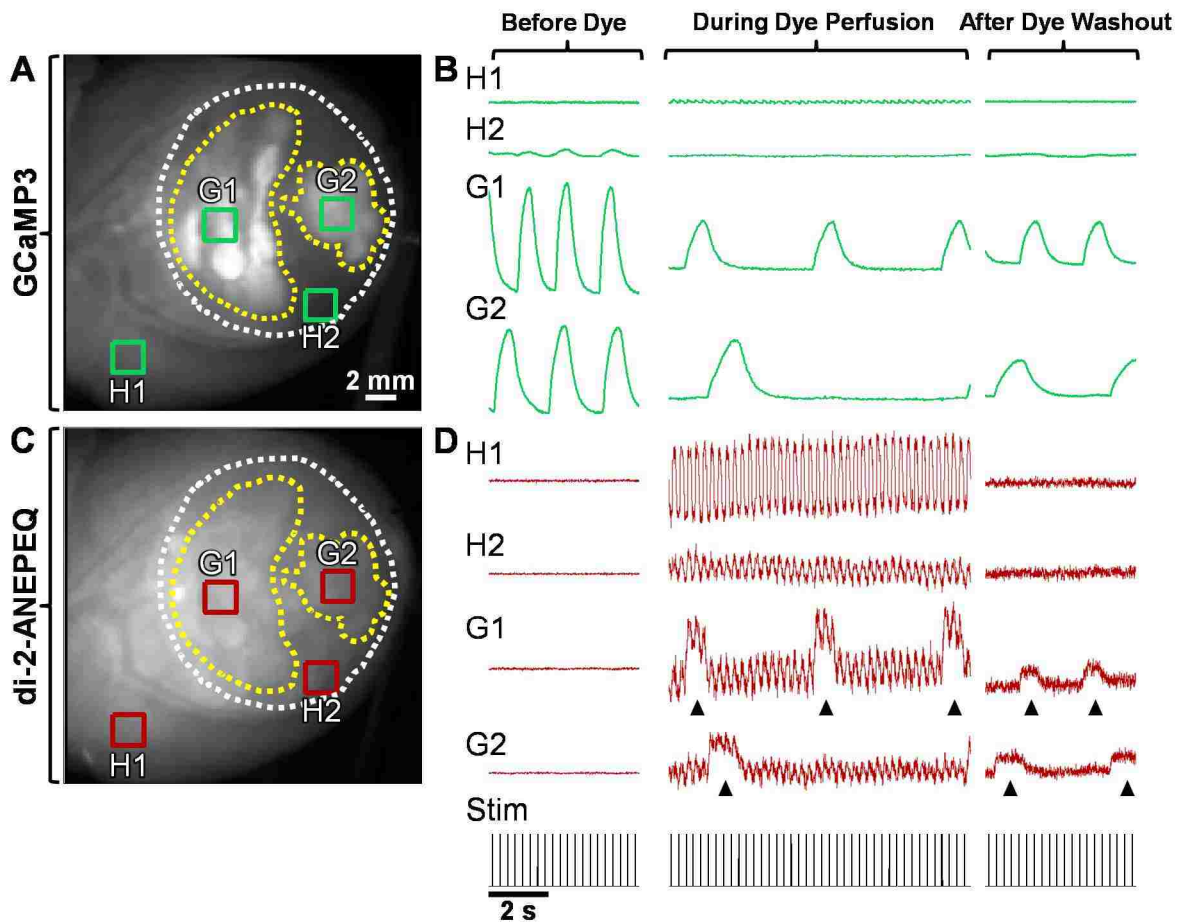
Figure 4.6. Simultaneous imaging of the water-soluble voltage dye di-2-ANEPEQ and hESC-CM grafts expressing GCaMP3 allow for reliable measurements of both host and graft myocardium electrical activity. Representative injured and GCaMP3+ hESC-CM engrafted heart simultaneously imaged for both GCaMP3 (graft calcium, **A-B**) and di-2-ANEPEQ (host and graft voltage, **C-D**) fluorescence activity. **A:** Epicardial still image of this representative heart as viewed through the GCaMP3 (green) channel, showing the cryoinjury zone (white dotted line) and within it two independent hESC-CM graft regions (yellow dotted lines). Four ROIs have been selected to assess the activity of viable host (H1), injured host (H2), and the two graft regions (G1&G2). **B:** Mean GCaMP3 fluorescence activity from ROIs identified in the corresponding GCaMP3 still image in **A**, assessed before di-2-ANEPEQ perfusion (left panel), during di-2-ANEPEQ recirculation (middle panel) and after dye washout (right panel). Grafts were uncoupled from the host and each other, so GCaMP3 transients occurred independently of the applied stimuli (black trace at bottom). **C&D:** Simultaneously recorded di-2-ANEPEQ (red) channel still image (**C**) and mean di-2-ANEPEQ fluorescence activity from the same ROIs identified in panels **A&C,** assessed before, during, and after di-2-ANEPEQ. This figure highlights several important aspects of combined GCaMP3 and di-2-ANEPEQ imaging. First, before dye perfusion we could verify no significant leakage of GCaMP3 fluorescence into the di-2-ANEPEQ channel (see left panels of **B&D**). Second, at a time point during dye perfusion where both host and graft tissues were maximally loaded (see middle panels of **B&D**), host ROIs showed rapid optical action potentials (oAPs) that occurred in sync with the

64

middle panels of **B&D**), host ROIs showed rapid optical action potentials (oAPs) that occurred in sync with the applied stimuli, with robust oAPs elicited from viable host as shown in ROI H1 but oAPs of reduced amplitude coming from surviving endocardial host tissue within the injury region as shown in ROI H2. These smaller amplitude oAPs from surviving host were also observed within graft ROIs G1&G2, however superimposed on top of them were graft-derived oAPs (arrowheads) with a different periodicity and duration than host that occurred in sync with the graft-autonomous GCaMP3 signals. Further, we could verify no significant leakage of di-2-ANEPEQ fluorescence into the GCaMP3 channel. Last, late into di-2-ANEPEQ washout (see right panels of **B&D**) we found all host-derived signals have disappeared, however graft tissues have retained the dye longer and continue to emit oAPs (arrowheads) that are again coincident with the graft-autonomous GCaMP3 transients.
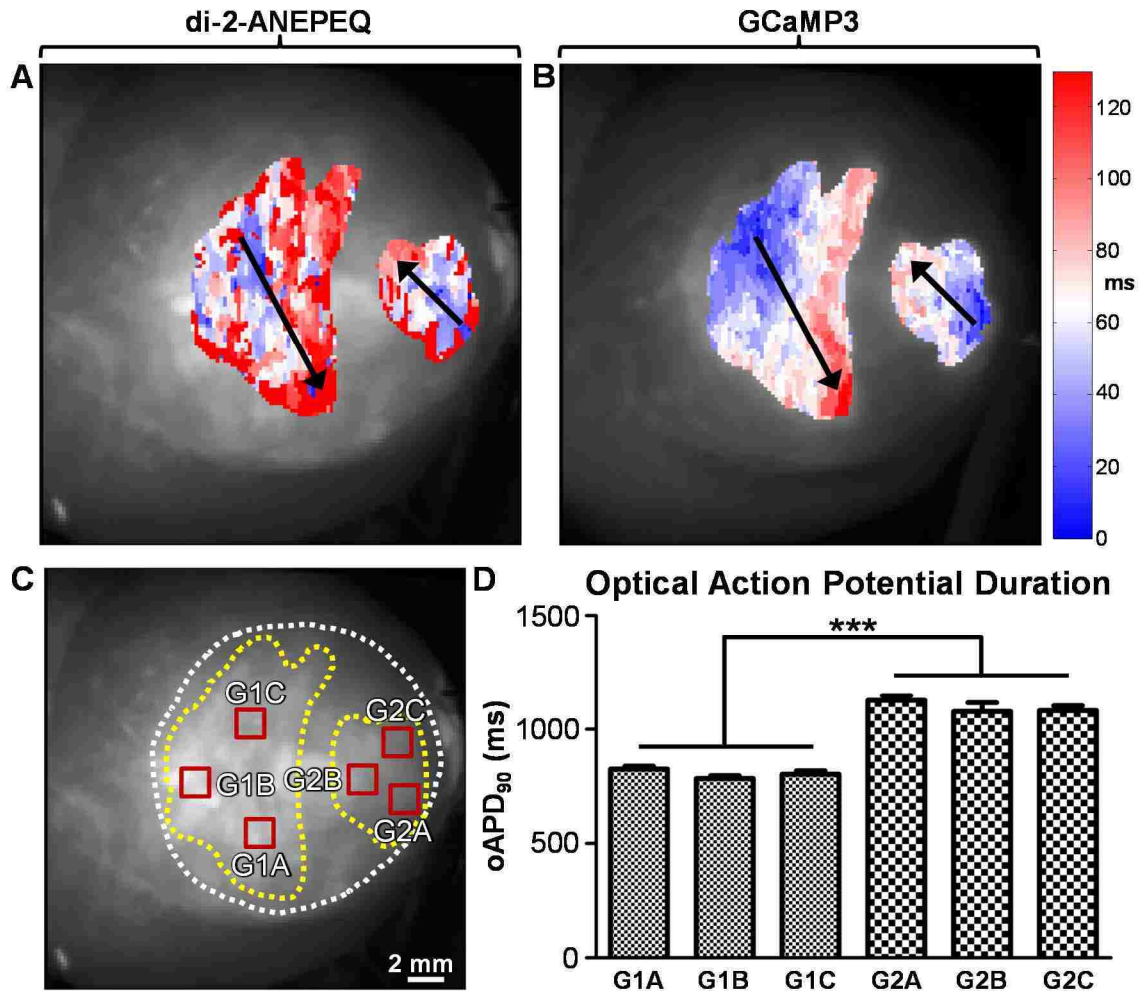
Figure 4.7. Good correlation between hESC-CM graft activation maps based on di-2-ANEPEQ and GCaMP3 signals. A-B: Activation maps based on a single beat for the same hESC-CM graft regions outlined in main figure 2, created using di-2-ANEPEQ (**A**) and GCaMP3 (**B**) optical signals. Activation time (ms) is expressed relative to the first active site within the ROI on a given channel. Note the two grafts activated independently but have been displayed with the same activation time scale. Also note the agreement in primary activation vectors, which have been demarked with black arrows. **C-D:** Optical action potential duration (oAPD) measurements from individual hESC-CM graft regions were not dependent on the location of ROIs selected for analysis. **C:** di-2-ANEPEQ channel still image of an injured and GCaMP3+ RUES2 hESC-CM engrafted heart after host voltage transients washed out but graft-derived di-2-ANEPEQ signals remained. In this heart the two graft regions (yellow-dotted lines) inside the injury region (white-dotted line) activated independently from one another and the host. Three ROIs were selected per graft region for an analysis of oAPD, to test if measurements of this parameter varied with location. **D:** Quantitation of oAPDs (reported at 90% repolarization, APD$_{90}$) measured from the ROIs identified in panel **C**. We found oAPDs measured from various locations within a single graft region were not significantly different, however were different between these independently active grafts. ***=P<0.001.
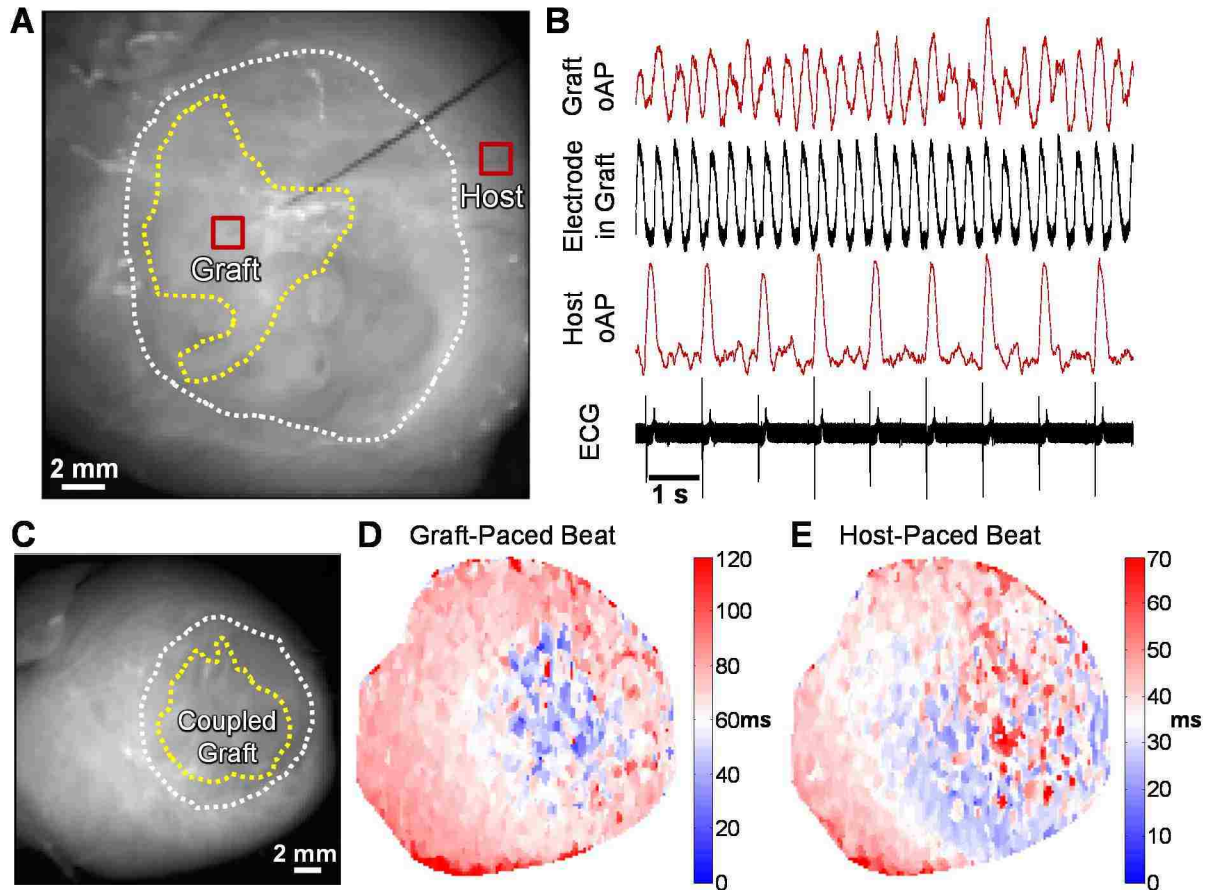
Figure 4.8. Simultaneous electrode and optical action potential recordings from an uncoupled hESC-CM graft, plus a heart with coupled hESC-CM graft in which the graft acted as an ectopic pacemaker. A&B: An injured and hESC-CM engrafted heart in which we successfully impaled graft tissue with a 1-2 µm diameter pure iridium intracellular recording electrode in order to compare di-2-ANEPEQ optical action potentials (oAPs) with direct electrode recordings. **A:** Epicardial still image taken on the di-2-ANEPEQ channel, showing the uncoupled hESC-CM graft footprint (yellow dotted line) inside the cryoinjury region (white dotted line) and the recording electrode stabbing into graft tissue. Note that the graft ROI selected to assess graft-derived di-2-ANEPEQ oAPs is centered over the termination of the recording electrode within graft tissue. Also note a ROI within viable host muscle remote to the injury region has been selected to compare host signals to the simultaneously recorded ECG. **B:** Simultaneously recorded di-2-ANEPEQ-derived oAPs and direct electrode recordings from hESC-CM graft tissue (top two traces) along with host oAPs and ECG data (bottom two traces), corresponding to the heart from panel **A**. Note the excellent agreement in these paired optical and electrode measurements. **C-E:** The injured and hESC-CM engrafted heart of this study in which we found the electrically coupled graft could ectopically pace the host heart. **C:** Epicardial still image taken on the di-2-ANEPEQ channel, showing the coupled hESC-CM graft footprint (yellow dotted line) inside the cryoinjury region (white dotted line). **D:** Voltage activation map for a single graft-paced beat, showing the earliest activating area (blue) starts in the coupled graft footprint, then propagates outward towards the LV base and apex (white to red). **E:** Voltage

67

activation map for a single host-paced beat, with earliest activation (blue) initiating at the LV apex, then propagating towards the LV base and finally back apically to activate the graft (white to red). Note the slower kinetics of the graft-paced versus host-paced beat. Also note that both activation maps represent information from a *single* beat.

4.3.4 Outcomes from optically mapping injured hearts transplanted with GCaMP3+ hESC-CM grafts

Given this capacity to reliably detect and distinguish between host- and graft-derived electrical activity, we next moved to experiments to investigate how parameters including cell line (RUES2 versus H7 hESCs), the timing of cell transplantation (cell delivery at 10- or 28-days post-injury) and spontaneous versus paced conditions would affect the electrical behavior of engrafted hearts. See Table 4.1 for a detailed summary of conditions tested and corresponding outcomes.

GCaMP3+ hESC Line	Cardiac Injury Model	# of Distinct Graft Regions	Host-Graft Coupling?	Graft Activation Vector Distinct from Host?	Pacing Affect Graft Behavior?	Graft oAPD$_{90}$ (ms)	Rate Corrected Graft oAPD$_{90}$ (ms)	Graft CV (cm/s)	Host CV (cm/s)
RUES2	Chronic	1	N	Y	N	716	556	3.7	69.4
RUES2	Chronic	1	N	Y	N	581	506	5.9	123.0
RUES2	Chronic	1	N	Y	N	611	526	6.5	188.0
RUES2	Chronic	1	N	Y	N	699	590	4.5	88.5
RUES2	Chronic	2	N	Y	N	842	685	10.1	62.2
			N	N	N	1088	699	6.2	
H7	Chronic	1	N	Y	N	212	257	12.5	77.2
H7	Chronic	1	N	Y	N	223	243	5.1	78.4
H7	Chronic	1	N	Y	N	336	357	8.4	74.5
H7	Chronic	1	N	Y	N	323	324	12.1	47.2
H7	Subacute	1	Y	Y	Y	211	288	5.7	75.2
H7	Subacute	1	N	Y	N	293	312	6.1	60.5
H7	Subacute	1	N	Y	N	303	297	8.4	58.0

Table 4.1. Summary data for injured hearts engrafted with GCaMP3+ hESC-CMs simultaneously imaged for GCaMP3 (graft calcium) and di-2-ANEPEQ (host and graft voltage).

One finding that was immediately apparent was the striking differences in the electrical behavior of grafts formed using either RUES2 or H7 GCaMP3+ hESC-CMs, regardless of the timing of cell transplantation (n=6 and n=7 animals per group, respectively). Unexpectedly, all RUES2-derived grafts displayed ultra-long oAPDs, which were not present in their H7 counterparts (APD$_{90}$ of 756±76 vs 272±21 ms, p<0.01) even after correcting for differences in firing rate (rate corrected APD$_{90}$ of 594±33 vs 297±15 ms, p<0.01, see Figure 4.9A-B). This difference in APD between lines was not confounded by underlying host-derived signals (as all graft oAPDs were assessed at a time after di-2-ANEPEQ washout when host-derived signals were no longer present), nor was it attributable to the variation within an individual graft (because each "island" of graft showed similar oAPDs throughout, see Figure 4.7C-D).
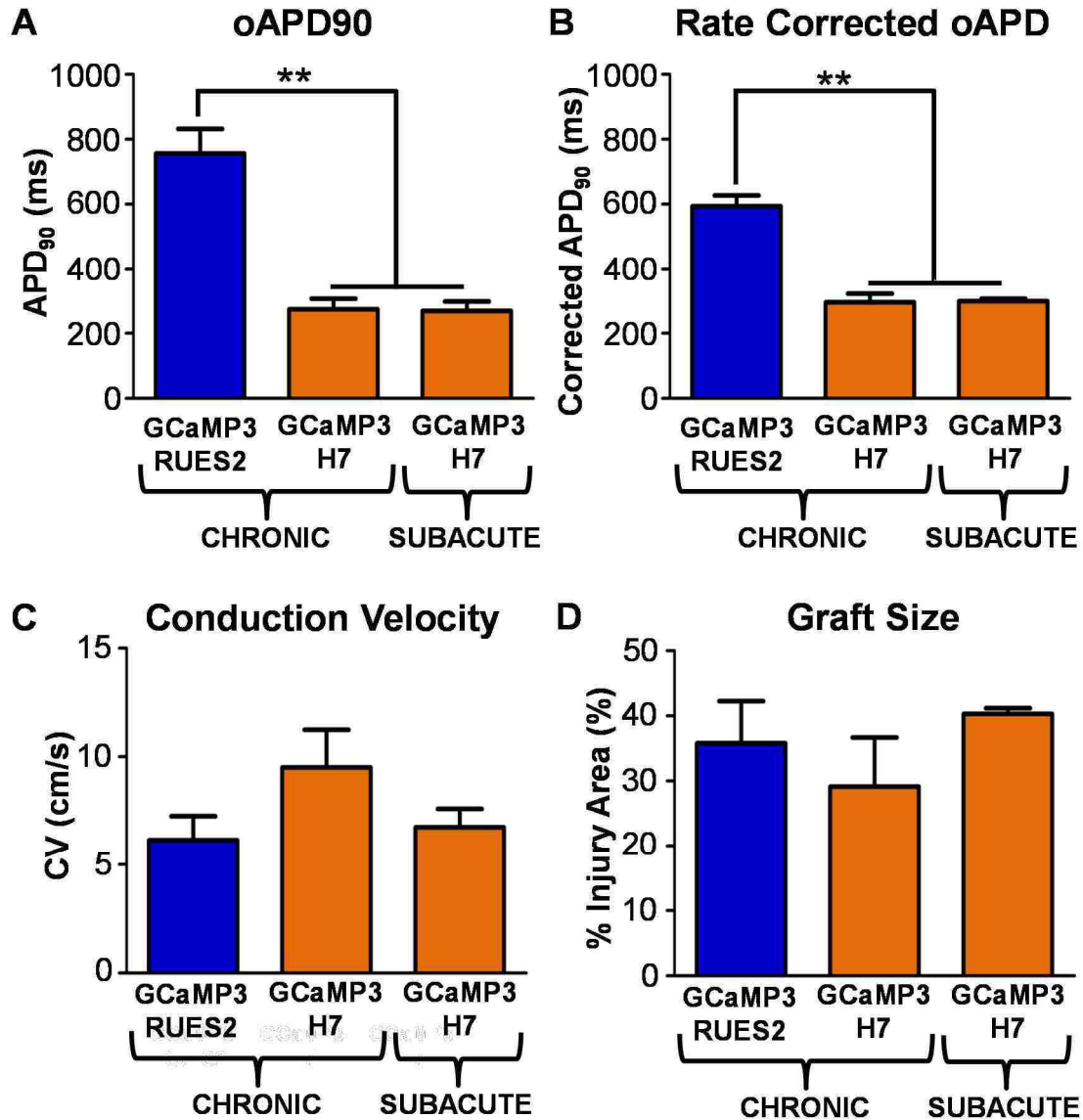
Figure 4.9. Grafts formed using RUES2- and H7-derived hESC-CMs show differences in action potential duration, but no difference in conduction velocity or size. Electrophysiological properties of RUES2- (blue) vs H7- (orange) derived hESC-CM grafts in injured hearts. **A:** Graft optical action potential durations (oAPDs), reported as the time from start until 90% repolarization (APD$_{90}$); H7-derived grafts transplanted in chronic and subacute injury models were remarkably similar in this parameter, however they were significantly different from transplanted RUES2-derived grafts which all showed ultra-long oAPDs. **B:** Since RUES2- and H7-derived grafts exhibited differential activation rates (0.53±0.06 vs 1.42±0.21 Hz, respectively), we applied Fridericia's rate correction to adjust oAPDs. Even after correcting for rate, RUES2-derived graft oAPDs remained significantly longer than their H7 counterparts. **C:** Graft conduction velocities (CV) were similar, averaging 7.4±0.8 cm/s. For comparison, adjacent host tissue measured 83.5±11.0 cm/s. **D:** Graft size, expressed as the % of injury area occupied by graft as viewed from the epicardial surface, was also similar. n=3-5 per condition, **=P<0.01.

A second unanticipated outcome in the study was the lack of any host-graft electrical coupling observed in the chronically injured and GCaMP3+ hESC-CM recipient hearts of this study (n=9), given an expected coupling rate of ~40% based on our previous work[82]. When combined with host-graft coupling outcomes from our lab for all hearts transplanted with GCaMP3+ hESC-CM grafts imaged at two weeks, we found the clear tendency of RUES2-derived grafts to not couple with host hearts (Figure 4.10). Thus we switched to our subacute injury model with H7-derived grafts (n=3) and found one of three hearts to contain a completely coupled graft. Surprisingly, when imaging at a time point when both host and graft were loaded with di-2-ANEPEQ, this coupled GCaMP3+ H7 hESC-CM graft was able to ectopically pace the host heart as well as follow host-led beats (Figure 4.8C-E) upon removal of overdrive pacing.

Although grafts formed using RUES2- and H7-derived GCaMP3+ hESC-CMs showed major differences in their oAPDs and capacity for host-graft coupling, we did not find significant differences in other parameters including graft CV (6.2±0.9 vs 8.3±1.1 cm/s, respectively, p=0.21, Figure 4.9C) or size (35.8±6.5% vs 33.9±4.6% graft area as % of injury area, p=0.81, Figure 4.9D). Importantly, however, CV in graft tissue overall was only ~9% of that in adjacent host myocardium (overall mean graft CV of 7.2±0.8 cm/s vs 83.5±11.0 cm/s, p<0.0001 for paired comparisons between graft and host within individual hearts). Moreover, both RUES2- and H7-derived grafts showed other potentially pro-arrhythmic behavior including propagation along vectors opposite from that in host tissue and/or spatial patterns of activation that varied from beat-to-beat.
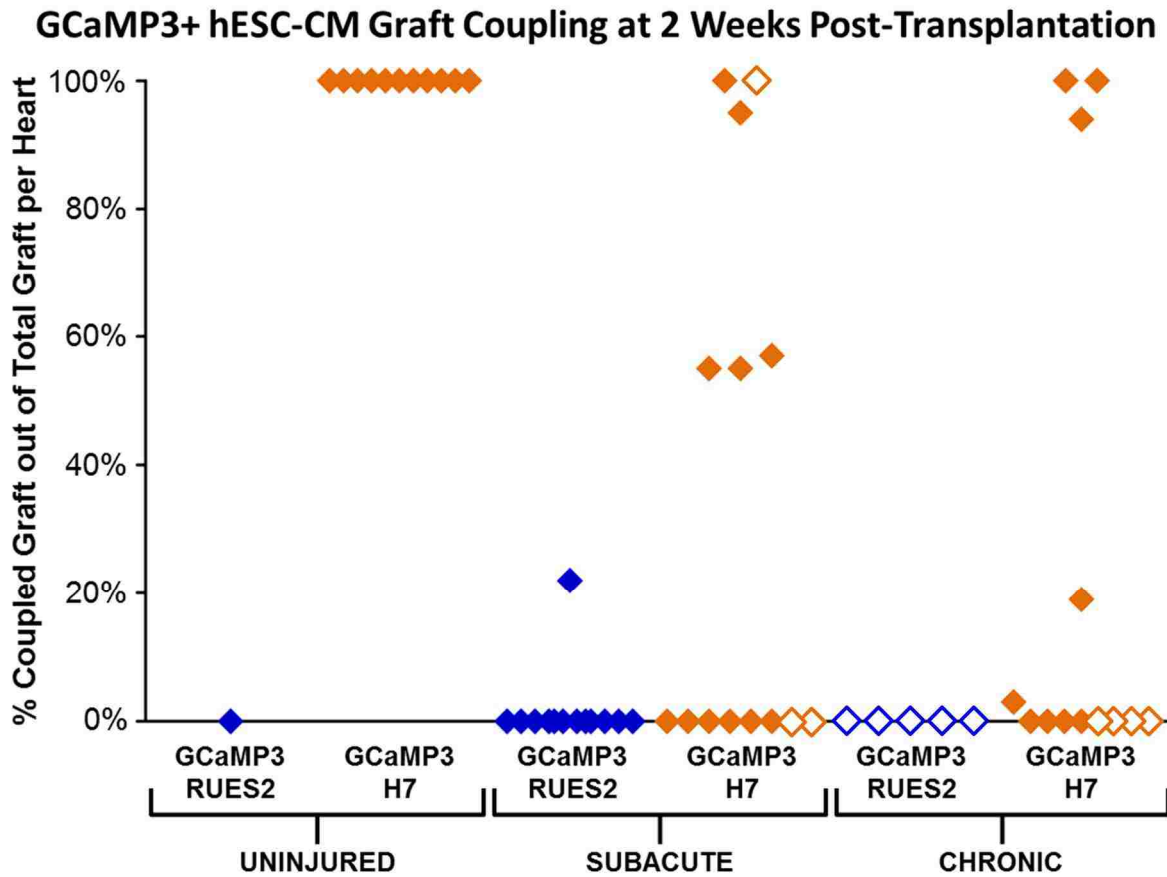
Figure 4.10. Collective host-graft electrical coupling at 2 weeks post-transplantation. % of visible GCaMP3+ hESC-CM graft area found to be 1:1 coupled in recipient hearts imaged two weeks post-transplantation (each data point represents a single heart; note hearts of this study have white centers). This data incorporates our experience with two cell preparations (cardiomyocytes derived from the RUES2 (blue) and H7 (orange) hESC lines) and three recipient models (uninjured, subacutely injured and chronically injured hearts). Note that GCaMP3+ RUES2 hESC-CMs consistently exhibit a lack of host-graft coupling.

4.3.5 Structure and gap junction expression in hESC-CM-engrafted hearts by histology

Although our group has previously examined in detail the composition of hESC-CM grafts as well as their structural effects on recipient hearts[47, 74, 80-82, 115], here we performed focused histological studies to specifically address whether differences in scar size, graft size, graft distribution or gap junction protein expression could account

for the aforementioned differences in the electrical behavior of grafts formed using

RUES2- versus H7-derived hESC-CMs. We also sought to understand why the fraction

of hearts showing 1:1 host-graft coupling was lower than in our earlier studies also

employing GCaMP3+ hESC-CMs and a similar experimental design[80, 82, 115]. Figure

4.11A-C depicts representative images of GCaMP3+ hESC-CM grafts in cryoinjured

hearts. As in our earlier work, we found that the transplantation of cardiomyocytes from

both lines resulted in irregular islands of human myocardium that were mostly located

within the cryoinjury scar. Importantly, hearts receiving RUES2- versus H7-derived

hESC-CMs showed no differences in terms of scar size or graft area (Figure 4.11D-F).

Interestingly, we found no points of host-graft contact whatsoever in the 4 hearts that

received H7 hESC-CMs 28 days post-injury, despite the presence of large graft

implants within the cryoinjury scar. While this is a potential explanation for the absence

of 1:1 host-graft coupling in these hearts, it should be noted that 2 of 5 equivalently

prepared RUES2 hESC-CM engrafted hearts showed areas of significant host-graft

contact (totaling 109.1 mm and 1.5 mm in the examined histological sections), and yet

these host-contacting graft regions were found to be uncoupled.

To rule out a difference in gap junction expression or localization, we compared

RUES2 and H7 hESC-CM grafts by immunohistochemistry using antibodies against the

adherins junction protein N-cadherin and the major gap junction protein connexin-43. In

brief, while we found that grafts formed from both cell lines showed levels of cadherin

expression that were comparable to that in adjacent host myocardium, cadherin

immunoreactivity in graft muscle tended to be distributed uniformly throughout the graft

cell sarcolemma rather than localized to intercalated discs at the transverse border

between individual cardiomyocytes as in host myocardium (Figure 4.12A). On the other hand, consistent with our prior work[80], we found connexin-43 expression to be relatively low in hESC-CM grafts of both lines and to lack the strong, anisotropic immunoreactivity at intercalated discs found in the adjacent host myocardium (Figure 4.12B). Moreover, connexin-43 immunoreactivity was slightly weaker in RUES2 hESC-CM grafts than H7 equivalents.
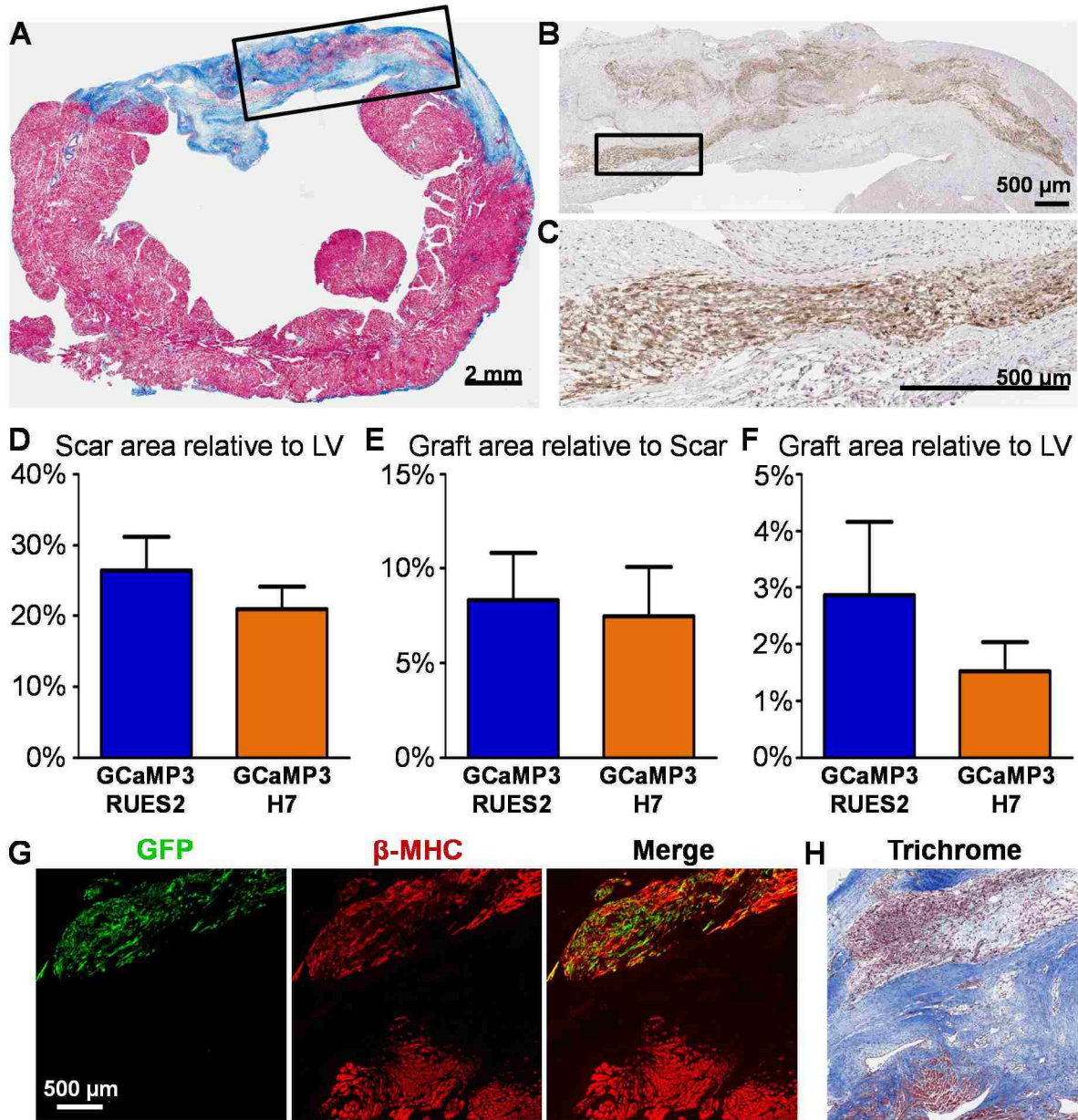
Figure 4.11. Histological analyses of injured hearts with GCaMP3+ hESC-CM grafts. A-C: Representative injured heart transplanted with GCaMP3+ hESC-CMs 28 days post-injury. The transplantation of GCaMP3+ hESC-CMs from both lines resulted in irregular islands of human myocardium that were mostly located within the cryoinjury scar, shown in this series of insets: panel **A** shows a transverse heart section masson's trichrome stained to demark muscle (red) and scar (blue), whereas an adjacent section shown in panels **B&C** stained for GFP (brown) confirms the viable muscle in the injury scar as graft. **D-F:** Quantitation of relative scar, graft, and LV areas for injured hearts receiving GCaMP3+ RUES2 (blue, n=5) or H7 (orange, n=4) hESC-CM grafts at 28 days post-injury. Note no significant differences in all parameters between hearts. **G-H:** GCaMP3+ hESC-CM graft near host tissue imaged by immunofluorescence on confocal for GFP (green) and the muscle marker β-MHC (red) in **G**, with masson's trichrome staining of an adjacent section in **H**.
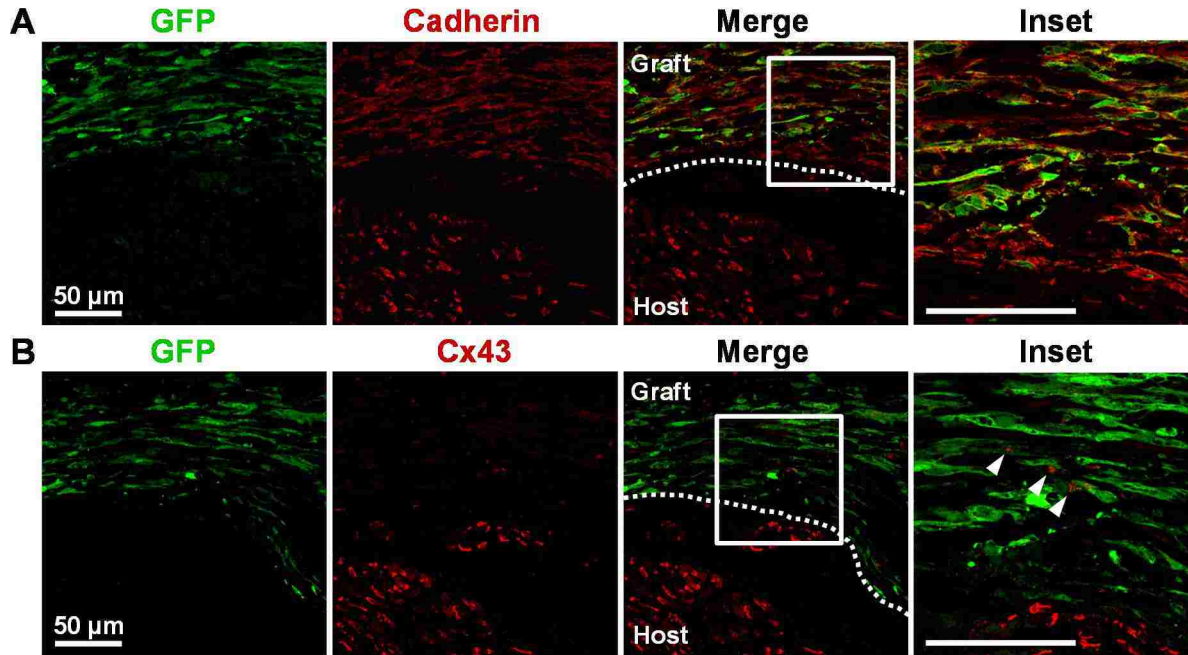
Figure 4.12. GCaMP3+ hESC-CM grafts have comparable cadherin expression as host myocardium, but much lower connexin-43 expression. Representative area of GCaMP3+ hESC-CM graft located in scar tissue near the injury border zone dual-labeled with antibodies against either GFP (green) and cadherin (red) (**A**), or GFP (green) and connexin-43 (Cx43, red) (**B**). **A:** All hESC-CM grafts displayed a comparable level of cadherin expression as host, however with a uniform sarcolemmal distribution rather than localized to intercalated discs as in host myocardium. **B:** Conversely, while punctate Cx43 gap junction plaques were observed in hESC-CM graft tissue (arrowheads in inset), grafts commonly lacked the strong and anisotropic immunoreactivity of Cx43 at intercalated discs as found in host muscle. Furthermore, Cx43 expression overall was much lower in hESC-CM graft tissues compared to host, and between lines RUES2-derived hESC-CM grafts showed slightly less expression than H7-derived equivalents.

4.3.6 GCaMP3 expression prolongs the action potential duration of hESC-CMs

In prior work, our group has used patch-clamp techniques to obtain measurements of APD in WT hESC-CMs from both H7 and RUES2 hESCs on the order of ~200 ms[53,63]. Hence, our finding here of ultra-long APDs in GCaMP3+ RUES2 hESC-CM grafts (but curiously not in their GCaMP3+ H7-derived counterparts) caused us to speculate that GCaMP3 expression itself might be causing "off-target", action

potential-prolonging effects. To address this issue in a higher-throughput fashion and

with a technology more amenable to multicellular preparations than patch-clamping, we

stained WT and GCaMP3+ cardiomyocytes from both lines with the voltage-sensitive

dyes di-2-ANEPEQ or RH237 and then acquired their respective oAPDs in vitro. oAPD

measurements were obtained from both individual cells and from cardiomyocytes

organized into ~300 µm diameter aggregates, under conditions of both spontaneous

contraction and field-stimulation. As depicted in Figure 4.13A-C, we found the

expression of GCaMP3 prolonged APDs of hESC-CMs derived from both RUES2s and

H7s (although only significantly in H7s at $\leq$0.5 Hz), while APDs of WT hESC-CMs from

both lines were not different in this parameter.
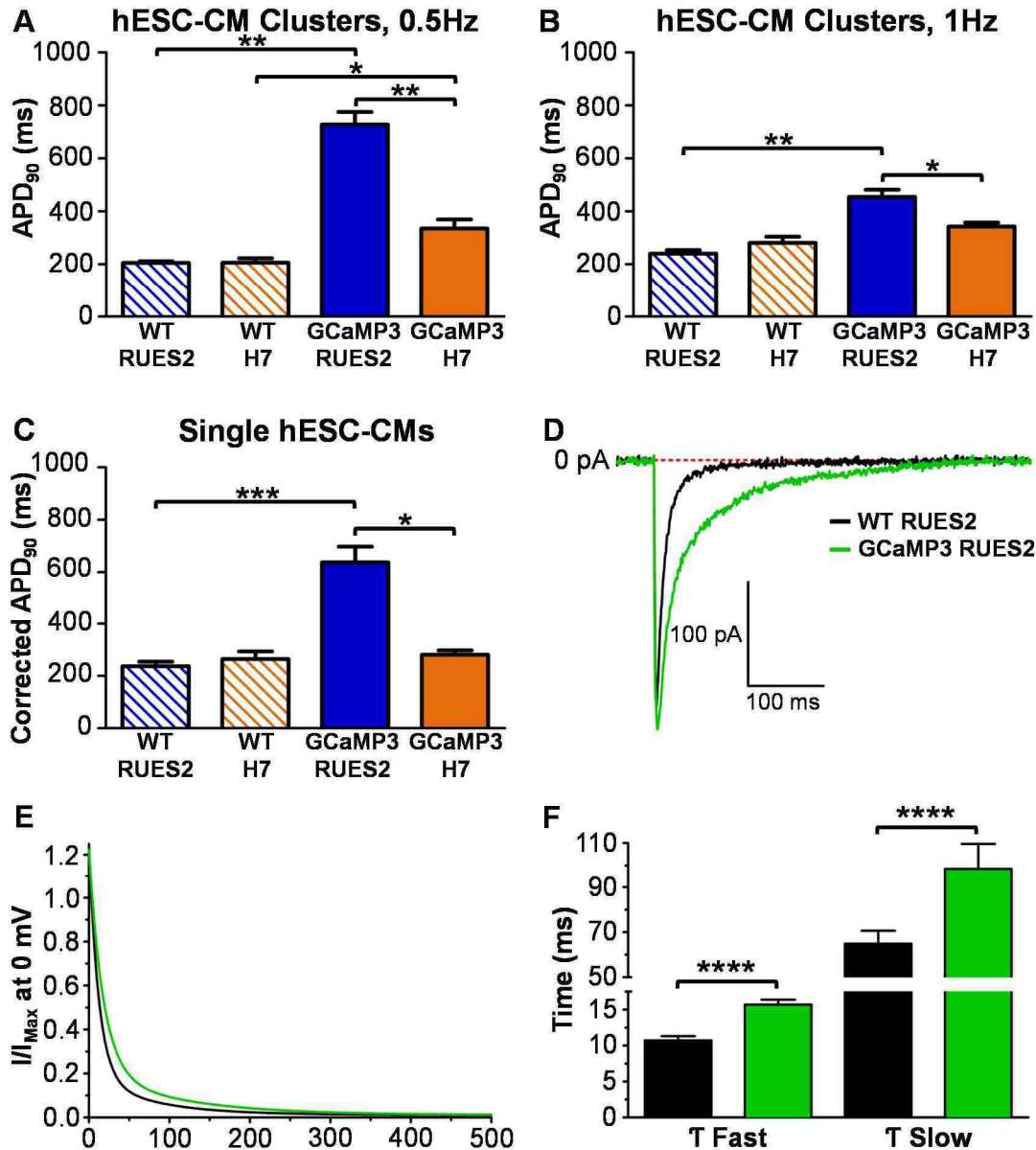
Figure 4.13. GCaMP3 expression prolongs hESC-CM action potentials and is associated with slower L-type calcium channel inactivation kinetics. **A-C:** hESC-CM optical action potential durations (oAPDs) measured in vitro for both RUES2 and H7 hESC-CMs correlate with oAPDs of grafts in injured hearts and show GCaMP3 expression prolongs this parameter. **A-B:** APD_{90} of hESC-CM aggregates, measured after loading with di-2-ANEPEQ, at 0.5Hz (**A**) and 1Hz (**B**). Interestingly, oAPDs of WT RUES2 and H7 hESC-CM aggregates were not significantly different, yet were significantly less than GCaMP3+ hESC-CM equivalents at 0.5Hz (**A**). Further, GCaMP3+ RUES2 hESC-CM aggregates showed ultra-long oAPDs similar to measurements from uncoupled grafts in injured hearts, and were significantly longer than GCaMP3+ H7 hESC-CM aggregate oAPDs. GCaMP3+ RUES2 and H7 hESC-CM aggregate oAPDs reduce with the increase in rate to 1Hz (**B**), however GCaMP3+ RUES2s continue to be significantly distinct. Results are from 3 biological replicates per group, n>12 aggregates per biological replicate, and >5 oAPDs measured per aggregate. **C:** Rate corrected APD_{90} of single

hESC-CMs in vitro, measured after loading with RH237. Single hESC-CM data shows GCaMP3+ RUES2 hESC-CMs have significantly longer oAPDs than WT RUES2- and GCaMP3+ H7-derived hESC-CM equivalents, and supports hESC-CM aggregate data as well as GCaMP3+ hESC-CM oAPDs of grafts in injured hearts. n>5 cells per group, with >4 oAPDs measured each. **D-F:** L-type calcium currents ($I_{Ca,L}$) of WT and GCaMP3+ RUES2 hESC-CMs measured by patch clamp show GCaMP3 expression is associated with slower $I_{Ca,L}$ inactivation. **D:** Representative $I_{Ca,L}$ from WT and GCaMP3+ RUES2 hESC-CMs (black and green traces, respectively), elicited by depolarization to 0 mV. **E:** Inactivation kinetics from **D** after normalization. **F:** Fast and slow decay time constants, quantified from a two-phase exponential decay fit to normalized current traces from **E**, were significantly longer in GCaMP3+ RUES2 hESC-CM vs WT equivalents (n>12 per group). *=P<0.05, **=P<0.01, ***=P<0.001, ****=P<0.0001.

GCaMP3 includes calcium-binding moieties from calmodulin[97, 117]. Because the overexpression of other recombinant calmodulin derivatives has been shown to affect inactivation of the L-type calcium current ($I_{Ca,L}$,)[132-134] in primary cardiomyocytes and this inward current plays an important role in maintaining the plateau phase of the cardiac action potential[135], we hypothesized that the AP-prolonging effects of GCaMP3 expression in hESC-CMs might be related in part to interference with $I_{Ca,L}$ inactivation. To test this, we used patch-clamp techniques to isolate and compare $I_{Ca,L}$ in WT and GCaMP3+ RUES2 hESC-CMs. Consistent with our hypothesis, while there were no differences in the amplitude and voltage dependence of this current, we did find that its inactivation kinetics were significantly slowed in GCaMP3+ myocytes (Figure 4.13D-F). Interestingly, while this effect on $I_{Ca,L}$ inactivation was readily apparent during experiments in which no exogenous calcium buffer was added to the patch-pipette, they were ablated by the addition of EGTA to the intracellar solution (data not shown), suggesting that it involves interference with calcium- rather than voltage-dependent components of channel inactivation.

4.4 Summary

The present study makes a number of important contributions to the field. We report herein the first unambiguous action potentials from engrafted hESC-CMs, using a new optical mapping technology based on the simultaneous imaging of a graft-autonomous reporter of activation (hESC-CM grafts expressing GCaMP3) and the water-soluble voltage dye di-2-ANEPEQ. Further, we confirmed our earlier finding (see Chapter 2) that conventional lipophilic voltage dyes label host but not transplanted hESC-CM graft myocardium. We then used, for the first time in this context, the water-soluble voltage dye di-2-ANEPEQ to overcome this limitation and validated its utility as a reporter of both host and hESC-CM graft electrical activity. Using this new technology, we identified a number of potentially pro-arrhythmic properties of GCaMP3+ hESC-CM grafts derived from two common hESC lines (RUES2 and H7), including incomplete host-graft coupling, poor graft CV relative to host, aberrant and variable patterns of graft activation from beat to beat, and graft-induced ectopy.

Chapter 5: Development and Application of Matlab Scripts to Analyze Human Embryonic Stem Cell-Derived Graft and Host Cardiomyocyte Activity Ex Vivo

5.1 Introduction

The visualization of hESC-CM graft and host cardiomyocyte activity by genetically encoded and perfused fluorescent reporters has served as the basis for the discoveries of this body of work. In order to extract meaningful data from ex vivo imaging experiments of hESC-CM engrafted hearts, de novo analysis tools had to be created. The reason being is that interpretations of optical signals from hearts transplanted with hESC-CM grafts, which could activate independently from each other and the host, presents a unique challenge. While a number of labs in recent years have made code freely available to analyze imaging data of heart tissue activation after loading with a voltage dye ex vivo (e.g. the "Rhythm" analysis package from the Efimov group and open source code from the Rollins group), these analysis tools all had limitations that precluded their use to analyze hESC-CM engrafted hearts. To be useful for our studies, we required an analysis tool capable of quickly assessing host activation kinetics as well as the coupling and activation kinetics of several distinct hESC-CM graft regions simultaneously. Further, and as found using the tools explained below, graft activation can be variable on a beat-to-beat basis, thus ensemble averaging of graft-derived signals cannot be employed and the ability to map single-beat spatial activation kinetics of the inherently low hESC-CM graft-derived fluorescent signals is required.

Detailed in this chapter are the key steps implemented in the analysis of imaging data from hESC-CM engrafted hearts. The core capabilities mentioned above have been incorporated in these novel tools, written de novo in the Matlab environment. See the Appendix for this source code used to analyze GCaMP3+ hESC-CM graft-derived calcium signals and both host- and hESC-CM graft-derived voltage signals.

5.2 Matlab Code Development and Application

The overall workflow for the Matlab-based analysis of ex-vivo imaging data is summarized in Figure 5.1. The key steps identified are explained in detail below.

```
┌─────────┐      ┌──────────────┐      ┌──────────────┐
│         │      │ Import and   │      │ Spatially and│
│  START  │ ───→ │ time sync    │ ───→ │ temporally   │
│         │      │ imaging &    │      │ filter       │
│         │      │ Labchart data│      │ imaging data │
└─────────┘      └──────────────┘      └──────────────┘
                                                │
   ┌────────────────────────────────────────────┘
   ↓
┌──────────────┐      ┌──────────────┐      ┌──────────────┐
│ Visualize z- │      │              │      │ Remove signal│
│ score of     │      │ Output plot  │      │ drift, auto  │
│ filtered     │      │ of normalized│      │ detect peaks │
│ imaging data,│ ───→ │ ROI FI means,│ ───→ │ and valleys, │
│ then select  │      │ ECG, and stim│      │ normalize,   │
│ ROIs for FI  │      │ signals vs   │      │ then         │
│ mean plots   │      │ time         │      │ savitsky-    │
│ and/or       │      │              │      │ golay filter │
│ activation   │      │              │      │              │
│ maps         │      │              │      │              │
└──────────────┘      └──────────────┘      └──────────────┘
                                                    │
   ┌────────────────────────────────────────────────┘
   ↓
┌──────────────┐      ┌──────────────┐      ┌──────────────┐
│              │      │ Determine    │      │              │
│ Select time  │      │ activation   │      │              │
│ window for   │      │ time per     │      │              │
│ activation   │ ───→ │ pixel for    │ ───→ │     END      │
│ map          │      │ each         │      │              │
│ generation   │      │ activation   │      │              │
│ per ROI      │      │ within       │      │              │
│              │      │ selected time│      │              │
│              │      │ window, then │      │              │
│              │      │ plot in      │      │              │
│              │      │ pseudocolor  │      │              │
└──────────────┘      └──────────────┘      └──────────────┘
```

Figure 5.1. Work-flow of ex vivo imaging data analysis using developed Matlab scripts. Simplified work-flow of ex vivo imaging data analysis (ROIs = regions of interest, FI = fluorescence intensity).

5.2.1 Standardization of data acquisition

In order to develop Matlab-based analysis tools, the settings used to capture imaging data through the Andor iXon 860 EM-CCD cameras operated by Andor Solis and other data such as the host heart ECG, pacing stimuli, and camera fire signals recorded through a PowerLab 430 system operated by LabChart had to be standardized. This standardization is the basis for successful post-processing analysis, and was arrived at after iterations of modifying imaging acquisition settings and assessing the quality of results after post-processing. In brief, all GCaMP3+ hESC-CM

graft-derived calcium signals were captured with an exposure time of 5 ms for 2600 frames, which without frame transfer mode enabled resulted in an overall kinetic cycle time of ~7 ms (or ~150 frames per second) and an overall duration of recording of ~18 seconds. Pre-amp gain for these recordings was set at 4.5x with an EM gain of 300. All host- and graft-derived voltage signals were captured with an exposure time of 2 ms for 9000 frames, which with frame transfer mode enabled kept the overall kinetic cycle time at ~2 ms (or ~500 frames per second) with an overall duration of recording of ~18 seconds. Pre-amp gain for these recordings was set at 2.2x with an EM gain of 80. In LabChart, the host ECG signal was recorded in channel 1, pacing stimuli delivered to the heart in channel 2, the stimulus pulse delivered to the cameras to start simultaneous recording in channel 3, the camera fire signals from the camera dedicated to recording GCaMP3 signals in channel 4, and last the camera fire signals from the camera dedicated to recording voltage signals in channel 5. It is imperative that these acquisition settings be utilized if our Matlab scripts will be used for analysis.

5.2.2 Import and time sync imaging and Labchart data in Matlab

The first step in post-processing analysis is importing imaging and Labchart data into the Matlab environment and ensuring this data is properly time synced. To do so, imaging data must be exported from Andor Solis as a 16 bit unsigned raw data file, and the corresponding Labchart data saved as a text file without headers, comments, or event markers. After initializing the Matlab code, the user is prompted to enter information about the dataset as well as the full names of these files for importation.

Time syncing of these files is then accomplished by utilizing the camera fire signals within the text file and the known kinetic cycle time between frames.

5.2.3 Data filtering

Careful consideration went into the choice and sequence of filters applied to ex vivo imaging data. Early in code development it was evident that over processing of raw imaging data could alter optical signals such that their integrity was not preserved; alternatively, too little processing and signals could not be used for automated detection of peaks, valleys, and activation times. Thus, the choice and order of filter methods was selected after testing over 15 different combinations of spatial, frequency and temporal filters on random sets of actual imaging data.

In brief, the following processing steps are applied to raw imaging data: user-defined data mask to remove background pixel data, spatial filtering consisting of a median filter (3x3) and then cone filter (width 3, slope 1), user-defined lowpass FIR filter (100Hz typical), and finally temporal filtering consisting of a median filter (width 3) and then a moving average filter (width 5). Next the first and last 15 frames are removed to get rid of the effects from filtering, and a polynomial curve fit used to remove global drift (to remove any photobleaching over the course of the 18 seconds recorded). The ECG data is also curve fit and baseline corrected by use of savitzky-golay and moving average filters.

Figure 5.2 displays the processing of data from a single active pixel of an uninjured and di-2-ANEPEQ loaded heart imaged ex vivo. As can be seen, the initially noisy fluorescent voltage signal from this single pixel has been successfully processed

to produce a signal that can be used for interpretation. Note that this assessment is printed to screen each time an analysis is performed so that the user can ensure proper processing has been implemented.

Raw Data

After Spatial 3x3 Median Filter

After Spatial 3x1 Cone Filter

After Temporal 100Hz Lowpass Filter

After Temporal 3-width Median Filter

After Temporal 5-width Moving Average Filter

Overlay of Final Filtered Signal Over Raw Data
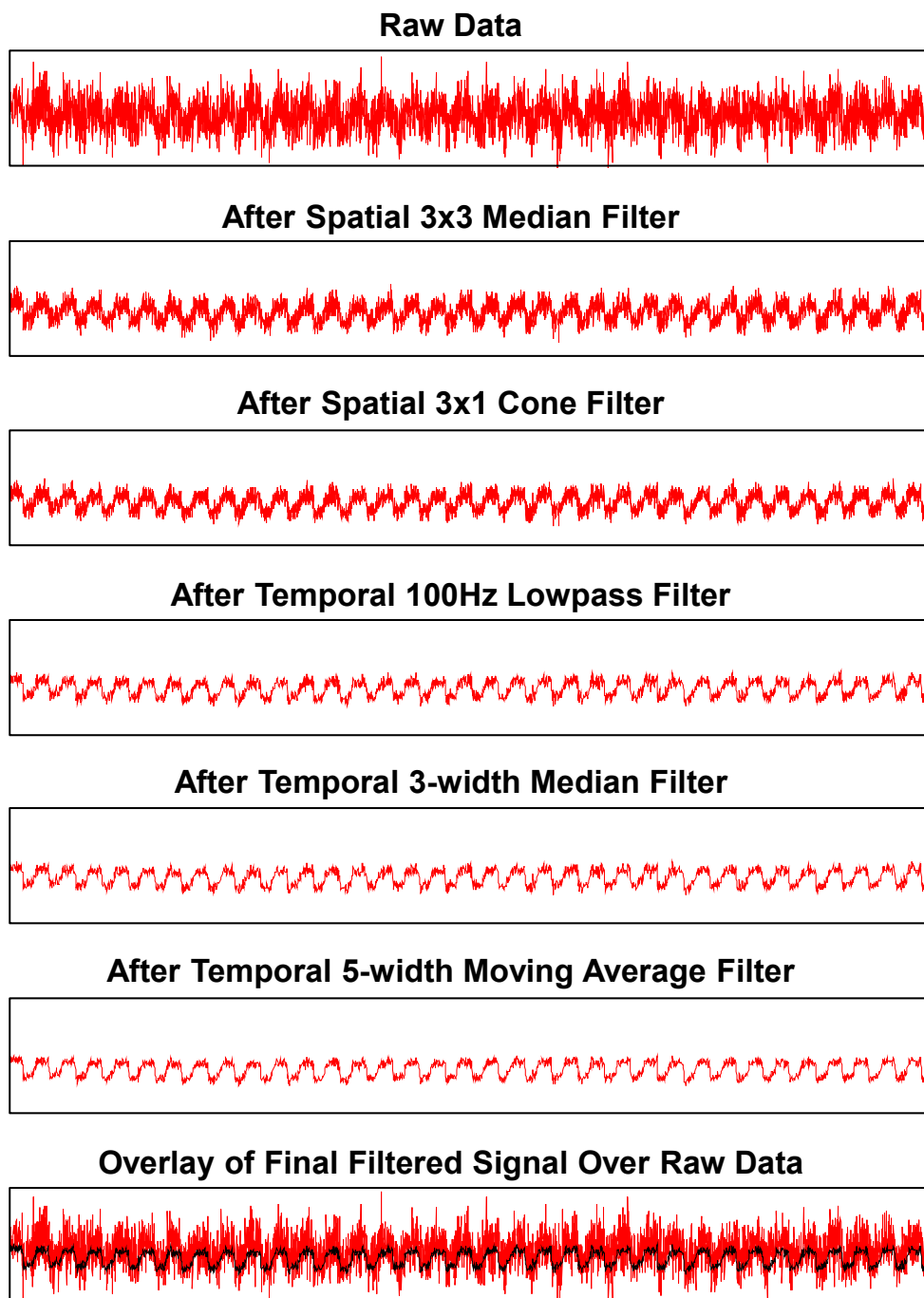
Figure 5.2. Careful selection of filters preserves signal integrity while reducing noise. Plotted is the raw fluorescence data of a single active pixel from a di-2-ANEPEQ loaded heart imaged ex vivo, along with the change in this raw data after the sequential filtering steps we found to preserve signal integrity yet reduce noise. 10 seconds plotted, all with the same y-axis range. Note this data is plotted before signal inversion has been performed, and represents typical results.

Last, before data is visualized to screen for ROI selection, the user is prompted to input whether or not the data needs to be inverted. For signals that increase in fluorescence upon activation, such as those from GCaMP3, no inversion is required; however, for signals that decrease in fluorescence upon activation, such as those from myocardium loaded with RH237 or di-2-ANEPEQ, the signals must be inverted for later peak detection.

5.2.4 Data visualization for ROI selection

To identify active graft and/or host regions for region of interest (ROI) selection, the z-score of each pixel through time is calculated and then visualized to the screen in pseudocolor. Visualization of the z-score, versus the processed data, was chosen because it allowed for the easier discrimination of active regions. Then as standard, a pseudocolored movie of this z-scored activity is saved to file at $1/10^{th}$ recorded speed. Using the displayed z-score data, the user is prompted to enter the number of ROIs and to select them in free-form from a standard deviation image printed to the screen.

5.2.5 Data plots and ROI summary data

After selecting the number of ROIs, be it either independent graft regions or host tissue, the mean fluorescence intensity of each ROI is calculated and normalized to the ROI mean with the max range. These ROI means are then plotted against time with the pacing stimuli and host ECG (vertically stacked upon one another). If graft ROIs were selected, this plot is used to determine the extent of host-graft coupling by comparing the pacing stimuli and/or ECG to the mean fluorescence activity of the graft ROIs.

Further drift removal is implemented if necessary, before a corresponding still image of the heart is generated (with ROI boundaries color-coded and numbered to match the ROI data plots) before all figures are saved to file. Note that this method of displaying all ROI, ECG, and pacing stimuli data on one plot versus time has greatly increased the efficiency of data analysis.

In addition to the still image and corresponding ROI data plot, other information such as the area and activation frequency of each ROI are printed to screen. The activation frequency of each ROI is determined by finding the dominant frequency of the ROI mean after conversion to the frequency domain. The average period for the ROI mean is then found from this dominant frequency, and input into an automatic peak detection algorithm used to find the start and peak of each ROI activation. These identified starts and peaks are then demarked on a plot printed to screen, where the user can modify the search length modifier of the algorithm until all starts and peaks are determined correctly. Note that, by feeding into the peak detection algorithm the ROI mean period, auto-detection of the starts and peaks is typically correct the first time. Also note that this process is performed for each ROI selected.

5.2.6 Additional processing for activation maps

While the activation of ROIs can be visualized by pseudocolored movies, creating 2D pseuodocolored activation maps requires additional post-processing. Again here, much consideration went into the method for carefully removing remaining noise so that algorithms in Matlab could be used to auto-determine spatial activation times on a per-pixel basis.

The first step taken is to normalize the imaging data on a per-pixel basis through time so that peak fluorescence corresponds to "activated" (i.e. depolarized) and baseline fluorescence corresponds to "resting." Next, imaging data is filtered by a savitzky-golay filter with settings found to consistently produce good results on a number of sample datasets, and the first and last 80 frames are removed to get rid of the effects from filtering. Again here, to ensure this critical filtering step which is necessary to remove remaining noise has been performed effectively, the results of filtering are printed to screen. A pseuodocolored movie of activation for selected ROIs is sent to the screen for the user to examine, and movies of actual and 1/10th speed saved to file.

The last steps before determining ROI spatial activation maps are to re-calculate the mean of each ROI and, using the same method described in section 5.2.5 above, auto-determine the start and peak of each activation on an individual ROI basis. Again here the user can modify the search length modifier of the algorithm until all starts and peaks are determined correctly. Note this step is critical for the determination of activation times, since the algorithm written for auto-detection will search between the start and peak of each activation of each ROI.

5.2.7 Activation time maps and histogram plots

The first step to auto-determine spatial activation time maps is to define the time window, per ROI, containing activations to be mapped. There is no limit here to the number of activations that can be mapped per ROI, which is a great advantage of this code. In selecting a time window, a time point before a start and a time point after a

90

peak should be selected so that each activation of an ROI has a paired start and peak for the search algorithm. Once this is done, the time associated with the maximum slope between these starts and peaks is determined on a single-pixel basis and stored in a matrix corresponding to each activation. These matrices, when pseuodocolored, are the spatial activation time maps, and they are printed to screen as well as automatically saved to file. In addition, activation time histogram plots are generated for each activation, printed to screen, and saved.

5.4 Summary

The Matlab code described herein for the analysis of hESC-CM engrafted hearts imaged ex vivo allows for the fast assessment of host activation kinetics, the extent of graft coupling, and graft activation kinetics. By allowing for multiple ROIs to be analyzed simultaneously and on a per-beat basis automatically, this code greatly increases the efficiency of data analysis. Further, by making the analysis process steps transparent and allowing for user feedback during implementation, the signal integrity of the inherently small dynamic signals recorded by ex vivo imaging of hESC-CM engrafted hearts can be preserved. These novel tools are a clear advancement over existing tools available that are limited to single ROI analysis and require user intervention to assess individual beat behavior.

Chapter 6: Gap Junction Modifiers to Improve the Electrical Integration and Activity of Human Embryonic Stem Cell-Derived Cardiomyocyte Grafts in Injured Hearts

6.1 Introduction

The overall goal of the work described in this Chapter is to the hypothesis that treatment with gap junction modifiers (GJMs) will improve the electrical integration and function of hESC-CM grafts after transplantation into injured hearts. Since the heart functions as an electrical syncytia, electrical integration is necessary for the graft to contribute new force-generating units. Using the guinea pig, we have shown that hESC-CM grafts are capable of coupling and beating synchronously with host heart muscle, but their integration is typically imperfect as described in Chapters 2 through 4. Most hearts show large islands of graft muscle that fire in no relation to the host sinus rhythm, with slow and variable patterns of activation. This is understandable, given the injury region in which hESC-CM grafts are located has insulating fibrosis and is a hypoxic environment likely to promote gap junction uncoupling via connexin-43 (Cx43) dephosphorylation[109, 110, 136]. To overcome this dilemma, we explore the novel approach of treating hESC-CM engrafted hearts with GJMs, which are peptide drugs that have been shown to prevent or reverse the dephosphorylation of Cx43 by factors like ischemia and elevated $[Ca^{2+}]_I$.

While current clinical investigations with GJMs have focused on the anti-arrhythmic potential of these small molecule drugs[136, 137], we are the first to test their ability to improve the electrophysiological behavior of hESC-CMs after transplantation

into injured hearts. Our work with the canonical GJM, AAP10[138-142], as well as its more stable and clinically relevant analogue Rotigaptide[136, 137, 143-146], give this work excellent translational potential.

6.2 Materials and Methods

6.2.1 Production of WT and GCaMP3+ hESC-CMs

Please see section 2.2.1 for details regarding the production of WT RUES2 hESC-CMs used here for in vitro screens and GCaMP3+ H7 and RUES2 hESC-CMs used for transplantation studies involving GJMs.

For in vitro hESC-CM Cx43 rescue experiments, WT RUES2 hESC-CM cultures were enzymatically dispersed to single-cells and replated onto gelatin- and polyethylenimine-coated glass coverslips at $2x10^5$ hESC-CMs per coverslip as previously described[66] to form small interconnected clusters. For Western Blot preparations, WT RUES2 hESC-CM cultures were left in the 6-well plate format used to induce differentiation, corresponding to $\sim3x10^6$ hESC-CMs per well.

6.2.2 In vitro rescue of Cx43 dephosphorylation in hESC-CMs by GJMs

To assess the ability of GJMs to rescue Cx43 dephosphorylation, we exposed hESC-CMs in vitro to the gap junction uncoupler aconitine (1 µM)[147, 148] via media for 30 minutes, followed by 20 minutes incubation with either media alone, media plus AAP10 (100 nM), or media plus control peptide (100 nM). The untreated group received changes of media at matched 30 and 20 minute timepoints. Samples were then fixed for further analysis. We also performed similar experiments using the less labile AAP10

analogue Rotigaptide, but instead with high (100 nM) and low (45 nM) doses of Rotigaptide versus its peptide control (100 nM).

6.2.3 Cx43 immunofluorescence and analysis

We dual immunofluorescently stained clusters of wild-type RUES2 hESC-CMs for phosphorylated Cx43 at serine 368 (rabbit polyclonal primary with 488 fluorescent secondary) and total Cx43 (mouse monoclonal primary with 594 fluorescent secondary) after Solan et al.[149] following the gap junction uncoupling challenge and treatments described in section 6.2.2 above. Fixed samples were then Hoechst counterstained and imaged on a Nikon A1R confocal microscope in frame scan mode. 10 scans at random were taken per sample, moving from one side of the sample to another, with 12 samples minimum per group. Image analysis was performed using custom scripts written in Matlab with final readout being the ratio of phosphorylated to total Cx43 per cell. For this, we utilized the blue (nuclear) channel to determine the number of cells per field, as well as to create a mask to delete from the green (phosphorylated Cx43) and red (total Cx43) channels so that when pixel counts were taken to assess the output ratio, nuclear staining which is not of interest was removed from the analysis. All analyses were assessed with identical pixel intensity thresholds.

6.2.4 Cx43 western blotting

Western blotting for phosphorylated and total Cx43 at serine 368 was performed on wild-type RUES2 hESC-CMs following the gap junction uncoupling challenge and treatments described in section 6.2.2 above per Solan et al[149].

6.2.5 Cardiac cryoinjury and GCaMP3+ hESC-CM transplantation

All animal procedures adhered to protocols approved by the University of Washington Institutional Animal Care and Use Committee (IACUC) and were conducted in accordance with federal guidelines. Please see sections 2.2.2 and 3.2.2 for details regarding our methods for the cardiac cryoinjury procedure and intra-cardiac cell injection. Note studies here were performed in subacutely (10 days between injury and cell transplantation, n=8) and chronically (28 days between injury and cell transplantation, n=2) injured guinea pig hearts transplanted with 1×10^8 GCaMP3+ H7 hESC-CMs, and subacutely (n=13) injured guinea pig hearts transplanted with 1×10^8 GCaMP3+ RUES2 hESC-CMs.

6.2.6 Acute treatment of AAP10 on injured and GCaMP3+ hESC-CM engrafted hearts ex vivo

Please see sections 2.2.3 and 3.2.3 for details regarding our methods for the ex vivo imaging of injured and GCaMP3+ hESC-CM engrafted guinea pig hearts. In pilot studies, we first imaged subacutely (n=8) and chronically (n=2) injured guinea pig hearts transplanted with GCaMP3+ H7 hESC-CMs before and during the perfusion of AAP10 (100 nM, GenScript, Piscataway, NJ, USA) in 2,3-butanedione monoxime (20mM, Sigma-Aldrich, St. Louis, Missouri, USA)) containing Langendorff buffer. These studies informed the properly controlled and dedicated experiments to test the capacity of AAP10 (100 nM, n=5) versus control peptide (100 nM, n=8) to mediate improvements in GCaMP3+ RUES2 hESC-CM graft function two-weeks after transplantation into

subacutely injured hearts. For this, once hearts were harvested, cannulated, and electrically stabilized ex vivo, we arrested motion by perfusing blebbistatin (10μM, Cayman Chemical, Ann Arbor, Michigan, USA) containing buffer, then switched to blebbistatin- and peptide-containing buffer for 30 minutes, followed by a 30 minute washout by switching back to blebbistating-containing buffer only. Hearts were paced just above their sinus rate (3.5-4 Hz) to remove heart rate as a confounding variable. Additionally, 0.05% BSA was added to all perfusion buffers to block the internals of our Langendorff system, and all peptide-containing buffers were prepared immediately before use.

6.2.7 Statistical analysis

GraphPad Prism (GraphPad Software, La Jolla, California, USA) was used to perform all statistical analyses. To test for the ability of GJMs to rescue Cx43 phosphorylation, the results from Matlab analyses of Cx43 immunofluorescence were compared using 1-way ANOVA with Tukey's multiple comparison test correction. A p value less than 0.05 was considered significant.

6.3 Results

6.3.1 GJM treatment rescues hESC-CM Cx43 dephosphorylation in vitro

To test the hypothesis that GJMs can rescue the phosphorylation status of hESC-CMs in vitro, we subjected clusters of hESC-CMs to the gap junction uncoupler aconitine followed by AAP10 or its stable analogue Rotigaptide and matched control peptides. We then fixed these samples and assessed for total and phosphorylated

Cx43 expression by immunofluorescence and western blot. Confocal images of immunofluorescently stained samples were quantitated by the use of custom Matlab scripts to assess the ratio of phosphorylated Cx43 to total Cx43 on a cellular basis after removal of nuclear staining. While we still consider this work to be preliminary, treatment with GJMs had the clear trend of increasing the ratio of phosphorylated to total Cx43 in hESC-CMs after the dephosphorylation of Cx43 by aconitine, consistent with a rescue of this parameter (see Figure 6.1). Further, GJM treatment appeared to enhance the phosphorylation status of hESC-CMs in vitro above baseline levels.
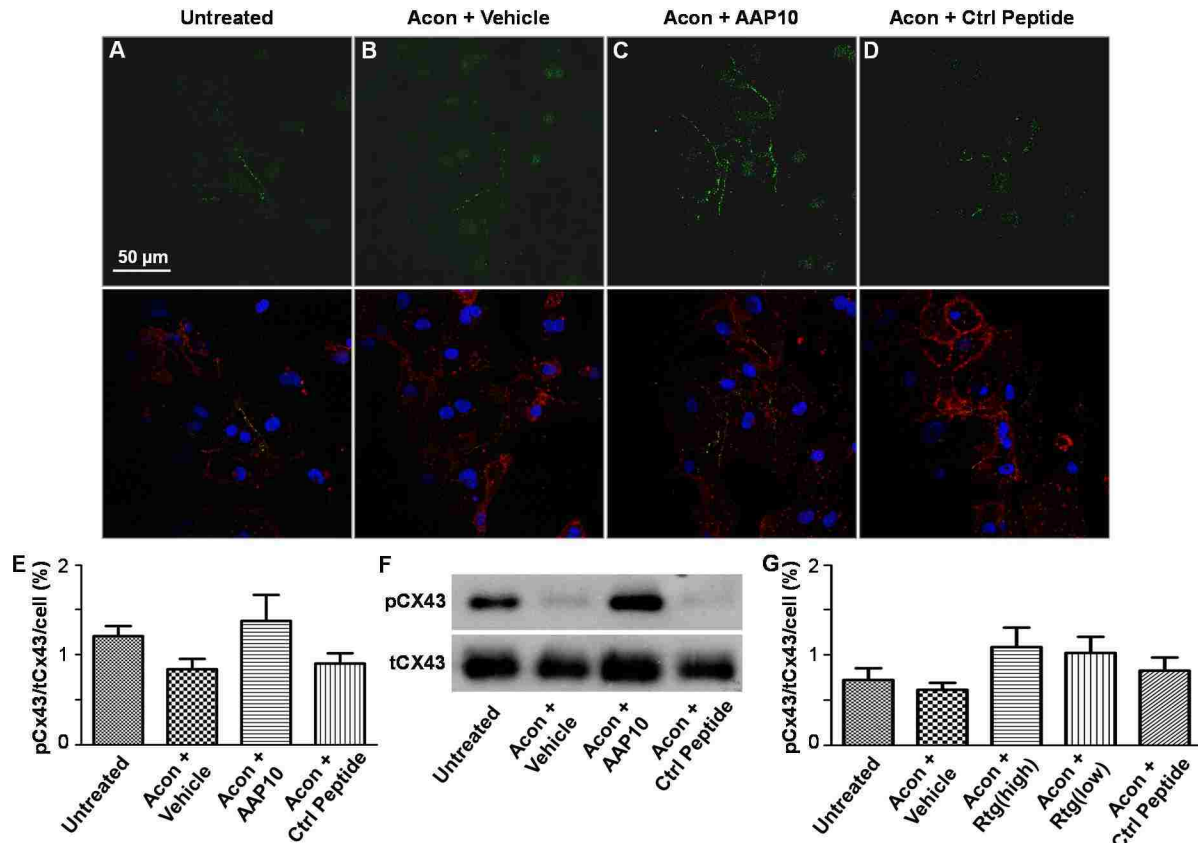
Figure 6.1. Gap junction modifiers rescue hESC-CM Cx43 dephosphorylation in vitro. A-D: Cx43 phosphorylation rescue experiment performed on clusters of hESC-CMs in vitro; upper panels show confocal images of hESC-CMs immunofluorescently labeled for phosphorylated Cx43 at serine 368 (green), bottom show merge with labels for total Cx43 (red) and nuclei (blue). Specifically, panels show baseline hESC-CMs in culture (**A**), and hESC-CMs treated with 30 minutes of aconitine (Acon) followed by: 20 minutes of vehicle (**B**), 20 minutes of AAP10 (**C**), and 20 minutes of control peptide (**D**). **E:** Quantitation of images from **A-D**, expressed as the percentage of phosphorylated Cx43 (pCx43) to total Cx43 (tCx43) per cell after removal of nuclear labeling. Data includes analysis of greater than 12 images per group (n>190 cells per group). Reassuringly, aconitine-mediated dephosphorylation of hESC-CM Cx43 was reversed by AAP10 but not the control peptide. **F:** Western blot results after performing the same Cx43 phophorylation challenge described in **A-D** on hESC-CMs in culture. Here also we see AAP10 treatment alone was able to rescue aconitine-mediated hESC-CM Cx43 dephosphorylation. **G:** Cx43 rescue experiment performed on clusters of hESC-CMs in vitro, as described in **A-D** except with the more stable AAP10 analogue Rotigaptide (Rtg). Data includes analysis of greater than 7 images per group (n>100 cells per group). Note that both a high and low dose of Rotigaptide were tested, and both rescued Cx43 phosphorylation. Unexpectedly, the control of scrambled Rotigaptide also rescued Cx43, but to a lesser extent.

6.3.2 GJM treatment improves H7- but not RUES2-derived GCaMP3+ hESC-CM graft coupling in injured hearts

The promising result that GJMs can improve the phosphorylation status of hESC-CMs after a gap junction uncoupling challenge in vitro led us to test their capacity to mediate short-term improvements in the coupling and conduction velocity of hESC-CM grafts transplanted into injured hearts. For this, we first transplanted GCaMP3+ H7 hESC-CMs into cryoinjured guinea pig hearts (n=10), and later imaged them ex vivo using a modified Langendorff preparation after mechanical arrest with BDM. We then used the graft-derived GCaMP3 signal to quantitatively assess the extent of graft coupling and activation kinetics before, during, and after the addition of AAP10 the Langendorff perfusate. As shown in Figure 6.2, acute treatment with AAP10 improved these measured parameters in H7-derived GCaMP3+ hESC-CM grafts. Notably, 4 of 7 hearts with imperfectly coupled grafts before treatment improved significantly in this parameter after 10 minutes of AAP10 perfusion, as assessed by comparing the graft-derived GCaMP3 signal to the host ECG (3 of the 10 hearts were excluded because they contained 100% coupled graft at baseline, and so no further improvement was possible in this parameter). AAP10 treatment also mediated an improvement in GCaMP3+ H7 hESC-CM graft conduction velocity, assessed by mapping the kinetics of the graft-derived GCaMP3 fluorescence signal. Figure 6.2D shows a representative graft region coupled to the host at baseline that took 45 ms to completely activate initially, but after AAP10 treatment activated fully in 27 ms, demonstrating an increase in conduction velocity from 2.3 cm/s to 3.9 cm/s.
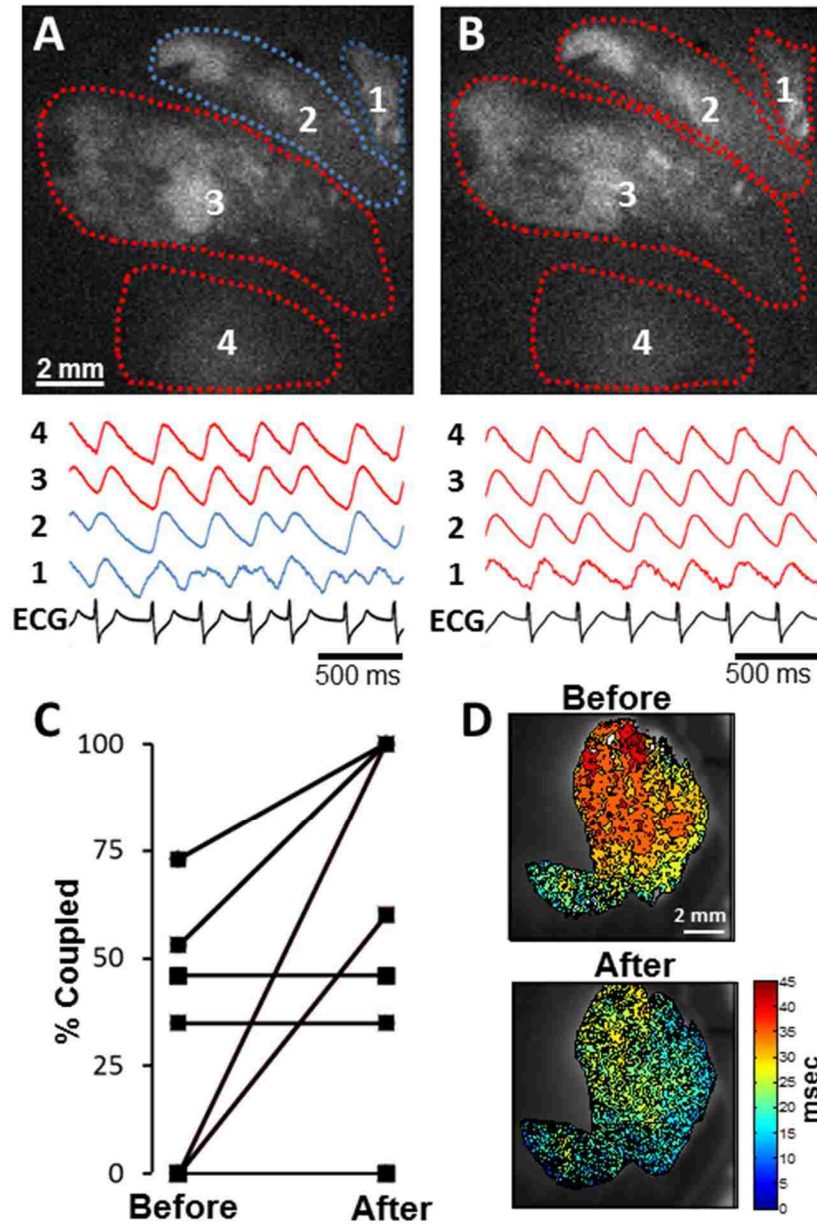
Figure 6.2. Acute treatment with AAP10 ex vivo improves the coupling and activation of GCaMP3+ H7 hESC-CMs in injured hearts. A-B: An injured and GCaMP3+ H7 hESC-CM engrafted heart with four distinct graft regions imaged ex vivo; shown is the calcium activity of all four graft regions before and after AAP10 treatment by the Langendorff perfusion. Note that before AAP10, graft regions 1&2 were not coupled to the host (see regions and traces marked in blue), however after AAP10 these regions activated in sync with the host and the already coupled graft regions (shown in red). **C:** % of coupled graft area for 7 injured and GCaMP3+ H7 hESC-CM engrafted hearts before and after AAP10. 4 of 7 hearts showed a robust improvement in coupling after AAP10; 3 hearts were excluded because they exhibited 100% coupling at baseline. **D:** GCaMP3+ H7 hESC-CM graft activation maps before and after AAP10. Notice the great reduction in the time required for complete activation, consistent with an increase in graft CV from 2.3 to 3.9 cm/s.

The positive results of acute AAP10 treatment on the electrical behavior of GCaMP3+ H7 hESC-CM grafts in injured hearts led us to perform properly controlled experiments with transplanted GCaMP3+ RUES2 hESC-CMs. For this, we similarly transplanted GCaMP3+ RUES2 hESC-CMs into cryoinjured guinea pig hearts and examined graft electrical behavior ex vivo after acute treatment with AAP10 (n=5) or control peptide (n=8). After discovering the potential for adverse effects from BDM on graft electrical behavior (as described in Chapter 2), we switched to blebbistatin as our preferred mechanical uncoupling agent for these ex vivo imaging experiments. In the control peptide group at baseline, we found only 2 of the 8 hearts had regions of coupled GCaMP3+ RUES2 hESC-CM graft, with the caveat that the coupled graft region in one of these hearts was directly adjacent to healthy host tissue at the injury border zone, and completely within healthy host tissue in the other heart. As expected from our in vitro studies with RUES2 hESC-CMs, the control peptide had no effect on GCaMP3+ RUES2 hESC-CM graft coupling in any of the hearts examined. Separately, in the AAP10 treatment group, none of the 5 hearts at baseline displayed evidence of host-graft electrical coupling. Unexpectedly, however, none of the 5 hearts showed an improvement in this parameter with acute AAP10 treatment. Since this negative result could likely be attributed to a lack of host-graft physical contact, we sought next to assess for improvements in GCaMP3+ RUES2 hESC-CM conduction velocity as found in H7-derived counterparts with AAP10 treatment. Unexpectedly, the signal quality from transplanted GCaMP3+ RUES2 hESC-CM grafts was too poor to make any assessments of improvement in function before and after AAP10 treatment. Intrigued, we investigated by histology and found that all transplanted GCaMP3+ RUES2 hESC-

CM grafts were heterogeneous for GCaMP3 expression (data not shown). As this was our first experience transplanting GCaMP3+ RUES2 hESC-CMs, this finding was not anticipated, and led us to cease a continued investigation of AAP10 treatment on GCaMP3+ RUES2 hESC-CM engrafted hearts.

6.4 Summary

Our work described here with GJMs presents a new and promising approach to improve the function of hESC-CM grafts after transplantation into injured hearts. We found both the canonical GJM AAP10 and its more stable and clinically relevant analogue Rotigaptide have the ability to rescue Cx43 phosphorylation of hESC-CMs after a gap junction uncoupling challenge in vitro. This ability extended to hESC-CM grafts transplanted into injured hearts, where the injury environment is suspected to reduce gap junctional coupling by Cx43 dephosphorylation. Indeed, we found acute AAP10 treatment ex vivo mediated robust improvements in the electrical coupling and conduction velocity of GCaMP3+ H7 hESC-CM grafts transplanted into injured hearts. However, these same robust improvements were not found in equivalently injured and GCaMP3+ RUES2 hESC-CM engrafted hearts.

Chapter 7: Discussion

The work described here makes a number of important contributions to the study of hESC-CMs as a therapy for heart repair after injury. Using the guinea pig and hESC-CMs expressing the fluorescent calcium sensor GCaMP3, we found the first direct evidence that hESC-CMs can integrate electrically in host hearts after transplantation, including in uninjured (see Chapter 2), recently injured (see Chapter 2), and chronically injured (see Chapter 3) hearts. Further, after attempting to map both host and hESC-CM graft electrical activity and finding conventional methods could not label grafts (see Chapters 2 and 4), we developed a new optical mapping technology based on the combined imaging of grafts expressing GCaMP3 and the water-soluble voltage dye di-2-ANEPEQ (see Chapters 4 and 5). Below follows a discussion of our various findings using these developed technologies along with their implications and limitations.

7.1 GCaMP3+ hESC-CM graft coupling in recipient hearts

With GCaMP3 as a graft-direct readout of graft activity, and an animal model with a heart rate more closely matched to humans (guinea pigs with a sinus rate 200-240 bpm), we observed unambiguous evidence for the ability of hESC-CMs to couple with host hearts. Previous studies in mice and rats, while necessary to build this therapy and prove still to be a testbed for discovery, did not serve as the best models to assess electrical integration due to their high intrinsic heart rates (~600 and ~450 bpm, respectively). In the guinea pig, we found hESC-CMs derived from the transgenic GCaMP3+ H7 hESC line coupled with intact host hearts 100% of the time. This

complete coupling, presumably due to many points of host-graft contact, also led to fast activation of hESC-CM graft tissue (see Chapter 2).

With established success in uninjured hearts, we moved on to test the capacity of hESC-CMs to couple in recently injured hearts using the same GCaMP3+ H7 hESC-CMs (see Chapter 2). In particular, we wanted to test whether the improvements in mechanical function and protection from arrhythmias could be explained by direct graft electromechanical coupling. We found GCaMP3+ H7 hESC-CM grafts to couple in 1:1 synchrony with host hearts ~60% of the time (4 of 7 hearts, with the area of coupled graft ranging from 55 to 95%), perhaps explaining the improvements in function in parallel experiments. Interestingly, and not altogether unexpectedly (see Discussion section 7.1.4 below), the activation kinetics of coupled graft regions located completely within the injury region were much slower than grafts residing within healthy host tissue. Thus, although this observed phenomenon of coupled but slowly activating graft theoretically pre-disposed recipient hearts to re-entrant phenomenon, such electrical disturbances were not observed.

Next we tested the ability of GCaMP3+ hESC-CM grafts to electrically integrate in guinea pig hearts with fully established scars (see Chapter 3). In this model, which represents the context in which hESC-CM therapy would likely first commence in the clinic, graft electrical coupling was found to be more limited. Only ~38% of recipient hearts were found to contain electrically integrated grafts (5 of 13 hearts, with the area of coupled graft ranging from 3 to 100%). This outcome likely explains our observation in parallel experiments in this model of no beneficial effects of hESC-CM transplantation on host heart mechanical function.

There are several reasons why the aforementioned studies in the guinea pig had such different outcomes. First, these experiments were not matched, so differences in cell dosage cannot be ruled out (see sections 2.2.2 and 3.2.2). Further, the subtle differences in the injuries created or the success of hESC-CM engraftment could be attributed to multiple personnel being involved in the surgical procedures. However, the most likely explanation for differences between outcomes in recent versus established injuries is attributable to the more hostile environment of the chronically injured hearts, where already established adverse remodeling and a greater extent of fibrosis are expected to oppose hESC-CM graft survival, integration, and potential mechanical benefits.

To further evaluate differences in hESC-CM engraftment between these established guinea pig cardiac injury models, test for differences between CMs derived from two common hESC lines (RUES2 and H7), and investigate host-graft electrical interactions directly, we developed an optical mapping technology using the same GCaMP3 hESC-CMs and the voltage dye di-2-ANEPEQ. A discussion of this work (detailed in Chapter 4) is provided next.

7.2 Optical mapping of hESC-CM graft electrical activity in injured hearts

hESC-CMs have emerged as an attractive cell source for cardiac repair, but, given concerns about the risk of graft-related arrhythmias, progress in the field will require new tools to investigate the electrophysiological properties of engrafted hearts. Optical mapping is an obviously attractive experimental modality for this application, and

our efforts to apply this technology in the work of Chapter 4 led to a number of observations of interest. First, we confirmed our earlier findings (see Chapter 2) that it can be challenging to distinguish between hESC-CM graft- and host-derived optical voltage signals; in fact, in our hands, conventional lipophilic voltage dyes do not even label hESC-CM graft tissue at all. To overcome this problem, we tested a novel strategy based on the simultaneous imaging of a graft-autonomous reporter of activation (hESC-CM grafts expressing GCaMP3) and the water-soluble voltage dye di-2-ANEPEQ (which stains both graft and host). This approach allowed us to acquire the first, unambiguously *graft-derived* oAPs from hESC-CM tissue in injured hearts, plus it revealed potentially pro-arrhythmic behavior by hESC-CM graft tissue including incomplete host-graft coupling, slow graft CVs, spatially abnormal patterns of graft activation that varied from beat to beat, and graft-induced ectopy.

The imaging system described in Chapter 4 has a number of important advantages that warrant further discussion. Its principal advantage is that, while earlier studies employing conventional, lipophilic dyes to study hESC-CM electrical activity should probably be interpreted with caution, our approach provides two independent means of distinguishing between graft- and host-derived electrical signals. First, we were able to verify all apparent graft-derived oAPs by correlating them with the simultaneously-acquired, graft-autonomous GCaMP3 signals. Moreover, the differential labeling kinetics of di-2-ANEPEQ in host and graft tissue provided a second way of confirming the origin of oAPs obtained using this voltage-sensitive dye. While di-2-ANEPEQ does eventually label both compartments, we found that it stains and washes out of host tissue much more rapidly than it does from graft. Hence, we were able to

separate between the two signals by performing serial wash-in and washout experiments: only host-derived oAPs were observed at early time-points during dye wash-in, while graft-derived oAPs (occurring in synchrony with GCaMP3 transients as expected) could be isolated at later time-points during dye washout. As an aside, this differential time-course of di-2-ANEPEQ labeling between graft and host is likely a consequence of the relatively poor perfusion of graft tissue, and this fact should be kept in mind during experiments in which engrafted hearts are treated with pharmacological agents that may take longer to reach the graft.

Optical mapping with di-2-ANEPEQ, while powerful, does come with its disadvantages. First, in contrast to lipophilic dyes which are typically introduced in a bolus, di-2-ANEPEQ has to be constantly perfused into the heart (via a recirculation loop) to maintain oAPs. While we did not observe differences in the electrical activity of hearts loaded with either di-2-ANEPEQ or RH237, off-target effects are always a potential concern when agents need to be continuously applied for long periods of time. Second, wash-in and wash-out experiments can be tedious and technically challenging to perform, and they provide a relatively narrow time-window for pharmacological or electrophysiological challenges because graft oAPs can only be reliably isolated and detected for ~10 minutes during dye wash-out. Further, serial wash-in and wash-out increases the total duration of each imaging experiment, thereby requiring an ex vivo heart preparation that is stable for up to 1.5 hours.

Despite these disadvantages, the imaging approaches employed in Chapter 4 allowed us to acquire important new insights into the electrophysiological properties of hESC-CM grafts in injured hearts. In addition to acquiring previously unknown

parameters such as paired graft and host CV and graft APD, we observed host-graft

electrical interactions directly by imaging an electrically coupled graft and found that it

could both ectopically pace the host as well as follow host-led beats. Some discussion

is necessary then to reconcile this and the other pro-arrhythmic properties of

transplanted hESC-CM grafts observed in this work to our earlier finding that hESC-CM

transplantation mediated an arrhythmia suppressive effect. Using the same subacute

guinea pig cardiac injury model, we previously found the transplantation of hESC-CMs

resulted in a small reduction of spontaneous arrhythmias (assessed by telemetric ECG)

but a large reduction in induced arrhythmias by programmed electrical stimulation

protocols in the intact animal[80]. Since ECG measures alone do not afford the same

spatiotemporal resolution of our optical mapping strategy employed here in ex vivo

preparations, we cannot rule out the presence of graft-induced ectopy in our prior work

if graft activation rates were closely matched to host sinus rates. However, it is likely

the high heart rate of the guinea pig (>200 beats per minute) succeeds in masking graft-

related arrhythmias.

Unexpectedly, we found stark differences in oAPDs and host-graft coupling

between GCaMP3+ hESC-CM grafts derived from RUES2 and H7 hESC lines, with

RUES2 derivatives universally displaying ultra-long oAPDs and seemingly lacking the

capacity to electrically couple with host hearts. All other parameters, including

histological assessments of recipient heart LV size, scar size and graft size, as well as

optical measures of recipient host CV, graft CV and graft size, were not significantly

different. We believed these characteristics of GCaMP3+ RUES2 hESC-CMs could be

a function of GCaMP3 expression itself, and indeed through optical techniques and

patch clamping in vitro found impaired $I_{Ca,L}$ inactivation relative to WT equivalents. H7 hESC-CMs were also negatively affected electrophysiologically by the expression of GCaMP3, however not to the same degree as RUES2 hESC-CMs. One hypothesis to explain this apparent discrepancy is that a greater outward rectifying potassium current density could rescue the phenotype in H7s, similar to the rescue of action potential durations observed by Mahajan et al[150] after delivering potassium channel agonists in a similar context.

Altogether, this finding of GCaMP3-mediated APD prolongation was not anticipated since mice hearts with systemic and cardiomyocyte-restricted overexpression of GCaMP3's predecessor, GCaMP2, displayed normal APDs as measured by RH237[116] as well as seemingly normal cardiac function. Further, we are not aware of any reports describing this off-target effect on cellular electrophysiology. Interestingly, here we found the GCaMP3-mediated APD prolongation diminishes with increased rate to a significant degree only in GCaMP3+ H7 hESC-CMs, perhaps explaining why we previously found coupled GCaMP3+ H7 hESC-CM grafts could keep pace with host hearts at pacing rates >5Hz[80]. We suspect then that the near complete lack of GCaMP3+ RUES2 hESC-CM graft coupling is a direct result of the electrical mismatch created between these graft cells and host myocardium by GCaMP3 expression, i.e. grafts are electrically refractory and cannot sync with host myocardium due to their abnormally long APDs.

Instead of pursuing the root cause of GCaMP3-mediated idiosyncratic effects, it would be more fruitful to force the hESC expression of a voltage sensitive protein to measure hESC-CM graft-derived optical voltage transients directly, such as VSFP2.3

after Chang Liao et al.[151] have done in the mouse. Combined with a spectrally separate

lipophilic voltage dye, which we have shown does not label graft tissue, optical mapping

of host and graft electrical activity could be accomplished. However, voltage-sensitive

proteins with better kinetics and dynamic fluorescence range would likely be required to

faithfully visualize transplanted hESC-CM grafts. Indeed, we have initiated work with

hESC-CMs expressing different voltage sensitive proteins to measure graft voltage

activity directly after transplantation (see Future Directions 8.2). Until this strategy

becomes standard, our strategy of di-2-ANEPEQ imaging is a valuable tool to study

transplanted grafts in injured hearts.

While the imaging of hearts with uncoupled grafts was useful for validating di-2-

ANEPEQ as both a host and hESC-CM graft electrical reporter, and a number of pro-

arrhythmic properties were observed from these studies, in the end these hearts could

not provide *direct* insights as to a mechanistic basis for the transient arrhythmias

observed in the recently reported non-human primate infarct mode[115]. After switching

from a chronic to a subacute guinea pig model of cardiac injury with GCaMP3+ H7

hESC-CM grafts, we finally observed a heart with a completely coupled graft. In this

heart, the coupled graft could follow sinus rhythm host-led beats as well as ectopically

pace the heart. Overdrive suppression by pacing at the LV apex abolished graft ectopy,

where instead the graft followed pacing just as with sinus rhythm beats. While this data

cannot rule out reentrant phenomena as a likely contributor to the aforementioned

arrhythmias in the non-human primate (especially considering the very slow graft CVs

measured here), nor can we discount the idiosyncratic effect of GCaMP3 expression in

these coupled RUES2 hESC-CM grafts as a contributing factor, the fact that overdrive

suppression eliminated graft ectopy provides evidence that graft-induced arrhythmias in the large animal context could be the result of enhanced graft automaticity relative to host. A plausible reason then for the cessation of VT observed with prolonged duration in vivo is that hESC-CM grafts matured and established a more polarized resting membrane potential, reducing the electrical mismatch between these tissues and reducing enhanced graft automaticity in kind. Studies must continue to make this discrimination.

Arguably, based on recent work of hESC-CM transplantation in the non-human primate, the next major hurdles in the clinical translation of hESC-CM based therapies for heart repair are graft electrical integration and graft-related arrhythmias. Combined, previous work from our group has shown that other translational concerns such as the risk of teratomas, the ability to produce at scale, and graft survival can be overcome. The next step in addressing these hurdles is to understand the source of the transient arrhythmias in the non-human primate, with tools already created as highlighted in Future Directions section 8.1.

7.3 Matlab scripts to analyze hESC-CM engrafted hearts

Prior to the development of Matlab scripts to analyze GCaMP3+ hESC-CM engrafted hearts, our ability to assess the activation kinetics and extent of coupling of grafts with host myocardium was limited. Specifically, no assessment of graft activation kinetics could be made quantitatively, as the standard analysis tools in AndorSolis limited the user to square ROIs and could only provide, by comparing the mean fluorescence activity of this square ROI to the host ECG, a binary assessment of graft

coupling after exporting into Excel.   In addition, early analyses were limited to the

singular assessments of graft ROIs, severely limiting analysis throughput. There was a

clear desire to map the activation kinetics of transplanted grafts, as well as be able to

clearly define multiple regions for analysis that were based on the actual graft footprints.

Using Matlab, we wrote scripts to overcome the limitations of combined

AndorSolis and Excel analysis. Initial work here was very successful, and allowed for

the finding that graft activation kinetics differed based on residing in healthy or injured

host tissue (see Chapter 2). However, since these scripts determined activation time

based on the time delta between the host R wave (or applied stimulus) and the initial

rise in graft GCaMP3 fluorescence, they could only be applied to coupled hESC-CM

grafts. Thus, we needed to develop new and more robust analysis tools that would

allow for this same analysis on uncoupled grafts as well. The work of Chapter 5 details

the development of these more robust analysis tools, which we have used extensively in

the work of Chapter 4.

Last, one separate point of discussion applicable to the analysis of graft activity is

our finding that hESC-CM graft activation can vary beat-to-beat. This phenomenon

brings to light a great word of caution when post-processing imaging data, namely that

ensemble averaging cannot be employed. Thus, Matlab post-processing analysis tools

had to be developed that would appropriately filter noise yet maintain signal integrity at

the single-pixel level, and any activation maps created could only be based on single

beats.

7.4 Treatment with gap junction modifiers

While inherent factors such as relatively small hESC-CM size and active inward currents, as well as low, isotropic distribution of Cx43 already limit hESC-CM graft propagation kinetics versus healthy host tissue, the environment of the injury area in which we transplant these grafts is a hypoxic environment likely to cause gap junction uncoupling. It is this adverse environmental factor that we aimed to treat with gap junction modifiers, a novel class of small molecule drugs. While our work with GJMs is still preliminary (see Chapter 6), we did find robust improvements in transplanted GCaMP3+ H7 hESC-CM electrical behavior after acute treatment ex vivo, including an increase in graft coupling and activation kinetics. Interestingly, we found no improvement in transplanted GCaMP3+ RUES2 hESC-CMs, although in vitro RUES2 hESC-CMs did respond after a gap junction uncoupling challenge. After developing the technologies to visualize for the first time graft electrical activity via the use of the water-soluble voltage dye di-2-ANEPEQ (see Chapter 4), the extremely prolonged APDs in all GCaMP3+ RUES2-derived hESC-CM grafts likely explain the negative result, i.e. that the presence of GCaMP3 created grafts that were so electrically mismatched that they could not couple to host myocardium because they were too often electrically refractory and could not pace with the guinea pig heart sinus rate. Indeed, collectively data from our lab suggests GCaMP3+ RUES2 hESC-CMs essentially lack the capacity to couple with guinea pig host hearts. The reason why H7-derived grafts likely responded to treatment are that APDs of GCaMP3+ H7 hESC-CMs were much less affected by GCaMP3, and so grafts from this cell source could still cycle fast enough to couple with host myocardium. Because of this promising work in H7-derived transplanted grafts, as

well as a reasonable explanation for why we saw no improvements in transplanted GCaMP3+ RUES2 grafts, the use of gap junction modifiers should be pursued in future studies as a novel means to improve graft coupling and CV.

Note that we would not expect all hearts to show an improvement in coupling following AAP10 treatment: GJMs may be able to rescue grafts with a functional block to coupling, but they are unlikely to improve the coupling of graft regions isolated by scar tissue. Also, it is not known whether potential improvements in graft CV and coupling via GJM treatment will be electrically stabilizing or destabilizing in engrafted hearts. Further animal studies, in particular telemetric ECG studies of injured and hESC-CM engrafted hearts treated chronically with GJMs via implantable osmotic mini pumps, will have to be pursued.

7.5 Study limitations

Limitations to the studies described herein should be acknowledged. As discussed previously[82], our experiments involved a relatively short duration of follow-up. Mummery and colleagues have pointed out the value of transplantation studies with longer endpoints; indeed, after transplanting hESC-CMs into acutely infarcted NOD-SCID mice, they observed beneficial effects on mechanical function at 4 weeks that disappeared by 12 weeks post-transplantation[152]. Our decision to limit studies to 2 or 4 weeks post-transplantation reflect an attempt to balance practical considerations related to work in an immunocompetent host, requiring daily immunosuppressive therapy to prevent hESC-CM graft rejection, with the end goal of assessing graft electrical integration. With recent work of the Russell group aiming to create universal donor cells

from embryonic stem cell sources that do not elicit a host immune response[153], studies with much longer duration without concern of the risks of prolonged immunosuppression may be possible.

Also mentioned previously[82], while arguably a better model than the mouse or rat, there are obviously major differences in the size and sinus rate of the guinea pig heart employed here versus that of the adult human. As such, we cannot rule out the possibility that graft-related arrhythmias will occur following hESC-CM transplantation in a larger, more relevant preclinical model or eventual human subjects. Indeed, Chong et al recently found transient electrical instability followed hESC-CM transplantation in a primate infarct model[154].   Hence, rather than replacing the need for eventual safety studies in a large animal model, we regard the higher-throughput guinea pig model as a more suitable platform to test strategies to promote host-graft integration (see Chapter 6) and screen for effects on electrical stability. Better integrated cardiomyocytes might show greater maturation and contribute more to force generation[155, 156], but they also might prove more arrhythmogenic. The technology described herein, as applied to the guinea pig model, is a reasonably high-throughput platform in which to conduct such testing.

Another limitation acknowledged previously[80, 82] is that due to the excellent coronary collateral system of the guinea pig[157], we must perform direct cryoinjury of the left ventricular wall to induce a model of myocardial infarction. Cryoinjury does have the advantage that it produces a very reproducible size and location of injury scar and so reduces animal-to-animal variability. On the other hand, because it results in the necrosis of all cell types and a near-transmural injury, it may create a more hostile

environment for cell engraftment than would be the case in an ischemia-reperfusion infarct model. If so, then our studies may be best regarded as a worst-case scenario for hESC-CM engraftment and integration. Indeed, recent work with hESC-CM transplantation in a non-human primate infarct model reported 100% host-graft integration in all recipient hearts[115], an outcome we found only with hESC-CM transplantation in uninjured guinea pig hearts (see Chapter 2). The probable explanation is the difference in pathophysiology of the ischemic injury to non-human primate hearts, likely to leave many points of contact between transplanted grafts and healthy myocardium.

While ex vivo imaging has many advantages for studying hESC-CM transplantation, including the ability to map in great spatiotemporal detail the activity and interactions of both host and transplanted graft tissues, and it allows for the potential to perform controlled perfusion experiments that cannot be performed in vivo, it does have its drawbacks. The most obvious is that it is a terminal procedure, thus serial measurements in the same heart cannot be made. While Chang Liao et al. have recently published on a system that would allow for the potential of serial optical mapping of hearts in vivo[151], this technology is still in its infancy and requires further development. Thus if serial measurements of myocardial spatial activation are a crucial component of the experimental design, in vivo electroanatomical mapping should be considered as an alternative if limits in resolution (1mm) are not a concern.

Further, the optical assessment of tissue electrical activity ex vivo generally requires the use of mechanical uncoupling agents, which in our own work has proven to have the propensity to affect the preparation's electrical stability. In particular, we found

BDM to exhibit off-target effects on uncoupled graft behavior (see chapter 3). While there are complex post-processing analysis methods that can obviate the need for use of these mechanical uncoupling agents[106], the incorporation of these methods in the analysis of hESC-CM engrafted hearts would not be straight forward considering the inherently low dynamic optical signals thus far observed from hESC-CM grafts. Fortunately, the mechanical uncoupler blebbistatin has not shown to interfere with host or graft electrical activity in any of the engrafted hearts in which we have utilized this agent. However, perfusion with this agent causes a high-degree of autofluorescence in myocardium at wavelengths that overlap with GCaMP3 (emission in the 500-530 nm range when excited at ~488 nm). This was not limiting in our experiments because the background fluorescence caused by blebbistatin is significant only in intact myocardium, so it actually helped to accentuate the border between viable muscle and the cryoinjury scar. Blebbistatin would likely be more problematic in an animal model in which myocardial infarction is induced by coronary ligation, as there would be overlying subepicardial host muscle.

Another limitation of ex vivo imaging is that heart tissues suffer edema over time as proteins are washed out in single-pass flow Langendorff systems, even though buffers are designed to be iso-osmotic. The resultant blebbing of tissue can lead to a reduction of captured fluorophore signal and hinder intravital imaging in general.

A limitation specific to our studies involving the imaging of host and graft voltage activity by di-2-ANEPEQ relates to our experimental goal of imaging *entire* hearts so as to capture global host-graft electrical interactions. Because of this, the spatial resolution for graft regions was not optimum. This made post-processing graft activation difficult,

especially with the limited dynamic range afforded by graft-derived di-2-ANEPEQ

signals at timepoints late into dye washout. For future work, it is advisable to select

optics that allow for zooming in on graft tissue alone in its entirety so that spatial

resolution can be maximized.

Chapter 8: Future Directions

8.1 Optical mapping of non-human primate hearts ex vivo

With the recent report of transient ventricular tachycardia observed in only hESC-CM engrafted hearts in the larger non-human primate infarct model[115], the ability to optically map both host and graft electrical activity has become even more important. While the graft-autonomous calcium reporter GCaMP3 was useful to show hESC-CM grafts could couple with host myocardium in this more clinically relevant injury model, it could not provide information as to host-graft electrical interactions and the mechanistic basis for these rhythm disturbances. With the success of the combined approach of optically mapping GCaMP3+ hESC-CM engrafted guinea pig hearts with the water-soluble voltage dye di-2-ANEPEQ described in Chapter 4, we sought to apply this same technique to map the electrical activity of non-human primate hearts ex vivo.

Due to the great difference in heart size between the guinea pig and non-human primate, however, optically mapping non-human primate hearts ex vivo in full field of view was not immediately possible. To accomplish this work, we built completely new imaging and ex vivo support systems. We then used this technology to optically map a number of infarcted non-human primate hearts after loading with di-2-ANEPEQ. Figure 8.1 provides an overview of this new optical mapping system, how it compares to the system previously used for guinea pig heart optical mapping, and evidence that this is a viable approach for future studies.
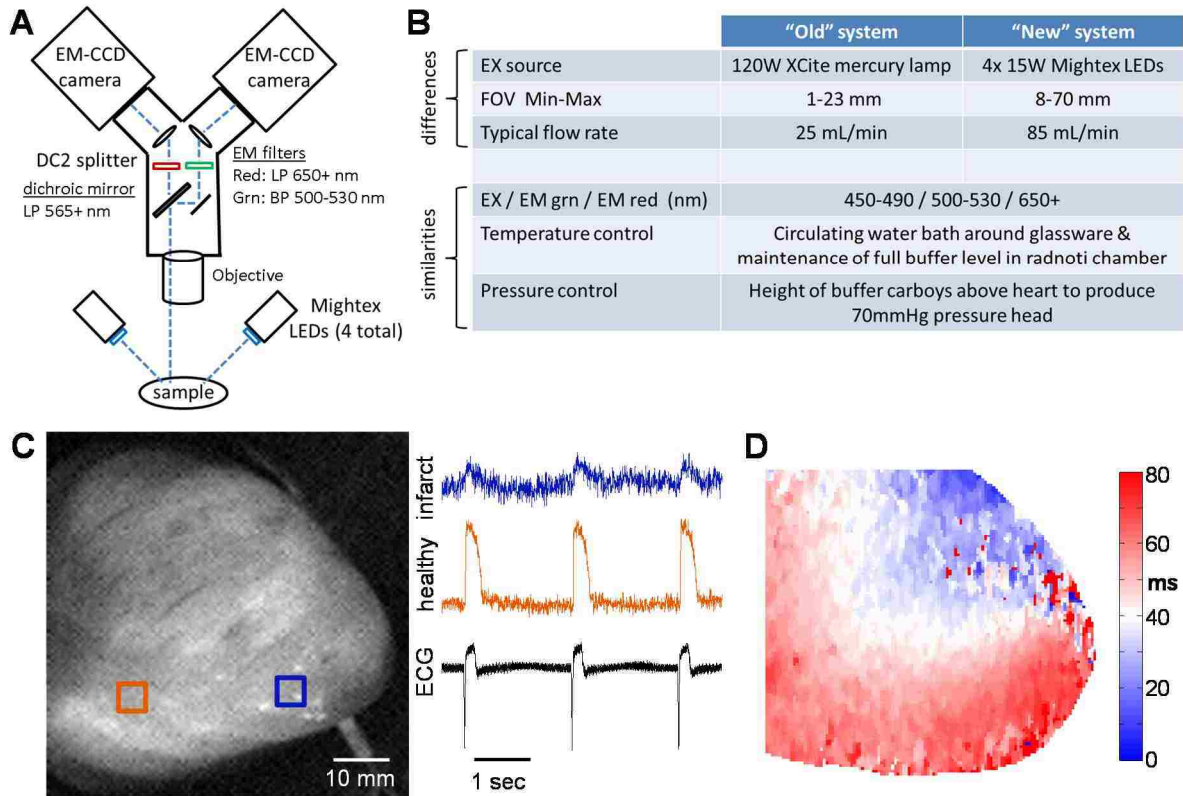
Figure 8.1. Successful ex vivo imaging of non-human primate hearts with di-2-ANEPEQ. A: Schematic of our dual EM-CCD-based imaging system designed for optical mapping of di-2-ANEPEQ in the larger non-human primate heart. For this we did away with the Nikon SMZ1000 stereomicroscope base and designed a structure to support the DC2 splitter and EM-CCD cameras directly. This allowed for direct mounting of C-mount telephoto lenses to the DC2 for image acquisition, and flexibility in working distances up to 24 inches. Excitation is now provided by 4 LEDs aimed at the heart surface. **B:** Summary of differences and similarities between the "old" imaging system (used for guinea pig and smaller heart ex vivo imaging) and "new" imaging system (with built-in flexibility to image non-human primate hearts down to rat hearts full field of view). **C:** Example imaging data from a non-human primate heart imaged full field of view after loading with di-2-ANEPEQ. Note the robust optical transients derived from healthy host tissue remote to the infarct region, similar to data measured from cryoinjured guinea pig hearts. **D:** Example pseudocolored activation map for a single beat of a di-2-ANEPEQ-loaded non-human primate heart indicating early (blue) to late (white to red) activation.

Moving forward, the method of optically mapping non-human primate hearts transplanted with hESC-CM grafts expressing a graft-autonomous reporter of activation ex vivo provides the spatiotemporal resolution required to investigate the mechanistic basis for the transient ventricular tachycardia observed in prior hESC-CM engraftment studies. Although actual values of host and graft tissue voltage cannot be measured,

this technique would allow for the determination of whether graft-related ectopy (potentially a result from enhanced graft automaticity relative to host) or re-entrant phenomenon (potentially due to conduction block or poor conduction through graft tissue) are the cause of graft-related arrhythmias.

8.2 Optical mapping of hESC-CM grafts expressing a voltage-sensitive fluorescent protein in hearts loaded with a lipophilic voltage dye

As detailed in Chapter 4 and discussed in Chapter 7, our finding that GCaMP3 expression adversely affects the electrophysiology of hESC-CMs was unexpected. This has led us to explore alternatives for measuring graft electrical activity for future studies. Recently, multiple new voltage-sensitive fluorescent proteins have been described, which show impressive dynamic fluorescence range and response speeds making them potentially suitable for the detection of transplanted hESC-CM graft activity[158-162]. Indeed, Chang Liao et al. recently reported on the cardiac expression of the voltage-sensitive protein VSFP2.3 in mice, and although in their study the dynamic range was low (~1% non-ratiometric) and response speed slow for measuring healthy heart tissue activation[151], this is a promising direction for the field.

Inspired by these advances, we have created multiple transgenic hESC lines that stably express one of two voltage-sensitive proteins, ArcLight[160, 161] or the archaerhodopsin mutant ArchD95H[162]. In vitro, hESC-CMs expressing these voltage-sensitive proteins exhibit robust optical APs, with ArchD95H+ hESC-CMs showing a particularly large change in fluorescence upon depolarization. More promising, when

transplanted into cryoinjured guinea pig hearts, oAPs from hESC-CM grafts expressing these voltage-sensitive were detectable (Figure 8.2). Again ArchD95H+ hESC-CMs provided the best signal, likely because of the protein's red-shifted spectrum, and appears to be the best candidate cell line at this time for future studies. The approach then, which has a number of advantages over the methods detailed in Chapter 4, would be to image hESC-CM grafts expressing a voltage-sensitive protein (providing a graft-autonomous reporter of electrical activation) after loading engrafted hearts ex vivo with a spectrally distinct lipophilic voltage dye (which we have shown do not label graft tissue).
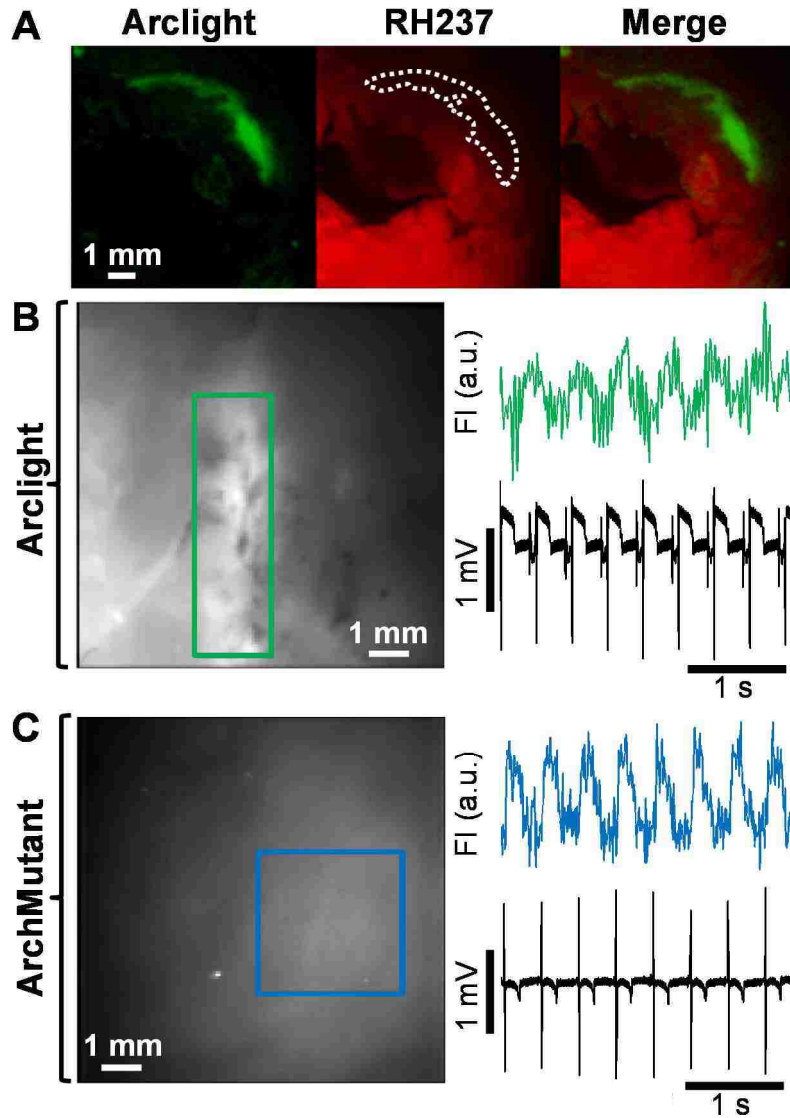
Figure 8.2. Successful ex vivo imaging of hESC-CM grafts expressing voltage-sensitive proteins after transplantation in guinea pig hearts. **A:** Transverse slices of a chronically injured heart transplanted with Arclight+ hESC-CM graft after loading with RH237. Note the complete lack of RH237 labelling in the Arclight+ hESC-CM graft denoted by the white dotted line. **B:** Optical action potentials detected from ArcLight+ hESC-CMs transplanted in an injured heart. Left: Epicardial surface of engrafted heart with Arclight+ hESC-CM graft (denoted in green) located in the injury region. Right: Mean fluorescence intensity of the graft-derived voltage activity through time (green trace) plotted with the host ECG (black trace). Note that Arclight+ hESC-CM depolarization results in an overall decrease in fluorescence intensity, so the graft optical signal has been inverted to match convention. Also note that this graft is electrically uncoupled from the host. **C:** Optical action potentials detected from ArchD95H+ hESC-CMs transplanted in an uninjured heart. Left: Epicardial surface of engrafted heart with ArchD95H+ graft region of interest (denoted in blue). Right: ArchD95H fluorescence (blue trace) and simultaneously acquired host ECG. ArchD95H+ hESC-CM depolarization results in a decrease in optical fluorescence intensity as measured by our 650 nm longpass filter, thus the graft optical signal has been inverted here as well. Note this graft was coupled to the host.

Appendix

A.1 Matlab script to analyze ex vivo voltage imaging data

```
% created by Dominic Filice, work in progress from 2010-2015.


%-------------------------------------------------------------------------
%%%%%%%%%%%%%%%%%%%%%%% SET POTENTIAL COLORMAPS %%%%%%%%%%%%%%%%%%%%%%%%%%%%
%
%Making blue to white to red cmap. Note, every colormap has exactly 3
columns,
%and I want to go from red [1 0 0] at top to white [1 1 1] at middle to
%blue [0 0 1] at bottom.  In order to get even distribution of colors
%between these (wiht # of rows at 128), I'll need to set middle two rows
%at white, and set the other rows as an interpolation between 0 and 1.
bwr=zeros(128,3);
others=(0:(1/63):1); others=transpose(others);
rwbhalf=zeros(64,3);
rwbhalf(:,1)=others; rwbhalf(:,2)=others; rwbhalf(:,3)=ones;
bwr(1:64,:)=rwbhalf; bwr(65:end,:)=fliplr(flipud(rwbhalf));
%the above produces a colormap that is blue for early, red for late

%the below here produces the opposite (red for early, blue for late); this
%is the one we will use:
rwb=flipud(bwr); %named "rwb" for red (early) to white to blue (late)

%-------

%Now to produce special colormaps for voltage dye specific ActMaps:
btr=bwr;
btr(1:64,3)=btr(1:64,2); %produces a colormap that goes from black (early) to
red (late)
rtb=flipud(btr); %produces an opposite colormap that goes from red (early) to
black (late)

%Now to produce special colormaps for GCaMP3 specific ActMaps:
btg=btr;
btg(65:end,1)=btg(65:end,2);
btg(65:end,2)=ones; %produces a colormap that goes from black (early) to
green (late)
gtb=flipud(btg); %produces an opposite colormap that goes from green (early)
to black (late)

%-------

%Colormaps for visualization of Activation, specifically for movies as this
%will have better contrast by design.  Producing two colormaps here, one
%for voltage movies and the other for GCaMP3 movies:
others2=(0:(1/42):1); others2=transpose(others2); %defining interpolation

bwyr=zeros(128,3);
bwyr(2:44,1)=others2; bwyr(2:44,2)=others2; bwyr(2:44,3)=others2;
```

```matlab
bwyr(44:86,1)=ones; bwyr(44:86,2)=ones; bwyr(44:86,3)=flipud(others2);
bwyr(86:128,1)=ones; bwyr(86:128,2)=flipud(others2);
%"bwyr" refers to black-white-yellow-red

%now make an equivalent colormap for going to green (swap 1st & 2nd columns):
bwyg=zeros(128,3);
bwyg(:,1)=bwyr(:,2); bwyg(:,2)=bwyr(:,1); bwyg(:,3)=bwyr(:,3);
%"bwyg" refers to black-white-yellow-green


%------
%creat colormaps that go from black directly to red ("br") and to green
%("bg") without the white intermediary:
br=gray(128); br(:,2)=0; br(:,3)=0;
bg=gray(128); bg(:,1)=0; bg(:,3)=0;
%%%%%%%%%%%%%%%%%%%%% READ DATA & USER INPUT %%%%%%%%%%%%%%%%%%%%%%%%%%%%%%%%%

% ANDOR DATA
%file and user input
%read *.dat files and obtain user input:
format long

%ask user for animal identifier & conditions (i.e., G345 acute with cells
2wks)
animal=input('Please enter the animal identifier and parameters: \n'  , 's');
%ask user for complete file name including extension
filename=input('Please enter the name of the Andor raw file you \nwish to
analyze including the file extension: \n'  ,'s');
%ask user for number of frames total
frame=input('How many frames total? \n');
%ask user for real time between each frame
tbwframe=input('How much time (sec) between each frame? \n');
%ask user for the field of view:
fov=input('What is the length of one side of the field of view (mm)? \n');
%ask user for the pixel depth (one dimension):
numpixs=input('How many pixels per side (e.g. 128)? \n');
%calc the mm per pixel:
pixsize=fov/numpixs;
%now below we are creating a "real time" vector that sets the first frame at
time 0,
%then increments on by the time between each frame until the end.
rtime=zeros(1,frame);
for i=2:frame, rtime(1,i)=tbwframe*(i-1); end;

%Import Data:
fid=fopen(filename, 'rb');
a=fread(fid,numpixs*numpixs*frame,'uint16');
fclose(fid);
DATA=reshape(a,numpixs, numpixs, frame);

%rotate the data matrix 90 degrees counter clockwise so that it is the
%same as the Andor Solis captured data:
for i=1:frame, DATA(:,:,i)=rot90(DATA(:,:,i)); end;

maxa=max(a);
mina=min(a);
```

```
clear a ans fid

% ECG data
%ECG data must be copied into text file, all rows deleted up until first
%row with the camera fire signal, and all rows after the last camera fire
%signal deleted. Also, only copy the Channel data, not the headers or any
%comments or event indicators (these can cause errors in reading).
%This will leave us with  rows - Range / Channel 1 / Channel 2 / Channel 3 /
%Channel 4 / Channel 5, of which only Channel 1 through 5 are of use.  Here,
Channel 1 is our ECG
%signal in mV, Channel 2 is the Stimulator to the Heart in V, Channel 3 is
the external Stim signal
%to the cameras in V, Channel 4 is the Green camera fire signal in V, and
Channel 5 is the Red camera fire signal in V.
ECGfilename=input('Please enter the name of the ECG text file you \nwish to
analyze including the file extension: \n'  ,'s');
fid=fopen(ECGfilename, 'rb');
[ECG position]=textscan(fid, '%*s %f %f %f %f %f');
fclose(fid);


%Create new folder to store all analyzed data, as well as set this new
%folder as the current directory:
formatOut='dd-mmm-yyyy-HH-MM-SS';
noww=datestr(now,formatOut);
newfolder=strcat(animal,'_',noww,'_',mfilename);
mkdir(newfolder);
cd(newfolder);


%Transform the cell array into an ordinary matrix with 5 columns:
ecg = ECG{1};
for i = 2:5
    ecg = [ecg ECG{i}];
end


%automatically remove leading and trailing zeros from Labchart import file:
[r,c,v]=find(ecg(:,5)>2.5);
beginning=r(1);
ecg(1:beginning-1,:)=[];


%[rg,cg,vg]=find(ecg(:,4)>2.5);
[rr,cr,vr]=find(ecg(:,5)>2.5);
%gending=rg(end);
rending=rr(end);
% if rending>gending
%     ending=rending;
% else
%     ending=gending;
% end
ending=rending;
ecg(ending+1:end,:)=[];


%now clear the no longer needed variable ECG and other variables not needed:
clear ECG i fid ans r c v rg cg vg rr cr vr


%add real time to ecg, starting with 0 and increasing every 0.001s:
```

```matlab
ecgtinterval=.001;
ecg(1,6)=0;
for k=2:length(ecg); ecg(k,6)=ecgtinterval*(k-1); end;

% ECG Baseline Drift Removal by median subtraction and curve fitting:
%median:
ecg(isnan(ecg(:,1)))=0; %in case any values did not copy well and were
assigned "NaN", set them to zero
ECGmedian=median(ecg(:,1));
ecg(:,7)=ecg(:,1)-ECGmedian;


%correcting drift using a combo of sgolay and removal of ringing at ends,
%replacing with mean value of closest 10 frames from sgolay fit:
ecgfit=smooth(ecg(:,7),10001,'sgolay',21);
ecgfit=smooth(ecgfit,500,'moving');
ecgfit(1:600)=0;ecgfit(1:600)=mean(ecgfit(601:611));
ecgfit(end-600:end)=0;ecgfit(end-600:end)=mean(ecgfit(end-611:end-601));
ecg(:,7)=ecg(:,7)-ecgfit;
figure()
subplot(2,1,1);plot(ecg(:,6),ecg(:,1),'b',ecg(:,6),ecgfit,'r'); title('raw
ECG w/ 1st curvefit');
subplot(2,1,2);plot(ecg(:,6),ecg(:,7),'b'); title('curve fit ECG');


% %curvefitting (using a 24th order polynomial to fit ECG)
% ecgpoly=polyfit(ecg(:,6),ecg(:,7),24);
% ecgpolyf=polyval(ecgpoly,ecg(:,6));
% figure()
% subplot(2,1,1);plot(ecg(:,6),ecg(:,7),'b',ecg(:,6),ecgpolyf,'r');
title('raw ECG w/ 1st curvefit');
% ecg(:,7)=ecg(:,7)-ecgpolyf;
% subplot(2,1,2);plot(ecg(:,6),ecg(:,7),'b'); title('curve fit ECG');
% %found that multiple curvefitting, using polyfit function, doesn't do much
% %after the first pass, thus removed the subsequent passes through:
% % %repeat ECG curvefitting
% % ecgpoly2=polyfit(ecg(:,6),ecg(:,7),24);
% % ecgpolyf2=polyval(ecgpoly2,ecg(:,6));
% % subplot(4,1,2);plot(ecg(:,6),ecg(:,7),'b',ecg(:,6),ecgpolyf2,'r');
title('1st corrected ECG w/ 2nd curvefit');
% % ecg(:,7)=ecg(:,7)-ecgpolyf2;
% % %repeat again:
% % ecgpoly3=polyfit(ecg(:,6),ecg(:,7),24);
% % ecgpolyf3=polyval(ecgpoly3,ecg(:,6));
% % subplot(4,1,3);plot(ecg(:,6),ecg(:,7),'b',ecg(:,6),ecgpolyf2,'r');
title('2nd corrected ECG w/ 3rd curvefit');
% % ecg(:,7)=ecg(:,7)-ecgpolyf3;
% % subplot(4,1,4);plot(ecg(:,6),ecg(:,7),'b',ecg(:,6),ecgpolyf2,'r');
title('Final corrected ECG');
%
% % %trying convolution:
% % ecgconv=conv(ecg(:,7),ones(1,100));
% % figure(), plot(ecgconv)

% Normalizing the ECG to between 0 and 1:
%normalizeddata=(data-min)./(max-mix)
ecg(:,8)=(ecg(:,7)-min(ecg(:,7)))./(max(ecg(:,7))-min(ecg(:,7)));
```

```matlab
%now add 1 to this normalization so that it can be plotted above the stim
%signal:
ecg(:,8)=ecg(:,8)+1;

% Normalizing the Stim to Heart to between 0 and 1, and then drop it's
%magnitude to 80% so that it doesn't take up entire bottom row height:
ecg(:,9)=(ecg(:,2)-min(ecg(:,2)))./(max(ecg(:,2))-min(ecg(:,2)));
ecg(:,9)=ecg(:,9).*0.8;
%% IN THE END, this leaves us with the following data in the "ecg" matrix:
% Column:   1           2              3            4             5
6           7            8             9
%   Info:  raw ECG  Stim to Heart  Stim to Cams  Grn Cam fire  Red Cam fire
real time   drift-ECG   norm ECG   norm Stim to Heart
% Units:   mV          V                           V                       V
sec        mV           mV           V

%-------------------------------------------------------------------------
%%%%%%%%%%%%%%%%%%%%%%%%%%%%% PLAY RAW DATA %%%%%%%%%%%%%%%%%%%%%%%%%%%%%%%%%

%play raw data:
titlestrraw=[animal, ' - Raw Data'];
figure('Name',titlestrraw,'NumberTitle','off'); for i=1:frame;
imagesc(DATA(:,:,i)); axis square;  set(gca, 'YTick', []);set(gca, 'XTick',
[]); set(gca,'clim', [mina*1.2 maxa*.8]); colormap(gray);
title(sprintf('Frame %i', i));  pause(tbwframe); end;

%-------------------------------------------------------------------------
%%%%%%%%%%%%%%%%%%%%%%%%%%%%% DATA MASK %%%%%%%%%%%%%%%%%%%%%%%%%%%%%%%%%%%%%
%goal here is to mask off only the heart, and not care about background
M=mean(DATA,3);
STD=std(DATA,0,3);
COMB=M+(40*STD);
titlestrmask=[animal, ' - Select Mask'];
figure('Name',titlestrmask,'NumberTitle','off');
imagesc(COMB); axis square; set(gca, 'YTick', []);set(gca, 'XTick', []);
colormap(gray(256));

%manual selection using roipoly, then apply mask to entire DATA 3D matrix
%and set all background to 0.
Active=roipoly;
%apply mask to Data stack:
for y=1:frame, DATA(:,:,y)=Active(:,:).*DATA(:,:,y);, end;

%-------------------------------------------------------------------------
%%%%%%%%%%%%%%%%%%%%%%%%%%% SPATIAL FILTERING %%%%%%%%%%%%%%%%%%%%%%%%%%%%%%%
%goal here is to implement a median filter (size 3) to remove noise, then a
%special cone filter with a width of 3 pixels

%spatial median filter first (default window of 3x3):
DATAfm=zeros(size(DATA));
for i=1:size(DATA,3), DATAfm(:,:,i)=medfilt2(DATA(:,:,i)); end

%conefilt (courtesy of Matthew Kay @ GW):
width=3;
slope=1;
```

```matlab
kernel=zeros(width,width);
for i=0:width-1;
 for j=0:width-1;
   kernel(i+1,j+1)=floor((width-1)*slope/2+1-slope*sqrt((i-(width-1)/2)^2+(j-
(width-1)/2)^2));
     if kernel(i+1,j+1)<0, kernel(i+1,j+1)=0; end;
 end
end
kernel=kernel.*(1/sum(sum(kernel)));

% apply spatial conefilt:
DATAfmc=zeros(size(DATA));
for i=1:size(DATA,3), DATAfmc(:,:,i)=conv2(DATAfm(:,:,i),kernel,'same'); end
%reapply mask:
for y=1:frame, DATAfmc(:,:,y)=Active(:,:).*DATAfmc(:,:,y);, end;

% %play spatially filtered data:
% titlestrsfd=[animal, ' - Spatially Filtered Data'];
% figure('Name',titlestrsfd,'NumberTitle','off'); for i=1:frame;
imagesc(DATAfmc(:,:,i)); axis square;  set(gca, 'YTick', []);set(gca,
'XTick', []); set(gca,'clim', [mina*1.2 maxa*.8]); colormap(gray);
title(sprintf('Frame %i', i));  pause(tbwframe); end;

%------------------------------------------------------------------------
%%%%%%%%%%%%%%%%%%%%%%%%%%%% TEMPORAL FILTERING %%%%%%%%%%%%%%%%%%%%%%%%%%%%%%
%goal is to use convert to frequency domain using FFT transform, and use a
%finite impulse filter (FIR) to remove frequencies above user input.  Need to
ensure
%a zero phase response so that the transform & filtering does not impart a
%time-domain delay (bi-directionally process it!).
Freq=1/tbwframe; %sampling freq is based on time between frames
order=50; %want a FIR of order 50
passupto=input('Enter lowpass FIR filter pass up to band (Hz):  ');
%if the Nyquist freq is lower than the desired pass up to band, then
%we need to drop passupto appropriately:
if (passupto*1.25)>(Freq/2),
    passupto=(Freq/2)/1.25;
    disp(['Sampling Freq too low to lowpass filter imaging data in time at
defined Hz.']);
    disp(['Resultant lowpass cutoff is:  ' num2str(passupto) 'Hz']);
end
f0=[0 passupto passupto*1.25 Freq/2]./(Freq/2);
a0=[1 1 0 0];
b=firpm(order,f0,a0);
a=1;

vector=reshape(DATAfmc,[],size(DATAfmc,3));
DATAfmcf=zeros(size(vector));
for n=1:size(vector,1)
    if sum(vector(n,:))~=0
        DATAfmcf(n,:)=filtfilt(b,a,vector(n,:));
    end
end
DATAfmcf=reshape(DATAfmcf,size(DATA,1),size(DATA,2),[]);

% median filter with a kernel of 3 through time
```

```matlab
DATAfmcfm=medfilt1(DATAfmcf,3,[],3);

%moving average smooth filter with kernel of 5 through time
vector2=reshape(DATAfmcfm,[],size(DATAfmcfm,3));
DATAf=smooth(vector2,5,'moving');
DATAf=reshape(DATAf,size(DATA,1),size(DATA,2),[]);

%reapply mask:
for y=1:frame, DATAf(:,:,y)=Active(:,:).*DATAf(:,:,y);, end;

% %sgolay average smooth filter with span 1001 and order 50
% vector2=reshape(DATAfmcfm,[],size(DATAfmcfm,3));
% DATAf=smooth(vector2,1001,'sgolay',50);
% DATAf=reshape(DATAf,size(DATA,1),size(DATA,2),[]);

% %play spatially & temporally filtered data:
% titlestrstfd=[animal, ' - Spatially & Temporally Filtered Data'];
% figure('Name',titlestrstfd,'NumberTitle','off'); for i=1:frame;
imagesc(DATAf(:,:,i)); axis square;  set(gca, 'YTick', []);set(gca, 'XTick',
[]); set(gca,'clim', [mina*1.2 maxa*.8]); colormap(gray);
title(sprintf('Frame %i', i));  pause(tbwframe); end;

% %let's look at a pixels through time, before and after filtering:
% data=reshape(DATA,[],size(DATA,3));
% dataf=reshape(DATAf,[],size(DATAf,3));
% figure(),plot(data(1998,:),'b'),hold,plot(dataf(1998,:),'r');


%-------------------------------------------------------------------------
%%%%%%%%%%%%%%%%%%%%%%%%% FILTER ASSESSMENT %%%%%%%%%%%%%%%%%%%%%%%%%%%%%%%%
%ask user for number of frames total
figure('Name','Select Active Pixel','NumberTitle','off');
imagesc(COMB); axis square; set(gca, 'YTick', []);set(gca, 'XTick', []);
colormap(gray(256));

disp('Select an active pixel to assess quality of filtering:');
[xactive,yactive] = ginput(1);
xactive=floor(xactive);yactive=floor(yactive);
titlestrfiltering=[animal, ' - Individual Pixel Data - for assessing
filtering'];
subplot714title=strcat('after Temporal Lowpass of', {' '}, num2str(passupto),
' Hz');
figure('Name',titlestrfiltering,'NumberTitle','off')
subplot(7,1,1),plot((reshape(DATA(xactive,yactive,:),1,[])),'b'), title('Raw
data');
subplot(7,1,2),plot((reshape(DATAfm(xactive,yactive,:),1,[])),'b'),
title('after Spatial 3x3 median');
subplot(7,1,3),plot((reshape(DATAfmc(xactive,yactive,:),1,[])),'b'),
title('after Spatial 3x3 conefilter');
subplot(7,1,4),plot((reshape(DATAfmcf(xactive,yactive,:),1,[])),'b'),
title(subplot714title);
subplot(7,1,5),plot((reshape(DATAfmcfm(xactive,yactive,:),1,[])),'b'),
title('after Temporal 3-span median');
subplot(7,1,6),plot((reshape(DATAf(xactive,yactive,:),1,[])),'b'),
title('after Temporal 5-span average');
```

```matlab
subplot(7,1,7),hold on;
plot((reshape(DATA(xactive,yactive,:),1,[])),'b');plot((reshape(DATAf(xactive
,yactive,:),1,[])),'r'), title('Overlay of raw & last');
h=gcf;
saveas(h,titlestrfiltering, 'tif');
saveas(h,titlestrfiltering);
%clear large matrices we no longer need:
clear DATAfm DATAfmc DATAfmcfm

titlestrfilteringdone=[animal, ' - Individual Pixel Data - Overlay of Raw &
Last'];
figure('Name', titlestrfilteringdone,'NumberTitle','off')
plot((reshape(DATA(xactive,yactive,:),1,[])),'b');hold
on;plot((reshape(DATAf(xactive,yactive,:),1,[])),'r'), title('Overlay of raw
& last');hold off;
h=gcf;
saveas(h,titlestrfilteringdone, 'tif');
saveas(h,titlestrfilteringdone);




save(animal)
%-------------------------------------------------------------------------
%%%%%%%%%%%%%% REMOVE EFFECTS OF FILTERING AT ENDS %%%%%%%%%%%%%%%%%%%%%%
%goal here is to remove the first 15 and last 15 frames due to effects from
%filtering.  But, since we have ECG here, we cant' just get rid of the
%first and last frames, we need to get rid of all time points corresponding
%to the first and last 15 frames:
DATAf(:,:,end-15+1:end)=[];DATAf(:,:,1:15)=[];
rtime(end-15+1:end)=[];rtime(1:15)=[];
newendtime=rtime(end);newstarttime=rtime(1);
ecg(:,10)=ecg(:,6).*1000;
removeend=find(abs(ecg(:,10) - newendtime*1000) <
0.5);removestart=find(abs(ecg(:,10) - newstarttime*1000) < 0.5);
ecg(removeend+1:end,:)=[];ecg(1:removestart-1,:)=[];
frame=frame-30;
%-------------------------------------------------------------------------
%%%%%%%%%%%%%%%%%%%%%%%%%% DRIFT REMOVAL %%%%%%%%%%%%%%%%%%%%%%%%%%%%%%%%%%
%goal here is to use polynomial fitting to fit the optical signal and then
%subtract this from the original signal to remove drift (4th order or
%higher probably needed) - this MUST be done if accurate calcs of
%activation times, etc., are going to be performed!

% %curvefitting
% %find mean of each frame, create a vector of these means, then find
% %polynomial fit to this and subtract each pixel in time by this fit:
% Mn=zeros(size(DATAf(3)));
% for m=1:frame; Mn(m)=mean2(DATAf(:,:,m));end;
% DATAfpoly=polyfit(rtime,Mn,4);
% DATAfpolyf=polyval(DATAfpoly,rtime);
%
% vector3=reshape(DATAf,[],size(DATAf,3));
% for v=1:size(vector3,1)
%     vector3d(v,:)=vector3(v,:)-DATAfpolyf;
% end
% DATAfd=reshape(vector3d,size(DATA,1),size(DATA,2),[]);
```

```matlab
% %after drift removal need to redo mask:
% for y=1:frame, DATAfd(:,:,y)=Active(:,:).*DATAfd(:,:,y);, end;
%
% Mnn=zeros(size(DATAfd(3)));
% for m=1:frame; Mnn(m)=mean2(DATAfd(:,:,m));end;
%
figure(),plot(Mn,'b'),hold,plot(DATAfpolyf,'r'),plot(Mnn,'m');title('curvefit
for signal drift removal');hold off;


%curvefitting
%find mean of each frame, create a vector of these means, then find
%sgolay fit to this and subtract each pixel in time by this fit:
Mn=zeros(size(DATAf(3)));
for m=1:frame; Mn(m)=mean2(DATAf(:,:,m));end;
DATAffit=smooth(Mn,2001,'sgolay',2);
DATAffit=transpose(DATAffit);
vector3=reshape(DATAf,[],size(DATAf,3));
DATAffit=repmat(DATAffit,size(vector3,1),1);
vector3d=vector3-DATAffit;
% for v=1:size(vector3,1)
%     vector3d(v,:)=vector3(v,:)-DATAffit;
% end
DATAfd=reshape(vector3d,size(DATA,1),size(DATA,2),[]);
%after drift removal need to redo mask:
for y=1:frame, DATAfd(:,:,y)=Active(:,:).*DATAfd(:,:,y);, end;

Mnn=zeros(size(DATAfd(3)));
for m=1:frame; Mnn(m)=mean2(DATAfd(:,:,m));end;
figure(),plot(Mn,'b'),hold,plot(DATAffit(1,:),'r'),plot(Mnn+DATAffit(1,1),'m'
);title('curvefit for signal drift removal');hold off;



%-------------------------------------------------------------------------
%%%%%%%%%%%%%%%%%%%%%%%%% ENSEMBLE AVERAGING %%%%%%%%%%%%%%%%%%%%%%%%%%%%%%%
%not performed at this time, not here


%-------------------------------------------------------------------------
%%%%%%%%%%%%%%%%%%%%%%%%%%%%% FLIP SIGN %%%%%%%%%%%%%%%%%%%%%%%%%%%%%%%%%%%%%
%goal here is to flip the signal only if we are working with a voltage dye
%signal (do not flip if working with GCaMP data).  The reason is the
%voltage dye signal inherently drops in fluorescence upon depolarization,
%but we need it, for thresholding purposes later, to increase in
%fluorescence:

%ask user for the type of signal being analyzed:
signaltype=input('GCaMP3 (G) or Voltage (V) signal being assessed?  ', 's');
if strcmp(signaltype,'V')
    DATAfd=-DATAfd;
    DATAfd=DATAfd-min(min(min(DATAfd)));
end;

%not in above, if voltage signal, we've now made it negative, so must
increase all values
%such that they are all positive (for proper 2nd drift removal later):
```

```matlab
%-------------------------------------------------------------------------
%%%%%%%%%%%%%%%%% PLAY (if desired) Z SCORED DATA %%%%%%%%%%%%%%%%%%%%%%%%%
DATAz=zeros(size(DATAfd));
    DATAz=zscore(DATAfd,0,3);
    Zmin=min(min(min(DATAz)));
    Zmax=max(max(max(DATAz)));
runZ=input('Play Z scored data (y/n)?  ', 's');
if strcmp(runZ,'y')
    %play Z scored data so that user can determine ROI:
    figure('Name','Z scored','NumberTitle','off');
    for i=1:frame;imagesc(DATAz(:,:,i)); axis square;
        set(gca, 'YTick', []); set(gca, 'XTick', []); set(gca,'clim',
[Zmin*1/3 Zmax*1/3]);
        colormap(br); title(sprintf('Frame %i', i));  pause(tbwframe);
    end;
end;

% Make a movie of the Z scored data:
figure('Name','Z scored','NumberTitle','off');
titlemovie=[animal,'_Z Scored Data_one tenth speed'];
vidObj=VideoWriter(titlemovie);
%set the framerate
vidObj.FrameRate=(round(1/(tbwframe*10)));
%write sequence of frames to the compressed AVI file:
open(vidObj);

for i=1:frame;imagesc(DATAz(:,:,i)); axis square;
        set(gca, 'YTick', []); set(gca, 'XTick', []);
        set(gca,'clim', [Zmin*1/3 Zmax*1/3]);
        colormap(br); title(sprintf('Time (s) = %.3f', rtime(i)));
        currFrame=getframe; writeVideo(vidObj,currFrame);
end;
close(vidObj);

% Plot the Zscore of the selected "active" pixel:
plot((reshape(DATAz(xactive,yactive,:),1,[])),'b');

% Save zcoredata as a matlab file:
save('zscoredata.mat','DATAz','Zmin','Zmax','frame','rtime','tbwframe',
'animal', 'br');

%-------------------------------------------------------------------------
%%%%%%%%%%%%%%%%%%%%%%%%% SAVE PROCESSED DATA %%%%%%%%%%%%%%%%%%%%%%%%%%%%%%
save processed.mat

%-------------------------------------------------------------------------
%%%%%%%%% ROI PLOTS - Mean of ROIs and Total FI against time %%%%%%%%%%%%
%ROIs:
Mnew=mean(DATAfd,3);
STDnew=std(DATAfd,0,3);STDnew=Active.*STDnew;
COMBnew=M+(40*STDnew);
```

```matlab
figure('Name','Standard Deviation
Image','NumberTitle','off'),imagesc(STDnew); axis square; set(gca, 'YTick',
[]);set(gca, 'XTick', []);colormap(gray(256));
maxSTD=max(max(STD));
minSTD=min(min(STD));
titlestrOpt=[animal, ' - Select ROI'];
figure('Name',titlestrOpt, 'NumberTitle','off');
imagesc(COMBnew(:,:)); axis square;  set(gca, 'YTick', []);set(gca, 'XTick',
[]);
%set(gca,'clim', [minSTD maxSTD]);
colormap(jet(256));


%ask user for the number of ROIs:
nROIs=input('How many ROIs?  ');


for i=1:nROIs; eval(['roimask_' num2str(i) '=roipoly;']); end;


%apply ROI masks to DATA image stacks:
for i=1:nROIs; eval(['roi_' num2str(i) '=zeros(numpixs,numpixs,frame);']);
for j=1:frame; eval(['roi_' num2str(i) '(:,:,j)=roimask_' num2str(i)
'(:,:).*DATAfd(:,:,j);']); end; end;


% INFARCT AREA:
titlestrinfarct=[animal, ' - Select Infarct'];
figure('Name',titlestrinfarct,'NumberTitle','off');
imagesc(M); axis square; set(gca, 'YTick', []);set(gca, 'XTick', []);
colormap(gray(256));
%Now ask user to select infarct region:
display('Now define the infarct region')
roimask_infarct=roipoly;


%Using regionprops to get means of ROIs and other info like area, perimeter,
min & max intensity, etc. need to preallocate structures...?
for i=1:nROIs; eval(['CC_' num2str(i) '=bwconncomp(roimask_' num2str(i)
'(:,:));']); end;
for i=1:nROIs; for j=1:frame; eval(['S_' num2str(i) '(j)=regionprops(CC_'
num2str(i) ', DATAfd(:,:,j), ''Area'', ''Perimeter'', ''Centroid'',
''PixelIdxList'', ''PixelList'', ''MaxIntensity'', ''MinIntensity'',
''MeanIntensity'');']); end; end;
%now do the same for the infarct region:
II=bwconncomp(roimask_infarct);
for j=1:frame; I=regionprops(II, DATAfd(:,:,j), 'Area', 'Perimeter',
'Centroid', 'PixelIdxList', 'PixelList', 'MaxIntensity', 'MinIntensity',
'MeanIntensity'); end;


%Trace ROI boundaries using bwboundaries:
for i=1:nROIs; eval(['[Bound_' num2str(i) ', L_' num2str(i)
']=bwboundaries(roimask_' num2str(i) ',''noholes'');']); end;
%Trace infarct boundary the same way:
[IBound, III]=bwboundaries(roimask_infarct,'noholes');


%plot these boundaries on image in a color and label them:
cblue=[0,112,192];cblue=cblue/255;
cred=[255,0,0];cred=cred/255;
cgreen=[0,176,80];cgreen=cgreen/255;
```

```
corange=[228,108,10];corange=corange/255;
cpurple=[112,48,160];cpurple=cpurple/255;
ctan=[148,138,84];ctan=ctan/255;
colors=[cblue; cred; cgreen; corange; cpurple; ctan];

titlestrrois=[animal, ' - ROIs'];
figure('Name',titlestrrois,'NumberTitle','off');
imagesc(M(:,:)); axis square;  set(gca, 'YTick', []);set(gca, 'XTick', []);
colormap(gray(256));
hold on; for i=1:nROIs; eval(['for k=1:length(Bound_' num2str(i) ');
boundary_' num2str(i) '= Bound_' num2str(i) '{k}; plot(boundary_' num2str(i)
'(:,2), boundary_' num2str(i) '(:,1), ''Color'',
colors(i,:),''LineWidth'',2); Row = ceil(length(boundary_' num2str(i) ')/2);
col = boundary_' num2str(i) '(Row,2); row = boundary_' num2str(i) '(Row,1); h
= text(col+2, row+5, num2str(i));
set(h,''Color'',colors(i,:),''FontSize'',14,''FontWeight'',''bold'');
end;']); end; set(gca, 'YTick', []);set(gca, 'XTick', []);hold off;
%now also draw over this the infarct region in a dotted white line:
hold on; for l=length(IBound); iboundary=IBound{l}; plot(iboundary(:,2),
iboundary(:,1), '--w', 'LineWidth',2); end; hold off;
%save figure to file (as both a tiff and matlab file):
h=gcf;
saveas(h,titlestrrois, 'tif');
saveas(h,titlestrrois);

%do trick to extract means from S_x into separate matrix, then plot this
for i=1:nROIs; eval(['roi_' num2str(i) 'means=[S_' num2str(i)
'.MeanIntensity];']); end;

% NOTE - need to look into plotting total FI in the region,
% not just the mean (could provide some usefull data). - NOT GOING TO DO

%find ranges (max-min) of each ROI means:
for i=1:nROIs, eval(['roi_' num2str(i) 'range=(max(roi_' num2str(i) 'means)-
min(roi_' num2str(i) 'means));']); end;
%now add these ranges to a vector called "ranges":
for i=1:nROIs, eval(['ranges(i)=roi_' num2str(i) 'range;']); end;
%now find max of the ranges:
[MAXrange roiwmax] = max(ranges);
%now normalize ROI means to ROI with max range:
for i=1:nROIs; eval(['roi_' num2str(i) 'normmeans=zeros(length(roi_'
num2str(i) 'means)); roi_' num2str(i) 'normmeans=(roi_' num2str(i) 'means-
min(roi_' num2str(i) 'means))./(MAXrange);']); end;
% %now normalize each ROI mean to itself for plotting:
% for i=1:nROIs; eval(['roi_' num2str(i) 'normmeans=zeros(length(roi_'
num2str(i) 'means)); roi_' num2str(i) 'normmeans=(roi_' num2str(i) 'means-
min(roi_' num2str(i) 'means))./(roi_' num2str(i) 'range);']); end;

%now increase each successive ROI by "1", "2", etc. so that they can be
%plotted and appear stacked on top of eachother (so we can easily correlate
%them):
increase=1;
for n=1:nROIs; eval(['roi_' num2str(n) 'normmeans=roi_' num2str(n)
'normmeans+increase; increase=increase+1;']); end; %note, can change the
"n=1:nROIs" to "n=2:nROIs" if I don't want the normalized ROI mean plots to
start at 2 (using "2" makes then start at 1)
```

135

```matlab
%then add 1 again to push up ROI normmeans because we have the stim signal
%plotting as well:
for n=1:nROIs; eval(['roi_' num2str(n) 'normmeans=roi_' num2str(n)
'normmeans+1;']); end;


%Now tell user that the movie is _ seconds long, then ask what time time
%range they want to plot:
disp(['The recording is ' num2str(max(rtime)) ' seconds long total.']);


%Don't want to ask any more, just plot starting from 0 and ending 0.5sec
%past max rtime from now on.
%starttime=input('Please enter the range you wish to plot the data:\nBegin at
time:  ');
%endtime=input('End at time:  ');
starttime=0;endtime=(max(rtime))+0.5;


%for figures (plot traces without ECG identifiers):
titlestrsupp=[animal, ' - Normalized ROI FI Means, Heart Stim & ECG'];
figure('Name',titlestrsupp,'NumberTitle','off'); hold on; axis([starttime
endtime 0 (nROIs+2)]); for i=1:nROIs; eval(['plot(rtime(1,:),roi_' num2str(i)
'normmeans(1,:), ''Color'',colors(i,:), ''LineWidth'',2);']); end;
plot(ecg(:,6),ecg(:,9),'r', 'LineWidth', 2); plot(ecg(:,6),ecg(:,8),'k',
'LineWidth', 2); xlabel('time (sec)'); %set(gca, 'YTick', []);
%title(sprintf(titlestrroisandecg, frselect));
%Display "ECG" and "ROI _" in appropriate places on the Y axis
%define number of labels required
nlabels=nROIs+2;
%divide Y axis into the appropriate number of sections:
set(gca, 'YTick', 0.5:1:nlabels);
%now display:
if nROIs==1, set(gca, 'YTickLabel', 'STIM|ECG|ROI 1'), elseif nROIs==2,
set(gca, 'YTickLabel', 'STIM|ECG|ROI 1|ROI 2'), elseif nROIs==3, set(gca,
'YTickLabel', 'STIM|ECG|ROI 1|ROI 2|ROI 3'), elseif nROIs==4, set(gca,
'YTickLabel', 'STIM|ECG|ROI 1|ROI 2|ROI 3|ROI 4'), elseif nROIs==5, set(gca,
'YTickLabel', 'STIM|ECG|ROI 1|ROI 2|ROI 3|ROI 4|ROI 5'), elseif nROIs==6,
set(gca, 'YTickLabel', 'STIM|ECG|ROI 1|ROI 2|ROI 3|ROI 4|ROI 5|ROI 6'),
elseif nROIs==7, set(gca, 'YTickLabel', 'STIM|ECG|ROI 1|ROI 2|ROI 3|ROI 4|ROI
5|ROI 6|ROI 7'),  elseif nROIs==8, set(gca, 'YTickLabel', 'STIM|ECG|ROI 1|ROI
2|ROI 3|ROI 4|ROI 5|ROI 6|ROI 7|ROI 8'), end;


%%%%%%%%%%%%%%%%%%%%%%
%ask user if drift removal is required again:
driftokay=input('Is another round of drift removal required (y/n)?:  ');
while driftokay==y


%redo drift removal per roi based on the mean of the roi:
for n=1:nROIs; eval(['roi_' num2str(n) 'meansfit=polyfit(rtime,roi_'
num2str(n) 'means,1); roi_' num2str(n) 'meansfitf=polyval(roi_' num2str(n)
'meansfit,rtime); vector_roi_' num2str(n)
'=reshape(DATAfd,[],size(DATAfd,3)); roi_' num2str(n) 'meansfitf=repmat(roi_'
num2str(n) 'meansfitf,size(vector_roi_' num2str(n) ',1),1); vector_roi_'
num2str(n) 'd=vector_roi_' num2str(n) '-roi_' num2str(n) 'meansfitf;
DATAfd_roi_' num2str(n) '=reshape(vector_roi_' num2str(n)
'd,size(DATAfd,1),size(DATAfd,2),[]);']); end;
if nROIs==1, DATAfd=DATAfd_roi_1; elseif nROIs==2,
DATAfd=DATAfd_roi_1+DATAfd_roi_2; elseif nROIs==3,
```

```matlab
DATAfd=DATAfd_roi_1+DATAfd_roi_2+DATAfd_roi_3; elseif nROIs==4,
DATAfd=DATAfd_roi_1+DATAfd_roi_2+DATAfd_roi_3+DATAfd_roi_4; elseif nROIs==5,
DATAfd=DATAfd_roi_1+DATAfd_roi_2+DATAfd_roi_3+DATAfd_roi_4+DATAfd_roi_5;
elseif nROIs==6,
DATAfd=DATAfd_roi_1+DATAfd_roi_2+DATAfd_roi_3+DATAfd_roi_4+DATAfd_roi_5+DATAf
d_roi_6; end;
%now redo evaluation of means per ROI:
%Using regionprops to get means of ROIs and other info like area, perimeter,
min & max intensity, etc. need to preallocate structures...?
for i=1:nROIs; eval(['CC_' num2str(i) '=bwconncomp(roimask_' num2str(i)
'(:,:));']); end;
for i=1:nROIs; for j=1:frame; eval(['S_' num2str(i) '(j)=regionprops(CC_'
num2str(i) ', DATAfd(:,:,j), ''Area'', ''Perimeter'', ''Centroid'',
''PixelIdxList'', ''PixelList'', ''MaxIntensity'', ''MinIntensity'',
''MeanIntensity'');']); end; end;
%now do the same for the infarct region:
II=bwconncomp(roimask_infarct);
for j=1:frame; I=regionprops(II, DATAfd(:,:,j), 'Area', 'Perimeter',
'Centroid', 'PixelIdxList', 'PixelList', 'MaxIntensity', 'MinIntensity',
'MeanIntensity'); end;
%do trick to extract means from S_x into separate matrix, then plot this
for i=1:nROIs; eval(['roi_' num2str(i) 'means=[S_' num2str(i)
'.MeanIntensity];']); end;
%apply ROI masks to DATA image stacks:
for i=1:nROIs; eval(['roi_' num2str(i) '=zeros(numpixs,numpixs,frame);']);
for j=1:frame; eval(['roi_' num2str(i) '(:,:,j)=roimask_' num2str(i)
'(:,:).*DATAfd(:,:,j);']); end; end;


%find ranges (max-min) of each ROI means:
for i=1:nROIs, eval(['roi_' num2str(i) 'range=(max(roi_' num2str(i) 'means)-
min(roi_' num2str(i) 'means));']); end;
%now add these ranges to a vector called "ranges":
for i=1:nROIs, eval(['ranges(i)=roi_' num2str(i) 'range;']); end;
%now find max of the ranges:
[MAXrange roiwmax] = max(ranges);
%now normalize ROI means to ROI with max range:
for i=1:nROIs; eval(['roi_' num2str(i) 'normmeans=zeros(length(roi_'
num2str(i) 'means)); roi_' num2str(i) 'normmeans=(roi_' num2str(i) 'means-
min(roi_' num2str(i) 'means))./(MAXrange);']); end;
% %now normalize each ROI mean to itself for plotting:
% for i=1:nROIs; eval(['roi_' num2str(i) 'normmeans=zeros(length(roi_'
num2str(i) 'means)); roi_' num2str(i) 'normmeans=(roi_' num2str(i) 'means-
min(roi_' num2str(i) 'means))./(roi_' num2str(i) 'range);']); end;


%now increase each successive ROI by "1", "2", etc. so that they can be
%plotted and appear stacked on top of eachother (so we can easily correlate
%them):
increase=1;
for n=1:nROIs; eval(['roi_' num2str(n) 'normmeans=roi_' num2str(n)
'normmeans+increase; increase=increase+1;']); end; %note, can change the
"n=1:nROIs" to "n=2:nROIs" if I don't want the normalized ROI mean plots to
start at 2 (using "2" makes then start at 1)
%then add 1 again to push up ROI normmeans because we have the stim signal
%plotting as well:
for n=1:nROIs; eval(['roi_' num2str(n) 'normmeans=roi_' num2str(n)
'normmeans+1;']); end;
```

```matlab
%Now tell user that the movie is _ seconds long, then ask what time time
range they want to plot:
disp(['The recording is ' num2str(max(rtime)) ' seconds long total.']);

%Don't want to ask any more, just plot starting from 0 and ending 0.5sec
%past max rtime from now on.
%starttime=input('Please enter the range you wish to plot the data:\nBegin at
time:   ');
%endtime=input('End at time:   ');
starttime=0;endtime=(max(rtime))+0.5;

%for figures (plot traces without ECG identifiers):
titlestrsupp=[animal, ' - Normalized ROI FI Means, Heart Stim & ECG'];
figure('Name',titlestrsupp,'NumberTitle','off'); hold on; axis([starttime
endtime 0 (nROIs+2)]); for i=1:nROIs; eval(['plot(rtime(1,:),roi_' num2str(i)
'normmeans(1,:), ''Color'',colors(i,:), ''LineWidth'',2);']); end;
plot(ecg(:,6),ecg(:,9),'r', 'LineWidth', 2); plot(ecg(:,6),ecg(:,8),'k',
'LineWidth', 2); xlabel('time (sec)'); %set(gca, 'YTick', []);
%title(sprintf(titlestrroisandecg, frselect));
%Display "ECG" and "ROI _" in appropriate places on the Y axis
%define number of labels required
nlabels=nROIs+2;
%divide Y axis into the appropriate number of sections:
set(gca, 'YTick', 0.5:1:nlabels);
%now display:
if nROIs==1, set(gca, 'YTickLabel', 'STIM|ECG|ROI 1'), elseif nROIs==2,
set(gca, 'YTickLabel', 'STIM|ECG|ROI 1|ROI 2'), elseif nROIs==3, set(gca,
'YTickLabel', 'STIM|ECG|ROI 1|ROI 2|ROI 3'), elseif nROIs==4, set(gca,
'YTickLabel', 'STIM|ECG|ROI 1|ROI 2|ROI 3|ROI 4'), elseif nROIs==5, set(gca,
'YTickLabel', 'STIM|ECG|ROI 1|ROI 2|ROI 3|ROI 4|ROI 5'), elseif nROIs==6,
set(gca, 'YTickLabel', 'STIM|ECG|ROI 1|ROI 2|ROI 3|ROI 4|ROI 5|ROI 6'),
elseif nROIs==7, set(gca, 'YTickLabel', 'STIM|ECG|ROI 1|ROI 2|ROI 3|ROI 4|ROI
5|ROI 6|ROI 7'),  elseif nROIs==8, set(gca, 'YTickLabel', 'STIM|ECG|ROI 1|ROI
2|ROI 3|ROI 4|ROI 5|ROI 6|ROI 7|ROI 8'), end;

driftokay=input('Is another round of drift removal required (y/n)?:   ');
end;

%-------------------------------------------------------------------------
%%%%%%%%%%%%%%%%%%% Ask User for Time Window to Analyze %%%%%%%%%%%%%%%%%%%
%After displaying the ROI plots against the ECG and stim, ask user for the
%time window that they'd like to proceed analyzing (for determining
%activation frequency, peaks/valleys, period of ROIs, and for later
%activation mapping:

nstarttime=input('Please enter the range you wish to plot the data:\nBegin at
time:   ');
nendtime=input('End at time:   ');

%Now get rid of data outside of the user selected window:
nstartframe=find(rtime(:)>nstarttime,1);
nendframe=find(rtime(:)>nendtime,1);
DATAfd(:,:,nendframe:end)=[];DATAfd(:,:,1:nstartframe)=[];
rtime(nendframe:end)=[];rtime(1:nstartframe)=[];
```

```matlab
newnewendtime=rtime(end);newnewstarttime=rtime(1);
newremoveend=find(ecg(:,3)==newnewendtime);newremovestart=find(ecg(:,3)==newn
ewstarttime);
ecg(newremoveend+1:end,:)=[];ecg(1:newremovestart-1,:)=[];
frame=nendframe-nstartframe-1;
for i=1:nROIs, eval(['roi_' num2str(i) '(:,:,nendframe:end)=[];']); end;
for i=1:nROIs, eval(['roi_' num2str(i) '(:,:,1:nstartframe)=[];']); end;
for i=1:nROIs, eval(['roi_' num2str(i) 'means(nendframe:end)=[];']); end;
for i=1:nROIs, eval(['roi_' num2str(i) 'means(1:nstartframe)=[];']); end;

%REDO normalization within the selected time range:
%find ranges (max-min) of each ROI means:
for i=1:nROIs, eval(['roi_' num2str(i) 'range=(max(roi_' num2str(i) 'means)-
min(roi_' num2str(i) 'means));']); end;
%now add these ranges to a vector called "ranges":
for i=1:nROIs, eval(['ranges(i)=roi_' num2str(i) 'range;']); end;
%now find max of the ranges:
[MAXrange roiwmax] = max(ranges);
%now normalize ROI means to ROI with max range:
for i=1:nROIs; eval(['roi_' num2str(i) 'normmeans=zeros(length(roi_'
num2str(i) 'means)); roi_' num2str(i) 'normmeans=(roi_' num2str(i) 'means-
min(roi_' num2str(i) 'means))./(MAXrange);']); end;

%now increase each successive ROI by "1", "2", etc. so that they can be
%plotted and appear stacked on top of eachother (so we can easily correlate
%them):
increase=1;
for n=1:nROIs; eval(['roi_' num2str(n) 'normmeans=roi_' num2str(n)
'normmeans+increase; increase=increase+1;']); end; %note, can change the
"n=1:nROIs" to "n=2:nROIs" if I don't want the normalized ROI mean plots to
start at 2 (using "2" makes then start at 1)
%then add 1 again to push up ROI normmeans because we have the stim signal
%plotting as well:
for n=1:nROIs; eval(['roi_' num2str(n) 'normmeans=roi_' num2str(n)
'normmeans+1;']); end;

%Now tell user that the movie is _ seconds long, then ask what time time
range they want to plot:
disp(['The selected window is ' num2str(max(rtime)) ' seconds long total.']);

%kick out new plot:
%for figures (plot traces without ECG identifiers):
titlestrsupp=[animal, ' - Normalized ROI FI Means, Heart Stim & ECG'];
figure('Name',titlestrsupp,'NumberTitle','off'); hold on; axis([nstarttime
nendtime 0 (nROIs+2)]); for i=1:nROIs; eval(['plot(rtime(1,:),roi_'
num2str(i) 'normmeans(1,:), ''Color'',colors(i,:), ''LineWidth'',2);']); end;
plot(ecg(:,6),ecg(:,9),'r', 'LineWidth', 2); plot(ecg(:,6),ecg(:,8),'k',
'LineWidth', 2); xlabel('time (sec)'); %set(gca, 'YTick', []);
%title(sprintf(titlestrroisandecg, frselect));
%Display "ECG" and "ROI _" in appropriate places on the Y axis
%divide Y axis into the appropriate number of sections:
set(gca, 'YTick', 0.5:1:nlabels);
%now display:
if nROIs==1, set(gca, 'YTickLabel', 'STIM|ECG|ROI 1'), elseif nROIs==2,
set(gca, 'YTickLabel', 'STIM|ECG|ROI 1|ROI 2'), elseif nROIs==3, set(gca,
'YTickLabel', 'STIM|ECG|ROI 1|ROI 2|ROI 3'), elseif nROIs==4, set(gca,
```

```matlab
    'YTickLabel', 'STIM|ECG|ROI 1|ROI 2|ROI 3|ROI 4'), elseif nROIs==5, set(gca,
    'YTickLabel', 'STIM|ECG|ROI 1|ROI 2|ROI 3|ROI 4|ROI 5'), elseif nROIs==6,
    set(gca, 'YTickLabel', 'STIM|ECG|ROI 1|ROI 2|ROI 3|ROI 4|ROI 5|ROI 6'),
    elseif nROIs==7, set(gca, 'YTickLabel', 'STIM|ECG|ROI 1|ROI 2|ROI 3|ROI 4|ROI
    5|ROI 6|ROI 7'),  elseif nROIs==8, set(gca, 'YTickLabel', 'STIM|ECG|ROI 1|ROI
    2|ROI 3|ROI 4|ROI 5|ROI 6|ROI 7|ROI 8'), end;

    %save figure to file (as both a tiff and matlab file):
    h=gcf;
    saveas(h,titlestrsupp, 'tif');
    saveas(h,titlestrsupp);

    %Output the voltage range of the ECG:
    disp(['The Voltage range of ECG (mV): Max ' num2str(max(ecg(:,1))) ', Min '
    num2str(min(ecg(:,1)))]);
    %Output at end the regionproperties for each ROI (in order):
    display('ROI REGION INFO')
    for i=1:nROIs; eval(['S_' num2str(i) '(1,1)']); end;
    %Then output the regionproperties for the infarct region:
    display('INFARCT REGION INFO')
    I(1,1)

    %save('timecoursedata','roi_1normmeans','roi_2normmeans','roi_3normmeans','ro
    i_4normmeans','rtime','MAXrange','roiwmax','ecg')

    %-------------------------------------------------------------------------
    %%%%%%%%%%%%%%%%%%%%%%%%% Activation Frequency %%%%%%%%%%%%%%%%%%%%%%%%%%%%%%
    %Convert each roi signal into the freq domain, then find the dominant
    %frequency and convert this back into a time interval for that roi that
    %represents it's periodicity.  (Then can use this time interval for
    %the min peakdistance, if desired, so that accurate peaks can be detected).

    % frequency = Freq, sample time = max(rtime), length = frame
    NFFT=2^nextpow2(frame);
    for i=1:nROIs, eval(['Y_' num2str(i) '=fft(roi_' num2str(i) 'means-mean(roi_'
    num2str(i) 'means),NFFT)/frame;']); end;
    for i=1:nROIs, eval(['f_' num2str(i) '=Freq/2*linspace(0,1,NFFT/2+1);']);
    end;
    for i=1:nROIs, eval(['[Y_' num2str(i) 'max, Yindex_' num2str(i)
    ']=max(2*abs(Y_' num2str(i) '(1:NFFT/2+1)));']); end;
    for i=1:nROIs, eval(['freq_' num2str(i) '=f_' num2str(i) '(Yindex_'
    num2str(i) ');']); end;
    for i=1:nROIs, eval(['period_' num2str(i) '=1/freq_' num2str(i) ';']); end;

    %  plotting:
    % figure(),plot(f_1,2*abs(Y_1(1:NFFT/2+1)))
    % title('Single-Sided Amplitude Spectrum of y(t)')
    % xlabel('Frequency (Hz)')
    % ylabel('|Y(f)1|')
    %
    % figure(),plot(f_2,2*abs(Y_2(1:NFFT/2+1)))
    % title('Single-Sided Amplitude Spectrum of y(t)')
    % xlabel('Frequency (Hz)')
    % ylabel('|Y(f)2|')
```

```
%need to output this info for all ROIs (actually will do later, with +/- SEM
based on peak & valley analysis):
%need to use this info to inform windows that will be used later in program
%- but can't use exact period info because could potentially miss some
%peaks, thus use 85% of this period to look for peaks:
for i=1:nROIs, eval(['MPD_' num2str(i) '=round((period_' num2str(i)
'/tbwframe)*.75);']); end;

%%% find peaks of the means of each ROI:
for n=1:nROIs, eval(['[Proi_' num2str(n) ' LProi_' num2str(n)
']=findpeaks(roi_' num2str(n) 'normmeans, ''MINPEAKDISTANCE'',MPD_'
num2str(n) ');']); end;
% valleys in the signals:
for n=1:nROIs, eval(['[Vroi_' num2str(n) ' LVroi_' num2str(n) ']=findpeaks(-
roi_' num2str(n) 'normmeans, ''MINPEAKDISTANCE'',MPD_' num2str(n) ');']);
end;
for n=1:nROIs, eval(['Vroi_' num2str(n) ' =-Vroi_' num2str(n) ';']); end;

%now plot and ask user for verification that peaks & valleys were properly
%identified:
titlestrpvs=[animal, ' - ROI peaks and valleys'];
figure('Name',titlestrpvs, 'NumberTitle','off');
for n=1:nROIs, eval(['subplot(nROIs, 1, n); hold; plot(roi_' num2str(n)
'normmeans, ''g''); title(''ROI ' num2str(n) '''); axis([0 length(roi_'
num2str(n) 'normmeans) min(roi_' num2str(n) 'normmeans) max(roi_' num2str(n)
'normmeans)]); ylabel(''FI''); plot(LProi_' num2str(n) ',Proi_' num2str(n)
',''bo''); plot(LVroi_' num2str(n) ',Vroi_' num2str(n) ',''ro'');hold
off;']); end;

pvsokay=input('Are the peaks and valleys for each ROI correctly identified
(y/n)?:  ');
while pvsokay==n
    newmod=input('Please enter new multiplier for peak detection
(default=0.75):  ');
    for i=1:nROIs, eval(['MPD_' num2str(i) '=round((period_' num2str(i)
'/tbwframe)*newmod);']); end;
    % find peaks of the means of each ROI:
    for n=1:nROIs, eval(['[Proi_' num2str(n) ' LProi_' num2str(n)
']=findpeaks(roi_' num2str(n) 'normmeans, ''MINPEAKDISTANCE'',MPD_'
num2str(n) ');']); end;
    % valleys in the signals:
    for n=1:nROIs, eval(['[Vroi_' num2str(n) ' LVroi_' num2str(n)
']=findpeaks(-roi_' num2str(n) 'normmeans, ''MINPEAKDISTANCE'',MPD_'
num2str(n) ');']); end;
    for n=1:nROIs, eval(['Vroi_' num2str(n) ' =-Vroi_' num2str(n) ';']); end;
    titlestrpvs=[animal, ' - ROI peaks and valleys'];
    figure('Name',titlestrpvs, 'NumberTitle','off');
    for n=1:nROIs, eval(['subplot(nROIs, 1, n); hold; plot(roi_' num2str(n)
'normmeans, ''g''); title(''ROI ' num2str(n) '''); axis([0 length(roi_'
num2str(n) 'normmeans) min(roi_' num2str(n) 'normmeans) max(roi_' num2str(n)
'normmeans)]); ylabel(''FI''); plot(LProi_' num2str(n) ',Proi_' num2str(n)
',''bo''); plot(LVroi_' num2str(n) ',Vroi_' num2str(n) ',''ro'');hold
off;']); end;
    pvsokay=input('Are the peaks and valleys for each ROI correclty
identified (y/n)?:  ');
end;
```

```matlab
disp('"Proi_x/LProi_x" & "Vroi_x/LVroi_x" have stored the value & frames of
the')
disp('peaks and valleys of each ROI, respectively.')
disp('Open these variables to perform statistics on ROI intervals.')


%-------------------------------------------------------------------------
%%%%%%%%%%%%%%%%%%%%%%%%%%%%%%% SAVE DATA %%%%%%%%%%%%%%%%%%%%%%%%%%%%%%%%%%%
save(animal)
%Save ROI Masks to a matlab file named "'animal'_ROI_Masks":
titlerois=[animal, '_ROI_Masks'];
save(titlerois, 'roimask_*');

%save('red18timecoursedata','roi_1normmeans','roi_2normmeans','roi_3normmeans
','roi_4normmeans','rtime','MAXrange','roiwmax','ecg')


%-------------------------------------------------------------------------
%%%%%%%%%%%%%%%%%%%%%%%%%%%%%% ACTIVATION MAPS %%%%%%%%%%%%%%%%%%%%%%%%%%%%%%%
%goal here is to create a single matrix that contains the activation time
%of each pixel for a given window of time (one complete activation).
% NOTE: skipping a re-normalization step for now.

%first ask user if Activation Maps are desired:
ActMapyeah=input('Do you want to continue with Activation Maps (y/n)?  ',
's');
if strcmp(ActMapyeah,'n')
    error('This concludes the analysis (disregard error message above).')
end;

%Apply a combined mask that keeps everything inside defined ROIs, but
%removes everything else:
combroimask=zeros(size(roimask_1));
for i=1:nROIs, eval(['combroimask=combroimask+roimask_' num2str(i) ';']);
end;
for y=1:frame, DATAfd(:,:,y)=combroimask(:,:).*DATAfd(:,:,y); end;

%%% NORMALIZING %%%
%goal here is to normalize the data to the same amplitude so
%that peak fluorescence (F=1) corresponds to a depolarized membrane
%potential and baseline fluorescence (F=0) corresponds to the resting
%membrane potential.  THIS IS DONE ON A SINGLE PIXEL LEVEL THROUGH TIME!
vector4=reshape(DATAfd,[],size(DATAfd,3));
vector4n=zeros(size(vector4));
for w=1:size(vector4,1)
    vector4n(w,:)=(vector4(w,:)-min(vector4(w,:)))./(max(vector4(w,:))-
min(vector4(w,:)));
end
DATAfdn=reshape(vector4n,size(DATAfd,1),size(DATAfd,2),[]);

%%% Visualize the activation of all ROIs over a still shot of the heart:
%find ranges (max-min) of the combined ROIs:
combroimax=max(max(max(DATAfdn)));
combroimin=min(min(min(DATAfdn)));
combroirange=combroimax-combroimin;
%also find range of background image, M:
```

142

```matlab
M=M.*Active;
Mmax=max(max(max(M)));
Mmin=min(min(min(M)));
Mrange=Mmax-Mmin;
%now scale the combined ROI data to between 128-256:
DATAscaled=zeros(size(DATAfdn));
DATAscaled=(((DATAfdn-combroimin)./combroirange).*128)+128;
for y=1:frame, DATAscaled(:,:,y)=combroimask(:,:).*DATAscaled(:,:,y); end;
%now set values of NaN in DATAscaled ==0:
DATAscaled(isnan(DATAscaled))=0;
%now scale the backfround image to between 0-128
Mscaled=zeros(size(M));
Mscaled=((M-Mmin)./Mrange).*128;
%now create a combined colormap of gray and jet so that the background and
%ROI data will be displayed with the appropriate color:
Ncolormap=[gray(128); br];
%now create a new, single data matrix of Mscaled and DATAscaled:
Mscaledcomplement=Mscaled.*imcomplement(combroimask);
Activation=zeros(size(DATAscaled));
for i=1:frame, Activation(:,:,i) = DATAscaled(:,:,i)+(Mscaledcomplement);end;
% %now play:
% titlestrfdnd=[animal, ' - Activation of ROIs'];
% figure('Name',titlestrfdnd,'NumberTitle','off');
% for i=1:frame; imagesc(Activation(:,:,i));axis square;  set(gca, 'YTick',
[]);set(gca, 'XTick', []); set(gca,'clim', [0 256]); colormap(Ncolormap);
title(sprintf('Frame %i', i));  pause(tbwframe); end;


% %want to see what an individual & active pixel trace looks like:
% figure(),plot((reshape(DATAscaled(xactive,yactive,:),1,[])),'b');



%FURTHER FILTERING REQ'D PER PIXEL FOR ACTIVATION & CV MAPS! Implement
%sgolay filter now on pixels within identified ROIs:
slength=100; %setting the length of the sgolay...
sgolayo=2;
%filter to a multiple of the number of frames total that through trial and
error I found to work well
vector5=reshape(DATAfdn,[],size(DATAfdn,3));
DATAsgolay=zeros(size(vector5));
for x=1:length(vector5),
    if isfinite(vector5(x))
        DATAsgolay(x,:)=smooth(vector5(x,:),slength,'sgolay',sgolayo); %need
to modify this here...
        %(as well as others below)...and instead of doing it for entire
    end;
end;
DATAsgolay=reshape(DATAsgolay,size(DATAfdn,1),size(DATAfdn,2),[]);

% %want to see what an individual & active pixel trace looks like:
%figure(),plot((reshape(DATAsgolay(xactive,yactive,:),1,[])),'b');


%-------------------------------------------------------------------------
%%%%%%%%%%%% REMOVE EFFECTS OF FILTERING AT ENDS AGAIN %%%%%%%%%%%%%%%%%%%%%
%goal here is to remove the first 80 and last 80 frames due to effects from
%filtering.  But, since we have ECG here, we cant' just get rid of the
%first and last frames, we need to get rid of all time points corresponding
```

```matlab
%to the first and last 80 frames:
DATAfdn(:,:,end-80+1:end)=[];DATAfdn(:,:,1:80)=[];
DATAsgolay(:,:,end-80+1:end)=[];DATAsgolay(:,:,1:80)=[];
rtime(end-80+1:end)=[];rtime(1:80)=[];
newendtime=rtime(end);newstarttime=rtime(1);
removeend=find(abs(ecg(:,10) - newendtime*1000) <
0.5);removestart=find(abs(ecg(:,10) - newstarttime*1000) < 0.5);
ecg(removeend+1:end,:)=[];ecg(1:removestart-1,:)=[];
frame=frame-160;
%-------------------------------------------------------------------

% want to see what an individual & active pixel trace looks like after the
sgolay:
titlestraddfiltering=[animal, ' - Individual Pixel Data - additional
filtering for ActMap'];
figure('Name',titlestraddfiltering,'NumberTitle','off')
subplot(3,1,1), plot((reshape(DATAfdn(xactive,yactive,:),1,[])),'r'),
title('previously filtered data');
subplot(3,1,2), plot((reshape(DATAsgolay(xactive,yactive,:),1,[])),'k'),
title('after sgolay');
subplot(3,1,3), plot((reshape(DATAfdn(xactive,yactive,:),1,[])),'r'); hold
on; plot((reshape(DATAsgolay(xactive,yactive,:),1,[])),'k'),title('overlay');
h=gcf;
saveas(h,titlestraddfiltering, 'tif');
saveas(h,titlestraddfiltering);


%Now redo the mean of each ROI:
for i=1:nROIs; eval(['CCnew_' num2str(i) '=bwconncomp(roimask_' num2str(i)
'(:,:));']); end;
for i=1:nROIs; for j=1:frame; eval(['S_' num2str(i)
'new(j)=regionprops(CCnew_' num2str(i) ', DATAsgolay(:,:,j), ''Area'',
''Perimeter'', ''Centroid'', ''PixelIdxList'', ''PixelList'',
''MaxIntensity'', ''MinIntensity'', ''MeanIntensity'');']); end; end;
%do trick to extract means from S_x into separate matrix, then plot this
for i=1:nROIs; eval(['roi_' num2str(i) 'sgolaymeans=[S_' num2str(i)
'new.MeanIntensity];']); end;
%NOTE that this method does not count the zeros that make up the 128x128
%matrices, which could adversely lower the mean values of ROIs

%Now re-normalize at each pixel (for use in mapping):
vector6=reshape(DATAsgolay,[],size(DATAsgolay,3));
vector6n=zeros(size(vector6));
for w=1:size(vector6,1)
    if isfinite(vector6(w))
    vector6n(w,:)=(vector6(w,:)-min(vector6(w,:)))./(max(vector6(w,:))-
min(vector6(w,:)));
    end;
end;
DATAsgolayn=reshape(vector6n,size(DATAsgolay,1),size(DATAsgolay,2),[]);

%%%%%%%%%%%%%%%%%%%%%%%%%%%%%%%%%%%%%
%Before moving too much far forward, play sgolay filtered data to see if it
%is sensical: scale to between 128-256:
combroimaxsgolayn=max(max(max(DATAsgolayn)));
combroiminsgolayn=min(min(min(DATAsgolayn)));
```

```matlab
combroirangesgolayn=combroimaxsgolayn-combroiminsgolayn;
DATAsgolayscaled=zeros(size(DATAsgolayn));
DATAsgolayscaled=(((DATAsgolayn-
combroiminsgolayn)./combroirangesgolayn).*128)+128;
for y=1:frame,
DATAsgolayscaled(:,:,y)=combroimask(:,:).*DATAsgolayscaled(:,:,y); end;
%now set values of NaN in DATAscaled ==0:
DATAsgolayscaled(isnan(DATAsgolayscaled))=0;
%now create a new, single data matrix of Mscaled and DATAsgolayscaled:
Activationsgolay=zeros(size(DATAsgolayscaled));
for i=1:frame, Activationsgolay(:,:,i) =
DATAsgolayscaled(:,:,i)+(Mscaledcomplement);end;
%now play:
titlestrfdnd=[animal, ' - Activation of ROIs'];
figure('Name',titlestrfdnd,'NumberTitle','off');
for i=1:frame; imagesc(Activationsgolay(:,:,i));axis square;  set(gca,
'YTick', []);set(gca, 'XTick', []); set(gca,'clim', [0 256]);
colormap(Ncolormap); title(sprintf('Frame %i', i));  pause(tbwframe); end;
% ----------------------------------------------
figure()
%Now create a movie of the above:
titlemovie=[animal,'_Activation of ROIs'];
vidObj=VideoWriter(titlemovie);
%set the framerate
vidObj.FrameRate=(round(1/tbwframe));
%write sequence of frames to the compressed AVI file:
open(vidObj);
for i=1:frame; imagesc(Activationsgolay(:,:,i)); axis square; set(gca,
'YTick', []);set(gca, 'XTick', []);
    set(gca,'clim', [0 256]); colormap(Ncolormap); title(sprintf('Time (s) =
%.3f', rtime(i)));
    currFrame=getframe; writeVideo(vidObj,currFrame); end;
close(vidObj);

%Now create a movie of sgolay activation at slower time:
figure()
titlemovie=[animal,'_Activation of ROIs_one tenth speed'];
vidObj=VideoWriter(titlemovie);
%set the framerate
vidObj.FrameRate=(round(1/(tbwframe*10)));
%write sequence of frames to the compressed AVI file:
open(vidObj);
for i=1:frame; imagesc(Activationsgolay(:,:,i)); axis square; set(gca,
'YTick', []);set(gca, 'XTick', []);
    set(gca,'clim', [0 256]); colormap(Ncolormap); title(sprintf('Time (s) =
%.3f', rtime(i)));
    currFrame=getframe; writeVideo(vidObj,currFrame); end;
close(vidObj);
%%%%%%%%%%%%%%%%%%%%%%%%%%%%%%%%%%%%%

% %apply ROI masks to recently filtered data:
% for i=1:nROIs; eval(['roi_' num2str(i) 'new=zeros(128,128,frame);']); for
j=1:frame; eval(['roi_' num2str(i) 'new(:,:,j)=roimask_' num2str(i)
'(:,:).*DATAsgolayn(:,:,j);']); end; end;

%%%%reshape for 1st derivative calculation:
```

```matlab
vector7=reshape(DATAsgolayn,[],size(DATAsgolayn,3));
vector7d=zeros((size(vector7,1)),(size(vector7,2))-1);
vector7d=diff(vector7,1,2);
% %normalize:
% for w=1:size(vector7d,1)
%     if isfinite(vector7d(w))
%     vector7d(w,:)=(vector7d(w,:)-min(vector7d(w,:)))./(max(vector7d(w,:))-
min(vector7d(w,:)));
%     end;
% end;
DATAsgolaynd=reshape(vector7d,size(DATAsgolayn,1),size(DATAsgolayn,2),[]);
% create a time vector for the 1st derivative stack:
drtime=zeros(1,frame-1);
for i=1:frame-1; drtime(i)=((rtime(i)+rtime(i+1))/2);end;
% filtering 1st Derivative signal for each pixel:
% Implement sgolay filter now on pixels within identified ROIs:
vector7ds=reshape(DATAsgolaynd,[],size(DATAsgolaynd,3));
DATA2sgolaynd=zeros(size(vector7ds));
for x=1:length(vector7ds),
    if isfinite(vector7ds(x))
        DATA2sgolaynd(x,:)=smooth(vector7ds(x,:),slength,'sgolay',sgolayo);
    end;
end;
DATA2sgolaynd=reshape(DATA2sgolaynd,size(DATAsgolayn,1),size(DATAsgolayn,2),[
]);

% % now mask this based on ROIs:
% for i=1:nROIs; eval(['roi_' num2str(i) 'd=zeros(128,128,frame-1);']); for
j=1:frame-1; eval(['roi_' num2str(i) 'd(:,:,j)=roimask_' num2str(i)
'(:,:).*DATAsgolaynd(:,:,j);']); end; end;
%roi_1d(isnan(roi_1dd))=0;

%Now find the mean of each ROId:
for i=1:nROIs; eval(['CCnew_' num2str(i) 'd=bwconncomp(roimask_' num2str(i)
'(:,:));']); end;
for i=1:nROIs; for j=1:frame-1; eval(['S_' num2str(i)
'newd(j)=regionprops(CCnew_' num2str(i) 'd, DATA2sgolaynd(:,:,j), ''Area'',
''Perimeter'', ''Centroid'', ''PixelIdxList'', ''PixelList'',
''MaxIntensity'', ''MinIntensity'', ''MeanIntensity'');']); end; end;
%do trick to extract means from S_x into separate matrix, then plot this
for i=1:nROIs; eval(['roi_' num2str(i) 'dmeans=[S_' num2str(i)
'newd.MeanIntensity];']); end;
%NOTE that this method does not count the zeros that make up the 128x128
%matrices, which could adversely lower the mean values of ROIs

%%%%reshape for 2nd derivative calculation:
vector8=reshape(DATA2sgolaynd,[],size(DATA2sgolaynd,3));
vector8d=zeros((size(vector8,1)),(size(vector8,2))-1);
vector8d=diff(vector8,1,2);
% %normalize:
% for w=1:size(vector8d,1)
%     if isfinite(vector8d(w))
%     vector8d(w,:)=(vector8d(w,:)-min(vector8d(w,:)))./(max(vector8d(w,:))-
min(vector8d(w,:)));
%     end;
% end;
```

```matlab
DATAsgolayndd=reshape(vector8d,size(DATA2sgolaynd,1),size(DATA2sgolaynd,2),[]
);
% create a time vector for the 2nd derivative stack:
ddrtime=zeros(1,frame-2);
for i=1:frame-2; ddrtime(i)=((drtime(i)+drtime(i+1))/2);end; %the same as
"rtime" but with first and last times gone
% filtering 2nd Derivative signal for each pixel:
% Implement sgolay filter now on pixels within identified ROIs:
vector8ds=reshape(DATAsgolayndd,[],size(DATAsgolayndd,3));
DATA2sgolayndd=zeros(size(vector8ds));
for x=1:length(vector8ds),
    if isfinite(vector8ds(x))
        DATA2sgolayndd(x,:)=smooth(vector8ds(x,:),slength,'sgolay',sgolayo);
    end;
end;
DATA2sgolayndd=reshape(DATA2sgolayndd,size(DATA2sgolaynd,1),size(DATA2sgolayn
d,2),[]);

%and plot norm, 1st diff, and 2nd diff signals for identified active pixel:
titlestrds=[animal, ' - Individual Pixel Data - Normal & Derivatives'];
figure('Name',titlestrds,'NumberTitle','off')
subplot(3,1,1), plot((reshape(DATAsgolayn(xactive,yactive,:),1,[])),'r'),
title('Normal time');
subplot(3,1,2), plot((reshape(DATA2sgolaynd(xactive,yactive,:),1,[])),'k'),
title('1st derivative');
subplot(3,1,3), plot((reshape(DATA2sgolayndd(xactive,yactive,:),1,[])),'b');
title('2nd derivative');
h=gcf;
saveas(h,titlestrds, 'tif');
saveas(h,titlestrds);

%NOT DONE AT THIS TIME
% % now mask this based on ROIs:
% for i=1:nROIs; eval(['roi_' num2str(i) 'dd=zeros(128,128,frame-2);']); for
j=1:frame-2; eval(['roi_' num2str(i) 'dd(:,:,j)=roimask_' num2str(i)
'(:,:).*DATAsgolayndd(:,:,j);']); end; end;

%Now find the mean of each ROIdd:
for i=1:nROIs; eval(['CCnew_' num2str(i) 'dd=bwconncomp(roimask_' num2str(i)
'(:,:));']); end;
for i=1:nROIs; for j=1:frame-2; eval(['S_' num2str(i)
'newdd(j)=regionprops(CCnew_' num2str(i) 'dd, DATA2sgolayndd(:,:,j),
''Area'', ''Perimeter'', ''Centroid'', ''PixelIdxList'', ''PixelList'',
''MaxIntensity'', ''MinIntensity'', ''MeanIntensity'');']); end; end;
%do trick to extract means from S_x into separate matrix, then plot this
for i=1:nROIs; eval(['roi_' num2str(i) 'ddmeans=[S_' num2str(i)
'newdd.MeanIntensity];']); end;
%NOTE that this method does not count the zeros that make up the 128x128
%matrices, which could adversely lower the mean values of ROIs

% %Create vector that is the mean of the 1st and 2nd derivative signals for
each ROI:
% for i=1:nROIs; eval(['roi_' num2str(i) 'dmeans=zeros(0,frame-1); for
n=1:frame-1; roi_' num2str(i) 'dmeans(n)=(mean2(roi_' num2str(i)
'd(:,:,n)));end;']); end;
```

147

```matlab
% for i=1:nROIs; eval(['roi_' num2str(i) 'ddmeans=zeros(0,frame-2); for
n=1:frame-2; roi_' num2str(i) 'ddmeans(n)=(mean2(roi_' num2str(i)
'dd(:,:,n)));end;']); end;

%need to refind the peaks & valleys for the sgolay filtered ROIs now!
for n=1:nROIs, eval(['[Proi_' num2str(n) 'sg LProi_' num2str(n)
'sg]=findpeaks(roi_' num2str(n) 'sgolaymeans, ''MINPEAKDISTANCE'',MPD_'
num2str(n) ');']); end;
for n=1:nROIs, eval(['[Vroi_' num2str(n) 'sg LVroi_' num2str(n)
'sg]=findpeaks(-roi_' num2str(n) 'sgolaymeans, ''MINPEAKDISTANCE'',MPD_'
num2str(n) ');']); end;
for n=1:nROIs, eval(['Vroi_' num2str(n) 'sg =-Vroi_' num2str(n) 'sg;']); end;
% Find peaks in 1st derivative signal for each ROI:
for n=1:nROIs, eval(['[Proi_' num2str(n) 'd LProi_' num2str(n)
'd]=findpeaks(roi_' num2str(n) 'dmeans, ''MINPEAKDISTANCE'',MPD_' num2str(n)
');']); end;
% Find peaks in 2nd derivative signal for each ROI:
for n=1:nROIs, eval(['[Proi_' num2str(n) 'dd LProi_' num2str(n)
'dd]=findpeaks(roi_' num2str(n) 'ddmeans, ''MINPEAKDISTANCE'',MPD_'
num2str(n) ');']); end;

%now plot the mean of the normal, 1st derivative, and 2nd derivative
%signals, for each ROI:
for n=1:nROIs;
    eval(['figure(),title(''ROI ' num2str(n) ' peaks & valleys'');
subplot(3,1,1), hold on; plot(roi_' num2str(n) 'sgolaymeans, ''g'');
title(''ROI ' num2str(n) '  Mean''); axis([0 length(roi_' num2str(n)
'sgolaymeans) min(roi_' num2str(n) 'sgolaymeans) max(roi_' num2str(n)
'sgolaymeans)]); ylabel(''FI''); plot(LProi_' num2str(n) 'sg,Proi_'
num2str(n) 'sg,''bo''); plot(LVroi_' num2str(n) 'sg,Vroi_' num2str(n)
'sg,''ro''); subplot(3,1,2), hold on; plot(roi_' num2str(n) 'dmeans, ''g'');
title(''ROI ' num2str(n) '  1st Deriv Mean''); axis([0 length(roi_'
num2str(n) 'dmeans) min(roi_' num2str(n) 'dmeans) max(roi_' num2str(n)
'dmeans)]); ylabel(''FI''); plot(LProi_' num2str(n) 'd,Proi_' num2str(n)
'd,''bo''); subplot(3,1,3), hold on; plot(roi_' num2str(n) 'ddmeans, ''g'');
title(''ROI ' num2str(n) '  2nd Deriv Mean''); axis([0 length(roi_'
num2str(n) 'ddmeans) min(roi_' num2str(n) 'ddmeans) max(roi_' num2str(n)
'ddmeans)]); ylabel(''FI''); plot(LProi_' num2str(n) 'dd,Proi_' num2str(n)
'dd,''bo'');']);
end;

pvsokay=input('Are the peaks and valleys for each ROI correctly identified
(y/n)?:  ');
while pvsokay==n
    newmod=input('Please enter new multiplier for peak detection
(default=0.75):  ');
    for i=1:nROIs, eval(['MPD_' num2str(i) '=round((period_' num2str(i)
'/tbwframe)*newmod);']); end;
    %need to refind the peaks & valleys for the sgolay filtered ROIs now!
    for n=1:nROIs, eval(['[Proi_' num2str(n) 'sg LProi_' num2str(n)
'sg]=findpeaks(roi_' num2str(n) 'sgolaymeans, ''MINPEAKDISTANCE'',MPD_'
num2str(n) ');']); end;
    for n=1:nROIs, eval(['[Vroi_' num2str(n) 'sg LVroi_' num2str(n)
'sg]=findpeaks(-roi_' num2str(n) 'sgolaymeans, ''MINPEAKDISTANCE'',MPD_'
num2str(n) ');']); end;
```

```matlab
    for n=1:nROIs, eval(['Vroi_' num2str(n) 'sg =-Vroi_' num2str(n) 'sg;']);
end;
    % Find peaks in 1st derivative signal for each ROI:
    for n=1:nROIs, eval(['[Proi_' num2str(n) 'd LProi_' num2str(n)
'd]=findpeaks(roi_' num2str(n) 'dmeans, ''MINPEAKDISTANCE'',MPD_' num2str(n)
');']); end;
    % Find peaks in 2nd derivative signal for each ROI:
    for n=1:nROIs, eval(['[Proi_' num2str(n) 'dd LProi_' num2str(n)
'dd]=findpeaks(roi_' num2str(n) 'ddmeans, ''MINPEAKDISTANCE'',MPD_'
num2str(n) ');']); end;
    %now plot the mean of the normal, 1st derivative, and 2nd derivative
    %signals, for each ROI:
    for n=1:nROIs;
        eval(['figure(),title(''ROI ' num2str(n) ' peaks & valleys'');
subplot(3,1,1), hold on; plot(roi_' num2str(n) 'sgolaymeans, ''g'');
title(''ROI ' num2str(n) '  Mean''); axis([0 length(roi_' num2str(n)
'sgolaymeans) min(roi_' num2str(n) 'sgolaymeans) max(roi_' num2str(n)
'sgolaymeans)]); ylabel(''FI''); plot(LProi_' num2str(n) 'sg,Proi_'
num2str(n) 'sg,''bo''); plot(LVroi_' num2str(n) 'sg,Vroi_' num2str(n)
'sg,''ro''); subplot(3,1,2), hold on; plot(roi_' num2str(n) 'dmeans, ''g'');
title(''ROI ' num2str(n) '  1st Deriv Mean''); axis([0 length(roi_'
num2str(n) 'dmeans) min(roi_' num2str(n) 'dmeans) max(roi_' num2str(n)
'dmeans)]); ylabel(''FI''); plot(LProi_' num2str(n) 'd,Proi_' num2str(n)
'd,''bo''); subplot(3,1,3), hold on; plot(roi_' num2str(n) 'ddmeans, ''g'');
title(''ROI ' num2str(n) '  2nd Deriv Mean''); axis([0 length(roi_'
num2str(n) 'ddmeans) min(roi_' num2str(n) 'ddmeans) max(roi_' num2str(n)
'ddmeans)]); ylabel(''FI''); plot(LProi_' num2str(n) 'dd,Proi_' num2str(n)
'dd,''bo'');']);
    end;
    pvsokay=input('Are the peaks and valleys for each ROI correctly
identified (y/n)?:  ');
end;


%-------------------------------------------------------------------------
%%%%%%%%%%%%%% Now to selecting windows for mapping %%%%%%%%%%%%%%%%%%%%%%
% Select time window for activation mapping (one window per ROI):
disp('For the following, use the cursor function and extract the frame (X)
values:')
for i=1:nROIs;
    eval(['roi_' num2str(i) 'fstart=input([''Enter a start frame to search
for activation of ROI ' num2str(i) ': '']);']);
    eval(['roi_' num2str(i) 'fend=input([''Enter end frame of activation(s)
for ROI ' num2str(i) ': '']);']);
end;

%STEPS (generally, specifics may change):
%1) using the window selected above for each ROI, find the next min in the
%normal ROI signal as well as the next maximum in the signal.
%2) using the locations of the minimums and subsequent maximums, search
%within each and find the max derivative between this small window on a per
%pixel basis for each ROI.
%3) for each ROI and each window, create an activation map
%4) end with plotting a montage of the activation maps for each ROI
%separately.  Can, for figures, etc. come into the code and specifically
%plot ones for figures.
%5) iff the activation maps are qualitatively the same, can ask user if
```

```matlab
%they want to average all of them for the generation of a single activation
%map
%6) next for CV maps, first ask user if CV maps are desired.  If so, then
%create a CV map for each separate activation map that was made in a
%similar montage fashion.  At the end can ask user if they want to generate
%one CV map that is based on the averaged activation map (iff the user
%elected to average the activation maps).


%find the identified valleys within the user selected frames:
for i=1:nROIs;
    eval(['roi_' num2str(i) 'ftemp=find(roi_' num2str(i) 'fstart <= LVroi_'
num2str(i) 'sg & LVroi_' num2str(i) 'sg <= roi_' num2str(i) 'fend);']);
    eval(['roi_' num2str(i) 'fvs=LVroi_' num2str(i) 'sg(roi_' num2str(i)
'ftemp);']);
end
%find the identified peaks within the user selected frames:
for i=1:nROIs;
    eval(['roi_' num2str(i) 'ftemp=find(roi_' num2str(i) 'fstart <= LProi_'
num2str(i) 'sg & LProi_' num2str(i) 'sg <= roi_' num2str(i) 'fend);']);
    eval(['roi_' num2str(i) 'fps=LProi_' num2str(i) 'sg(roi_' num2str(i)
'ftemp);']);
end

%now break up each ROI trace into sections, and search vector7ds for a max
%at each pixel.  Where ever this max occurs, mark the frame number where it
%happens in the separate matrix ActMapF_X_Y (X=roi #, Y=activation #), then
%later find the times that correspond to the frames and create the matrix
%ActMap_X_Y.  Then plot these ActMap_X_Y in a montage fashion for the user.
%NOTE: the benefit of breaking up into sections first then finding maximums
%is that I don't have to implement a peakfinding algorithm and double check
%it for the continuous time series.

for i=1:nROIs,
    eval(['elements(i)=numel(roi_' num2str(i) 'fvs)-1;']);
end;

%create vector9's that contain ROI specific data of the 1st derivative
for i=1:nROIs; eval(['vector9_' num2str(i) '=zeros(numpixs,numpixs,frame-
1);']); for j=1:frame-1; eval(['vector9_' num2str(i) '(:,:,j)=roimask_'
num2str(i) '(:,:).*DATA2sgolaynd(:,:,j);']); end; end;
for i=1:nROIs; eval(['vector9_' num2str(i) '(vector9_' num2str(i) ' == 0) =
NaN;']); end;
for i=1:nROIs; eval(['vector9_' num2str(i) '=reshape(vector9_' num2str(i)
',[],size(DATA2sgolaynd,3));']);end;
%now perform all operations to create activation maps for each activation
%of each ROI - VERY IMPORTANT STEPS HERE!!!! Note time is in milliseconds!
j=1;
for i=1:nROIs,
    for j=1:elements(i);
        eval(['roi_' num2str(i) '_' num2str(j) 'f=[roi_' num2str(i)
'fvs(j):roi_' num2str(i) 'fvs(j+1)]; roi_' num2str(i) '_' num2str(j)
'=vector9_' num2str(i) '(:,roi_' num2str(i) 'fvs(j):roi_' num2str(i)
'fvs(j+1)); [roi_' num2str(i) '_' num2str(j) 'maxd roi_' num2str(i) '_'
num2str(j) 'maxc] = max(roi_' num2str(i) '_' num2str(j) ', [], 2); roi_'
num2str(i) '_' num2str(j) 'fmax = roi_' num2str(i) '_' num2str(j) 'f(roi_'
```

150

```matlab
num2str(i) '_' num2str(j) 'maxc); roi_' num2str(i) '_' num2str(j) 'acttime =
drtime(roi_' num2str(i) '_' num2str(j) 'fmax); roi_' num2str(i) '_'
num2str(j) 'actmap = reshape(roi_' num2str(i) '_' num2str(j) 'acttime,
size(DATA2sgolaynd,1), size(DATAsgolaynd,2),[]); roi_' num2str(i) '_'
num2str(j) 'correction = min(min(roi_' num2str(i) '_' num2str(j) 'actmap));
roi_' num2str(i) '_' num2str(j) 'actmap = roi_' num2str(i) '_' num2str(j)
'actmap - roi_' num2str(i) '_' num2str(j) 'correction*ones(size(roi_'
num2str(i) '_' num2str(j) 'actmap,1),size(roi_' num2str(i) '_' num2str(j)
'actmap,2)); roi_' num2str(i) '_' num2str(j) 'actmap(roi_' num2str(i) '_'
num2str(j) 'actmap == 0) = NaN; roi_' num2str(i) '_' num2str(j) 'correction2
= nanmin(nanmin(roi_' num2str(i) '_' num2str(j) 'actmap)); roi_' num2str(i)
'_' num2str(j) 'actmap = roi_' num2str(i) '_' num2str(j) 'actmap - roi_'
num2str(i) '_' num2str(j) 'correction2*ones(size(roi_' num2str(i) '_'
num2str(j) 'actmap,1),size(roi_' num2str(i) '_' num2str(j) 'actmap,2)); roi_'
num2str(i) '_' num2str(j) 'actmap=roi_' num2str(i) '_' num2str(j)
'actmap*1000;']);
    end;
end;


%find max (longest time) of actmaps for plotting all actmaps:
for i=1:nROIs
    for j=1:elements(i);
        eval(['roi_' num2str(i) 'actmapmaxs(j)=max(max(roi_' num2str(i) '_'
num2str(j) 'actmap));']);
    end;
        eval(['roi_' num2str(i) 'actmapmax=max(roi_' num2str(i)
'actmapmaxs);']);
end;

%plot all actmaps as imagesc:
for i=1:nROIs
    for j=1:elements(i);
        eval(['figure(''Name'',''roi_' num2str(i) '_' num2str(j) ' Activation
(imagesc)'',''NumberTitle'',''off''),imagesc(roi_' num2str(i) '_' num2str(j)
'actmap), title(sprintf(''Time Range: %.3f to %.3f sec'',min(roi_' num2str(i)
'_' num2str(j) 'acttime),max(roi_' num2str(i) '_' num2str(j) 'acttime)));
axis off, colorbar, colormap(btr), axis square; caxis([0, roi_' num2str(i)
'actmapmax]), set(gca, ''YTick'', []);set(gca, ''XTick'', []), hgsave(''roi_'
num2str(i) '_' num2str(j) ' Activation (imagesc)''); print(''-dpng'',''roi_'
num2str(i) '_' num2str(j) ' Activation (imagesc)'');']);
    end;
end;

%Save all activation maps as a matrix:
titleActMaps=[animal, '_AllActMaps'];
save(titleActMaps, 'roi_*'); %note this will also save all roi_* data as well

% NO LONGER PLOTTING AND SAVING THESE CONTOUR MAPS, NOT FOUND TO BE USEFUL
% %plot all actmaps as contourf w/o lines:
% for i=1:nROIs
%     for j=1:elements(i);
%         eval(['figure(''Name'',''roi_' num2str(i) '_' num2str(j) '
Activation (contourf)'',''NumberTitle'',''off''),contourf(flipud(roi_'
num2str(i) '_' num2str(j) 'actmap),''LineColor'',''none''),
title(sprintf(''Time Range: %.3f to %.3f sec'',min(roi_' num2str(i) '_'
```

```matlab
num2str(j) 'acttime),max(roi_' num2str(i) '_' num2str(j) 'acttime))); axis
off, colorbar, axis square; caxis([0, roi_' num2str(i) 'actmapmax]), set(gca,
''YTick'', []);set(gca, ''XTick'', []), hgsave(''roi_' num2str(i) '_'
num2str(j) ' Activation (contourf)''); print(''-dpng'',''roi_' num2str(i) '_'
num2str(j) ' Activation (contourf)'');']);
%     end;
% end;


%need to plot histograms also, to get a visual of really how long
%activation takes and to discern whether or not the min & max limits used
%to plot are good:
%1st reshape the actmaps into a vector each, then sort these vectors in
%ascending order, then use the hist function to plot histograms of each:
for i=1:nROIs
    for j=1:elements(i);
        eval(['roi_' num2str(i) '_' num2str(j) 'hist = reshape(roi_'
num2str(i) '_' num2str(j) 'actmap,1,[]); roi_' num2str(i) '_' num2str(j)
'hist=sort(roi_' num2str(i) '_' num2str(j) 'hist); figure(''Name'',''roi_'
num2str(i) '_' num2str(j) ' Activation Time
Histogram'',''NumberTitle'',''off''), hist(roi_' num2str(i) '_' num2str(j)
'hist),title(sprintf(''Time Range: %.3f to %.3f sec'',min(roi_' num2str(i)
'_' num2str(j) 'acttime),max(roi_' num2str(i) '_' num2str(j) 'acttime)));
xlabel(''Activation Time (ms)''),ylabel(''Counts''),hgsave(''roi_' num2str(i)
'_' num2str(j) ' Activation Time Histogram''); print(''-dpng'',''roi_'
num2str(i) '_' num2str(j) ' Activation Time Histogram'');']);
    end;
end;

%save data:
save(animal)
```

A.2 Matlab script to analyze ex vivo calcium imaging data

```matlab
% created by Dominic Filice, work in progress from 2010-2015.


%------------------------------------------------------------------------
%%%%%%%%%%%%%%%%%%%%% SET POTENTIAL COLORMAPS %%%%%%%%%%%%%%%%%%%%%%%%%%%%%
%
%Making blue to white to red cmap. Note, every colormap has exactly 3
columns,
%and I want to go from red [1 0 0] at top to white [1 1 1] at middle to
%blue [0 0 1] at bottom.  In order to get even distribution of colors
%between these (wiht # of rows at 128), I'll need to set middle two rows
%at white, and set the other rows as an interpolation between 0 and 1.
bwr=zeros(128,3);
others=(0:(1/63):1); others=transpose(others);
rwbhalf=zeros(64,3);
rwbhalf(:,1)=others; rwbhalf(:,2)=others; rwbhalf(:,3)=ones;
bwr(1:64,:)=rwbhalf; bwr(65:end,:)=fliplr(flipud(rwbhalf));
%the above produces a colormap that is blue for early, red for late

%the below here produces the opposite (red for early, blue for late); this
%is the one we will use:
rwb=flipud(bwr); %named "rwb" for red (early) to white to blue (late)


%-------

%Now to produce special colormaps for voltage dye specific ActMaps:
btr=bwr;
btr(1:64,3)=btr(1:64,2); %produces a colormap that goes from black (early) to
red (late)
rtb=flipud(btr); %produces an opposite colormap that goes from red (early) to
black (late)

%Now to produce special colormaps for GCaMP3 specific ActMaps:
btg=btr;
btg(65:end,1)=btg(65:end,2);
btg(65:end,2)=ones; %produces a colormap that goes from black (early) to
green (late)
gtb=flipud(btg); %produces an opposite colormap that goes from green (early)
to black (late)


%-------

%Colormaps for visualization of Activation, specifically for movies as this
%will have better contrast by design.  Producing two colormaps here, one
%for voltage movies and the other for GCaMP3 movies:
others2=(0:(1/42):1); others2=transpose(others2); %defining interpolation

bwyr=zeros(128,3);
bwyr(2:44,1)=others2; bwyr(2:44,2)=others2; bwyr(2:44,3)=others2;
bwyr(44:86,1)=ones; bwyr(44:86,2)=ones; bwyr(44:86,3)=flipud(others2);
bwyr(86:128,1)=ones; bwyr(86:128,2)=flipud(others2);
%"bwyr" refers to black-white-yellow-red
```

```matlab
%now make an equivalent colormap for going to green (swap 1st & 2nd columns):
bwyg=zeros(128,3);
bwyg(:,1)=bwyr(:,2); bwyg(:,2)=bwyr(:,1); bwyg(:,3)=bwyr(:,3);
%"bwyg" refers to black-white-yellow-green

%------
%creat colormaps that go from black directly to red ("br") and to green
%("bg") without the white intermediary:
br=gray(128); br(:,2)=0; br(:,3)=0;
bg=gray(128); bg(:,1)=0; bg(:,3)=0;
%----------------------------------------------------------------------
%%%%%%%%%%%%%%%%%%%%%%% READ DATA & USER INPUT %%%%%%%%%%%%%%%%%%%%%%%%%%%%%%

% ANDOR DATA
%file and user input
%read *.dat files and obtain user input:
format long

%ask user for animal identifier & conditions (i.e., G345 acute with cells
2wks)
animal=input('Please enter the animal identifier and parameters: \n'  , 's');
%ask user for complete file name including extension
filename=input('Please enter the name of the Andor raw file you \nwish to
analyze including the file extension: \n'  ,'s');
%ask user for number of frames total
frame=input('How many frames total? \n');
%ask user for real time between each frame
tbwframe=input('How much time (sec) between each frame? \n');
%ask user for the field of view:
fov=input('What is the length of one side of the field of view (mm)? \n');
%ask user for the pixel depth (one dimension):
numpixs=input('How many pixels per side (e.g. 128)? \n');
%calc the mm per pixel:
pixsize=fov/numpixs;
%now below we are creating a "real time" vector that sets the first frame at
time 0,
%then increments on by the time between each frame until the end.
rtime=zeros(1,frame);
for i=2:frame, rtime(1,i)=tbwframe*(i-1); end;

%Import Data:
fid=fopen(filename, 'rb');
a=fread(fid,numpixs*numpixs*frame,'uint16');
fclose(fid);
DATA=reshape(a,numpixs, numpixs, frame);

%rotate the data matrix 90 degrees counter clockwise so that it is the
%same as the Andor Solis captured data:
for i=1:frame, DATA(:,:,i)=rot90(DATA(:,:,i)); end;

maxa=max(a);
mina=min(a);
clear a ans fid

% ECG data
```

```matlab
%ECG data must be copied into text file, all rows deleted up until first
%row with the camera fire signal, and all rows after the last camera fire
%signal deleted. Also, only copy the Channel data, not the headers or any
%comments or event indicators (these can cause errors in reading).
%This will leave us with  rows - Range / Channel 1 / Channel 2 / Channel 3 /
%Channel 4 / Channel 5, of which only Channel 1 through 5 are of use.  Here,
Channel 1 is our ECG
%signal in mV, Channel 2 is the Stimulator to the Heart in V, Channel 3 is
the external Stim signal
%to the cameras in V, Channel 4 is the Green camera fire signal in V, and
Channel 5 is the Red camera fire signal in V.
ECGfilename=input('Please enter the name of the ECG text file you \nwish to
analyze including the file extension: \n'  ,'s');
fid=fopen(ECGfilename, 'rb');
[ECG position]=textscan(fid, '%*s %f %f %f %f %f');
fclose(fid);


%Create new folder to store all analyzed data, as well as set this new
%folder as the current directory:
formatOut='dd-mmm-yyyy-HH-MM-SS';
noww=datestr(now,formatOut);
newfolder=strcat(animal,'_',noww,'_',mfilename);
mkdir(newfolder);
cd(newfolder);


%Transform the cell array into an ordinary matrix with 5 columns:
ecg = ECG{1};
for i = 2:5
    ecg = [ecg ECG{i}];
end


%automatically remove leading and trailing zeros from Labchart import file:
[r,c,v]=find(ecg(:,4)>2.5);
beginning=r(1);
ecg(1:beginning-1,:)=[];


[rg,cg,vg]=find(ecg(:,4)>2.5);
%[rr,cr,vr]=find(ecg(:,5)>2.5);
gending=rg(end);
%rending=rr(end);


% if rending>gending
%     ending=rending;
% else
%     ending=gending;
% end
ending=gending;
ecg(ending+1:end,:)=[];


%now clear the no longer needed variable ECG and other variables not needed:
clear ECG i fid ans r c v rg cg vg %rr cr vr


%add real time to ecg, starting with 0 and increasing every 0.001s:
ecgtinterval=.001;
ecg(1,6)=0;
```

```matlab
for k=2:length(ecg); ecg(k,6)=ecgtinterval*(k-1); end;


% ECG Baseline Drift Removal by median subtraction and curve fitting:
%median:
ecg(isnan(ecg(:,1)))=0; %in case any values did not copy well and were
assigned "NaN", set them to zero
ECGmedian=median(ecg(:,1));
ecg(:,7)=ecg(:,1)-ECGmedian;


%correcting drift using a combo of sgolay and removal of ringing at ends,
%replacing with mean value of closest 10 frames from sgolay fit:
ecgfit=smooth(ecg(:,7),10001,'sgolay',21);
ecgfit=smooth(ecgfit,500,'moving');
ecgfit(1:600)=0;ecgfit(1:600)=mean(ecgfit(601:611));
ecgfit(end-600:end)=0;ecgfit(end-600:end)=mean(ecgfit(end-611:end-601));
ecg(:,7)=ecg(:,7)-ecgfit;
figure()
subplot(2,1,1);plot(ecg(:,6),ecg(:,1),'b',ecg(:,6),ecgfit,'r'); title('raw
ECG w/ 1st curvefit');
subplot(2,1,2);plot(ecg(:,6),ecg(:,7),'b'); title('curve fit ECG');



% %curvefitting (using a 24th order polynomial to fit ECG)
% ecgpoly=polyfit(ecg(:,6),ecg(:,7),24);
% ecgpolyf=polyval(ecgpoly,ecg(:,6));
% figure()
% subplot(2,1,1);plot(ecg(:,6),ecg(:,7),'b',ecg(:,6),ecgpolyf,'r');
title('raw ECG w/ 1st curvefit');
% ecg(:,7)=ecg(:,7)-ecgpolyf;
% subplot(2,1,2);plot(ecg(:,6),ecg(:,7),'b'); title('curve fit ECG');
% %found that multiple curvefitting, using polyfit function, doesn't do much
% %after the first pass, thus removed the subsequent passes through:
% % %repeat ECG curvefitting
% % ecgpoly2=polyfit(ecg(:,6),ecg(:,7),24);
% % ecgpolyf2=polyval(ecgpoly2,ecg(:,6));
% % subplot(4,1,2);plot(ecg(:,6),ecg(:,7),'b',ecg(:,6),ecgpolyf2,'r');
title('1st corrected ECG w/ 2nd curvefit');
% % ecg(:,7)=ecg(:,7)-ecgpolyf2;
% % %repeat again:
% % ecgpoly3=polyfit(ecg(:,6),ecg(:,7),24);
% % ecgpolyf3=polyval(ecgpoly3,ecg(:,6));
% % subplot(4,1,3);plot(ecg(:,6),ecg(:,7),'b',ecg(:,6),ecgpolyf2,'r');
title('2nd corrected ECG w/ 3rd curvefit');
% % ecg(:,7)=ecg(:,7)-ecgpolyf3;
% % subplot(4,1,4);plot(ecg(:,6),ecg(:,7),'b',ecg(:,6),ecgpolyf2,'r');
title('Final corrected ECG');
%
% % %trying convolution:
% % ecgconv=conv(ecg(:,7),ones(1,100));
% % figure(), plot(ecgconv)


% Normalizing the ECG to between 0 and 1:
%normalizeddata=(data-min)./(max-mix)
ecg(:,8)=(ecg(:,7)-min(ecg(:,7)))./(max(ecg(:,7))-min(ecg(:,7)));
%now add 1 to this normalization so that it can be plotted above the stim
%signal:
```

```matlab
ecg(:,8)=ecg(:,8)+1;

% Normalizing the Stim to Heart to between 0 and 1, and then drop it's
% magnitude to 80% so that it doesn't take up entire bottom row height:
ecg(:,9)=(ecg(:,2)-min(ecg(:,2)))./(max(ecg(:,2))-min(ecg(:,2)));
ecg(:,9)=ecg(:,9).*0.8;
% IN THE END, this leaves us with the following data in the "ecg" matrix:
% Column:  1        2           3               4             5
6          7           8           9
%   Info:  raw ECG  Stim to Heart  Stim to Cams  Grn Cam fire  Red Cam fire
real time  drift-ECG   norm ECG   norm Stim to Heart
%  Units:  mV        V             V               V             V
sec        mV          mV          V


%-------------------------------------------------------------------------
%%%%%%%%%%%%%%%%%%%%%%%%%%%% PLAY RAW DATA %%%%%%%%%%%%%%%%%%%%%%%%%%%%%%%%%

%play raw data:
titlestrraw=[animal, ' - Raw Data'];
figure('Name',titlestrraw,'NumberTitle','off'); for i=1:frame;
imagesc(DATA(:,:,i)); axis square;  set(gca, 'YTick', []);set(gca, 'XTick',
[]); set(gca,'clim', [mina*1.2 maxa*.8]); colormap(gray);
title(sprintf('Frame %i', i));  pause(tbwframe); end;


%-------------------------------------------------------------------------
%%%%%%%%%%%%%%%%%%%%%%%%%%%% DATA MASK %%%%%%%%%%%%%%%%%%%%%%%%%%%%%%%%%%%%%%
%goal here is to mask off only the heart, and not care about background
M=mean(DATA,3);
STD=std(DATA,0,3);
COMB=M+(40*STD);
titlestrmask=[animal, ' - Select Mask'];
figure('Name',titlestrmask,'NumberTitle','off');
imagesc(COMB); axis square; set(gca, 'YTick', []);set(gca, 'XTick', []);
colormap(gray(256));

%manual selection using roipoly, then apply mask to entire DATA 3D matrix
%and set all background to 0.
Active=roipoly;
%apply mask to Data stack:
for y=1:frame, DATA(:,:,y)=Active(:,:).*DATA(:,:,y);, end;


%-------------------------------------------------------------------------
%%%%%%%%%%%%%%%%%%%%%%%%%%%% SPATIAL FILTERING %%%%%%%%%%%%%%%%%%%%%%%%%%%%%%
%goal here is to implement a median filter (size 3) to remove noise, then a
%special cone filter with a width of 3 pixels

%spatial median filter first (default window of 3x3):
DATAfm=zeros(size(DATA));
for i=1:size(DATA,3), DATAfm(:,:,i)=medfilt2(DATA(:,:,i)); end

%conefilt (courtesy of Matthew Kay @ GW):
width=3;
slope=1;
kernel=zeros(width,width);
for i=0:width-1;
```

```matlab
   for j=0:width-1;
      kernel(i+1,j+1)=floor((width-1)*slope/2+1-slope*sqrt((i-(width-1)/2)^2+(j-
(width-1)/2)^2));
        if kernel(i+1,j+1)<0, kernel(i+1,j+1)=0; end;
    end
end
kernel=kernel.*(1/sum(sum(kernel)));

% apply spatial conefilt:
DATAfmc=zeros(size(DATA));
for i=1:size(DATA,3), DATAfmc(:,:,i)=conv2(DATAfm(:,:,i),kernel,'same'); end
%reapply mask:
for y=1:frame, DATAfmc(:,:,y)=Active(:,:).*DATAfmc(:,:,y);, end;

% %play spatially filtered data:
% titlestrsfd=[animal, ' - Spatially Filtered Data'];
% figure('Name',titlestrsfd,'NumberTitle','off'); for i=1:frame;
imagesc(DATAfmc(:,:,i)); axis square;  set(gca, 'YTick', []);set(gca,
'XTick', []); set(gca,'clim', [mina*1.2 maxa*.8]); colormap(gray);
title(sprintf('Frame %i', i));  pause(tbwframe); end;

%-------------------------------------------------------------------------
%%%%%%%%%%%%%%%%%%%%%%%%%%% TEMPORAL FILTERING %%%%%%%%%%%%%%%%%%%%%%%%%%%%%%
%goal is to use convert to frequency domain using FFT transform, and use a
%finite impulse filter (FIR) to remove frequencies above user input.  Need to
ensure
%a zero phase response so that the transform & filtering does not impart a
%time-domain delay (bi-directionally process it!).
Freq=1/tbwframe; %sampling freq is based on time between frames
order=50; %want a FIR of order 50
passupto=input('Enter lowpass FIR filter pass up to band (Hz):  ');
%if the Nyquist freq is lower than the desired pass up to band, then
%we need to drop passupto appropriately:
if (passupto*1.25)>(Freq/2),
    passupto=(Freq/2)/1.25;
    disp(['Sampling Freq too low to lowpass filter imaging data in time at
defined Hz.']);
    disp(['Resultant lowpass cutoff is:  ' num2str(passupto) 'Hz']);
end
f0=[0 passupto passupto*1.25 Freq/2]./(Freq/2);
a0=[1 1 0 0];
b=firpm(order,f0,a0);
a=1;

vector=reshape(DATAfmc,[],size(DATAfmc,3));
DATAfmcf=zeros(size(vector));
for n=1:size(vector,1)
    if sum(vector(n,:))~=0
        DATAfmcf(n,:)=filtfilt(b,a,vector(n,:));
    end
end
DATAfmcf=reshape(DATAfmcf,size(DATA,1),size(DATA,2),[]);

% median filter with a kernel of 3 through time
DATAfmcfm=medfilt1(DATAfmcf,3,[],3);
```

```matlab
%moving average smooth filter with kernel of 5 through time
vector2=reshape(DATAfmcfm,[],size(DATAfmcfm,3));
DATAf=smooth(vector2,5,'moving');
DATAf=reshape(DATAf,size(DATA,1),size(DATA,2),[]);

%reapply mask:
for y=1:frame, DATAf(:,:,y)=Active(:,:).*DATAf(:,:,y);, end;

% %sgolay average smooth filter with span 1001 and order 50
% vector2=reshape(DATAfmcfm,[],size(DATAfmcfm,3));
% DATAf=smooth(vector2,1001,'sgolay',50);
% DATAf=reshape(DATAf,size(DATA,1),size(DATA,2),[]);

% %play spatially & temporally filtered data:
% titlestrstfd=[animal, ' - Spatially & Temporally Filtered Data'];
% figure('Name',titlestrstfd,'NumberTitle','off'); for i=1:frame;
imagesc(DATAf(:,:,i)); axis square;  set(gca, 'YTick', []);set(gca, 'XTick',
[]); set(gca,'clim', [mina*1.2 maxa*.8]); colormap(gray);
title(sprintf('Frame %i', i));  pause(tbwframe); end;

% %let's look at a pixels through time, before and after filtering:
% data=reshape(DATA,[],size(DATA,3));
% dataf=reshape(DATAf,[],size(DATAf,3));
% figure(),plot(data(1998,:),'b'),hold,plot(dataf(1998,:),'r');

%-----------------------------------------------------------------------
%%%%%%%%%%%%%%%%%%%%%%%%%% FILTER ASSESSMENT %%%%%%%%%%%%%%%%%%%%%%%%%%%%%%
%ask user for number of frames total
figure('Name','Select Active Pixel','NumberTitle','off');
imagesc(COMB); axis square; set(gca, 'YTick', []);set(gca, 'XTick', []);
colormap(gray(256));

disp('Select an active pixel to assess quality of filtering:');
[xactive,yactive] = ginput(1);
xactive=floor(xactive);yactive=floor(yactive);
titlestrfiltering=[animal, ' - Individual Pixel Data - for assessing
filtering'];
subplot714title=strcat('after Temporal Lowpass of', {' '}, num2str(passupto),
' Hz');
figure('Name',titlestrfiltering,'NumberTitle','off')
subplot(7,1,1),plot((reshape(DATA(xactive,yactive,:),1,[])),'b'), title('Raw
data');
subplot(7,1,2),plot((reshape(DATAfm(xactive,yactive,:),1,[])),'b'),
title('after Spatial 3x3 median');
subplot(7,1,3),plot((reshape(DATAfmc(xactive,yactive,:),1,[])),'b'),
title('after Spatial 3x3 conefilter');
subplot(7,1,4),plot((reshape(DATAfmcf(xactive,yactive,:),1,[])),'b'),
title(subplot714title);
subplot(7,1,5),plot((reshape(DATAfmcfm(xactive,yactive,:),1,[])),'b'),
title('after Temporal 3-span median');
subplot(7,1,6),plot((reshape(DATAf(xactive,yactive,:),1,[])),'b'),
title('after Temporal 5-span average');
subplot(7,1,7),hold on;
plot((reshape(DATA(xactive,yactive,:),1,[])),'b');plot((reshape(DATAf(xactive
,yactive,:),1,[])),'r'), title('Overlay of raw & last');
h=gcf;
```

159

```matlab
saveas(h,titlestrfiltering, 'tif');
saveas(h,titlestrfiltering);
%clear large matrices we no longer need:
% clear DATAf DATAfm DATAfmc DATAfmcfm


%-------------------------------------------------------------------------
%%%%%%%%%%%%%%% REMOVE EFFECTS OF FILTERING AT ENDS %%%%%%%%%%%%%%%%%%%%%%%
%goal here is to remove the first 15 and last 15 frames due to effects from
%filtering.  But, since we have ECG here, we cant' just get rid of the
%first and last frames, we need to get rid of all time points corresponding
%to the first and last 15 frames:
DATAf(:,:,end-15+1:end)=[];DATAf(:,:,1:15)=[];
rtime(end-15+1:end)=[];rtime(1:15)=[];
newendtime=rtime(end);newstarttime=rtime(1);
ecg(:,10)=ecg(:,6).*1000;
removeend=find(abs(ecg(:,10) - newendtime*1000) <
0.5);removestart=find(abs(ecg(:,10) - newstarttime*1000) < 0.5);
ecg(removeend+1:end,:)=[];ecg(1:removestart-1,:)=[];
frame=frame-30;
%-------------------------------------------------------------------------
%%%%%%%%%%%%%%%%%%%%%%%%%%% DRIFT REMOVAL %%%%%%%%%%%%%%%%%%%%%%%%%%%%%%%%%%
%goal here is to use polynomial fitting to fit the optical signal and then
%subtract this from the original signal to remove drift (4th order or
%higher probably needed) - this MUST be done if accurate calcs of
%activation times, etc., are going to be performed!

%curvefitting
%find mean of each frame, create a vector of these means, then find
%polynomial fit to this and subtract each pixel in time by this fit:
Mn=zeros(size(DATAf(3)));
for m=1:frame; Mn(m)=mean2(DATAf(:,:,m));end;
DATAfpoly=polyfit(rtime,Mn,4);
DATAfpolyf=polyval(DATAfpoly,rtime);

vector3=reshape(DATAf,[],size(DATAf,3));
for v=1:size(vector3,1)
    vector3d(v,:)=vector3(v,:)-DATAfpolyf;
end
DATAfd=reshape(vector3d,size(DATA,1),size(DATA,2),[]);
%after drift removal need to redo mask:
for y=1:frame, DATAfd(:,:,y)=Active(:,:).*DATAfd(:,:,y);, end;

Mnn=zeros(size(DATAfd(3)));
for m=1:frame; Mnn(m)=mean2(DATAfd(:,:,m));end;
figure(),plot(Mn,'b'),hold,plot(DATAfpolyf,'r'),plot(Mnn,'m');title('curvefit
for signal drift removal');hold off;


%-------------------------------------------------------------------------
%%%%%%%%%%%%%%%%%%%%%%%%%%% ENSEMBLE AVERAGING %%%%%%%%%%%%%%%%%%%%%%%%%%%%%
%not performed at this time, not here


%-------------------------------------------------------------------------
%%%%%%%%%%%%%%%%%%%%%%%%%%%%%%% FLIP SIGN %%%%%%%%%%%%%%%%%%%%%%%%%%%%%%%%%%
%goal here is to flip the signal only if we are working with a voltage dye
%signal (do not flip if working with GCaMP data).  The reason is the
%voltage dye signal inherently drops in fluorescence upon depolarization,
```

```matlab
%but we need it, for thresholding purposes later, to increase in
%fluorescence:

%ask user for the type of signal being analyzed:
signaltype=input('GCaMP3 (G) or Voltage (V) signal being assessed?  ', 's');
if strcmp(signaltype,'V')
    DATAfd=-DATAfd;
end;


%-------------------------------------------------------------------------
%%%%%%%%%%%%%%%%% PLAY (if desired) Z SCORED DATA %%%%%%%%%%%%%%%%%%%%%%%%
DATAz=zeros(size(DATAfd));
    DATAz=zscore(DATAfd,0,3);
    Zmin=min(min(min(DATAz)));
    Zmax=max(max(max(DATAz)));
runZ=input('Play Z scored data (y/n)?  ', 's');
if strcmp(runZ,'y')
    %play Z scored data so that user can determine ROI:
    figure('Name','Z scored','NumberTitle','off');
    for i=1:frame;imagesc(DATAz(:,:,i)); axis square;
        set(gca, 'YTick', []); set(gca, 'XTick', []); set(gca,'clim',
[Zmin*1/3 Zmax*1/3]);
        colormap(bg); title(sprintf('Frame %i', i));  pause(tbwframe);
    end;
end;


% Make a movie of the Z scored data:
figure('Name','Z scored','NumberTitle','off');
titlemovie=[animal,'_Z Scored Data_one tenth speed'];
vidObj=VideoWriter(titlemovie);
%set the framerate
vidObj.FrameRate=(round(1/(tbwframe*10)));
%write sequence of frames to the compressed AVI file:
open(vidObj);

for i=1:frame;imagesc(DATAz(:,:,i)); axis square;
        set(gca, 'YTick', []); set(gca, 'XTick', []);
        set(gca,'clim', [Zmin*1/3 Zmax*1/3]);
        colormap(bg); title(sprintf('Time (s) = %.3f', rtime(i)));
        currFrame=getframe; writeVideo(vidObj,currFrame);
end;
close(vidObj);

% Plot the Zscore of the selected "active" pixel:
plot((reshape(DATAz(xactive,yactive,:),1,[])),'b');

% Save zcoredata as a matlab file:
save('zscoredata.mat','DATAz','Zmin','Zmax','frame','rtime','tbwframe',
'animal', 'bg');

%-------------------------------------------------------------------------
%%%%%%%%%%%%%%%%%%%%%%%%%%% SAVE PROCESSED DATA %%%%%%%%%%%%%%%%%%%%%%%%%%%
save processed.mat

%-------------------------------------------------------------------------
```

161

```matlab
%%%%%%%%%% ROI PLOTS - Mean of ROIs and Total FI against time %%%%%%%%%%%%%%
%ROIs:
Mnew=mean(DATAfd,3);
STDnew=std(DATAfd,0,3);STDnew=Active.*STDnew;
COMBnew=M+(40*STDnew);

figure('Name','Standard Deviation
Image','NumberTitle','off'),imagesc(STDnew); axis square; set(gca, 'YTick',
[]);set(gca, 'XTick', []);colormap(gray(256));
maxSTD=max(max(STD));
minSTD=min(min(STD));
titlestrOpt=[animal, ' - Select ROI'];
figure('Name',titlestrOpt, 'NumberTitle','off');
imagesc(COMBnew(:,:)); axis square;  set(gca, 'YTick', []);set(gca, 'XTick',
[]);
%set(gca,'clim', [minSTD maxSTD]);
colormap(jet(256));

%ask user for the number of ROIs:
nROIs=input('How many ROIs?  ');

for i=1:nROIs; eval(['roimask_' num2str(i) '=roipoly;']); end;
%apply ROI masks to DATA image stacks:
for i=1:nROIs; eval(['roi_' num2str(i) '=zeros(numpixs,numpixs,frame);']);
for j=1:frame; eval(['roi_' num2str(i) '(:,:,j)=roimask_' num2str(i)
'(:,:).*DATAfd(:,:,j);']); end; end;


% INFARCT AREA:
titlestrinfarct=[animal, ' - Select Infarct'];
figure('Name',titlestrinfarct,'NumberTitle','off');
imagesc(M); axis square; set(gca, 'YTick', []);set(gca, 'XTick', []);
colormap(gray(256));
%Now ask user to select infarct region:
display('Now define the infarct region')
roimask_infarct=roipoly;

%Using regionprops to get means of ROIs and other info like area, perimeter,
min & max intensity, etc. need to preallocate structures...?
for i=1:nROIs; eval(['CC_' num2str(i) '=bwconncomp(roimask_' num2str(i)
'(:,:));']); end;
for i=1:nROIs; for j=1:frame; eval(['S_' num2str(i) '(j)=regionprops(CC_'
num2str(i) ', DATAfd(:,:,j), ''Area'', ''Perimeter'', ''Centroid'',
''PixelIdxList'', ''PixelList'', ''MaxIntensity'', ''MinIntensity'',
''MeanIntensity'');']); end; end;
%now do the same for the infarct region:
II=bwconncomp(roimask_infarct);
for j=1:frame; I=regionprops(II, DATAfd(:,:,j), 'Area', 'Perimeter',
'Centroid', 'PixelIdxList', 'PixelList', 'MaxIntensity', 'MinIntensity',
'MeanIntensity'); end;

%Trace ROI boundaries using bwboundaries:
for i=1:nROIs; eval(['[Bound_' num2str(i) ', L_' num2str(i)
']=bwboundaries(roimask_' num2str(i) ',''noholes'');']); end;
%Trace infarct boundary the same way:
```

162

```matlab
[IBound, III]=bwboundaries(roimask_infarct,'noholes');

%plot these boundaries on image in a color and label them:
cblue=[0,112,192];cblue=cblue/255;
cred=[255,0,0];cred=cred/255;
cgreen=[0,176,80];cgreen=cgreen/255;
corange=[228,108,10];corange=corange/255;
cpurple=[112,48,160];cpurple=cpurple/255;
ctan=[148,138,84];ctan=ctan/255;
colors=[cblue; cred; cgreen; corange; cpurple; ctan];

titlestrrois=[animal, ' - ROIs'];
figure('Name',titlestrrois,'NumberTitle','off');
imagesc(M(:,:)); axis square;  set(gca, 'YTick', []);set(gca, 'XTick', []);
colormap(gray(256));
hold on; for i=1:nROIs; eval(['for k=1:length(Bound_' num2str(i) ');
boundary_' num2str(i) '= Bound_' num2str(i) '{k}; plot(boundary_' num2str(i)
'(:,2), boundary_' num2str(i) '(:,1), ''Color'',
colors(i,:),''LineWidth'',2); Row = ceil(length(boundary_' num2str(i) ')/2);
col = boundary_' num2str(i) '(Row,2); row = boundary_' num2str(i) '(Row,1); h
= text(col+2, row+5, num2str(i));
set(h,''Color'',colors(i,:),''FontSize'',14,''FontWeight'',''bold'');
end;']); end; set(gca, 'YTick', []);set(gca, 'XTick', []);hold off;
%now also draw over this the infarct region in a dotted white line:
hold on; for l=length(IBound); iboundary=IBound{l}; plot(iboundary(:,2),
iboundary(:,1), '--w', 'LineWidth',2); end; hold off;
%save figure to file (as both a tiff and matlab file):
h=gcf;
saveas(h,titlestrrois, 'tif');
saveas(h,titlestrrois);
%do trick to extract means from S_x into separate matrix, then plot this
for i=1:nROIs; eval(['roi_' num2str(i) 'means=[S_' num2str(i)
'.MeanIntensity];']); end;

% NOTE - need to look into plotting total FI in the region,
% not just the mean (could provide some usefull data). - NOT GOING TO DO

%find ranges (max-min) of each ROI means:
for i=1:nROIs, eval(['roi_' num2str(i) 'range=(max(roi_' num2str(i) 'means)-
min(roi_' num2str(i) 'means));']); end;
%now add these ranges to a vector called "ranges":
for i=1:nROIs, eval(['ranges(i)=roi_' num2str(i) 'range;']); end;
%now find max of the ranges:
[MAXrange roiwmax] = max(ranges);
%now normalize ROI means to ROI with max range:
for i=1:nROIs; eval(['roi_' num2str(i) 'normmeans=zeros(length(roi_'
num2str(i) 'means)); roi_' num2str(i) 'normmeans=(roi_' num2str(i) 'means-
min(roi_' num2str(i) 'means))./(MAXrange);']); end;
% %now normalize each ROI mean to itself for plotting:
% for i=1:nROIs; eval(['roi_' num2str(i) 'normmeans=zeros(length(roi_'
num2str(i) 'means)); roi_' num2str(i) 'normmeans=(roi_' num2str(i) 'means-
min(roi_' num2str(i) 'means))./(roi_' num2str(i) 'range);']); end;

%now increase each successive ROI by "1", "2", etc. so that they can be
%plotted and appear stacked on top of eachother (so we can easily correlate
%them):
```

163

```
increase=1;
for n=1:nROIs; eval(['roi_' num2str(n) 'normmeans=roi_' num2str(n)
'normmeans+increase; increase=increase+1;']); end; %note, can change the
"n=1:nROIs" to "n=2:nROIs" if I don't want the normalized ROI mean plots to
start at 2 (using "2" makes then start at 1)
%then add 1 again to push up ROI normmeans because we have the stim signal
%plotting as well:
for n=1:nROIs; eval(['roi_' num2str(n) 'normmeans=roi_' num2str(n)
'normmeans+1;']); end;

%Now tell user that the movie is _ seconds long, then ask what time time
range they want to plot:
disp(['The recording is ' num2str(max(rtime)) ' seconds long total.']);

%Don't want to ask any more, just plot starting from 0 and ending 0.5sec
%past max rtime from now on.
%starttime=input('Please enter the range you wish to plot the data:\nBegin at
time:  ');
%endtime=input('End at time:  ');
starttime=0;endtime=(max(rtime))+0.5;

%for figures (plot traces without ECG identifiers):
titlestrsupp=[animal, ' - Normalized ROI FI Means, Heart Stim & ECG'];
figure('Name',titlestrsupp,'NumberTitle','off'); hold on; axis([starttime
endtime 0 (nROIs+2)]); for i=1:nROIs; eval(['plot(rtime(1,:),roi_' num2str(i)
'normmeans(1,:), ''Color'',colors(i,:), ''LineWidth'',2);']); end;
plot(ecg(:,6),ecg(:,9),'r', 'LineWidth', 2); plot(ecg(:,6),ecg(:,8),'k',
'LineWidth', 2); xlabel('time (sec)'); %set(gca, 'YTick', []);
%title(sprintf(titlestrroisandecg, frselect));
%Display "ECG" and "ROI _" in appropriate places on the Y axis
%define number of labels required
nlabels=nROIs+2;
%divide Y axis into the appropriate number of sections:
set(gca, 'YTick', 0.5:1:nlabels);
%now display:
if nROIs==1, set(gca, 'YTickLabel', 'STIM|ECG|ROI 1'), elseif nROIs==2,
set(gca, 'YTickLabel', 'STIM|ECG|ROI 1|ROI 2'), elseif nROIs==3, set(gca,
'YTickLabel', 'STIM|ECG|ROI 1|ROI 2|ROI 3'), elseif nROIs==4, set(gca,
'YTickLabel', 'STIM|ECG|ROI 1|ROI 2|ROI 3|ROI 4'), elseif nROIs==5, set(gca,
'YTickLabel', 'STIM|ECG|ROI 1|ROI 2|ROI 3|ROI 4|ROI 5'), elseif nROIs==6,
set(gca, 'YTickLabel', 'STIM|ECG|ROI 1|ROI 2|ROI 3|ROI 4|ROI 5|ROI 6'),
elseif nROIs==7, set(gca, 'YTickLabel', 'STIM|ECG|ROI 1|ROI 2|ROI 3|ROI 4|ROI
5|ROI 6|ROI 7'),  elseif nROIs==8, set(gca, 'YTickLabel', 'STIM|ECG|ROI 1|ROI
2|ROI 3|ROI 4|ROI 5|ROI 6|ROI 7|ROI 8'), end;



%-------------------------------------------------------------------------
%%%%%%%%%%%%%%%%%%% Ask User for Time Window to Analyze %%%%%%%%%%%%%%%%%%%%
%After displaying the ROI plots against the ECG and stim, ask user for the
%time window that they'd like to proceed analyzing (for determining
%activation frequency, peaks/valleys, period of ROIs, and for later
%activation mapping:
```

```
nstarttime=input('Please enter the range you wish to plot the data:\nBegin at
time:  ');
nendtime=input('End at time:  ');

%Now get rid of data outside of the user selected window:
nstartframe=find(rtime(:)>nstarttime,1);
nendframe=find(rtime(:)>nendtime,1);
DATAfd(:,:,nendframe:end)=[];DATAfd(:,:,1:nstartframe)=[];
rtime(nendframe:end)=[];rtime(1:nstartframe)=[];
newnewendtime=rtime(end);newnewstarttime=rtime(1);
newremoveend=find(ecg(:,3)==newnewendtime);newremovestart=find(ecg(:,3)==newn
ewstarttime);
ecg(newremoveend+1:end,:)=[];ecg(1:newremovestart-1,:)=[];
frame=nendframe-nstartframe-1;
for i=1:nROIs, eval(['roi_' num2str(i) '(:,:,nendframe:end)=[];']); end;
for i=1:nROIs, eval(['roi_' num2str(i) '(:,:,1:nstartframe)=[];']); end;
for i=1:nROIs, eval(['roi_' num2str(i) 'means(nendframe:end)=[];']); end;
for i=1:nROIs, eval(['roi_' num2str(i) 'means(1:nstartframe)=[];']); end;

%REDO normalization within the selected time range:
%find ranges (max-min) of each ROI means:
for i=1:nROIs, eval(['roi_' num2str(i) 'range=(max(roi_' num2str(i) 'means)-
min(roi_' num2str(i) 'means));']); end;
%now add these ranges to a vector called "ranges":
for i=1:nROIs, eval(['ranges(i)=roi_' num2str(i) 'range;']); end;
%now find max of the ranges:
[MAXrange roiwmax] = max(ranges);
%now normalize ROI means to ROI with max range:
for i=1:nROIs; eval(['roi_' num2str(i) 'normmeans=zeros(length(roi_'
num2str(i) 'means)); roi_' num2str(i) 'normmeans=(roi_' num2str(i) 'means-
min(roi_' num2str(i) 'means))./(MAXrange);']); end;

%now increase each successive ROI by "1", "2", etc. so that they can be
%plotted and appear stacked on top of eachother (so we can easily correlate
%them):
increase=1;
for n=1:nROIs; eval(['roi_' num2str(n) 'normmeans=roi_' num2str(n)
'normmeans+increase; increase=increase+1;']); end; %note, can change the
"n=1:nROIs" to "n=2:nROIs" if I don't want the normalized ROI mean plots to
start at 2 (using "2" makes then start at 1)
%then add 1 again to push up ROI normmeans because we have the stim signal
%plotting as well:
for n=1:nROIs; eval(['roi_' num2str(n) 'normmeans=roi_' num2str(n)
'normmeans+1;']); end;

%Now tell user that the movie is _ seconds long, then ask what time time
range they want to plot:
disp(['The selected window is ' num2str(max(rtime)) ' seconds long total.']);

%kick out new plot:
%for figures (plot traces without ECG identifiers):
titlestrsupp=[animal, ' - Normalized ROI FI Means, Heart Stim & ECG'];
figure('Name',titlestrsupp,'NumberTitle','off'); hold on; axis([nstarttime
nendtime 0 (nROIs+2)]); for i=1:nROIs; eval(['plot(rtime(1,:),roi_'
num2str(i) 'normmeans(1,:), ''Color'',colors(i,:), ''LineWidth'',2);']); end;
plot(ecg(:,6),ecg(:,9),'r', 'LineWidth', 2); plot(ecg(:,6),ecg(:,8),'k',
```

165

```
'LineWidth', 2); xlabel('time (sec)'); %set(gca, 'YTick', []);
%title(sprintf(titlestrroisandecg, frselect));
%Display "ECG" and "ROI _" in appropriate places on the Y axis
%divide Y axis into the appropriate number of sections:
set(gca, 'YTick', 0.5:1:nlabels);
%now display:
if nROIs==1, set(gca, 'YTickLabel', 'STIM|ECG|ROI 1'), elseif nROIs==2,
set(gca, 'YTickLabel', 'STIM|ECG|ROI 1|ROI 2'), elseif nROIs==3, set(gca,
'YTickLabel', 'STIM|ECG|ROI 1|ROI 2|ROI 3'), elseif nROIs==4, set(gca,
'YTickLabel', 'STIM|ECG|ROI 1|ROI 2|ROI 3|ROI 4'), elseif nROIs==5, set(gca,
'YTickLabel', 'STIM|ECG|ROI 1|ROI 2|ROI 3|ROI 4|ROI 5'), elseif nROIs==6,
set(gca, 'YTickLabel', 'STIM|ECG|ROI 1|ROI 2|ROI 3|ROI 4|ROI 5|ROI 6'),
elseif nROIs==7, set(gca, 'YTickLabel', 'STIM|ECG|ROI 1|ROI 2|ROI 3|ROI 4|ROI
5|ROI 6|ROI 7'),  elseif nROIs==8, set(gca, 'YTickLabel', 'STIM|ECG|ROI 1|ROI
2|ROI 3|ROI 4|ROI 5|ROI 6|ROI 7|ROI 8'), end;

%save figure to file (as both a tiff and matlab file):
h=gcf;
saveas(h,titlestrsupp, 'tif');
saveas(h,titlestrsupp);

%Output the voltage range of the ECG:
disp(['The Voltage range of ECG (mV): Max ' num2str(max(ecg(:,1))) ', Min '
num2str(min(ecg(:,1)))]);
%Output at end the regionproperties for each ROI (in order):
display('ROI REGION INFO')
for i=1:nROIs; eval(['S_' num2str(i) '(1,1)']); end;
%Then output the regionproperties for the infarct region:
display('INFARCT REGION INFO')
I(1,1)

%save('timecoursedata','roi_1normmeans','roi_2normmeans','roi_3normmeans','ro
i_4normmeans','rtime','MAXrange','roiwmax','ecg')

%-------------------------------------------------------------------------
%%%%%%%%%%%%%%%%%%%%%%%% Activation Frequency %%%%%%%%%%%%%%%%%%%%%%%%%%%%%%%
%Convert each roi signal into the freq domain, then find the dominant
%frequency and convert this back into a time interval for that roi that
%represents it's periodicity.  (Then can use this time interval for
%the min peakdistance, if desired, so that accurate peaks can be detected).

% frequency = Freq, sample time = max(rtime), length = frame
NFFT=2^nextpow2(frame);
for i=1:nROIs, eval(['Y_' num2str(i) '=fft(roi_' num2str(i) 'means-mean(roi_'
num2str(i) 'means),NFFT)/frame;']); end;
for i=1:nROIs, eval(['f_' num2str(i) '=Freq/2*linspace(0,1,NFFT/2+1);']);
end;
for i=1:nROIs, eval(['[Y_' num2str(i) 'max, Yindex_' num2str(i)
']=max(2*abs(Y_' num2str(i) '(1:NFFT/2+1)));']); end;
for i=1:nROIs, eval(['freq_' num2str(i) '=f_' num2str(i) '(Yindex_'
num2str(i) ');']); end;
for i=1:nROIs, eval(['period_' num2str(i) '=1/freq_' num2str(i) ';']); end;

%  plotting:
% figure(),plot(f_1,2*abs(Y_1(1:NFFT/2+1)))
% title('Single-Sided Amplitude Spectrum of y(t)')
```

```matlab
% xlabel('Frequency (Hz)')
% ylabel('|Y(f)1|')
%
% figure(),plot(f_2,2*abs(Y_2(1:NFFT/2+1)))
% title('Single-Sided Amplitude Spectrum of y(t)')
% xlabel('Frequency (Hz)')
% ylabel('|Y(f)2|')


%need to output this info for all ROIs (actually will do later, with +/- SEM
based on peak & valley analysis):
%need to use this info to inform windows that will be used later in program
%- but can't use exact period info because could potentially miss some
%peaks, thus use 85% of this period to look for peaks:
for i=1:nROIs, eval(['MPD_' num2str(i) '=round((period_' num2str(i)
'/tbwframe)*.85);']); end;


%%% find peaks of the means of each ROI:
for n=1:nROIs, eval(['[Proi_' num2str(n) ' LProi_' num2str(n)
']=findpeaks(roi_' num2str(n) 'normmeans, ''MINPEAKDISTANCE'',MPD_'
num2str(n) ');']); end;
% valleys in the signals:
for n=1:nROIs, eval(['[Vroi_' num2str(n) ' LVroi_' num2str(n) ']=findpeaks(-
roi_' num2str(n) 'normmeans, ''MINPEAKDISTANCE'',MPD_' num2str(n) ');']);
end;
for n=1:nROIs, eval(['Vroi_' num2str(n) ' =-Vroi_' num2str(n) ';']); end;


%now plot and ask user for verification that peaks & valleys were properly
%identified:
titlestrpvs=[animal, ' - ROI peaks and valleys'];
figure('Name',titlestrpvs, 'NumberTitle','off');
for n=1:nROIs, eval(['subplot(nROIs, 1, n); hold; plot(roi_' num2str(n)
'normmeans, ''g''); title(''ROI ' num2str(n) '''); axis([0 length(roi_'
num2str(n) 'normmeans) min(roi_' num2str(n) 'normmeans) max(roi_' num2str(n)
'normmeans)]); ylabel(''FI''); plot(LProi_' num2str(n) ',Proi_' num2str(n)
',''bo''); plot(LVroi_' num2str(n) ',Vroi_' num2str(n) ',''ro'');hold
off;']); end;


pvsokay=input('Are the peaks and valleys for each ROI correctly identified
(y/n)?:  ');
while pvsokay==n
    newmod=input('Please enter new multiplier for peak detection
(default=0.85):  ');
    for i=1:nROIs, eval(['MPD_' num2str(i) '=round((period_' num2str(i)
'/tbwframe)*newmod);']); end;
    % find peaks of the means of each ROI:
    for n=1:nROIs, eval(['[Proi_' num2str(n) ' LProi_' num2str(n)
']=findpeaks(roi_' num2str(n) 'normmeans, ''MINPEAKDISTANCE'',MPD_'
num2str(n) ');']); end;
    % valleys in the signals:
    for n=1:nROIs, eval(['[Vroi_' num2str(n) ' LVroi_' num2str(n)
']=findpeaks(-roi_' num2str(n) 'normmeans, ''MINPEAKDISTANCE'',MPD_'
num2str(n) ');']); end;
    for n=1:nROIs, eval(['Vroi_' num2str(n) ' =-Vroi_' num2str(n) ';']); end;
    titlestrpvs=[animal, ' - ROI peaks and valleys'];
    figure('Name',titlestrpvs, 'NumberTitle','off');
```

```matlab
    for n=1:nROIs, eval(['subplot(nROIs, 1, n); hold; plot(roi_' num2str(n)
'normmeans, ''g''); title(''ROI ' num2str(n) '''); axis([0 length(roi_'
num2str(n) 'normmeans) min(roi_' num2str(n) 'normmeans) max(roi_' num2str(n)
'normmeans)]); ylabel(''FI''); plot(LProi_' num2str(n) ',Proi_' num2str(n)
',''bo''); plot(LVroi_' num2str(n) ',Vroi_' num2str(n) ',''ro'');hold
off;']); end;
    pvsokay=input('Are the peaks and valleys for each ROI correclty
identified (y/n)?:  ');
end;

disp('"Proi_x/LProi_x" & "Vroi_x/LVroi_x" have stored the value & frames of
the')
disp('peaks and valleys of each ROI, respectively.')
disp('Open these variables to perform statistics on ROI intervals.')

%-------------------------------------------------------------------------
%%%%%%%%%%%%%%%%%%%%%%%%%%%%%% SAVE DATA %%%%%%%%%%%%%%%%%%%%%%%%%%%%%%%%%%%%
save(animal)
%Save ROI Masks to a matlab file named "'animal'_ROI_Masks":
titlerois=[animal, '_ROI_Masks'];
save(titlerois, 'roimask_*');

%-------------------------------------------------------------------------
%%%%%%%%%%%%%%%%%%%%%%%%%%%%% ACTIVATION MAPS %%%%%%%%%%%%%%%%%%%%%%%%%%%%%%%
%goal here is to create a single matrix that contains the activation time
%of each pixel for a given window of time (one complete activation).
% NOTE: skipping a re-normalization step for now.

%first ask user if Activation Maps are desired:
ActMapyeah=input('Do you want to continue with Activation Maps (y/n)?  ',
's');
if strcmp(ActMapyeah,'n')
    error('This concludes the analysis (disregard error message above).')
end;

%Apply a combined mask that keeps everything inside defined ROIs, but
%removes everything else:
combroimask=zeros(size(roimask_1));
for i=1:nROIs, eval(['combroimask=combroimask+roimask_' num2str(i) ';']);
end;
for y=1:frame, DATAfd(:,:,y)=combroimask(:,:).*DATAfd(:,:,y);, end;

%%% NORMALIZING %%%
%goal here is to normalize the data to the same amplitude so
%that peak fluorescence (F=1) corresponds to a depolarized membrane
%potential and baseline fluorescence (F=0) corresponds to the resting
%membrane potential.  THIS IS DONE ON A SINGLE PIXEL LEVEL THROUGH TIME!
vector4=reshape(DATAfd,[],size(DATAfd,3));
vector4n=zeros(size(vector4));
for w=1:size(vector4,1)
    vector4n(w,:)=(vector4(w,:)-min(vector4(w,:)))./(max(vector4(w,:))-
min(vector4(w,:)));
end
DATAfdn=reshape(vector4n,size(DATAfd,1),size(DATAfd,2),[]);
```

```matlab
%%% Visualize the activation of all ROIs over a still shot of the heart:
%find ranges (max-min) of the combined ROIs:
combroimax=max(max(max(DATAfdn)));
combroimin=min(min(min(DATAfdn)));
combroirange=combroimax-combroimin;
%also find range of background image, M:
M=M.*Active;
Mmax=max(max(max(M)));
Mmin=min(min(min(M)));
Mrange=Mmax-Mmin;
%now scale the combined ROI data to between 128-256:
DATAscaled=zeros(size(DATAfdn));
DATAscaled=(((DATAfdn-combroimin)./combroirange).*128)+128;
for y=1:frame, DATAscaled(:,:,y)=combroimask(:,:).*DATAscaled(:,:,y); end;
%now set values of NaN in DATAscaled ==0:
DATAscaled(isnan(DATAscaled))=0;
%now scale the backfround image to between 0-128
Mscaled=zeros(size(M));
Mscaled=((M-Mmin)./Mrange).*128;
%now create a combined colormap of gray and jet so that the background and
%ROI data will be displayed with the appropriate color:
Ncolormap=[gray(128); bg];
%now create a new, single data matrix of Mscaled and DATAscaled:
Mscaledcomplement=Mscaled.*imcomplement(combroimask);
Activation=zeros(size(DATAscaled));
for i=1:frame, Activation(:,:,i) = DATAscaled(:,:,i)+(Mscaledcomplement);end;
% %now play:
% titlestrfdnd=[animal, ' - Activation of ROIs'];
% figure('Name',titlestrfdnd,'NumberTitle','off');
% for i=1:frame; imagesc(Activation(:,:,i));axis square;  set(gca, 'YTick',
[]);set(gca, 'XTick', []); set(gca,'clim', [0 256]); colormap(Ncolormap);
title(sprintf('Frame %i', i));  pause(tbwframe); end;


% %want to see what an individual & active pixel trace looks like:
% figure(),plot((reshape(DATAscaled(xactive,yactive,:),1,[])),'b');
sgolayo=68;
%FURTHER FILTERING REQ'D PER PIXEL FOR ACTIVATION & CV MAPS! Implement
%sgolay filter now on pixels within identified ROIs:
slength=round(((0.36*frame)-1)/2)*2+1; %setting the length of the sgolay...
%filter to a multiple of the number of frames total that through trial and
error I found to work well
vector5=reshape(DATAfdn,[],size(DATAfdn,3));
DATAsgolay=zeros(size(vector5));
for x=1:length(vector5),
    if isfinite(vector5(x))
        DATAsgolay(x,:)=smooth(vector5(x,:),slength,'sgolay',sgolayo); %need
to modify this here...
        %(as well as others below)...and instead of doing it for entire
    end;
end;
DATAsgolay=reshape(DATAsgolay,size(DATAfdn,1),size(DATAfdn,2),[]);


% %want to see what an individual & active pixel trace looks like:
% figure(),plot((reshape(DATAsgolay(xactive,yactive,:),1,[])),'b');


%----------------------------------------------------------------------
```

169

```matlab
%%%%%%%%%%% REMOVE EFFECTS OF FILTERING AT ENDS AGAIN %%%%%%%%%%%%%%%%%%%%%
%goal here is to remove the first 80 and last 80 frames due to effects from
%filtering.  But, since we have ECG here, we cant' just get rid of the
%first and last frames, we need to get rid of all time points corresponding
%to the first and last 80 frames:
DATAfdn(:,:,end-80+1:end)=[];DATAfdn(:,:,1:80)=[];
DATAsgolay(:,:,end-80+1:end)=[];DATAsgolay(:,:,1:80)=[];
rtime(end-80+1:end)=[];rtime(1:80)=[];
newendtime=rtime(end);newstarttime=rtime(1);
removeend=find(abs(ecg(:,10) - newendtime*1000) <
0.5);removestart=find(abs(ecg(:,10) - newstarttime*1000) < 0.5);
ecg(removeend+1:end,:)=[];ecg(1:removestart-1,:)=[];
frame=frame-160;
%-----------------------------------------------------------------------

% want to see what an individual & active pixel trace looks like after the
sgolay:
titlestraddfiltering=[animal, ' - Individual Pixel Data - additional
filtering for ActMap'];
figure('Name',titlestraddfiltering,'NumberTitle','off')
subplot(3,1,1), plot((reshape(DATAfdn(xactive,yactive,:),1,[])),'r'),
title('previously filtered data');
subplot(3,1,2), plot((reshape(DATAsgolay(xactive,yactive,:),1,[])),'k'),
title('after sgolay');
subplot(3,1,3), plot((reshape(DATAfdn(xactive,yactive,:),1,[])),'r'); hold
on; plot((reshape(DATAsgolay(xactive,yactive,:),1,[])),'k'),title('overlay');
h=gcf;
saveas(h,titlestraddfiltering, 'tif');
saveas(h,titlestraddfiltering);



%Now redo the mean of each ROI:
for i=1:nROIs; eval(['CCnew_' num2str(i) '=bwconncomp(roimask_' num2str(i)
'(:,:));']); end;
for i=1:nROIs; for j=1:frame; eval(['S_' num2str(i)
'new(j)=regionprops(CCnew_' num2str(i) ', DATAsgolay(:,:,j), ''Area'',
''Perimeter'', ''Centroid'', ''PixelIdxList'', ''PixelList'',
''MaxIntensity'', ''MinIntensity'', ''MeanIntensity'');']); end; end;
%do trick to extract means from S_x into separate matrix, then plot this
for i=1:nROIs; eval(['roi_' num2str(i) 'sgolaymeans=[S_' num2str(i)
'new.MeanIntensity];']); end;
%NOTE that this method does not count the zeros that make up the 128x128
%matrices, which could adversely lower the mean values of ROIs

%Now re-normalize at each pixel (for use in mapping):
vector6=reshape(DATAsgolay,[],size(DATAsgolay,3));
vector6n=zeros(size(vector6));
for w=1:size(vector6,1)
    if isfinite(vector6(w))
    vector6n(w,:)=(vector6(w,:)-min(vector6(w,:)))./(max(vector6(w,:))-
min(vector6(w,:)));
    end;
end;
DATAsgolayn=reshape(vector6n,size(DATAsgolay,1),size(DATAsgolay,2),[]);

%%%%%%%%%%%%%%%%%%%%%%%%%%%%%%%%%%%%%%%
```

```matlab
%Before moving too much far forward, play sgolay filtered data to see if it
%is sensical: scale to between 128-256:
combroimaxsgolayn=max(max(max(DATAsgolayn)));
combroiminsgolayn=min(min(min(DATAsgolayn)));
combroirangesgolayn=combroimaxsgolayn-combroiminsgolayn;
DATAsgolayscaled=zeros(size(DATAsgolayn));
DATAsgolayscaled=(((DATAsgolayn-
combroiminsgolayn)./combroirangesgolayn).*128)+128;
for y=1:frame,
DATAsgolayscaled(:,:,y)=combroimask(:,:).*DATAsgolayscaled(:,:,y); end;
%now set values of NaN in DATAscaled ==0:
DATAsgolayscaled(isnan(DATAsgolayscaled))=0;
%now create a new, single data matrix of Mscaled and DATAsgolayscaled:
Activationsgolay=zeros(size(DATAsgolayscaled));
for i=1:frame, Activationsgolay(:,:,i) =
DATAsgolayscaled(:,:,i)+(Mscaledcomplement);end;
%now play:
titlestrfdnd=[animal, ' - Activation of ROIs'];
figure('Name',titlestrfdnd,'NumberTitle','off');
for i=1:frame; imagesc(Activationsgolay(:,:,i));axis square;  set(gca,
'YTick', []);set(gca, 'XTick', []); set(gca,'clim', [0 256]);
colormap(Ncolormap); title(sprintf('Frame %i', i));  pause(tbwframe); end;
% -------------------------------------------------
figure()
%Now create a movie of the above:
titlemovie=[animal,'_Activation of ROIs_one tenth speed'];
vidObj=VideoWriter(titlemovie);
%set the framerate
vidObj.FrameRate=(round(1/(tbwframe*10)));
%write sequence of frames to the compressed AVI file:
open(vidObj);
for i=1:frame; imagesc(Activationsgolay(:,:,i)); axis square; set(gca,
'YTick', []);set(gca, 'XTick', []);
    set(gca,'clim', [0 256]); colormap(Ncolormap); title(sprintf('Time (s) =
%.3f', rtime(i)));
    currFrame=getframe; writeVideo(vidObj,currFrame); end;
close(vidObj);
%%%%%%%%%%%%%%%%%%%%%%%%%%%%%%%%%%%

% %apply ROI masks to recently filtered data:
% for i=1:nROIs; eval(['roi_' num2str(i) 'new=zeros(128,128,frame);']); for
j=1:frame; eval(['roi_' num2str(i) 'new(:,:,j)=roimask_' num2str(i)
'(:,:).*DATAsgolayn(:,:,j);']); end; end;

%%%%reshape for 1st derivative calculation:
vector7=reshape(DATAsgolayn,[],size(DATAsgolayn,3));
vector7d=zeros((size(vector7,1)),(size(vector7,2))-1);
vector7d=diff(vector7,1,2);
% %normalize:
% for w=1:size(vector7d,1)
%     if isfinite(vector7d(w))
%     vector7d(w,:)=(vector7d(w,:)-min(vector7d(w,:)))./(max(vector7d(w,:))-
min(vector7d(w,:)));
%     end;
% end;
DATAsgolaynd=reshape(vector7d,size(DATAsgolayn,1),size(DATAsgolayn,2),[]);
```

```matlab
% create a time vector for the 1st derivative stack:
drtime=zeros(1,frame-1);
for i=1:frame-1; drtime(i)=((rtime(i)+rtime(i+1))/2);end;
% filtering 1st Derivative signal for each pixel:
% Implement sgolay filter now on pixels within identified ROIs:
vector7ds=reshape(DATAsgolaynd,[],size(DATAsgolaynd,3));
DATA2sgolaynd=zeros(size(vector7ds));
for x=1:length(vector7ds),
    if isfinite(vector7ds(x))
        DATA2sgolaynd(x,:)=smooth(vector7ds(x,:),slength,'sgolay',sgolayo);
    end;
end;
DATA2sgolaynd=reshape(DATA2sgolaynd,size(DATAsgolayn,1),size(DATAsgolayn,2),[
]);

% % now mask this based on ROIs:
% for i=1:nROIs; eval(['roi_' num2str(i) 'd=zeros(128,128,frame-1);']); for
j=1:frame-1; eval(['roi_' num2str(i) 'd(:,:,j)=roimask_' num2str(i)
'(:,:).*DATAsgolaynd(:,:,j);']); end; end;
%roi_1d(isnan(roi_1dd))=0;

%Now find the mean of each ROId:
for i=1:nROIs; eval(['CCnew_' num2str(i) 'd=bwconncomp(roimask_' num2str(i)
'(:,:));']); end;
for i=1:nROIs; for j=1:frame-1; eval(['S_' num2str(i)
'newd(j)=regionprops(CCnew_' num2str(i) 'd, DATA2sgolaynd(:,:,j), ''Area'',
''Perimeter'', ''Centroid'', ''PixelIdxList'', ''PixelList'',
''MaxIntensity'', ''MinIntensity'', ''MeanIntensity'');']); end; end;
%do trick to extract means from S_x into separate matrix, then plot this
for i=1:nROIs; eval(['roi_' num2str(i)
'dmeans=[S_' num2str(i)
'newd.MeanIntensity];']); end;
%NOTE that this method does not count the zeros that make up the 128x128
%matrices, which could adversely lower the mean values of ROIs

%%%%reshape for 2nd derivative calculation:
vector8=reshape(DATA2sgolaynd,[],size(DATA2sgolaynd,3));
vector8d=zeros((size(vector8,1)),(size(vector8,2))-1);
vector8d=diff(vector8,1,2);
% %normalize:
% for w=1:size(vector8d,1)
%     if isfinite(vector8d(w))
%     vector8d(w,:)=(vector8d(w,:)-min(vector8d(w,:)))./(max(vector8d(w,:))-
min(vector8d(w,:)));
%     end;
% end;
DATAsgolayndd=reshape(vector8d,size(DATA2sgolaynd,1),size(DATA2sgolaynd,2),[]
);
% create a time vector for the 2nd derivative stack:
ddrtime=zeros(1,frame-2);
for i=1:frame-2; ddrtime(i)=((drtime(i)+drtime(i+1))/2);end; %the same as
"rtime" but with first and last times gone
% filtering 2nd Derivative signal for each pixel:
% Implement sgolay filter now on pixels within identified ROIs:
vector8ds=reshape(DATAsgolayndd,[],size(DATAsgolayndd,3));
DATA2sgolayndd=zeros(size(vector8ds));
for x=1:length(vector8ds),
```

```
    if isfinite(vector8ds(x))
        DATA2sgolayndd(x,:)=smooth(vector8ds(x,:),slength,'sgolay',sgolayo);
    end;
end;
DATA2sgolayndd=reshape(DATA2sgolayndd,size(DATA2sgolaynd,1),size(DATA2sgolayn
d,2),[]);


%and plot norm, 1st diff, and 2nd diff signals for identified active pixel:
titlestrds=[animal, ' - Individual Pixel Data - Normal & Derivatives'];
figure('Name',titlestrds,'NumberTitle','off')
subplot(3,1,1), plot((reshape(DATAsgolayn(xactive,yactive,:),1,[])),'r'),
title('Normal time');
subplot(3,1,2), plot((reshape(DATA2sgolaynd(xactive,yactive,:),1,[])),'k'),
title('1st derivative');
subplot(3,1,3), plot((reshape(DATA2sgolayndd(xactive,yactive,:),1,[])),'b');
title('2nd derivative');
h=gcf;
saveas(h,titlestrds, 'tif');
saveas(h,titlestrds);


%NOT DONE AT THIS TIME
% % now mask this based on ROIs:
% for i=1:nROIs; eval(['roi_' num2str(i) 'dd=zeros(128,128,frame-2);']); for
j=1:frame-2; eval(['roi_' num2str(i) 'dd(:,:,j)=roimask_' num2str(i)
'(:,:).*DATAsgolayndd(:,:,j);']); end; end;


%Now find the mean of each ROIdd:
for i=1:nROIs; eval(['CCnew_' num2str(i) 'dd=bwconncomp(roimask_' num2str(i)
'(:,:));']); end;
for i=1:nROIs; for j=1:frame-2; eval(['S_' num2str(i)
'newdd(j)=regionprops(CCnew_' num2str(i) 'dd, DATA2sgolayndd(:,:,j),
''Area'', ''Perimeter'', ''Centroid'', ''PixelIdxList'', ''PixelList'',
''MaxIntensity'', ''MinIntensity'', ''MeanIntensity'');']); end; end;
%do trick to extract means from S_x into separate matrix, then plot this
for i=1:nROIs; eval(['roi_' num2str(i) 'ddmeans=[S_' num2str(i)
'newdd.MeanIntensity];']); end;
%NOTE that this method does not count the zeros that make up the 128x128
%matrices, which could adversely lower the mean values of ROIs


% %Create vector that is the mean of the 1st and 2nd derivative signals for
each ROI:
% for i=1:nROIs; eval(['roi_' num2str(i) 'dmeans=zeros(0,frame-1); for
n=1:frame-1; roi_' num2str(i) 'dmeans(n)=(mean2(roi_' num2str(i)
'd(:,:,n)));end;']); end;
% for i=1:nROIs; eval(['roi_' num2str(i) 'ddmeans=zeros(0,frame-2); for
n=1:frame-2; roi_' num2str(i) 'ddmeans(n)=(mean2(roi_' num2str(i)
'dd(:,:,n)));end;']); end;


%need to refind the peaks & valleys for the sgolay filtered ROIs now!
for n=1:nROIs, eval(['[Proi_' num2str(n) 'sg LProi_' num2str(n)
'sg]=findpeaks(roi_' num2str(n) 'sgolaymeans, ''MINPEAKDISTANCE'',MPD_'
num2str(n) ');']); end;
for n=1:nROIs, eval(['[Vroi_' num2str(n) 'sg LVroi_' num2str(n)
'sg]=findpeaks(-roi_' num2str(n) 'sgolaymeans, ''MINPEAKDISTANCE'',MPD_'
num2str(n) ');']); end;
for n=1:nROIs, eval(['Vroi_' num2str(n) 'sg =-Vroi_' num2str(n) 'sg;']); end;
```

```matlab
% Find peaks in 1st derivative signal for each ROI:
for n=1:nROIs, eval(['[Proi_' num2str(n) 'd LProi_' num2str(n)
'd]=findpeaks(roi_' num2str(n) 'dmeans, ''MINPEAKDISTANCE'',MPD_' num2str(n)
');']); end;
% Find peaks in 2nd derivative signal for each ROI:
for n=1:nROIs, eval(['[Proi_' num2str(n) 'dd LProi_' num2str(n)
'dd]=findpeaks(roi_' num2str(n) 'ddmeans, ''MINPEAKDISTANCE'',MPD_'
num2str(n) ');']); end;

%now plot the mean of the normal, 1st derivative, and 2nd derivative
%signals, for each ROI:
for n=1:nROIs;
    eval(['figure(),title(''ROI ' num2str(n) ' peaks & valleys'');
subplot(3,1,1), hold on; plot(roi_' num2str(n) 'sgolaymeans, ''g'');
title(''ROI ' num2str(n) '  Mean''); axis([0 length(roi_' num2str(n)
'sgolaymeans) min(roi_' num2str(n) 'sgolaymeans) max(roi_' num2str(n)
'sgolaymeans)]); ylabel(''FI''); plot(LProi_' num2str(n) 'sg,Proi_'
num2str(n) 'sg,''bo''); plot(LVroi_' num2str(n) 'sg,Vroi_' num2str(n)
'sg,''ro''); subplot(3,1,2), hold on; plot(roi_' num2str(n) 'dmeans, ''g'');
title(''ROI ' num2str(n) '  1st Deriv Mean''); axis([0 length(roi_'
num2str(n) 'dmeans) min(roi_' num2str(n) 'dmeans) max(roi_' num2str(n)
'dmeans)]); ylabel(''FI''); plot(LProi_' num2str(n) 'd,Proi_' num2str(n)
'd,''bo''); subplot(3,1,3), hold on; plot(roi_' num2str(n) 'ddmeans, ''g'');
title(''ROI ' num2str(n) '  2nd Deriv Mean''); axis([0 length(roi_'
num2str(n) 'ddmeans) min(roi_' num2str(n) 'ddmeans) max(roi_' num2str(n)
'ddmeans)]); ylabel(''FI''); plot(LProi_' num2str(n) 'dd,Proi_' num2str(n)
'dd,''bo'');']);
end;

pvsokay=input('Are the peaks and valleys for each ROI correctly identified
(y/n)?:  ');
while pvsokay==n
    newmod=input('Please enter new multiplier for peak detection
(default=0.85):  ');
    for i=1:nROIs, eval(['MPD_' num2str(i) '=round((period_' num2str(i)
'/tbwframe)*newmod);']); end;
    %need to refind the peaks & valleys for the sgolay filtered ROIs now!
    for n=1:nROIs, eval(['[Proi_' num2str(n) 'sg LProi_' num2str(n)
'sg]=findpeaks(roi_' num2str(n) 'sgolaymeans, ''MINPEAKDISTANCE'',MPD_'
num2str(n) ');']); end;
    for n=1:nROIs, eval(['[Vroi_' num2str(n) 'sg LVroi_' num2str(n)
'sg]=findpeaks(-roi_' num2str(n) 'sgolaymeans, ''MINPEAKDISTANCE'',MPD_'
num2str(n) ');']); end;
    for n=1:nROIs, eval(['Vroi_' num2str(n) 'sg =-Vroi_' num2str(n) 'sg;']);
end;
    % Find peaks in 1st derivative signal for each ROI:
    for n=1:nROIs, eval(['[Proi_' num2str(n) 'd LProi_' num2str(n)
'd]=findpeaks(roi_' num2str(n) 'dmeans, ''MINPEAKDISTANCE'',MPD_' num2str(n)
');']); end;
    % Find peaks in 2nd derivative signal for each ROI:
    for n=1:nROIs, eval(['[Proi_' num2str(n) 'dd LProi_' num2str(n)
'dd]=findpeaks(roi_' num2str(n) 'ddmeans, ''MINPEAKDISTANCE'',MPD_'
num2str(n) ');']); end;
    %now plot the mean of the normal, 1st derivative, and 2nd derivative
    %signals, for each ROI:
    for n=1:nROIs;
```

```matlab
        eval(['figure(),title(''ROI ' num2str(n) ' peaks & valleys'');
subplot(3,1,1), hold on; plot(roi_' num2str(n) 'sgolaymeans, ''g'');
title(''ROI ' num2str(n) '  Mean''); axis([0 length(roi_' num2str(n)
'sgolaymeans) min(roi_' num2str(n) 'sgolaymeans) max(roi_' num2str(n)
'sgolaymeans)]); ylabel(''FI''); plot(LProi_' num2str(n) 'sg,Proi_'
num2str(n) 'sg,''bo''); plot(LVroi_' num2str(n) 'sg,Vroi_' num2str(n)
'sg,''ro''); subplot(3,1,2), hold on; plot(roi_' num2str(n) 'dmeans, ''g'');
title(''ROI ' num2str(n) '  1st Deriv Mean''); axis([0 length(roi_'
num2str(n) 'dmeans) min(roi_' num2str(n) 'dmeans) max(roi_' num2str(n)
'dmeans)]); ylabel(''FI''); plot(LProi_' num2str(n) 'd,Proi_' num2str(n)
'd,''bo''); subplot(3,1,3), hold on; plot(roi_' num2str(n) 'ddmeans, ''g'');
title(''ROI ' num2str(n) '  2nd Deriv Mean''); axis([0 length(roi_'
num2str(n) 'ddmeans) min(roi_' num2str(n) 'ddmeans) max(roi_' num2str(n)
'ddmeans)]); ylabel(''FI''); plot(LProi_' num2str(n) 'dd,Proi_' num2str(n)
'dd,''bo'');']);
    end;
    pvsokay=input('Are the peaks and valleys for each ROI correclty
identified (y/n)?:  ');
end;


%-------------------------------------------------------------------------
%%%%%%%%%%%%%% Now to selecting windows for mapping %%%%%%%%%%%%%%%%%%%%%%%
% Select time window for activation mapping (one window per ROI):
disp('For the following, use the cursor function and extract the frame (X)
values:')
for i=1:nROIs;
    eval(['roi_' num2str(i) 'fstart=input([''Enter a start frame to search
for activation of ROI ' num2str(i) ': '']);']);
    eval(['roi_' num2str(i) 'fend=input([''Enter end frame of activation(s)
for ROI ' num2str(i) ': '']);']);
end;

%STEPS (generally, specifics may change):
%1) using the window selected above for each ROI, find the next min in the
%normal ROI signal as well as the next maximum in the signal.
%2) using the locations of the minimums and subsequent maximums, search
%within each and find the max derivative between this small window on a per
%pixel basis for each ROI.
%3) for each ROI and each window, create an activation map
%4) end with plotting a montage of the activation maps for each ROI
%separately.  Can, for figures, etc. come into the code and specifically
%plot ones for figures.
%5) iff the activation maps are qualitatively the same, can ask user if
%they want to average all of them for the generation of a single activation
%map
%6) next for CV maps, first ask user if CV maps are desired.  If so, then
%create a CV map for each separate activation map that was made in a
%similar montage fashion.  At the end can ask user if they want to generate
%one CV map that is based on the averaged activation map (iff the user
%elected to average the activation maps).


%find the identified valleys within the user selected frames:
for i=1:nROIs;
    eval(['roi_' num2str(i) 'ftemp=find(roi_' num2str(i) 'fstart <= LVroi_'
num2str(i) 'sg & LVroi_' num2str(i) 'sg <= roi_' num2str(i) 'fend);']);
```

```matlab
    eval(['roi_' num2str(i) 'fvs=LVroi_' num2str(i) 'sg(roi_' num2str(i)
'ftemp);']);
end
%find the identified peaks within the user selected frames:
for i=1:nROIs;
    eval(['roi_' num2str(i) 'ftemp=find(roi_' num2str(i) 'fstart <= LProi_'
num2str(i) 'sg & LProi_' num2str(i) 'sg <= roi_' num2str(i) 'fend);']);
    eval(['roi_' num2str(i) 'fps=LProi_' num2str(i) 'sg(roi_' num2str(i)
'ftemp);']);
end

%now break up each ROI trace into sections, and search vector7ds for a max
%at each pixel.  Where ever this max occurs, mark the frame number where it
%happens in the separate matrix ActMapF_X_Y (X=roi #, Y=activation #), then
%later find the times that correspond to the frames and create the matrix
%ActMap_X_Y.  Then plot these ActMap_X_Y in a montage fashion for the user.
%NOTE: the benefit of breaking up into sections first then finding maximums
%is that I don't have to implement a peakfinding algorithm and double check
%it for the continuous time series.

for i=1:nROIs,
    eval(['elements(i)=numel(roi_' num2str(i) 'fvs)-1;']);
end;

%create vector9's that contain ROI specific data of the 1st derivative
for i=1:nROIs; eval(['vector9_' num2str(i) '=zeros(numpixs,numpixs,frame-
1);']); for j=1:frame-1; eval(['vector9_' num2str(i) '(:,:,j)=roimask_'
num2str(i) '(:,:).*DATA2sgolaynd(:,:,j);']); end; end;
for i=1:nROIs; eval(['vector9_' num2str(i) '(vector9_' num2str(i) ' == 0) =
NaN;']); end;
for i=1:nROIs; eval(['vector9_' num2str(i) '=reshape(vector9_' num2str(i)
',[],size(vector9_' num2str(i) ',3));']);end; %PROBLEM HERE - size of
DATA2sgolaynd not coming out right...
%now perform all operations to create activation maps for each activation
%of each ROI - VERY IMPORTANT STEPS HERE!!!! Note time is in milliseconds!
j=1;
for i=1:nROIs,
    for j=1:elements(i);
        eval(['roi_' num2str(i) '_' num2str(j) 'f=[roi_' num2str(i)
'fvs(j):roi_' num2str(i) 'fvs(j+1)]; roi_' num2str(i) '_' num2str(j)
'=vector9_' num2str(i) '(:,roi_' num2str(i) 'fvs(j):roi_' num2str(i)
'fvs(j+1)); [roi_' num2str(i) '_' num2str(j) 'maxd roi_' num2str(i) '_'
num2str(j) 'maxc] = max(roi_' num2str(i) '_' num2str(j) ', [], 2); roi_'
num2str(i) '_' num2str(j) 'fmax = roi_' num2str(i) '_' num2str(j) 'f(roi_'
num2str(i) '_' num2str(j) 'maxc); roi_' num2str(i) '_' num2str(j) 'acttime =
drtime(roi_' num2str(i) '_' num2str(j) 'fmax); roi_' num2str(i) '_'
num2str(j) 'actmap = reshape(roi_' num2str(i) '_' num2str(j) 'acttime,
size(DATA2sgolaynd,1), size(DATAsgolaynd,2),[]); roi_' num2str(i) '_'
num2str(j) 'correction = min(min(roi_' num2str(i) '_' num2str(j) 'actmap));
roi_' num2str(i) '_' num2str(j) 'actmap = roi_' num2str(i) '_' num2str(j)
'actmap - roi_' num2str(i) '_' num2str(j) 'correction*ones(size(roi_'
num2str(i) '_' num2str(j) 'actmap,1),size(roi_' num2str(i) '_' num2str(j)
'actmap,2)); roi_' num2str(i) '_' num2str(j) 'actmap(roi_' num2str(i) '_'
num2str(j) 'actmap == 0) = NaN; roi_' num2str(i) '_' num2str(j) 'correction2
= nanmin(nanmin(roi_' num2str(i) '_' num2str(j) 'actmap)); roi_' num2str(i)
'_' num2str(j) 'actmap = roi_' num2str(i) '_' num2str(j) 'actmap - roi_'
```

```matlab
num2str(i) '_' num2str(j) 'correction2*ones(size(roi_' num2str(i) '_'
num2str(j) 'actmap,1),size(roi_' num2str(i) '_' num2str(j) 'actmap,2)); roi_'
num2str(i) '_' num2str(j) 'actmap=roi_' num2str(i) '_' num2str(j)
'actmap*1000;']);
    end;
end;


%find max (longest time) of actmaps for plotting all actmaps:
for i=1:nROIs
    for j=1:elements(i);
        eval(['roi_' num2str(i) 'actmapmaxs(j)=max(max(roi_' num2str(i) '_'
num2str(j) 'actmap));']);
    end;
        eval(['roi_' num2str(i) 'actmapmax=max(roi_' num2str(i)
'actmapmaxs);']);
end;

%plot all actmaps as imagesc:
for i=1:nROIs
    for j=1:elements(i);
        eval(['figure(''Name'',''roi_' num2str(i) '_' num2str(j) ' Activation
(imagesc)'',''NumberTitle'',''off''),imagesc(roi_' num2str(i) '_' num2str(j)
'actmap), title(sprintf(''Time Range: %.3f to %.3f sec'',min(roi_' num2str(i)
'_' num2str(j) 'acttime),max(roi_' num2str(i) '_' num2str(j) 'acttime)));
axis off, colorbar, colormap(btg), axis square; caxis([0, roi_' num2str(i)
'actmapmax]), set(gca, ''YTick'', []);set(gca, ''XTick'', []), hgsave(''roi_'
num2str(i) '_' num2str(j) ' Activation (imagesc)''); print(''-dpng'',''roi_'
num2str(i) '_' num2str(j) ' Activation (imagesc)'');']);
    end;
end;


%Save all activation maps as a matrix:
titleActMaps=[animal, '_AllActMaps'];
save(titleActMaps, 'roi_*'); %note this will also save all roi_* data as well

% NO LONGER PLOTTING AND SAVING THESE CONTOUR MAPS, NOT FOUND TO BE USEFUL
% %plot all actmaps as contourf w/o lines:
% for i=1:nROIs
%     for j=1:elements(i);
%         eval(['figure(''Name'',''roi_' num2str(i) '_' num2str(j) '
Activation (contourf)'',''NumberTitle'',''off''),contourf(flipud(roi_'
num2str(i) '_' num2str(j) 'actmap),''LineColor'',''none''),
title(sprintf(''Time Range: %.3f to %.3f sec'',min(roi_' num2str(i) '_'
num2str(j) 'acttime),max(roi_' num2str(i) '_' num2str(j) 'acttime))); axis
off, colorbar, axis square; caxis([0, roi_' num2str(i) 'actmapmax]), set(gca,
''YTick'', []);set(gca, ''XTick'', []), hgsave(''roi_' num2str(i) '_'
num2str(j) ' Activation (contourf)''); print(''-dpng'',''roi_' num2str(i) '_'
num2str(j) ' Activation (contourf)'');']);
%     end;
% end;

%need to plot histograms also, to get a visual of really how long
%activation takes and to discern whether or not the min & max limits used
```

```matlab
%to plot are good:
%1st reshape the actmaps into a vector each, then sort these vectors in
%ascending order, then use the hist function to plot histograms of each:
for i=1:nROIs
    for j=1:elements(i);
        eval(['roi_' num2str(i) '_' num2str(j) 'hist = reshape(roi_'
num2str(i) '_' num2str(j) 'actmap,1,[]); roi_' num2str(i) '_' num2str(j)
'hist=sort(roi_' num2str(i) '_' num2str(j) 'hist); figure(''Name'',''roi_'
num2str(i) '_' num2str(j) ' Activation Time
Histogram'',''NumberTitle'',''off''), hist(roi_' num2str(i) '_' num2str(j)
'hist),title(sprintf(''Time Range: %.3f to %.3f sec'',min(roi_' num2str(i)
'_' num2str(j) 'acttime),max(roi_' num2str(i) '_' num2str(j) 'acttime)));
xlabel(''Activation Time (ms)''),ylabel(''Counts''),hgsave(''roi_' num2str(i)
'_' num2str(j) ' Activation Time Histogram''); print(''-dpng'',''roi_'
num2str(i) '_' num2str(j) ' Activation Time Histogram'');']);
    end;
end;

%save data:
save(animal)
```

178

Bibliography

1. Buja, L.M. & Vela, D. Cardiomyocyte death and renewal in the normal and diseased heart. *Cardiovasc Pathol* **17**, 349-374 (2008).
2. Senyo, S.E. et al. Mammalian heart renewal by pre-existing cardiomyocytes. *Nature* **493**, 433-436 (2013).
3. Laflamme, M.A. & Murry, C.E. Heart regeneration. *Nature* **473**, 326-335 (2011).
4. Murray, C.J. et al. Disability-adjusted life years (DALYs) for 291 diseases and injuries in 21 regions, 1990-2010: a systematic analysis for the Global Burden of Disease Study 2010. *Lancet* **380**, 2197-2223 (2012).
5. Heidenreich, P.A. et al. Forecasting the future of cardiovascular disease in the United States: a policy statement from the American Heart Association. *Circulation* **123**, 933-944 (2011).
6. Yancy, C.W. et al. 2013 ACCF/AHA guideline for the management of heart failure: a report of the American College of Cardiology Foundation/American Heart Association Task Force on Practice Guidelines. *Journal of the American College of Cardiology* **62**, e147-239 (2013).
7. Go, A.S. et al. Heart disease and stroke statistics--2013 update: a report from the American Heart Association. *Circulation* **127**, e6-e245 (2013).
8. Rose, E.A. et al. Long-term use of a left ventricular assist device for end-stage heart failure. *N Engl J Med* **345**, 1435-1443 (2001).
9. Soonpaa, M.H., Koh, G.Y., Klug, M.G. & Field, L.J. Formation of nascent intercalated disks between grafted fetal cardiomyocytes and host myocardium. *Science* **264**, 98-101 (1994).
10. Koh, G.Y. et al. Stable fetal cardiomyocyte grafts in the hearts of dystrophic mice and dogs. *The Journal of clinical investigation* **96**, 2034-2042 (1995).
11. Leor, J., Patterson, M., Quinones, M.J., Kedes, L.H. & Kloner, R.A. Transplantation of fetal myocardial tissue into the infarcted myocardium of rat - A potential method for repair of infarcted myocardium? *Circulation* **94**, 332-336 (1996).
12. Li, R.K. et al. Natural history of fetal rat cardiomyocytes transplanted into adult rat myocardial scar tissue. *Circulation* **96**, II-179-186; discussion 186-177 (1997).
13. Sakai, T. et al. Fetal cell transplantation: a comparison of three cell types. *J Thorac Cardiovasc Surg* **118**, 715-724 (1999).
14. Scorsin, M. et al. Comparison of the effects of fetal cardiomyocyte and skeletal myoblast transplantation on postinfarction left ventricular function. *J Thorac Cardiovasc Surg* **119**, 1169-1175 (2000).
15. Yao, M. et al. Long-term outcome of fetal cell transplantation on postinfarction ventricular remodeling and function. *Journal of molecular and cellular cardiology* **35**, 661-670 (2003).
16. Murry, C.E., Wiseman, R.W., Schwartz, S.M. & Hauschka, S.D. Skeletal myoblast transplantation for repair of myocardial necrosis. *The Journal of clinical investigation* **98**, 2512-2523 (1996).
17. Taylor, D.A. et al. Regenerating functional myocardium: improved performance after skeletal myoblast transplantation. *Nat Med* **4**, 929-933 (1998).
18. Atkins, B.Z. et al. Intracardiac transplantation of skeletal myoblasts yields two populations of striated cells in situ. *Ann Thorac Surg* **67**, 124-129 (1999).

19. Reinecke, H. & Murry, C.E. Transmural replacement of myocardium after skeletal myoblast grafting into the heart. Too much of a good thing? *Cardiovasc Pathol* **9**, 337-344 (2000).

20. Ghostine, S. et al. Long-term efficacy of myoblast transplantation on regional structure and function after myocardial infarction. *Circulation* **106**, I131-136 (2002).

21. Al Attar, N. et al. Long-term (1 year) functional and histological results of autologous skeletal muscle cells transplantation in rat. *Cardiovascular research* **58**, 142-148 (2003).

22. Leobon, B. et al. Myoblasts transplanted into rat infarcted myocardium are functionally isolated from their host. *Proceedings of the National Academy of Sciences of the United States of America* **100**, 7808-7811 (2003).

23. Abraham, M.R. et al. Antiarrhythmic engineering of skeletal myoblasts for cardiac transplantation. *Circulation research* **97**, 159-167 (2005).

24. Menasche, P. et al. The Myoblast Autologous Grafting in Ischemic Cardiomyopathy (MAGIC) trial: first randomized placebo-controlled study of myoblast transplantation. *Circulation* **117**, 1189-1200 (2008).

25. Reinecke, H., Poppa, V. & Murry, C.E. Skeletal muscle stem cells do not transdifferentiate into cardiomyocytes after cardiac grafting. *Journal of molecular and cellular cardiology* **34**, 241-249 (2002).

26. Orlic, D. et al. Bone marrow cells regenerate infarcted myocardium. *Nature* **410**, 701-705 (2001).

27. Orlic, D. et al. Mobilized bone marrow cells repair the infarcted heart, improving function and survival. *Proceedings of the National Academy of Sciences of the United States of America* **98**, 10344-10349 (2001).

28. Lunde, K. et al. Intracoronary injection of mononuclear bone marrow cells in acute myocardial infarction. *N Engl J Med* **355**, 1199-1209 (2006).

29. Wollert, K.C. et al. Intracoronary autologous bone-marrow cell transfer after myocardial infarction: the BOOST randomised controlled clinical trial. *Lancet* **364**, 141-148 (2004).

30. Schachinger, V. et al. Intracoronary bone marrow-derived progenitor cells in acute myocardial infarction. *N Engl J Med* **355**, 1210-1221 (2006).

31. Strauer, B.E., Yousef, M. & Schannwell, C.M. The acute and long-term effects of intracoronary Stem cell Transplantation in 191 patients with chronic heARt failure: the STAR-heart study. *Eur J Heart Fail* **12**, 721-729 (2010).

32. Murry, C.E. et al. Haematopoietic stem cells do not transdifferentiate into cardiac myocytes in myocardial infarcts. *Nature* **428**, 664-668 (2004).

33. Balsam, L.B. et al. Haematopoietic stem cells adopt mature haematopoietic fates in ischaemic myocardium. *Nature* (2004).

34. Mirotsou, M. et al. Secreted frizzled related protein 2 (Sfrp2) is the key Akt-mesenchymal stem cell-released paracrine factor mediating myocardial survival and repair. *Proceedings of the National Academy of Sciences of the United States of America* **104**, 1643-1648 (2007).

35. Mirotsou, M., Jayawardena, T.M., Schmeckpeper, J., Gnecchi, M. & Dzau, V.J. Paracrine mechanisms of stem cell reparative and regenerative actions in the heart. *Journal of molecular and cellular cardiology* **50**, 280-289 (2011).

36. Shintani, Y. et al. Donor cell-type specific paracrine effects of cell transplantation for post-infarction heart failure. *Journal of molecular and cellular cardiology* **47**, 288-295 (2009).

37. Gnecchi, M., Zhang, Z., Ni, A. & Dzau, V.J. Paracrine mechanisms in adult stem cell signaling and therapy. *Circulation research* **103**, 1204-1219 (2008).

38. Gnecchi, M. et al. Evidence supporting paracrine hypothesis for Akt-modified mesenchymal stem cell-mediated cardiac protection and functional improvement. *FASEB journal : official publication of the Federation of American Societies for Experimental Biology* **20**, 661-669 (2006).

39. Gnecchi, M. et al. Paracrine action accounts for marked protection of ischemic heart by Akt-modified mesenchymal stem cells. *Nat Med* **11**, 367-368 (2005).

40. Smith, R.R. et al. Regenerative potential of cardiosphere-derived cells expanded from percutaneous endomyocardial biopsy specimens. *Circulation* **115**, 896-908 (2007).

41. Li, T.S. et al. Direct comparison of different stem cell types and subpopulations reveals superior paracrine potency and myocardial repair efficacy with cardiosphere-derived cells. *Journal of the American College of Cardiology* **59**, 942-953 (2012).

42. Makkar, R.R. et al. Intracoronary cardiosphere-derived cells for heart regeneration after myocardial infarction (CADUCEUS): a prospective, randomised phase 1 trial. *Lancet* **379**, 895-904 (2012).

43. Malliaras, K. et al. Intracoronary cardiosphere-derived cells after myocardial infarction: evidence of therapeutic regeneration in the final 1-year results of the CADUCEUS trial (CArdiosphere-Derived aUtologous stem CElls to reverse ventricUlar dySfunction). *Journal of the American College of Cardiology* **63**, 110-122 (2014).

44. Yee, K. et al. Allogeneic cardiospheres delivered via percutaneous transendocardial injection increase viable myocardium, decrease scar size, and attenuate cardiac dilatation in porcine ischemic cardiomyopathy. *PloS one* **9**, e113805 (2014).

45. Kanazawa, H. et al. Cellular postconditioning: allogeneic cardiosphere-derived cells reduce infarct size and attenuate microvascular obstruction when administered after reperfusion in pigs with acute myocardial infarction. *Circulation. Heart failure* **8**, 322-332 (2015).

46. Thomson, J.A. et al. Embryonic stem cell lines derived from human blastocysts. *Science* **282**, 1145-1147 (1998).

47. Laflamme, M.A. et al. Cardiomyocytes derived from human embryonic stem cells in pro-survival factors enhance function of infarcted rat hearts. *Nature biotechnology* **25**, 1015-1024 (2007).

48. Zhu, W.Z., Filice, D., Palpant, N.J. & Laflamme, M.A. Methods for assessing the electromechanical integration of human pluripotent stem cell-derived cardiomyocyte grafts. *Methods in molecular biology* **1181**, 229-247 (2014).

49. Lopaschuk, G.D., Collins-Nakai, R.L. & Itoi, T. Developmental changes in energy substrate use by the heart. *Cardiovascular research* **26**, 1172-1180 (1992).

50. Porter, G.A., Jr. et al. Bioenergetics, mitochondria, and cardiac myocyte differentiation. *Progress in pediatric cardiology* **31**, 75-81 (2011).

51. Kehat, I. et al. Human embryonic stem cells can differentiate into myocytes with structural and functional properties of cardiomyocytes. *The Journal of clinical investigation* **108**, 407-414 (2001).

52. Lieu, D.K. et al. Absence of transverse tubules contributes to non-uniform Ca(2+) wavefronts in mouse and human embryonic stem cell-derived cardiomyocytes. *Stem cells and development* **18**, 1493-1500 (2009).

53. Lundy, S.D., Zhu, W.Z., Regnier, M. & Laflamme, M.A. Structural and functional maturation of cardiomyocytes derived from human pluripotent stem cells. *Stem Cells Dev* **22**, 1991-2002 (2013).

54. Mummery, C.L., Ward, D. & Passier, R. Differentiation of human embryonic stem cells to cardiomyocytes by coculture with endoderm in serum-free medium. *Current protocols in stem cell biology* **Chapter 1**, Unit 1F 2 (2007).

55. Snir, M. et al. Assessment of the ultrastructural and proliferative properties of human embryonic stem cell-derived cardiomyocytes. *American journal of physiology. Heart and circulatory physiology* **285**, H2355-2363 (2003).

56. Xu, C., Police, S., Rao, N. & Carpenter, M.K. Characterization and enrichment of cardiomyocytes derived from human embryonic stem cells. *Circulation research* **91**, 501-508 (2002).

57. Hazeltine, L.B. et al. Effects of substrate mechanics on contractility of cardiomyocytes generated from human pluripotent stem cells. *International journal of cell biology* **2012**, 508294 (2012).

58. Cui, L., Johkura, K., Takei, S., Ogiwara, N. & Sasaki, K. Structural differentiation, proliferation, and association of human embryonic stem cell-derived cardiomyocytes in vitro and in their extracardiac tissues. *J Struct Biol* **158**, 307-317 (2007).

59. McDevitt, T.C., Laflamme, M.A. & Murry, C.E. Proliferation of cardiomyocytes derived from human embryonic stem cells is mediated via the IGF/PI 3-kinase/Akt signaling pathway. *Journal of molecular and cellular cardiology* **39**, 865-873 (2005).

60. He, J.Q., Ma, Y., Lee, Y., Thomson, J.A. & Kamp, T.J. Human embryonic stem cells develop into multiple types of cardiac myocytes: action potential characterization. *Circulation research* **93**, 32-39 (2003).

61. Sartiani, L. et al. Developmental changes in cardiomyocytes differentiated from human embryonic stem cells: a molecular and electrophysiological approach. *Stem cells* **25**, 1136-1144 (2007).

62. Mummery, C. et al. Differentiation of human embryonic stem cells to cardiomyocytes: role of coculture with visceral endoderm-like cells. *Circulation* **107**, 2733-2740 (2003).

63. Zhu, W.Z. et al. Neuregulin/ErbB signaling regulates cardiac subtype specification in differentiating human embryonic stem cells. *Circulation research* **107**, 776-786 (2010).

64. Robertson, C., Tran, D.D. & George, S.C. Concise review: maturation phases of human pluripotent stem cell-derived cardiomyocytes. *Stem cells* **31**, 829-837 (2013).

65. Satin, J. et al. Mechanism of spontaneous excitability in human embryonic stem cell derived cardiomyocytes. *The Journal of physiology* **559**, 479-496 (2004).

66. Zhu, W.Z., Santana, L.F. & Laflamme, M.A. Local control of excitation-contraction coupling in human embryonic stem cell-derived cardiomyocytes. *PloS one* **4**, e5407 (2009).

67. Liu, J., Fu, J.D., Siu, C.W. & Li, R.A. Functional Sarcoplasmic Reticulum for Calcium-Handling of Human Embryonic Stem Cell-Derived Cardiomyocytes: Insights for Driven Maturation. *Stem cells* (2007).

68. Satin, J. et al. Calcium handling in human embryonic stem cell-derived cardiomyocytes. *Stem cells* **26**, 1961-1972 (2008).

69. Lee, P. et al. Simultaneous voltage and calcium mapping of genetically purified human induced pluripotent stem cell-derived cardiac myocyte monolayers. *Circulation research* **110**, 1556-1563 (2012).

70. Zhang, D. et al. Tissue-engineered cardiac patch for advanced functional maturation of human ESC-derived cardiomyocytes. *Biomaterials* **34**, 5813-5820 (2013).

71. Kehat, I., Gepstein, A., Spira, A., Itskovitz-Eldor, J. & Gepstein, L. High-resolution electrophysiological assessment of human embryonic stem cell-derived cardiomyocytes: a novel in vitro model for the study of conduction. *Circulation research* **91**, 659-661 (2002).

72. Valderrabano, M. Influence of anisotropic conduction properties in the propagation of the cardiac action potential. *Prog Biophys Mol Biol* **94**, 144-168 (2007).

73. Zhuang, J., Yamada, K.A., Saffitz, J.E. & Kleber, A.G. Pulsatile stretch remodels cell-to-cell communication in cultured myocytes. *Circulation research* **87**, 316-322 (2000).

74. Laflamme, M.A. et al. Formation of human myocardium in the rat heart from human embryonic stem cells. *Am J Pathol* **167**, 663-671 (2005).

75. Dai, W. et al. Survival and maturation of human embryonic stem cell-derived cardiomyocytes in rat hearts. *Journal of molecular and cellular cardiology* **43**, 504-516 (2007).

76. Caspi, O. et al. Transplantation of human embryonic stem cell-derived cardiomyocytes improves myocardial performance in infarcted rat hearts. *J Am Coll Cardiol* **50**, 1884-1893 (2007).

77. van Laake, L.W. et al. Human embryonic stem cell-derived cardiomyocytes survive and mature in the mouse heart and transiently improve function after myocardial infarction. *Stem cell research* **1**, 9-24 (2007).

78. van Laake, L.W. et al. Improvement of mouse cardiac function by hESC-derived cardiomyocytes correlates with vascularity but not graft size. *Stem cell research* **3**, 106-112 (2009).

79. van Laake, L.W., Passier, R., Doevendans, P.A. & Mummery, C.L. Human embryonic stem cell-derived cardiomyocytes and cardiac repair in rodents. *Circulation research* **102**, 1008-1010 (2008).

80. Shiba, Y. et al. Human ES-cell-derived cardiomyocytes electrically couple and suppress arrhythmias in injured hearts. *Nature* **489**, 322-325 (2012).

81. Fernandes, S. et al. Human embryonic stem cell-derived cardiomyocytes engraft but do not alter cardiac remodeling after chronic infarction in rats. *Journal of molecular and cellular cardiology* **49**, 941-949 (2010).

82. Shiba, Y. et al. Electrical Integration of Human Embryonic Stem Cell-Derived Cardiomyocytes in a Guinea Pig Chronic Infarct Model. *Journal of Cardiovascular Pharmacology and Therapeutics* **19**, 368-381 (2014).

83. Kehat, I. et al. Electromechanical integration of cardiomyocytes derived from human embryonic stem cells. *Nature biotechnology* **22**, 1282-1289 (2004).

84. Christie, J.D. et al. The Registry of the International Society for Heart and Lung Transplantation: Twenty-sixth Official Adult Lung and Heart-Lung Transplantation Report-2009. *J Heart Lung Transplant* **28**, 1031-1049 (2009).

85. Pouleur, A.C. et al. Pathogenesis of sudden unexpected death in a clinical trial of patients with myocardial infarction and left ventricular dysfunction, heart failure, or both. *Circulation* **122**, 597-602 (2010).

86. van Laake, L.W. et al. Human embryonic stem cell-derived cardiomyocytes survive and mature in the mouse heart and transiently improve function after myocardial infarction. *Stem Cell Research* **1**, 9-24 (2007).

87. Menard, C. et al. Transplantation of cardiac-committed mouse embryonic stem cells to infarcted sheep myocardium: a preclinical study. *Lancet* **366**, 1005-1012 (2005).

88. Blin, G. et al. A purified population of multipotent cardiovascular progenitors derived from primate pluripotent stem cells engrafts in postmyocardial infarcted nonhuman primates. *The Journal of clinical investigation* **120**, 1125-1139 (2010).

89. Chen, H.S., Kim, C. & Mercola, M. Electrophysiological challenges of cell-based myocardial repair. *Circulation* **120**, 2496-2508 (2009).

90. Gepstein, L. Electrophysiologic implications of myocardial stem cell therapies. *Heart Rhythm* **5**, S48-52 (2008).

91. Jonsson, M.K. et al. Quantified proarrhythmic potential of selected human embryonic stem cell-derived cardiomyocytes. *Stem cell research* **4**, 189-200 (2010).

92. Liao, S.Y. et al. Proarrhythmic risk of embryonic stem cell-derived cardiomyocyte transplantation in infarcted myocardium. *Heart rhythm : the official journal of the Heart Rhythm Society* **7**, 1852-1859 (2010).

93. Zhang, Y.M., Hartzell, C., Narlow, M. & Dudley, S.C., Jr. Stem cell-derived cardiomyocytes demonstrate arrhythmic potential. *Circulation* **106**, 1294-1299 (2002).

94. Roell, W. et al. Engraftment of connexin 43-expressing cells prevents post-infarct arrhythmia. *Nature* **450**, 819-824 (2007).

95. Thompson, S.A. et al. Engraftment of human embryonic stem cell derived cardiomyocytes improves conduction in an arrhythmogenic in vitro model. *J Mol Cell Cardiol* **53**, 15-23 (2012).

96. Xue, T. et al. Functional integration of electrically active cardiac derivatives from genetically engineered human embryonic stem cells with quiescent recipient ventricular cardiomyocytes: insights into the development of cell-based pacemakers. *Circulation* **111**, 11-20 (2005).

97. Kotlikoff, M.I. Genetically encoded Ca2+ indicators: using genetics and molecular design to understand complex physiology. *J Physiol* **578**, 55-67 (2007).

98. Hockemeyer, D. et al. Efficient targeting of expressed and silent genes in human ESCs and iPSCs using zinc-finger nucleases. *Nature biotechnology* **27**, 851-857 (2009).

99. Xu, C. et al. Efficient generation and cryopreservation of cardiomyocytes derived from human embryonic stem cells. *Regen Med* **6**, 53-66 (2011).

100. Zhu, W.Z., Van Biber, B. & Laflamme, M.A. Methods for the derivation and use of cardiomyocytes from human pluripotent stem cells. *Methods in molecular biology* **767**, 419-431 (2011).

101. Zhang, M. et al. Cardiomyocyte grafting for cardiac repair: graft cell death and anti-death strategies. *Journal of molecular and cellular cardiology* **33**, 907-921 (2001).

102. Biermann, M. et al. Differential effects of cytochalasin D and 2,3 butanedione monoxime on isometric twitch force and transmembrane action potential in isolated ventricular muscle: implications for optical measurements of cardiac repolarization. *J Cardiovasc Electrophysiol* **9**, 1348-1357 (1998).

103. Laurita, K.R. & Singal, A. Mapping action potentials and calcium transients simultaneously from the intact heart. *American journal of physiology. Heart and circulatory physiology* **280**, H2053-2060 (2001).

104. Fedorov, V.V. et al. Application of blebbistatin as an excitation-contraction uncoupler for electrophysiologic study of rat and rabbit hearts. *Heart rhythm : the official journal of the Heart Rhythm Society* **4**, 619-626 (2007).

105. Kolega, J. Phototoxicity and photoinactivation of blebbistatin in UV and visible light. *Biochem Biophys Res Commun* **320**, 1020-1025 (2004).

106. Asfour, H., Swift, L.M., Sarvazyan, N., Doroslovacki, M. & Kay, M.W. Signal decomposition of transmembrane voltage-sensitive dye fluorescence using a multiresolution wavelet analysis. *IEEE Trans Biomed Eng* **58**, 2083-2093 (2011).

107. Kay, M., Swift, L., Martell, B., Arutunyan, A. & Sarvazyan, N. Locations of ectopic beats coincide with spatial gradients of NADH in a regional model of low-flow reperfusion. *American journal of physiology. Heart and circulatory physiology* **294**, H2400-2405 (2008).

108. Swift, L. et al. Controlled regional hypoperfusion in Langendorff heart preparations. *Physiol Meas* **29**, 269-279 (2008).

109. Matsushita, S. et al. Alterations of phosphorylation state of connexin 43 during hypoxia and reoxygenation are associated with cardiac function. *The journal of histochemistry and cytochemistry : official journal of the Histochemistry Society* **54**, 343-353 (2006).

110. Matsushita, S. et al. Inhibition of connexin43 dephosphorylation is involved in protective effects of diltiazem on cardiac function during hypoxic injury. *Histol Histopathol* **26**, 315-322 (2011).

111. Weyers, J.J. et al. Effects of cell grafting on coronary remodeling after myocardial infarction. *J Am Heart Assoc* **2**, e000202 (2013).

112. Mummery, C. et al. Cardiomyocyte differentiation of mouse and human embryonic stem cells. *Journal of anatomy* **200**, 233-242 (2002).

113. Binah, O. et al. Functional and developmental properties of human embryonic stem cells-derived cardiomyocytes. *J Electrocardiol* **40**, S192-196 (2007).

114. Leor, J. et al. Human embryonic stem cell transplantation to repair the infarcted myocardium. *Heart* **93**, 1278-1284 (2007).

115. Chong, J.J. et al. Human embryonic-stem-cell-derived cardiomyocytes regenerate non-human primate hearts. *Nature* **510**, 273-277 (2014).

116. Tallini, Y.N. et al. Imaging cellular signals in the heart in vivo: Cardiac expression of the high-signal Ca2+ indicator GCaMP2. *Proc Natl Acad Sci U S A* **103**, 4753-4758 (2006).

117. Tian, L. et al. Imaging neural activity in worms, flies and mice with improved GCaMP calcium indicators. *Nature methods* **6**, 875-881 (2009).

118. Fast, V.G. & Kleber, A.G. Cardiac tissue geometry as a determinant of unidirectional conduction block: assessment of microscopic excitation spread by optical mapping in patterned cell cultures and in a computer model. *Cardiovascular research* **29**, 697-707 (1995).

119. Fast, V.G., Darrow, B.J., Saffitz, J.E. & Kleber, A.G. Anisotropic activation spread in heart cell monolayers assessed by high-resolution optical mapping. Role of tissue discontinuities. *Circulation research* **79**, 115-127 (1996).

120. Girouard, S.D., Pastore, J.M., Laurita, K.R., Gregory, K.W. & Rosenbaum, D.S. Optical mapping in a new guinea pig model of ventricular tachycardia reveals mechanisms for multiple wavelengths in a single reentrant circuit. *Circulation* **93**, 603-613 (1996).

121. Laurita, K.R., Girouard, S.D. & Rosenbaum, D.S. Modulation of ventricular repolarization by a premature stimulus. Role of epicardial dispersion of repolarization kinetics demonstrated by optical mapping of the intact guinea pig heart. *Circulation research* **79**, 493-503 (1996).

122. Qian, Y.W., Sung, R.J., Lin, S.F., Province, R. & Clusin, W.T. Spatial heterogeneity of action potential alternans during global ischemia in the rabbit heart. *American journal of physiology. Heart and circulatory physiology* **285**, H2722-2733 (2003).

123. Rogers, J.M., Walcott, G.P., Gladden, J.D., Melnick, S.B. & Kay, M.W. Panoramic optical mapping reveals continuous epicardial reentry during ventricular fibrillation in the isolated swine heart. *Biophysical journal* **92**, 1090-1095 (2007).

124. Ding, C. et al. High-resolution optical mapping of ventricular tachycardia in rats with chronic myocardial infarction. *Pacing Clin Electrophysiol* **33**, 687-695 (2010).

125. Omichi, C. et al. Comparing cardiac action potentials recorded with metal and glass microelectrodes. *American journal of physiology. Heart and circulatory physiology* **279**, H3113-3117 (2000).

126. Fridericia, L.S. The duration of systole in an electrocardiogram in normal humans and in patients with heart disease. 1920. *Annals of noninvasive electrocardiology : the official journal of the International Society for Holter and Noninvasive Electrocardiology, Inc* **8**, 343-351 (2003).

127. Hossain, M.Z., Ao, P. & Boynton, A.L. Rapid disruption of gap junctional communication and phosphorylation of connexin43 by platelet-derived growth factor in T51B rat liver epithelial cells expressing platelet-derived growth factor receptor. *J Cell Physiol* **174**, 66-77 (1998).

128. Cooper, C.D. & Lampe, P.D. Casein kinase 1 regulates connexin-43 gap junction assembly. *J Biol Chem* **277**, 44962-44968 (2002).

129. Ferreira, G., Yi, J., Rios, E. & Shirokov, R. Ion-dependent inactivation of barium current through L-type calcium channels. *The Journal of general physiology* **109**, 449-461 (1997).

130. Tampo, A., Hogan, C.S., Sedlic, F., Bosnjak, Z.J. & Kwok, W.M. Accelerated inactivation of cardiac L-type calcium channels triggered by anaesthetic-induced preconditioning. *Br J Pharmacol* **156**, 432-443 (2009).

131. Omichi, C. et al. Comparing cardiac action potentials recorded with metal and glass microelectrodes. *American journal of physiology. Heart and circulatory physiology* **279**, H3113-3117 (2000).

132. Erickson, M.G., Alseikhan, B.A., Peterson, B.Z. & Yue, D.T. Preassociation of calmodulin with voltage-gated Ca(2+) channels revealed by FRET in single living cells. *Neuron* **31**, 973-985 (2001).

133. Alseikhan, B.A., DeMaria, C.D., Colecraft, H.M. & Yue, D.T. Engineered calmodulins reveal the unexpected eminence of Ca2+ channel inactivation in controlling heart excitation. *Proceedings of the National Academy of Sciences of the United States of America* **99**, 17185-17190 (2002).

134. Limpitikul, W.B. et al. Calmodulin mutations associated with long QT syndrome prevent inactivation of cardiac L-type Ca(2+) currents and promote proarrhythmic behavior in ventricular myocytes. *Journal of molecular and cellular cardiology* **74**, 115-124 (2014).

135. Papp, Z., Peineau, N., Szigeti, G., Argibay, J. & Kovacs, L. Calcium-dependent modulation of the plateau phase of action potential in isolated ventricular cells of rabbit heart. *Acta physiologica Scandinavica* **167**, 119-129 (1999).

136. Kjolbye, A.L., Haugan, K., Hennan, J.K. & Petersen, J.S. Pharmacological modulation of gap junction function with the novel compound rotigaptide: a promising new principle for prevention of arrhythmias. *Basic Clin Pharmacol Toxicol* **101**, 215-230 (2007).

137. Udata, C., Micalizzi, M., Katz, A., Giogio, Q.M. & Meng, X. Six days continuous IV infusion study of the safety, tolerability and pharmacokinetics of rotigaptide (ZP123) administered intravenously to healthy subjects. *Clin Pharmacol Ther* **79**, 77 (2006a).

138. Dhein, S. et al. A new synthetic antiarrhythmic peptide reduces dispersion of epicardial activation recovery interval and diminishes alterations of epicardial activation patterns induced by regional ischemia. A mapping study. *Naunyn-Schmiedeberg's archives of pharmacology* **350**, 174-184 (1994).

139. Hagen, A., Dietze, A. & Dhein, S. Human cardiac gap-junction coupling: effects of antiarrhythmic peptide AAP10. *Cardiovascular research* **83**, 405-415 (2009).

140. Weng, S. et al. Pharmacological modification of gap junction coupling by an antiarrhythmic peptide via protein kinase C activation. *FASEB Journal* **16**, 1114-1116 (2002).

141. Grover, R. & Dhein, S. Spatial structure determination of antiarrhythmic peptide using nuclear magnetic resonance spectroscopy. *Peptides* **19**, 1725-1729 (1998).

142. Grover, R. & Dhein, S. Structure-activity relationships of novel peptides related to the antiarrhythmic peptide AAP10 which reduce the dispersion of epicardial action potential duration. *Peptides* **22**, 1011-1021 (2001).

143. Axelsen, L.N. et al. Identification of ischemia-regulated phosphorylation sites in connexin43: A possible target for the antiarrhythmic peptide analogue rotigaptide (ZP123). *Journal of molecular and cellular cardiology* **40**, 790-798 (2006).

144. Haugan, K. et al. Treatment with the gap junction modifier rotigaptide (ZP123) reduces infarct size in rats with chronic myocardial infarction. *J Cardiovasc Pharmacol* **47**, 236-242 (2006).

145. Hennan, J.K. et al. Rotigaptide (ZP123) prevents spontaneous ventricular arrhythmias and reduces infarct size during myocardial ischemia/reperfusion injury in open-chest dogs. *J Pharmacol Exp Ther* **317**, 236-243 (2006).

146. Stahlhut, M., Petersen, J.S., Hennan, J.K. & Ramirez, M.T. The antiarrhythmic peptide rotigaptide (ZP123) increases connexin 43 protein expression in neonatal rat ventricular cardiomyocytes. *Cell Commun Adhes* **13**, 21-27 (2006).

147. Dhein, S. et al. Protein kinase Calpha mediates the effect of antiarrhythmic peptide on gap junction conductance. *Cell Commun Adhes* **8**, 257-264 (2001).

148. Zhang, S.W., Liu, Y., Huang, G.Z. & Liu, L. Aconitine alters connexin43 phosphorylation status and [Ca2+] oscillation patterns in cultured ventricular myocytes of neonatal rats. *Toxicology in vitro : an international journal published in association with BIBRA* **21**, 1476-1485 (2007).

149. Solan, J.L., Fry, M.D., TenBroek, E.M. & Lampe, P.D. Connexin43 phosphorylation at S368 is acute during S and G2/M and in response to protein kinase C activation. *Journal of cell science* **116**, 2203-2211 (2003).

150. Mahajan, A. et al. Modifying L-type calcium current kinetics: consequences for cardiac excitation and arrhythmia dynamics. *Biophysical journal* **94**, 411-423 (2008).

151. Chang Liao, M.L. et al. Sensing Cardiac Electrical Activity With a Cardiac Myocyte Targeted Optogenetic Voltage Indicator. *Circulation research* (2015).

152. van Laake, L.W., Passier, R., Doevendans, P.A. & Mummery, C.L. Human embryonic stem cell-derived cardiomyocytes and cardiac repair in rodents. *Circ Res* **102**, 1008-1010 (2008).

153. Riolobos, L. et al. HLA engineering of human pluripotent stem cells. *Mol Ther* **21**, 1232-1241 (2013).
154. Christoffels, V.M. & Pu, W.T. Developing insights into cardiac regeneration. *Development* **140**, 3933-3937 (2013).
155. Halbach, M. et al. Electrophysiological maturation and integration of murine fetal cardiomyocytes after transplantation. *Circulation research* **101**, 484-492 (2007).
156. Pillekamp, F. et al. Force measurements of human embryonic stem cell-derived cardiomyocytes in an in vitro transplantation model. *Stem cells* **25**, 174-180 (2007).
157. Maxwell, M.P., Hearse, D.J. & Yellon, D.M. Species variation in the coronary collateral circulation during regional myocardial ischaemia: a critical determinant of the rate of evolution and extent of myocardial infarction. *Cardiovascular research* **21**, 737-746 (1987).
158. Cao, G. et al. Genetically targeted optical electrophysiology in intact neural circuits. *Cell* **154**, 904-913 (2013).
159. Han, Z. et al. Fluorescent protein voltage probes derived from ArcLight that respond to membrane voltage changes with fast kinetics. *PloS one* **8**, e81295 (2013).
160. Jin, L. et al. Single action potentials and subthreshold electrical events imaged in neurons with a fluorescent protein voltage probe. *Neuron* **75**, 779-785 (2012).
161. Leyton-Mange, J.S. et al. Rapid Cellular Phenotyping of Human Pluripotent Stem Cell-Derived Cardiomyocytes using a Genetically Encoded Fluorescent Voltage Sensor. *Stem Cell Reports* **2**, 163-170 (2014).
162. Park, J. et al. Screening fluorescent voltage indicators with spontaneously spiking HEK cells. *PloS one* **8**, e85221 (2013).